View metadata, citation and similar papers at core.ac.uk

brought to you by CORE

provided by University of Saskatchewan's Research Archive

# Performance Issues in Cellular Wireless Mesh Networks

A Thesis Submitted to the College of
Graduate Studies and Research
In Partial Fulfillment of the Requirements
For the Degree of Doctor of Philosophy
In the Department of Computer Science
University of Saskatchewan
Saskatoon, Saskatchewan

By

Dong Zhang

© Copyright Dong Zhang, September, 2010. All rights reserved.

## Permission to Use

In presenting this thesis in partial fulfilment of the requirements for a Postgraduate degree from the University of Saskatchewan, I agree that the Libraries of this University may make it freely available for inspection. I further agree that permission for copying of this thesis in any manner, in whole or in part, for scholarly purposes may be granted by the professor or professors who supervised my thesis work or, in their absence, by the Head of the Department or the Dean of the College in which my thesis work was done. It is understood that any copying or publication or use of this thesis or parts thereof for financial gain shall not be allowed without my written permission. It is also understood that due recognition shall be given to me and to the University of Saskatchewan in any scholarly use which may be made of any material in my thesis.

Requests for permission to copy or to make other use of material in this thesis in whole or part should be addressed to:

Head of the Department of Computer Science
University of Saskatchewan
Saskatoon, Saskatchewan, Canada (S7N 5C9)

# Abstract

This thesis proposes a potential solution for future ubiquitous broadband wireless access networks, called a cellular wireless mesh network (CMESH), and investigates a number of its performance issues. A CMESH is organized in multi-radio, multi-channel, multi-rate and multi-hop radio cells. It can operate on abundant high radio frequencies, such as 5-50 GHz, and thus may satisfy the bandwidth requirements of future ubiquitous wireless applications.

Each CMESH cell has a single Internet-connected gateway and serves up to hundreds of mesh nodes within its coverage area. This thesis studies performance issues in a CMESH, focusing on cell capacity, expressed in terms of the max-min throughput. In addition to introducing the concept of a CMESH, this thesis makes the following contributions.

The first contribution is a new method for analyzing theoretical cell capacity. This new method is based on a new concept called Channel Transport Capacity (CTC), and derives new analytic expressions for capacity bounds for carrier-sense-based CMESH cells.

The second contribution is a new algorithm called the Maximum Channel Collision Time (MCCT) algorithm and an expression for the nominal capacity of CMESH cells. This thesis proves that the nominal cell capacity is achievable and is the exact cell capacity for small cells within the abstract models.

Finally, based on the MCCT algorithm, this thesis proposes a series of greedy algorithms for channel assignment and routing in CMESH cells. Simulation results show that these greedy algorithms can significantly improve the capacity of CMESH cells, compared with algorithms proposed by other researchers.

# Table of Contents

# Acknowledgements

I would like to give ninety-percent of my thankfulness to my supervisor, Dr. Rick Bunt. I am lucky to have Dr. Bunt as my supervisor because this thesis is impossible without his help: he sent me to attend the Mobicom 2004 conference, where I found the thesis topic on wireless mesh networks; he gave me invaluable freedom to explore this unfamiliar but important area and tolerated my countless failures; he also gave me many useful comments on my thesis research and supported me financially.

I would like to thank my co-supervisor, Dr. Nathaniel Osgood. Dr. Osgood has wonderful knowledge about wireless communications. He showed me his research skills and gave me many useful comments on my research. His consideration and encouragement were very helpful, and I enjoyed talking with him about various topics.

I want to show my special thankfulness to Dr. Derek Eager and Dr. Ralph Deters. Dr. Eager gave me some of the most insightful comments on my thesis research and taught me how to do research by modelling systems in the course CMPT 815. He also suggested the MASCOTS conference, where my paper on cell capacity bounds got published. Dr. Deters taught me the C# language in the course CMPT 852, and the C# language later became one of the two major programming languages in my research and saved me tremendous time.

I want to acknowledge the other two committee members: Dr. Dwight Makaroff and Dr. David Klymyshyn, for their useful comments on my thesis and their help in our meetings. I must thank my external examiner Dr. Ehab Elmallah, who traveled to attend my defence.

I am very grateful to Brian Gallaway and Greg Oster, our system administrators, for their professional and timely technical support. I would like to thank the office staff members of my department, especially Jan Thompson, our graduate correspondent, whose help and mother-like love have become the sweetest memory during my Ph.D. study. I also want to thank Sheena Rowan, the executive assistant of Dr. Bunt, for all kinds of her help related to Dr. Bunt.

Finally, I would thank all of my family members, whose accompany and support in my most difficult days filled me with strength. Their love is the most precious gift in my life.

# List of Tables

# List of Figures

# List of Notation

| Symbol | Definition | Unit |
|---|---|---|
| $\vec{a} = (a_1, a_2, ...a_n)$ | Vector of active (traffic demand > 0) user nodes | |
| $\widehat{a}$ | The set form of a vector $\vec{a}$, i.e., $\widehat{a} = \{a_1, a_2, ...a_n\}$ | |
| $A_e$ | The number of active user nodes in $\widehat{V}_e$: $A_e = \left\|\widehat{a} \bigcap \widehat{V}_e\right\|$ | |
| $c$ (or $c_k$) | The maximum channel transport capacity (on channel $k$) | m · bit/s |
| $C$ | Number of orthogonal channels | |
| $C_e$ | Channel on edge $e$ | |
| $\vec{C}_E$ | Vector of the channels on the edges in $\vec{E}$ | |
| $\vec{C}_V$ | Vector of the channels assigned to the down radios in $\vec{V}$ | |
| $\widehat{C}$ | Set of orthogonal channels | |
| $d_c$ (or $d_{kc}$) | The transmission range that gives $c$ (on channel $k$) | m |
| $D$ (or $D_k$) | Carrier sense range (on channel $k$) | m |
| $e$ | An edge in $\vec{E}$ | |
| $e_v$ | The edge from $H_v$ to $v$ | |
| $\vec{E}$ | Vector of all the edges (directed wireless links) in a cell | |
| $\widehat{E}_A$ | Set of edges whose $A_e > 0$: $\widehat{E}_A = \{e \mid \forall e \in \widehat{E}, A_e > 0\}$ | |
| $\widehat{E}_v$ | Set of the child edges of down radio $v$ | |
| $G$ | The gateway in a cell | |
| $\vec{G}$ | Vector of the down radios of $G$ | |
| $H_v$ | Next-hop down radio of up radio $v$ on its path to $G$ | |
| $\widehat{I}_e$ | Set of edges interfering with edge $e$ if on the same channel | |
| $\widehat{I}_e(k)$ | Set of edges on channel $k$ in $\widehat{I}_e$ | |
| $\widehat{I}_e^+(C_e)$ | Set $\widehat{I}_e(C_e) \bigcup \{e\}$ | |
| $\vec{I}_E$ | Interference vector: $\vec{I}_E = (\widehat{I}_1, ..., \widehat{I}_{\left\|\vec{E}\right\|})$ | |

| | | |
|---|---|---|
| $\vec{m} = (m_1, m_2, ..., m_n)$ | Vector of the traffic demands for $\vec{a}$ | |
| $N$ | Number of user nodes | |
| $\vec{N}$ | Vector of nodes or their unique down/up radios in a cell | |
| $R$ | Cell radius | m |
| $\hat{R}_v$ | Path (a set of edges) between $v$ and $G$ | |
| $\vec{R}_V$ | Vector $\vec{R}_V = (\hat{R}_1, ...\hat{R}_{\lvert\vec{V}\rvert})$ | |
| $S$ | Packet size | |
| $T_e$ | Transmission time on edge $e$ for $A_e$ bits: $T_e = A_e \cdot \tau_e$ | s |
| $T_v$ | Sum of $T_e$ for all the edges in $\hat{E}_v$ | s |
| $\tau_e$ | Transmission time on edge $e$ for 1 bit | s |
| $v$ | An vertex in $\vec{V}$ | |
| $\vec{V}$ | Vector of vertexes: $\vec{V} = (\vec{N}, \vec{G})$ | |
| $\hat{V}_e$ | Set of nodes whose paths to $G$ include edge $e$ | |
| $w_c$ (or $w_{kc}$) | The corresponding bit rate for $d_c$ (on channel $k$) | bit/s |
| $w_e$ | Bit rate of edge $e$ | bit/s |
| $\vec{w}_E$ | Vector $\vec{w}_E = (w_1, ..., w_{\lvert\vec{E}\rvert})$ | bit/s |
| $x$ | Throughput achievable by each active user node | bit/s |
| $\vec{x} = (x_1, x_2, ..., x_n)$ | Vector of feasible throughput allocations for $\vec{a}$ | |

## List of Abbreviations

**4G** – Fourth-generation

**AAA** – Authentication, authorization, and accounting

**AP** – Access point

**BCD** – Bottleneck collision domain

**CBR** – Constant bit rate

**CCD** – Channel collision domain

**CCT** – Channel collision time

**CDMA** – Code division multiple access

**CMESH** – Cellular wireless mesh network

**CSMA/CA** – Carrier sense multiple access with collision avoidance

**CTC** – Channel transport capacity

**CTCD** – Channel transport capacity demand

**CTCS** – Channel transport capacity supply

**CTS** – Clear to send

**DCF** – Distributed coordination function

**DSL** – Digital subscriber line/loop

**ETT** – Estimated transmission time

**GMCCT** – Greedy maximum channel collision time

**GSM** – Global system for mobile communications

**LAN** – Local area network

**MAC** – Media access control

**MANET** – Mobile ad hoc network

**MCCT** – Maximum channel collision time

**MIMO** – Multiple input and multiple output

**MMAP** – Mesh mobility access point

**NIC** – Network interface card

**PCF** – Point coordination function

**PDA** – Personal digital assistant

**PLB** – Priority least busy

**RTS** – Request to send

**SINR** – Signal to interference and noise ratio

**TCP** – Transmission control protocol

**UDP** – User datagram protocol

**VoIP** – Voice over IP

**WLAN** – Wireless local area network

**WMN** – Wireless mesh network

## Glossary of Terms

**Bandwidth** – The difference between the upper and lower radio frequencies, in a contiguous set of radio frequencies, typically measured in hertz.

**Cell capacity** – The maximized minimum throughput of active user nodes each with infinite traffic demand. The general definition of cell capacity is the maximized minimum throughput of unsatisfied user nodes.

**Cellular wireless mesh network (or CMESH)** – A special ubiquitous wireless access network made up of multi-radio, multi-channel, multi-rate and multi-hop cells, each served by a gateway. A cellular wireless mesh network is also a special wireless mesh network organized in cells, where each cell has a single gateway and an exclusive coverage area.

**Channel** – Band of radio frequencies. In a CMESH, its all available radio frequencies are divided into multiple non-overlapping (or orthogonal) channels. Transmissions on different orthogonal channels are assumed to do not interfere with each other.

**CMESH cell (or cell)** – A cell in CMESHs has a single Internet-connected gateway that serves up to hundreds of mesh nodes within its coverage area. A CMESH cell is a multi-radio, multi-channel, multi-rate and multi-hop wireless network.

**Down radio** – The radio of a node that serves as a next-hop candidate for the up radios of other nodes to use the path of the node to access the gateway.

**Downstream** – The direction from the gateway to mesh nodes in a cell.

**Edge** – Directed wireless link.

**Gateway** – A CMESH cell has only a single gateway; the gateway has the only direct Internet connection in the cell.

**Helper radio** – The radio of a node that works on channels other than the two used by the down radio and the up radio of the node.

**Interference (edge)** – Edge $e$ interferes with edge $e'$ (or edges $e$ and $e'$ interfere with each other) if either of the following two cases hold. Case 1: a transmission on $e$ causes the failure of a simultaneous transmission on $e'$; Case 2: a transmission on $e'$ causes the failure of a simultaneous transmission on $e$. Let $\widehat{I}'_e$ and $\widehat{I}''_e$ denote all the edges that play the role of $e'$ in Case 1 and Case 2, respectively, if they are on the same channel as $e$ in a CMESH cell. In the thesis, the set of edges that interfere with $e$, denoted by $\widehat{I}_e$, is given by $\widehat{I}_e = \widehat{I}'_e \cup \widehat{I}''_e$.

**Max-min fairness** – A feasible allocation of throughput is max-min fair if and only if an increase of any throughput by any feasible allocation must come at the cost of a decrease of some already smaller throughput.

**Mesh (or Mobile) client** – A mobile user device such as a laptop that accesses a CMESH by communicating with MMAPs using mesh mobility software.

**Mesh mobility access point (or MMAP)** – A MMAP is an access point attached to a relay node for mesh clients to access a CMESH.

**Mesh node (or node)** – A node refers to either a user node or a relay node, both of which are stationary wireless nodes. Note that nodes in this thesis do not include gateways, MMAPs or mesh clients.

**Mobile ad hoc network** – A mobile ad hoc network is an autonomous system consisting of mobile nodes acting as both routers and hosts, connected by wireless links. Ad hoc means that the connection is established for the duration of one session and requires no base station.

**ns-2** – A popular discrete event simulator designed for network research.

**Path (or route)** – In a CMESH cell, a path of a node is a sequence of consecutive wireless links that connect the node to a gateway radio, along which user traffic is delivered between the node and the gateway.

**Post-CA Routing algorithm** – A routing algorithm that runs after channel assignment is done.

**Pre-CA Routing algorithm** – A routing algorithm that runs before channel assignment starts.

**Relay node** – A stationary wireless node that has no local user traffic and only relays the traffic of other nodes.

**Routing** – The process of selecting paths to the gateway for nodes in a CMESH cell.

**Sub-tree** – Node X is a sub-tree node of node or edge Y if X's path to the gateway passes through Y.

**Up radio** – The radio of a node that finds the path between the node and the gateway.

**Upstream** – The direction from mesh nodes to the gateway in a cell.

**User node** – A stationary wireless node that has local user traffic.

**Wireless mesh network (or WMN)** – A general-purpose wireless ad hoc network, whose nodes, each equipped with one or more radios, form a stationary backbone.

# CHAPTER 1
# INTRODUCTION

Recent years have witnessed a blossoming of wireless mesh networks (WMNs), which are expected to be one of the key technologies for next-generation wireless networking. This chapter gives an introduction to WMNs, focusing particularly on a new architecture of WMNs—named a cellular wireless mesh network or CMESH—proposed in this thesis.

A CMESH is organized in multi-radio, multi-channel, multi-rate and multi-hop cells. Each cell has a single Internet-connected gateway which serves up to hundreds of mesh nodes. A CMESH can operate on abundant high radio frequencies, such as 5-50 GHz, and thus offers the potential for satisfying the bandwidth requirements of future ubiquitous wireless applications.

This thesis studies a number of performance issues in CMESHs, focusing on cell capacity, expressed in terms of the max-min throughput. There are many factors that affect the capacity of a CMESH cell, such as the number of user nodes and their locations, wireless relay node deployment, the number of radios per mesh node, the number of orthogonal channels and their assignment, routing and transmission scheduling. This thesis addresses these factors in four research topics spread across four chapters: cell capacity bounds in Chapter 3, nominal cell capacity in Chapter 4, channel assignment in Chapter 5 and routing in Chapter 6.

The remainder of this chapter is organized as follows. Section 1.1 provides an overview of WMNs. Section 1.2 introduces a CMESH, including its definitions, architectures, applications and design goals. Section 1.3 summarizes the main assumptions that are made in the thesis. The contributions of this thesis are described in Section 1.4. Section 1.5 outlines the organization of the remainder of the thesis.

## 1.1 An Overview of Wireless Mesh Networks

This section gives a brief introduction to WMNs, including their definitions, applications, architectures, standards and their commercial and experimental deployments.

### Definitions

In general, a WMN can be defined as a wireless ad hoc network [126] organized in a mesh topology. A wireless ad hoc network was once a synonym for mobile ad hoc network (MANET) [91], which was also called a mobile multi-hop wireless ad hoc network. A mobile ad hoc network is an autonomous system consisting of mobile nodes acting as both routers and hosts, connected by wireless links. These mobile nodes can move freely and organize themselves dynamically to form a temporary network without pre-existing infrastructure. A wireless sensor network can also be considered as another type of wireless ad hoc network made up of sensors. Note that this general definition of a WMN allows all WMN nodes to be mobile.

In this thesis, a WMN is defined as a general-purpose wireless ad hoc network, whose nodes, each equipped with one or more radios, form a stationary backbone. According to this definition, there are two significant differences between WMNs and MANETs, as follows.

The first difference is in their application focus. MANETs were designed initially for military applications (e.g., thousands of mobile nodes need to communicate with each other on battlefields) and later for specialized civilian applications such as disaster recovery and cooperative mobile data exchange, and these applications are far from the general requirements of civilian use. By contrast, WMNs are designed for general-purpose applications, such as residential broadband Internet access, wireless community networks and corporate network backhauls, all of which seek to benefit the daily lives of ordinary citizens.

The second difference is in the network node types. In contrast to the mobile nodes in MANETs, most nodes in WMNs—and especially the backbone nodes—are stationary. Backbone nodes are the nodes that relay packets and connect all network components together. Stationary nodes are notes for which it is possible to have access to a sustained power supply. Therefore, WMN research can focus on performance issues without some critical constraints of MANETs, such as energy consumption and frequent topology changes.

### Applications

A primary anticipated application of WMNs is residential broadband Internet access. Residential broadband Internet access is expected to bring profound benefits to people's lives and the world's economy [8]. Such benefits may include, for example, home education, elderly citizens' health care, house energy monitoring and public safety.

Although wired technologies such as cable modem and DSL have already been able to provide broadband access to residences, they are relatively expensive, especially for those living in rural areas or developing countries, due particularly to the last-kilometre (or last-mile) problem [8]. High costs suppress users' demand, which further inhibits corporate investments in the infrastructure for residential broadband access.

Existing wireless communication technologies show great potential as a route to residential broadband access, but currently have limitations. Satellite systems have enough bandwidth but suffer from significant delay and may be too expensive for many families. The cellular networks have expensive base stations and limited bandwidth, so their broadband services are currently relatively expensive. Current Wi-Fi [125], i.e., IEEE 802.11 wireless LANs, can also provide broadband access, but their individual service coverage is very limited. As a result, a city-wide coverage may need a large number of access points, whose overall cost could be very high due to their expensive wired backhauls and management.

WMN technology offers an alternative approach that seeks to use cheap wireless devices to provide broadband Internet access with fewer wired backhauls. This approach appeals to many academic research groups [94, 95] and companies [17, 42].

Another application of WMNs is to use them as enterprise backbones [17, 42]. Corporations need to deploy an Intranet in an office, in a building, or among a number of buildings. Although 802.11 access points have been widely deployed in offices, they traditionally have to be inter-connected by wired lines. WMNs can be used to inter-connect these office access points with wireless links and save the expense of wired backbones.

Some other applications include security surveillance, community networks, and networks in difficult environments such as tunnels and oil rigs.

**Architectures**

A WMN consists of gateways, wireless mesh routers and wireless mesh clients [6]. Gateways (also called hot spots or access points [25]) are the special mesh routers that connect to the wired Internet directly or via other networks (such as satellite). Wireless mesh routers (also called transit access points (TAPs) [72]) are stationary nodes with full mesh functions, acting as network backbone routers and providing packet relay for themselves, wireless mesh clients and other networks. Wireless mesh clients are either stationary nodes or low-speed mobile nodes

serving end users and may or may not install mesh routing and other mesh functions. Mesh routers form the backbones (or trunks) of the network, while mesh clients are the network periphery serving end users.

Architectures of WMNs may be classified into three types: Infrastructure/Backbone WMNs, Client WMNs and Hybrid WMNs. Backbone WMNs are formed by mesh routers and provide an infrastructure for clients. Client WMNs are formed by mesh clients and provide peer-to-peer networks among client devices. Hybrid WMNs offer a combination of infrastructure and client meshing, and a mesh client can access gateways via either mesh routers or other mesh clients.

**Standards**

The IEEE 802.11 study group is pursuing the 802.11s project [54], termed IEEE 802.11 Extended Service Set (ESS) Mesh Networking. The IEEE 802.11s protocol is based on IEEE 802.11 MAC/PHY layers and provides an architecture and protocol for auto-configuring routing among access points (APs) using radio-aware metrics over a multi-hop topology in a wireless distribution system to support both broadcast/multicast and unicast traffic.

A joint proposal of SEEMesh (Simple, Efficient and Extensible Mesh) and Wi-Mesh has been accepted as a draft of 802.11s. SEEMesh introduces Mesh portals, which are compatible with the older wireless standard technology, and is supported by Intel, Motorola, Nokia, NTT DoCoMo and Texas Instruments. Wi-Mesh provides communications for consumer, small business and military applications.

**Commercial WMN Companies**

BelAir Networks [17] advocated a multi-radio, cellular LAN architecture and provided a system that delivered Wi-Fi access over large, dense, urban areas. It used antennas with high gain and a narrow horizontal beamwidth to enhance radio performance and reach extension. The radios could adapt to constant environmental changes on a packet-by-packet basis. The radio-aware routing algorithms continuously calculated the best route based on available capacity and latency, and each traffic source load balanced across a minimum of two routes. BelAir also provided single-radio systems as a low-cost and modest performance solution.

Firetide [42] focused on mesh infrastructure, whose nodes have multiple Ethernet interfaces that could be connected to Ethernet-capable devices. With the rapid growth of public safety and

homeland security markets, Firetide was interested in mesh-based video surveillance technology.

Strix Systems [116] designed the Access/One architecture, which was presented as a cost effective wireless mesh platform. Its indoor wireless system had up to three radios in a single mesh node. Its outdoor wireless system combined up to six radios in a single enclosure.

Tropos Networks [122] had a network architecture called MetroMesh for building metro-area wireless broadband networks. Its predictive wireless routing protocol could optimize the routing algorithm and reduce overhead and scaled to thousands of nodes.

Some other corporations, such as Cisco [30] and Motorola [96], that are currently providing commercial WMN solutions.

**Experimental WMNs**

Drunen *et al.* [37] presented a wireless community network based on IEEE 802.11b and directional channel techniques in the Netherlands. The network covered an area of 25 $km^2$, and home computers were interconnected via wireless links. Each node used two or more directional antennas to connect at least two other nodes to form a mesh network and one omni-directional antenna for local access. The OSPF (Open Shortest Path First) routing protocol [97] was used. Experiments showed that planning the network was difficult, so continuous configuration was needed, and changing antenna directions was difficult after initial setup. They also found that PC machines were not reliable, and that dedicated systems may solve this problem.

The MIT Roofnet [95] was another experimental IEEE 802.11b wireless mesh network. The experimental area was about 6 $km^2$ in Cambridge, Massachusetts. The network had 37 nodes, which were connected to the Internet via three to four wired gateways (12 nodes were within one hop of the gateways), whose antennas were on the top of some buildings. Each mesh node consisted of a PC, and a single Ethernet port, an 802.11b card, and an omni-directional antenna mounted on a roof or outside a window.

Microsoft Research had a research project called Self Organizing Wireless Mesh Networks [94]. Its testbed consisted of 23 nodes placed in a fixed location on one floor of an office building. Each node was a desktop equipped with two 802.11 cards, configured in an ad hoc mode and each tuned to a fixed channel.

The Experimental Computer Systems Lab at the Stony Brook University had an 802.11-based multi-channel WMN architecture called Hyacinth [107]. The Hyacinth testbed consisted of nine

nodes placed in a 20m×10m area spanning two lab rooms. Each node was a desktop computer equipped with two network interface cards (NICs), configured in an 802.11a ad hoc mode. Two of the nodes were the gateway nodes that were connected to the wired campus network.

## 1.2 Cellular Wireless Mesh Networks

One of the main contributions of this thesis is the introduction of a new form of WMN called a cellular wireless mesh network (CMESH), which is envisioned as one of the potential solutions for future ubiquitous broadband wireless access networks. This section gives an introduction to this new network.

Among all potential approaches to satisfying the traffic demand of future ubiquitous wireless applications, a CMESH chooses to utilize abundant high radio frequencies, such as 5-50 GHz. These radio frequencies cannot be utilized by traditional single-hop cellular networks because when radio frequencies are so high, even tree leaves may absorb signals. Transmissions have to place greater reliance on line-of-sight paths, which generally means shorter transmission distances, and thus user packets need to travel multiple hops before they can reach base stations.

### 1.2.1 Definitions

A CMESH is a special multi-hop cellular network. It has a similar cell structure to a traditional cellular network, but its cells are distinguished from the single-hop cells in a traditional cellular network by having multiple hops. A CMESH can also be defined as a special wireless mesh network organized in cells, where each cell has a single gateway and an exclusive coverage area.

A CMESH has the following advantages:

1. **High bandwidth**. This is an important advantage of a CMESH. As explained earlier in this section, a CMESH can utilize abundant high radio frequencies, such as above 5 GHz, which cannot be utilized by traditional single-hop cellular networks. Therefore, a CMESH may have high bandwidth available in high radio frequencies. Note that IEEE 802.16 uses the 10–66 GHz bands for office applications [60].
2. **Stable (elevated) cells.** Nodes in a CMESH are installed high above the ground away from sources of interference (see Section 1.2.2), so that moving people and vehicles will not block their transmissions. These nodes are stationary and are always powered on once installed. In addition, transmissions in a CMESH rely mainly on line-of-sight

paths, and multi-path fading may not be significant because signals fade quickly with distance in high radio frequencies. Because of these reasons, topology and link quality may be stable in a CMESH cell. Note that in case of precipitation, some wireless links may become broken; but because a node may have multiple neighbours due to a mesh topology, stable links may still be found during the precipitation by routing algorithms.

3. **Network robustness**. Single-hop cellular networks are vulnerable to a single point of failure, but a CMESH does not have this problem because each node may find multiple paths to multiple gateways. If a node in a CMESH cell cannot communicate with its next-hop neighbour (e.g., due to blockage) on its current path, it will choose another neighbour as its next hop. In addition, a CMESH cell is likely to have multiple neighbour cells. If the gateway of a cell fails, its nodes will be automatically split into several groups and join nearby cells. Ideally, unless all gateways in a CMESH are down, nodes should be able to find a healthy gateway.
4. **Ease of management**. A CMESH is organized in cells, bringing the advantages of simplicity and ease of management and making it possible for a CMESH to provide guaranteed throughput and delay for user nodes. For example, it is much easier for a CMESH to plan the coverage area of its cells and to manage inter-cell interference. Channel allocations among cells become simple: small random cells are like GSM cells, where neighbouring cells use a different set of channels to avoid inter-cell interference; large random cells, whose gateways are spaced with enough distance, may share a common set of channels without losing each cell's capacity, just like CDMA cells.
5. **Low costs**. Gateways in a CMESH can be personal computers (see Section 1.2.2), which are much cheaper than base stations and towers. A node may be inexpensive due to its simple functions and small sizes (see Section 1.2.2). Moreover, a CMESH is able to utilize its user nodes at users' locations (schemes will protect users' privileges): if a city-wide CMESH has one million users, the CMESH will have one million user nodes that relay packets, so the costs of wireless relay nodes are significantly reduced. With abundant radio frequencies, managed inter-cell interference and reduced interference from other sources, each gateway in a CMESH may serve a large number of user nodes in a large area. Thus, a CMESH may have reduced overall infrastructure costs for city-wide coverage.

6. **Low radiation**. Transmit power in a CMESH is low due to short transmission ranges. Transmit power in an indoor CMESH is even lower because the transmission distance may be only a few metres. In addition, mesh nodes (note: not clients) would be installed away from people (see Section 1.2.2): outdoor mesh nodes are installed typically 5-50 metres high where no people are nearby; indoor mesh nodes are installed on the ceiling with beams adjusted to travel along the ceiling. Finally, high radio frequencies have high path loss and may not penetrate walls of buildings. For these reasons, people may suffer from low radiation exposure from a CMESH.

The main disadvantage of a CMESH may be in supporting fast-moving users because of its short transmission range and high radio frequencies. To support such users, a traditional single-hop cellular network may be more suitable, because its longer transmission range reduces the need for handovers, and its lower radio frequencies perform better in the case of drastic changes in transmission conditions caused by rapid movement of mobile devices.

Being able to utilize abundant high radio frequencies and serve a large number of mesh nodes in a large area, a CMESH may have the potential to become another major public ubiquitous wireless access network, in addition to the existing satellite networks, cellular networks and other wireless access networks.

### 1.2.2 Architectures

A CMESH system consists of radio cells, AAA (authentication, authorization, and accounting) servers and network management servers, as shown in Figure 1.1. A CMESH cell consists of a single gateway, up to hundreds of user nodes and relay nodes, and optional mesh mobility access points (MMAPs), as shown in Figure 1.2.

Residents' personal computers are connected to user nodes via Ethernet. MMAPs can be attached to some selected relay nodes and serve as the entry points for mobile clients to access a CMESH. From CMESH users' point of view, their devices are automatically connected to the Internet once powered up, requiring no users' interaction with a CMESH.

A CMESH in a city is much like the lights of a city: both are installed high above the ground (see below), both need only power supply, and both rely on line-of-sight transmissions. A city-wide CMESH can contain thousands of cells, which can have millions of mesh nodes and can provide high-speed Internet to every corner of the city.

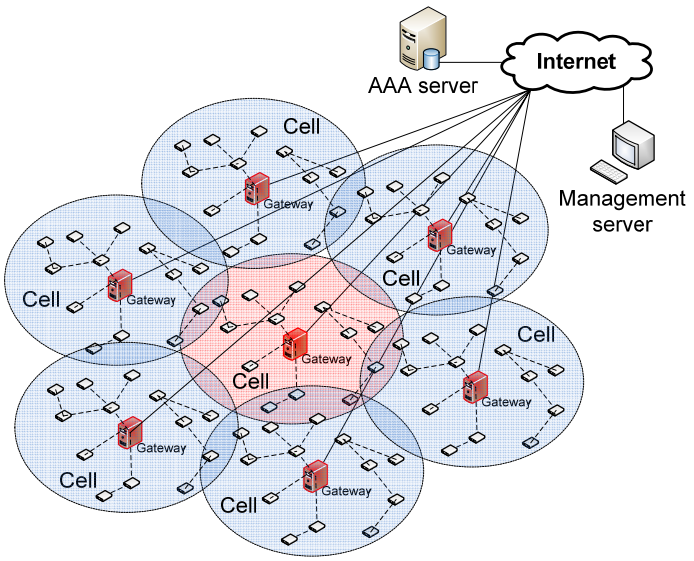


Figure 1.1: Architecture of a CMESH system

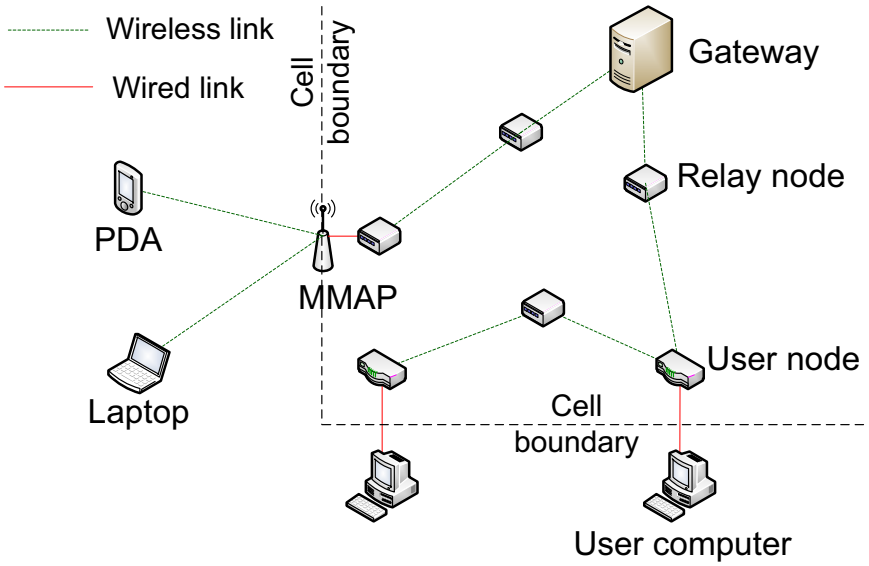


Figure 1.2: A CMESH cell

**Gateways**

A gateway is distinguished in a CMESH cell by possessing of a link offering direct access to the Internet. This Internet link would typically be realized via either a wired backhaul or directional wireless connections, such as satellite links. A gateway is also responsible for

organizing the mesh nodes in its cell so as to provide Internet access for them.

A gateway can be a high-performance personal computer, which is typically placed inside a secure room in a building. Each gateway has multiple external radios (up to the number of channels available in the cell), operating on different orthogonal channels, typically installed on the roof or the sides of a building.

**Mesh Nodes**

Mesh nodes (also named nodes) refer to either user nodes or relay nodes. A mesh node is a modem-like small wireless device that is stationary and needs only power supply. A mesh node is assumed to be always powered on.

A mesh node has the following components:

1. Multiple (three by default) radios.
2. A micro controller unit.
3. An Ethernet interface with Power over Ethernet (PoE).
4. An enclosure.

The research on channel assignment (Chapter 5) and routing (Chapter 6) uses a two-data-radio node design, where each node has two data radios: an up radio and a down radio. The up radio of a node finds a path for the node to access the gateway; the down radio of the node provides this path for other nodes to access the gateway. This design is a trade-off between multi-channel usage and per node cost: one radio cannot use multiple channels simultaneously, but more radios increase per node cost.

Existing simulation results and theoretical results support the use of a small number of radios per node in multi-channel wireless networks. For example, Alicherry *et al.*'s simulation results [7] show that using more than two radios has much lower marginal throughput gains. Kyasanur and Vaidya's theoretical results [82] show that if the number of channels is small compared to the number of nodes, the capacity of a random network, where nodes are uniformly located and each node has only a few radios, is not reduced.

As the number of channels in a cell increases, more data radios are necessary to utilize all the channels fully. If each node has only two data radios, this requires adding more nodes to a cell. For example, if a user requires more throughput than what one up radio can provide, the user can install more user nodes because the fairness model (see Section 1.2.4) is based on user nodes. If

there are bottleneck wireless links that severely limit cell capacity, more relay nodes can be deployed, because adding one relay node adds two data radios. Therefore, the two-data-radio node design can handle general scenarios.

A mesh node may also have a helper radio. A helper radio is useful because it enables a mesh node to simultaneously run tasks, such as link measurement, on a channel different from the two used by the up radio and the down radio. A helper radio can improve the performance of a mesh node. For example, if a data radio of a node is about to switch to a new channel, the helper radio of the node can operate on its current channel to avoid packet loss during the channel switching period. The three-radio node design is the default design for nodes in a CMESH.

A mesh node can be made small in size for the following reasons. First, as discussed above, a node typically has only three radios. Second, its antennas operate above 5 GHz and thus can be smaller than 1.5 cm ( $\lambda / 4 = 3 \times 10^8 / (5 \times 10^9) / 4 \times 100 = 1.5$ cm). Third, a node has only one interface, an Ethernet port, which also provides power using the Power over Ethernet technology. Finally, a node requires only a micro controller unit to run simple functions.

**Network Types**

A CMESH refers to either an outdoor CMESH or an indoor CMESH. It may have an add-on network, named a mobile CMESH, to provide mobility for mesh clients.

Outdoor CMESHs are deployed to provide broadband Internet access for residents and companies. A resident (or an office user) rents a modem-like user node and installs it or only its radios outdoors typically on an outside wall or a window of a building at a height ranging from 5-50 metres. This height range should be mandatory for all radios, including radios on high-rises, because typical transmission ranges in outdoor CMESHs are less than 200 metres. As mentioned earlier, user nodes and relay nodes may be small in size, so as to impose little detrimental impact on the appearance of buildings.

Indoor CMESHs are used for home/office networking. A building or a floor has a gateway that serves user nodes in rooms. Mesh nodes are installed on the ceiling. An indoor CMESH typically uses the highest available radio frequencies and shortest transmission ranges, such as only several metres. Radio frequencies that are very high may not penetrate or get around walls and thus reduce interference. If enough radio frequencies are available, the throughput of indoor CMESHs may be comparable to wired LANs.

Mobile CMESHs provide Internet access for indoor and outdoor mobile users at typical walking speed. A mobile CMESH is not an independent network: it is an add-on network to either outdoor CMESHs or indoor CMESHs, as shown in Figure 1.2. A mobile CMESH is composed of special modules called mesh mobility access points (MMAPs), which are attached to some selected relay nodes. On the client side, mesh mobility software must be installed in order to access MMAPs. A client (e.g., laptop) with mesh mobility software installed is called a mobile client or a mesh client. A mobile CMESH can use low radio frequencies to improve mobility support, and its radio frequencies should not be used by outdoor CMESHs and indoor CMESHs to avoid interference. If a mobile CMESH relies mainly on line-of-sight transmissions, a MMAP works like an overhead light, serving only mesh clients in a small area beneath it.

**Cell Initialization**

Cell initialization is started by an online gateway. The gateway periodically broadcasts cell-info messages composed of CMESH ID, cell ID and other public information at the link layer. Mesh nodes that hear the gateway broadcasts will send AAA requests to the gateway to join the cell (see Section 1.2.4). If a node is authenticated by AAA servers, it is assigned an IP address and an initial path to the gateway. Then the node can update its paths to the gateway and assign a channel to its down radio. Finally, the down radio of the node also periodically broadcasts cell-info messages so that its neighbouring nodes can also join the cell.

If a node is at the boundary of multiple cells, it joins all these cells. However, it broadcasts only the information of one cell whose gateway provides the most preferable path (e.g., based on the shortest hops to the gateway).

**Traffic Pattern in Cells**

In a CMESH cell, user traffic is only between user nodes and the gateway. This traffic pattern is also valid for traffic among user nodes in the same cell. If user node $A$ needs to send user packets to user node $B$ that is in the same cell, $A$ must first send its packets to the gateway and let the gateway forward the packets to $B$.

The reasons for this traffic pattern design are as follows. First, a CMESH cell is a local access network for Internet services, so most of its user traffic is for the Internet, not for internal communications. Second, wireless transmissions need to be encrypted, so a CMESH cell needs

a symmetric key scheme (see Section 1.2.4), in which the gateway and node $A$ share the key of node $A$, but it is unsafe for other nodes to share the key of node $A$. Third, a CMESH cell provides max-min throughput using a source rate control scheme (see Section 4.3.1), in which the gateway needs to count all user traffic in the cell, so internal traffic is also required to pass the gateway. Finally, this traffic pattern can bring a desirable benefit: it can simplify the routing process in a CMESH cell (see Chapter 6).

### 1.2.3 Applications

A CMESH provides one of the solutions for "last-kilometre" broadband Internet access for both residents and mobile clients. A typical application scenario in CMESHs could be as follows. A residential user rents a user node in order to become an outdoor CMESH user. The services may include broadband Internet access at home, VoIP (Voice over IP) services and TV programs by peer-to-peer technologies for a full year. Moreover, without any extra charges, a CMESH user can use mobile CMESHs (see below).

Another application scenario is home/office networking which extends the Internet access provided by outdoor CMESHs to the inside of buildings. A user of outdoor CMESHs can set up an indoor CMESH that allows all his computers and electrical appliances to join a family/office wireless network and access the Internet via the outdoor user node. An indoor CMESH cell consists of its own gateway and multiple user/relay nodes.

Mobile CMESHs allow people to access the high-speed Internet with mobile devices, such as laptops, and roam anywhere in the world where mobile CMESHs are available. For example, users can use mobile CMESHs to make VoIP calls while walking on streets or surf websites while waiting for buses. Mobile CMESHs can also let users locate themselves or track their belongings (see below). Because of short transmission distance and multiple available MMAPs due to a mesh topology, the localization can be precise.

Widely deployed CMESHs may serve as a high-performance ubiquitous Internet wireless access network and have many applications. For example, automatic meter reading systems require a large number of user nodes but have light traffic, so they may be not charged because their user nodes mainly relay packets. A user may attach tiny simplified mesh clients to his belongings such as cars or luggage and monitor their locations using a PDA. The only task of such a simplified mesh client is to periodically (e.g., per-minute or monthly) send authentication

packets to its AAA server. In the same way, industries can monitor their products (e.g., bottles for recycling purposes).

### 1.2.4 Design Goals

To support the above applications, a CMESH needs to meet the following design goals: high performance, low cost, secure, mobile and manageable.

#### Performance

A CMESH has four basic performance issues. In decreasing order of priority they are fairness, stability, throughput and delay. This thesis focuses on two of them: fairness and throughput. Stability and delay are discussed briefly, but their research is left for future work.

Fairness is a critical performance and research issue because the application goal requires a CMESH to serve all user nodes. Network throughput without fairness constraints is meaningless in a CMESH. For example, if the goal is simply to maximize the overall throughput in a CMESH cell, the result will be that a few user nodes nearest to the gateway take up all the throughput and other user nodes get nothing. Obviously, this is contrary to the application goal of a CMESH, and is thus not acceptable.

There are two common types of fairness: max-min fairness [19] (see Section 4.1.3 for details) and proportional fairness [93]. A CMESH needs to use max-min fairness because it is desirable for a CMESH cell, which is designed as a local access network, to provide equal service quality to all its user nodes independent of their locations. In contrast, proportional fairness penalizes multi-hop flows and thus would appear far less desirable in a CMESH.

As a single-gateway multi-hop wireless network, a CMESH cell needs special mechanisms to enforce max-min fairness for user nodes. Otherwise, severe unfairness may occur. Figure 1.3 shows an example. In the example, user node X has a sub-tree containing 50 user nodes (i.e., the paths of these 50 user nodes to the gateway pass through user node X). User node X has two 10 Mbps wireless links, W1 and W2, and a local wired Ethernet link W0 of bit rate 100 Mbps. The two wireless links W1 and W2 are operating on two different orthogonal channels.

Suppose that all the links are busy and node X treats all the received packets equally. Absent enforcement of max-min fairness mechanisms, a user node in user node X's sub-tree can achieve an average throughput that is only $1/500$ of user node X's local throughput, calculated by:

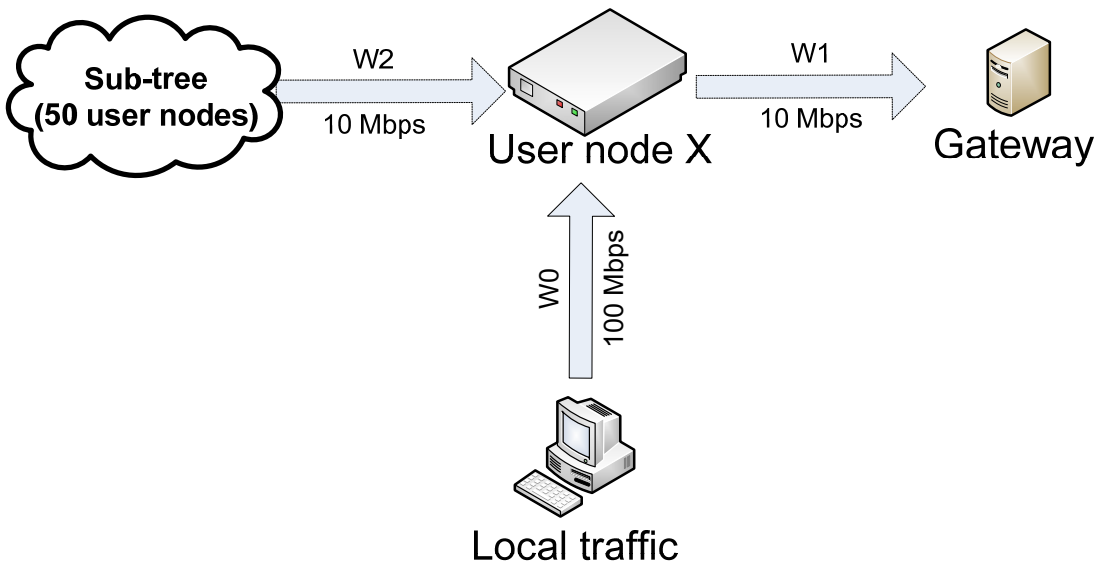


Figure 1.3: An example of throughput unfairness

$$\frac{100 \cdot 10}{(10+100)} : \frac{10 \cdot 10}{(10+100) \cdot 50} = 500:1 .$$

Throughput is another critical performance and research issue in a CMESH. Future wireless applications are expected to demand more user throughput. For example, 4G networks (the next-generation wireless networks that will be deployed in the 2010-15 period) require 1 Gbps data rate for a stationary user [61]. Because a CMESH cell has only limited network resources, such as the available orthogonal channels, it is critical to study how to optimize network schemes in order to maximize user node throughput.

Stability is a critical performance issue but is a less critical research issue because a CMESH cell is assumed to have stable topology and wireless link quality, as explained in Section 1.2.1. This provides a basis for the stability of channel assignment and routing. Further supported by schemes such as the max-min fairness mechanism (see Section 4.3.1), a CMESH cell may achieve stable throughput and packet delay.

Packet delay is considered to be a less critical performance issue compared with throughput in a CMESH because most Internet applications can tolerate some packet delay. Packet delay inside a CMESH cell may comprise propagation delay, processing delay, transmission delay, queuing delay and channel access delay. First, propagation delay can be assumed to be negligible because the radius of a CMESH cell is usually shorter than 1 km. Second, processing

delay should be low due to the simple routing process (see Chapter 6). For example, because an upstream packet is always sent to the gateway, it requires little routing processing. Third, packet transmission delay at each hop can be assumed to be low due to high link rates. In addition, retransmissions should be less frequent due to stable wireless links (see Section 1.2.1). Fourth, intra-flow (packets for the same user node) queuing delay at each hop can be assumed to be low because the max-min fairness mechanism (see Section 4.3.1) may avoid network congestion and use small private round robin queues. Fifth, channel access delay at each hop may be reduced by group packet transmissions (see Section 4.3.1) and should be low because the number of nodes competing for the same channel should be small due to multiple channels. Finally, the topology of a cell (a tree rooted at the gateway) should be controllable by wireless relay node deployment, so the maximum hop count should be under control.

Based on the above considerations, this thesis research focuses on max-min throughput in CMESH cells, instead of stability and delay.

**Costs**

The costs of a CMESH are introduced by three parts: wireless spectrum (i.e., radio frequencies), gateways and mesh nodes. A CMESH may use license-exempt radio bands—such as the 5 GHz band—to reduce spectrum costs. Costs introduced by licensed spectrum are beyond the scope of this thesis.

Gateways are the most expensive individual devices in CMESHs because of the requirements for their hardware performance, safe storage, broadband wired backhauls, power supply and backup. A gateway can be a high-performance personal computer.

Mesh nodes are likely to be inexpensive and energy-saving due to their small size (see Section 1.2.2). Mesh nodes are envisioned to generally use omni-directional radios so that they can stay connected in case of changes in their environment, and thus reduce costs in reconfiguration or regular maintenance. User nodes may also relay packets for other nodes, so fewer wireless relay nodes need to be deployed and the costs in relay nodes are reduced.

**Security**

There are a number of ways to deal with security concerns. A CMESH may use asymmetric encryption (public key cryptography) to authorize its nodes. The participants include one or

multiple AAA servers, the gateway, user/relay nodes, MMAPs and mesh mobility software installed on mobile clients. If a node passes the authentication, it becomes an authorized node and is assigned its symmetric key by its AAA server.

A cell should protect users' information privacy. To prevent eavesdropping, user packets can be encrypted while they are transmitted inside the cell. When user packets leave/enter the cell, user nodes and the gateway transparently decrypt/encrypt them with symmetric keys.

A cell could use a white-list technology to block traffic from unauthorized nodes. Each node maintains a white list that records authorized nodes. If node Y is not on the white list of node X, X forwards only Y's AAA requests via X's AAA server at a "safe" rate (e.g., one 40-byte packet every 30 seconds). This may reduce the risk of congestion caused by illegal traffic.

A cell should be able to detect hackers and notify healthy nodes to isolate malicious nodes, so that their detrimental effect is confined to their local areas (within one hop). The gateway may collect traffic statistics and warning reports from the authorized nodes in the cell. Warning reports may include conflicts of IP or MAC addresses caused by illegal nodes. Traffic statistics could be used to detect hacked nodes by recognition of traffic discrepancies.

**Mobility and Roaming**

As introduced earlier, mobility of mesh clients could be provided by MMAPs in a CMESH. Roaming is the process of handover from one MMAP to another without losing connections. Mobility and roaming should be provided using pure software methods, i.e., mobile clients need only install mesh mobility software that communicates with a CMESH.

Because a CMESH would be an all-IP network, handovers could be as simple as route changes. However, when a mesh client moves to another cell, its physical IP address changes, so a mobile-IP [100] scheme may be necessary for the mesh client to maintain transport and higher-layer connections while the mesh client is roaming.

**Management**

A city-wide CMESH can consist of millions of mesh nodes. Because of the large scale, it is impractical to manually monitor, configure or upgrade a CMESH. Therefore, a centralized network management platform, called a CMESH management system, would be necessary to control a CMESH. A CMESH management system could be designed to remotely monitor and

operate nodes and gateways in a CMESH. In emergencies, such as earth-quakes, it should be able to allocate network resources exclusively to the most important nodes. The system could have both programming interfaces and graphical interfaces. Programming interfaces would allow programs to automatically control a CMESH. Graphical interfaces would generate graphs such as topology maps and links for operators, who could analyze the network at a high level.

## 1.3 Assumptions

In this thesis, different research subjects have different assumptions. For example, channel assignment in Chapter 5 assumes that the single-path routes in a cell are given. Post-CA routing in Chapter 6 assumes that the channels on the down radios in a cell are given. Chapter 4 assumes that both the single-path routes and the channels on wireless links in a cell are given. This section groups the major assumptions in the thesis (excluding the ones just listed) into five topics: architecture, cell topology, packet loss, wireless interference model and user traffic.

### Architecture

A CMESH is envisioned as a future network, so it is hard to foresee its complete architectural assumptions. The following lists only basic assumptions about the CMESH architecture.

First, the thesis assumes that nodes or their radios can be installed overhead with power supplies and are always powered on. An outdoor CMESH may need permission to install some nodes on public lamp posts, and an indoor CMESH may need permission to install some nodes on the ceiling of a building where power supply is available.

Second, the thesis assumes that some radio bands in high radio frequencies can be allocated to a CMESH. The license-exempt radio bands such as the 5 GHz bands may not provide enough bandwidth, so a CMESH may need permission to use licensed bands.

Third, the thesis assumes that a CMESH uses IEEE 802.11-based WMN technology, featuring short transmission ranges and the CSMA/CA mechanism. Other types of WMNs, such as IEEE 802.16-based WMNs, are out of scope of the thesis.

Finally, the thesis assumes that technologies other than omni-directional radios can be used to handle special networking issues in real CMESH deployment. It can be anticipated that there will be many special scenarios in real deployment of a CMESH. In an indoor CMESH, for example, wireless transmissions using high radio frequencies may not penetrate interior walls, so

a wireless link between two mesh nodes that are blocked by a wall may be replaced with a wired Ethernet cable which passes the wall either over the top of the wall or through a penetration.

**Cell Topology**

The basic assumption about cell topology in the thesis is that mesh nodes and the gateway are stationary and all user nodes are connected to the gateway. Because user nodes in a cell may be sparsely located, they may not be able to connect to the gateway through themselves due to short transmission ranges, so cell connectivity has to be ensured by wireless relay node deployment.

Chapter 3 assumes that user nodes are either uniformly distributed or arbitrarily located, and a wireless link between two nodes exists if the distance between the two nodes is within the maximum transmission range. Chapter 3 studies theoretical cell capacity, so it assumes that wireless relay nodes can always be deployed in prescribed locations.

Chapters 4, 5 and 6 assume that cell topology (including node locations and wireless links) is given, and all user nodes have already been connected to the gateway by wireless relay node deployment. The simulations in Chapters 4, 5 and 6 assume that wireless relay nodes are deployed by two algorithms, called Least-RN and Cut-Hop.

The number of radios per mesh node is not an assumption. Chapters 3 and 4 allow arbitrary number of radios per mesh node. Chapters 5 and 6 studies the channel assignment and routing problems where a CMESH cell has a two-data-radio node design, so the number of radios per mesh node in the two chapters is always two.

**Packet Loss and Bit Rate**

Packet loss on wireless links is studied as an extension of the MCCT algorithm in Section 4.2.3. Chapter 4 assumes that packet loss on wireless links is given and is independent of packet size. Chapters 5 and 6 assume that packet loss on wireless links is given and is stable, and use the extension to deal with packet loss. Because Chapter 3 studies cell capacity limits, it assumes no packet loss. Chapter 5 also assumes that packet loss is independent of channels.

In the ns-2 simulations in this thesis, packet loss happens if during the reception of a packet, the SINR (signal to interference and noise ratio) at its receiver ever falls below the required threshold. Typical reasons for packet loss in the ns-2 simulations include the failure of either the carrier-sense scheme or the backoff algorithm in 802.11a MAC. All simulations in this thesis

assume no other types of packet loss. For example, packet loss caused by outside sources is not considered, because a CMESH may be away from sources of interference (see Section 1.2.1).

The assumptions about the bit rates of wireless links are as follows. Chapter 3 assumes that the bit rate of a wireless link between two nodes is determined by the maximum bit rate whose corresponding transmission range is no smaller than the distance between the two nodes. Chapters 4, 5 and 6 assume that the bit rates of the wireless links in a cell are given and stable. Chapter 5 also assumes that the bit rates of wireless links are independent of channels.

**Wireless Interference Model**

Chapter 3 assumes a multi-rate and carrier-sense-based interference model. This interference model can be interpreted as a multi-rate extension to the interference model in traditional cellular networks: if two transmitters on the same channel are spaced with enough distance, then they can successfully send packets to their own receivers within the transmission range without interfering with each other; higher transmission rates have reduced transmission ranges.

Chapters 4, 5 and 6 assume an arbitrary interference model (such as a conflict graph [64]), which requires that whether two wireless links interfere with each other is not affected by others. Chapter 5 also assumes that the interference model is independent of channels.

**User Traffic**

This thesis assumes that user traffic in a CMESH cell is only between the user nodes and the gateway (see Section 1.2.2). Chapters 5 and 6 assume downstream (but can be extended to upstream and bi-stream) user traffic for simplicity purposes. Chapter 4 assumes that user traffic can be either downstream or upstream (but can be extended to bi-stream user traffic). Chapter 3 assumes downstream, upstream and bi-stream user traffic, but its analytic expressions for capacity upper bounds are derived for upstream user traffic only.

All ns-2 simulations in this thesis assume UDP packets only. TCP was not used because its congestion control mechanism (which approximately provides proportional fair rate sharing) conflicts with the max-min fairness, and thus prevents the identification of cell capacity, which is defined by the max-min throughput. Research on TCP in a CMESH is left for future work.

## 1.4 Contributions of the Thesis

There are the four main contributions of this thesis.

- The notion of a cellular wireless mesh network (CMESH) is proposed as a potential solution for future ubiquitous broadband wireless access networks. A CMESH can operate on abundant high radio frequencies, such as 5-50 GHz, and thus may satisfy the bandwidth requirements of future ubiquitous wireless applications.
- A new method is proposed for analyzing theoretical cell capacity based on a new concept called Channel Transport Capacity (CTC), and new analytic expressions are derived for capacity bounds for carrier-sense-based cells in CMESHs. The results are first proven within the abstract models and then validated via simulations.
- A new algorithm called Maximum Channel Collision Time (MCCT) is proposed, which derives an expression for the nominal cell capacity. Within the abstract models, the nominal cell capacity is proven to be achievable and to be the exact cell capacity for small cells. The results are validated using ns-2 simulations.
- New greedy algorithms are proposed for channel assignment and routing in CMESH cells. Simulation results show that these greedy algorithms can significantly improve cell capacity, compared with algorithms proposed by other researchers.

Besides these main contributions, this thesis makes the following minor contributions. First, a max-min fairness mechanism is proposed for CMESH cells, which includes a source rate control scheme and a scheme of round robin queues and group packet transmissions. Second, this thesis extends the ns-2 simulator to support multi-radio, multi-channel, multi-rate and IEEE 802.11a networks. Also, this thesis designs two algorithms for wireless relay node deployment in CMESH cells, called Least-RN and Cut-Hop.

The following subsections elaborate on the main research contributions.

### 1.4.1 Capacity Bounds for CMESH Cells

Cell capacity is a key research issue for a CMESH. Given $C$ orthogonal channels and $N$ user nodes randomly uniformly located in a cell of radius $R$, what is the maximum expected throughput that can be guaranteed for each user node?

Without knowing relay node locations in a cell, most existing research tools, such as linear programming, have difficulties in determining cell capacity, because they traditionally require complete knowledge of cell topology and interference among wireless links. Another widely used research tool, asymptotic analysis, also cannot reveal the capacity of a CMESH cell because

a typical CMESH cell has tens or hundreds of user nodes, and the scale is too small for asymptotic analysis to derive cell capacity. Therefore, a new method is required to derive cell capacity in CMESHs.

This thesis proposes a new notion called Channel Transport Capacity (CTC) and derives analytic expressions for the capacity bounds for carrier-sense-based cells within the abstract models. Upper bounds for cell capacity are derived by analyzing the supply and demand of CTC, and lower bounds are derived by finding a joint scheme of wireless relay node deployment, routing, channel assignment and transmission scheduling that achieves a certain throughput.

### 1.4.2 Nominal Capacity of CMESH Cells

Jun and Sichitiu's Bottleneck Collision Domain (BCD) algorithm [68], Akhtar and Moessner's multi-channel variant [4] and Aoun *et al.*'s max-min fairness variants [10, 11] can calculate the nominal network capacity for a single-gateway and single-rate WMN. This thesis extends their work and proposes a new algorithm, the Maximum Channel Collision Time (MCCT) algorithm, which derives an expression for the nominal capacity of a CMESH cell.

The MCCT algorithm makes three new contributions. First, the MCCT algorithm works for multi-radio, multi-channel, multi-rate and multi-hop WMNs. In contrast, Jun and Sichitiu's and Aoun *et al.*'s algorithms do not work for multi-channel and multi-rate WMNs, and Akhtar and Moessner's algorithm does not work for multi-rate WMNs. Second, this thesis proves that the nominal capacity derived from the MCCT algorithm is achievable within the abstract models. In contrast, none of the above papers proved that the capacity derived from their algorithms is achievable. Third, this thesis derives an expression for the nominal capacity of a multi-radio, multi-channel, multi-rate and multi-hop cell, which has not been given by previous research.

### 1.4.3 Channel Assignment and Routing Algorithms for CMESH Cells

When the topology and the wireless technologies (e.g., IEEE 802.11a) of a cell are given, channel assignment and routing are the two major approaches to improve cell capacity. Although channel assignment and routing can be jointly studied, a joint problem has increased computational complexity and it is not feasible to find the optimal solution for any practical network scale [7]. Thus, this thesis studies channel assignment and routing separately.

Based on the MCCT algorithm, this thesis proposes a series of new greedy algorithms for channel assignment and routing in CMESH cells. In particular, this thesis gives theorems that

provide deeper insights into the channel assignment and routing problems in small CMESH cells. Simulation results show that these greedy algorithms can significantly improve the capacity of CMESH cells, compared with algorithms proposed by other researchers.

## 1.5 Thesis Organization

The remainder of the thesis is organized as follows. Chapter 2 provides an overview of related research on WMNs. Analytic expressions for capacity bounds for carrier-sense-based CMESH cells are presented in Chapter 3. Chapter 4 proposes the MCCT algorithm, which derives an expression for the nominal cell capacity. The channel assignment problem is studied in Chapter 5, and some greedy channel assignment algorithms are proposed. Chapter 6 proposes some greedy routing algorithms that run either before or after channel assignment. Chapter 7 summarizes the thesis and discusses future work.

# CHAPTER 2
# RELATED RESEARCH

Wireless mesh networks (WMNs) are expected to be a key technology for next-generation wireless networking and have attracted significant industry and academic attention in recent years. This chapter reviews related research on WMNs, ranging from the physical layer to the transport layer.

This chapter is organized as follows. Section 2.1 discusses the network capacity problem. Section 2.2 summarizes physical layer issues, focusing on wireless models. Section 2.3 overviews some link layer issues, focusing on the IEEE 802.11 MAC. Section 2.4 and Section 2.5 review channel assignment and routing algorithms for WMNs, respectively. Section 2.6 briefly introduces research on the transport layer.

## 2.1 Network Capacity

Capacity limitation is a well-known problem for all kinds of wireless networks. In multi-hop wireless ad hoc networks, network capacity suffers significantly as the number of wireless nodes increases. That is, wireless ad hoc networks do not scale well. For wireless ad hoc networks to scale, the traffic pattern may need to be constrained to local nodes. A WMN is a special type of wireless ad hoc network, so it shares the same capacity problem.

### 2.1.1 Capacity of Wireless Networks

Gupta and Kumar [47] estimated the per node network transport capacity of wireless ad hoc networks with omni-directional antennas. They studied two network models. The first, the arbitrary network model, has no restrictions on the locations of the nodes, the transmission powers, the source-destination associations, the routing protocol, or the spatial-temporal transmission scheduling scheme. The other, the random network model, has three additional restrictions: random node locations, random traffic pattern, and fixed transmission power. Gupta and Kumar assumed that transport capacity is equally divided among all $n$ nodes, and that each source node has its destination about 1 metre away, and then they calculated the throughput to be

$\Theta\left(1/\sqrt{n}\right)$ bits per second for arbitrary networks and $\Theta\left(1/\sqrt{n\log(n)}\right)$ for random networks under the protocol model (see Section 2.2.2). Under the physical model (see Section 2.2.2), the throughput is $\mathrm{O}\left(1/n^{1/\gamma}\right)$ for arbitrary networks and $\mathrm{O}\left(1/\sqrt{n}\right)$ for random networks, where $\gamma$ is the path loss exponent. They also showed that splitting a channel into sub-channels gives the same results. Finally, they suggested that the network designer may have to either constrict the number of total nodes or confine the traffic of each node to its nearby neighbours.

Based on their own previous work [47], Gupta and Kumar [48] further studied arbitrary size and topology networks over a general channel model called the vector discrete memoryless channel, and they pointed out that an information-theoretic transport capacity of $\Theta(n)$ bit-metres per second is achievable for more advanced receivers that do not treat interference as mere noise in a specific class of networks. They concluded that more sophisticated multi-user coding schemes may provide extra gains to some large wireless networks.

Li *et al.* [84] showed that the traffic pattern determines the scalability of per node capacity in a wireless ad hoc network when they studied the interactions of 802.11 MAC and ad hoc forwarding. They showed by simulations that only local traffic patterns can be scalable. They suggested that the scalability problem could be solved by keeping average distance between the source and the destination nodes small, no matter the overall size of the ad hoc network.

Arpacioglu and Haas [12] showed that the maximum achievable per-node end-to-end throughput in a wireless network of $N$ nodes with omni-directional antennas in a fixed area is $\Theta(1/N)$. This holds for optimal choices of the mobility pattern, the spatial-temporal transmission scheduling policy, the temporal variation of transmission powers, the source-destination pairs, and the possible multi-path routes. It also holds when multiple transmissions and receptions occur at the same time and channels are divided into sub-channels. The upper bound is given by $\lambda \le \frac{W_{\max} U}{\bar{H} N}$, where $W_{\max}$ is the maximum rate that can be transmitted, $\bar{H}$ is the average number of hops between the source and the destination of a bit, $N$ is the number of nodes, and $U$ is a function of $A$ (area), $\gamma$ (path loss exponent), $G$ (processing gain) and $\beta$ (signal-to-noise threshold). They argued that in order to make the system scalable, one or more of the parameters $W_{\max}$, $\gamma$, $G$, $\beta$ or $A$ must grow with $N$. In practical systems, the only

feasible parameter that may grow with $N$ is the area $A$, and $N$ must be $\mathrm{O}\left(A^{\min(\gamma/2,1)}\right)$ if $\gamma \neq 2$, and $\mathrm{O}\left(A/\log(A)\right)$ if $\gamma$=2. In addition, $\bar{H}$ must be $\Theta(1)$ with respect to $N$.

### 2.1.2 Capacity Improvement

It is possible to improve the capacity of wireless ad hoc networks under certain circumstances. The following shows how mobility, directional antennas and infrastructures can be utilized to improve network capacity.

#### Capacity Improvement by Mobility

Gupta and Kumar's work [47] assumed that the network is not mobile, while Grossglauser and Tse [46] showed that mobility can help improve network capacity. Grossglauser and Tse studied random networks under the physical reception model, assuming that node movement obeys a stationary ergodic process and node locations have a stationary uniform distribution. In addition, they assumed that source-destination pairs do not change and end-to-end delay can tolerate any large values. They concluded that there is a routing and scheduling scheme that can deliver a packet to its destination with at most two hops, and thus end-to-end per node throughput can be $\Theta(1)$ as the number of nodes grows large.

#### Capacity Improvement by Multiple Channels and Multiple Interfaces

Kyasanur and Vaidya [82] studied the capacity of multi-channel wireless networks, in which the number of radios per node is smaller than the number of channels. They showed that the capacity of multi-channel wireless networks depends on the ratio between the number of channels and the number of radios per node. They showed that for a random network with $n$ nodes and up to $\mathrm{O}(\log n)$ channels, the network capacity has the same bound given by Gupta and Kumar [47]. Their research shows that using a small number of radios per node may not decrease the capacity of multi-channel random wireless networks if the number of channels are small compared with the number of nodes.

#### Capacity Improvement by Directional Antennas

Yi *et al.* [131] studied wireless ad hoc networks with directional antennas in the arbitrary network and random network models. They showed that the use of directional antennas can

reduce radio interference and thus improve throughput capacity by a factor. When both sender and receiver nodes use directional antennas, they showed that the factor is $2\pi/\sqrt{\alpha\beta}$, where $\alpha$ and $\beta$ are the beamwidths of transmission and reception antennas, respectively, in arbitrary networks, and that the factor is $4\pi^2/(\alpha\beta)$ in random networks.

**Capacity Improvement by Infrastructures**

Kozat *et al.* [79] focused on the throughput capacity of wireless ad hoc networks in the scenario where infrastructure (wired access points, etc.) exists. They assumed that the number of ad hoc nodes that each access point serves is limited, all nodes have fixed transmission range, and that all ad hoc nodes are connected. Based on these assumptions, they showed that each ad hoc node can gain throughput capacity $\Theta(1/\log N)$ in a random network scenario, where $N$ is the total number of nodes. The gain in performance comes from the fact that infrastructure allows the number of hops from a source to a destination to be reduced to a constant number.

### 2.1.3 Capacity of WMNs

Jun and Sichitiu [68] studied the nominal capacity of WMNs. They defined a bottleneck collision domain as the geographical area that limits the throughput of the network. They assumed that the network has only one gateway, every node has infinite data to send to the gateway, and all $N$ nodes share the capacity absolutely fairly. They showed that asymptotic throughput capacity for each node decreases with the number of nodes as $O(1/N)$. Later, Aoun *et al.* gave the algorithm's max-min variant [10, 11], and Akhtar and Moessner gave the multi-channel variant [4] of the algorithm.

BelAir Networks [18] studied the capacity that is available to a large number of users in wireless mesh systems. They showed that the capacity of its single-radio mesh is between $1/h$ and $1/2^h$ of the channel capacity, where $h$ is the number of longest hops between the end users and the wired gateway. They pointed out that the capacity will be even lower if interference and contention are considered.

Previous research [7, 64, 80, 119] employed linear programming to study the network capacity of WMNs and other wireless networks. Algorithms based on linear programming were proposed but these algorithms did not derive analytic expressions for network capacity.

## 2.2 Physical Layer

Physical layer techniques deal with data encoding, signalling, transmission and reception functions. Physical layer techniques can significantly impact the performance of WMNs. For example, directional antennas can increase transmission range as far as 80 km [20], and multiple-input multiple-output (MIMO) antennas can increase throughput by dealing with multi-path propagation. By using MIMO and 40 MHz channels, the IEEE 802.11n [59] specifies the maximum raw data rate of 54-600 Mbps.

The following summarizes wireless communication models, including propagation models, reception models and channel models. Wireless communication models are the basis for research on wireless networks. It is preferable that upper layers get some information on important parameters such as signal strength and signal-to-noise ratios from the physical layer.

### 2.2.1 Wireless Propagation Models

The simplest wireless propagation model is the free space model as noted by Sheikh [109], in which a radio signal transmission path is free of objects that absorb, diffract or reflect radio energy. The model is described with the ratio of received power and the transmitted power and is given by $\frac{P_r}{P_s} = \left(\frac{\lambda}{4\pi d}\right)^2 g_s g_r$, where $P_r$ is the received power, $P_s$ is the transmitted power of the sender, $\lambda$ is the wavelength (metres), $d$ is the distance between the sender and the receiver, $g_s$ is the power gain ratio of the sender's antenna and $g_r$ is the power gain ratio of the receiver's antenna.

Another simple but useful model is the plane earth model [49], in which the ground may absorb and reflect signal power. This model is given by $\frac{P_r}{P_s} = \left(\frac{h_s h_r}{d^2}\right)^2 g_s g_r$, where $h_s$ and $h_r$ are the effective height of the sender's and the receiver's antennas, respectively.

### 2.2.2 Wireless Reception Models

A wireless reception model or interference model is used to determine when transmitted packets can be successfully received by the intended receiver.

A simplified assumption of packet transmissions in wireless networks is that any overlap in time of packet transmissions at the receiver side will cause an unsuccessful reception of the

involved packets, as in the original ALOHA [1]. MACA [71], MACAW [21] and FAMA [43] are all later schemes based on this model (any amount of interference is fatal for packet reception).

Shepard [110] studied a multi-hop packet radio network, consisting of millions or billions of nodes. The author assumed a reception model that a packet can be successfully received at the receiver if $\frac{S}{N} \geq \gamma(2^{c/w} - 1)$, where $S$ is the average power at the receiver, $N$ is the average interfering noise power at the receiver, $w$ is the bandwidth, $c$ is the data rate, and $\gamma$>1, during the whole reception period.

The two commonly used reception models are the protocol model and the physical model [47]. The protocol model supposes that a receiver $\mathrm{Rx}$ is able to receive packets from a transmitter $\mathrm{Tx}$ if the receiver is not in the interference ranges of any other transmitters $\mathrm{Tx}'$ on the same channel, i.e., $|\mathrm{Tx}' - \mathrm{Rx}| \geq (1+\delta) \cdot r$, where $r$ is the common transmission range and $\delta > 0$. In contrast, the physical model presumes that a receiver can successfully receive packets if Signal-to-Interference-and-Noise ratio (SINR) is above a given threshold during the packet transmission period.

### 2.3 Link Layer

Research on the link layer has focused mainly on the Media Access Control (MAC) sub-layer and the bit rate selection problem.

The IEEE 802.11 MAC [55] is assumed by most research, because of its simplicity and popularity. Nodes conforming to the IEEE 802.11 standards can operate in two configurations: independent configuration (called the ad hoc model), in which nodes communicate directly with each other, and infrastructure configuration, in which nodes communicate with access points. The IEEE 802.11 standards specify only the air-interface between nodes and between nodes and access points.

#### 2.3.1 IEEE 802.11b/g/a/n

The original version of the IEEE 802.11 standard released in 1997 specified two raw data rates of 1 and 2 Mbps. The IEEE 802.11b standard published in 1999 [57] was the first widely accepted standard, followed by the 802.11a [56] and 802.11g [58] standards. The 802.11b and

802.11g standards use the license-exempt 2.4 GHz band and operate at a maximum raw data rate of 11 Mbps and 54 Mbps, respectively. The 802.11a standard uses the 5 GHz band and operates at a maximum raw data rate of 54 Mbps.

The IEEE 802.11n standard [59] is built on MIMO (Multiple-Input and Multiple-Output), OFDM (Orthogonal Frequency-Division Multiplexing) and 40 MHz channels. It achieves up to 600 Mbps raw data rate with the use of four spatial streams, and offering a better operating distance than is available in current networks.

### 2.3.2 The Hidden Terminal Problem

The hidden terminal problem [121] describes packets collisions at a receiver because two senders cannot hear each other and transmit at the same time. To reduce the probability of the hidden terminal problem, a mechanism called virtual carrier sense (virtual CS) is devised.

In the virtual CS scheme, a sender sends a short control packet called Request to Send (RTS) before transmitting the data packets. The RTS packet contains the source, destination and duration of delivery of the intended packet and its ACK packet. The receiver responds with a Clear-to-Send (CTS) control packet, which contains the same duration information. When all other nodes receive the RTS/CTS packets, they will set their virtual CS indicator, called a Network Allocation Vector (NAV), and wait for the notified duration. The NAV and the physical carrier sensing function together indicate the busy state of the wireless medium. With the virtual CS mechanism, nodes that happen to hear RTS/CTS will reserve the medium as busy until the packet transmission is finished. Since RTS/CTS packets are short, the chance of collisions is small, and even if collisions do happen, they can be found faster.

### 2.3.3 Distributed Coordination Function (DCF)

The architecture of the IEEE 802.11 MAC sub-layer defines two access methods: the Distributed Coordination Function (DCF) and the Point Coordination Function (PCF). The fundamental access method is DCF, which uses CSMA/CA (Carrier Sense Multiple Access with Collision Avoidance) to access the wireless medium and provide best-effort service. The PCF method provides access via a point coordinator, so that contention can be avoided. PCF is suitable for real-time traffic, but PCF is not implemented in most 802.11 products.

In the DCF method, if a node has a packet to send out, it should sense the channel and wait for a period called Distributed Inter Frame Space (DIFS), and if the channel is still idle, it can

transmit the packet. To avoid a single sender sending sustained packets, and thus preventing the chances of other senders, a random interval is inserted between each transmission. If the packet is correctly received, the receiver sends an ACK packet after a period called Short Inter Frame Space (SIFS). If the sender receives the ACK, the transmitted packet is considered to be successfully delivered. Otherwise, the sender will retransmit the packet after the channel is idle for the DIFS period for a maximum of seven times. An Extended Inter Frame Space (EIFS) must be used whenever a MAC frame transmission begins but the complete frame is not correctly received.

If the sender senses that the channel is busy, it enters a collision avoidance phase by executing an exponential backoff algorithm: it will wait for a random interval, which is uniformly distributed between [0, CW]×SLOT, where CW is the contention window, which varies from 31 to 1023, and SLOT is 20 μs in 802.11b. Among the contending senders, the sender that happens to have chosen the smallest interval will win the right to transmit, and other senders will wait. If the medium is busy at any time during a backoff slot, the backoff procedure is suspended, and the backoff timer stops decreasing until the channel is idle for the duration of DIFS. Whenever the backoff timer reaches zero, the transmission should begin. Each time a sender collides, it doubles CW up to the maximum CW value. Based on the above analysis, the overall packet delivery time T is:

$$T = \mathrm{DIFS} + t_{cont} + t_{PLCP} + t_{tran} + t_{prop} + \mathrm{SIFS} + t_{PLCP} + t_{ack},$$

where SIFS = 10 μs, DIFS = 50 μs in 802.11b, $t_{cont}$ is the time spent on contention (as described above), $t_{tran}$ is the packet transmission time, $t_{ack}$ is the ACK packet transmission time, $t_{PLCP}$ is the time spent on the physical layer protocol overhead, and $t_{prop}$ is the propagation delay.

The DCF mechanism has been extensively studied and some problems with the DCF mechanism have also been found. Ergen *et al.* [39] proposed a Markov model to analyze DCF performance and found that the throughput first increases and then decreases when the number of active nodes increases.

Li *et al.* [85] identified an unfairness problem of EIFS, and suggested setting the EIFS duration to the same value as DIFS. Fang *et al.* [41] found an unfairness problem caused by setting the contention window to its minimum value upon a successful transmission. If a node sets a minimum contention window upon finishing a transmission, it will have a higher chance of

recapturing the channel than other nodes, whose contention windows remain higher.

Heusse *et al.* [50] found that the 802.11b DCF access method penalizes throughput for nodes with high bit rates. The reason is that 802.11b guarantees that the channel access chance for all nodes will tend to be equal in the long term. Equal chance means that, for the same packet size, slow senders occupy the channel longer than faster nodes, so the overall throughput suffers. Later, Yuan *et al.* [132] proposed a scheme that provides nodes with high bit rates temporal fairness and low-bit-rate nodes proportional temporal fairness in the long term. In addition, they also proposed an adaptive batch transmission scheme to improve throughput by decreasing protocol overhead of the DCF mechanism.

Lundgren *et al.* [90] found what they called communication grey zones in experiments in IEEE 802.11b networks. In such a zone, broadcast packets can be received, but unicast packets are not able to be received, so routing protocols that broadcast HELLO messages could actually establish wrong routes. The authors summarized the reasons as due to four factors: different transmission rate, no acknowledgements, small packet size, and fluctuating links. They suggested that this phenomenon could be solved by building routing tables according to end-to-end quality or by using broadcast and unicast packets correctly.

Xu *et al.* [128] studied IEEE 802.11 MAC in multi-hop environments through simulations and found some serious TCP problems, including TCP instability and unfairness problems. One reason is the exposed terminal problem [21]: they found that a receiver can successfully receive RTS but cannot send CTS back because it senses a busy channel. The other reason is that the random backoff scheme favours the latest successful nodes (in the short term). They studied a chain topology where two senders are too far apart to sense each other, and two receivers are between them. They found that a TCP connection with longer hops will suffer broken routes when packet retransmitting at the MAC layer fails seven times. They concluded that 802.11 MAC is not suitable for multi-hop ad hoc networks.

### 2.3.4 Bit Rate Selection

IEEE 802.11 [55] has multiple bit rates for a transmitter to choose. For example, 802.11b [57] transmitters can choose from rates of 1, 2, 5.5 or 11 Mbps, while 802.11a/g [56, 58] transmitters can select one of 6, 9, 12, 18, 24, 36, 48 or 54 Mbps. The automatic bit rate adaptation feature is an important function that many wireless protocols use to choose high quality and low loss rate

links. The following introduces some bit rate selection algorithms.

Auto Rate Fallback (ARF) [69] is the first published bit rate selection algorithm, developed for WaveLAN-II 802.11 wireless cards. ARF adapts to the dynamic conditions and it starts a timer upon rate dropping. After either the timer expires or 10 successive transmissions without retransmissions, ARF tries to tune to higher bit rate opportunities. It moves to lower bit rate whenever 1 or 2 consecutive packets are not acknowledged.

Bicket [22] evaluated a bit rate selection algorithm called SampleRate to maximize throughput over wireless links. SampleRate periodically samples with data packets at a bit rate that possibly has higher throughput in a ten-second window, and switches to the bit rate that has the highest estimated throughput.

Other rate-adaptive algorithms include Adaptive Auto Rate Fallback (AARF) [83], Receiver Based Auto-Rate (RBAR) [51] and Opportunistic Auto-Rate (OAR) [108]. The OAR protocol allows a high rate sender to send multiple packets if the total transmission time is equal to the transmission time that a slow rate sender needs to send a single packet, and thus provides temporal fairness in terms of channel occupancy time. The OAR dramatically improved channel efficiency over the 802.11 model whose fairness is based on an equal number of packets sent by each node over a long period.

### 2.3.5 Measurement of 802.11 Networks

Aguayo *et al.* [3] measured and analyzed packet loss in the MIT Roofnet network, an 802.11b-based mesh network. At the time of their study, the MIT Roofnet consisted of 38 nodes distributed over 6 $km^2$ in urban areas, each node equipped with an 802.11b card operating in an ad hoc model and connected to an omni-directional antenna mounted on a roof. In their experiment, each node in turn sent broadcast packets for 90 seconds and all other nodes passively listened. They found that most node pairs experience loss rates uniformly distributed over all possible values with no distinct loss rate thresholds to distinguish neighbours. They also showed that the delivery probability showed little relation to distance even for very close senders. Most links had loss rates varying slightly over time, but only a small number of links varied more than 10% in loss rates. In most cases, the measurement of current loss rates is a good predictor for future loss rates. In general, a higher signal to noise ratio (S/N) gives a lower loss rate, but there were many cases that disobeyed this rule, so S/N could not accurately predict loss rates. They

also measured interference, but found no relationship between interference and loss rate. Finally, the authors did experiments that emulated signal delay and attenuation, and they found multi-path fading could be an important reason for so many intermediate loss rates.

Anastasi *et al.* [9] also investigated the performance of IEEE 802.11b ad hoc networks by experiments. They found that the system behaviour is complex because the physical frame preamble is always transmitted at 1 Mbps, the RTS/CTS packets are transmitted at up to 2 Mbps, and the data packets can be sent at up to 11 Mbps. Therefore, no nodes can monopolize the channel. They also found that the transmission and physical carrier sensing ranges are much shorter than the assumptions in simulators and are highly variable depending on weather, place, time and other factors. They showed that the virtual carrier sensing mechanism (RTS/CTS) could not solve all hidden and exposed terminal problems.

Cheung *et al.* [28] compared path loss between 5 GHz 802.11a and 2.4 GHz 802.11b networks through experiments. They did more than 2100 measurements in a townhouse and an office over a period of three months. They found that 802.11a radios suffer much more propagation loss than 802.11b radios because of people walking or path loss through flooring, water, etc. They modeled the deterministic path loss with the following equation:

$$\text{path\_loss}(d) = 20\log_{10}\frac{4\pi d_0}{\lambda} + 10\gamma\log_{10}\frac{d}{d_0},$$

where path loss is in dB, $\lambda$ is wavelength, $d$ is distance, $d_0$ is a reference distance, and the path loss exponent $\gamma$ is 2 or free space. They measured that the best-fit $\gamma$ is 1.9 for line-of-sight distance (1-10 metres), and otherwise 3.7 and 4.6 for 802.11b and 802.11a, respectively.

Yarvis *et al.* [130] deployed a wireless testbed consisting of 6 nodes in three houses, and studied the link quality of 802.11a and 802.11b home networks. They showed that even in small areas like a home there is no guarantee of connectivity among wireless nodes, regardless of transmission power or rate. Wireless links tend to be stable over time, but they are highly asymmetric and have highly variable quality, which seems to be determined by node locations. Although 802.11a and 802.11b show similar characteristics, there is one major difference. The loss rates of 802.11a seem to display quite "binary" behaviour, either very high or very low, while loss rates in 802.11b appear to be uniformly distributed.

Kotz *et al.* [78] measured Wi-Fi networks on the Dartmouth College campus consisting of over 500 802.11b access points and had the following findings. First, their nodes were located at

different floors, i.e., their networks are non-planar. Second, radio ranges were found not to be circular and signal strength varied even in the innermost circles. Third, transmission ranges of wireless nodes had a large variance. Fourth, many asymmetric links existed in the experiments. Fifth, some transmission errors occurred even when mobile clients were in the range of access points. Finally, the experiments showed poor correlation between distance and signal strength. They explained that obstacles in their experimental environments might reflect or attenuate signals. Therefore, simulations that consider three dimensions, asymmetric links, and traces were suggested.

## 2.4 Channel Assignment

WMNs suffer capacity reduction due to many negative factors, such as multi-path fading, link interference and multi-hop packet delivery. For instance, previous research [18, 47] has shown that the end-to-end throughput of individual flows decreases rapidly as node density and the number of hops increases in multi-hop wireless networks.

Fortunately, WMNs have multiple orthogonal (also called non-overlapping) channels that do not interfere with each other and thus can increase the network capacity. For example, IEEE 802.11b has 3 orthogonal channels in the 2.4 GHz spectrum [57], and IEEE 802.11a has 12 orthogonal channels in the 5 GHz spectrum [56]. However, a mesh node usually has fewer radios than the available orthogonal channels due to cost or size constraints. Therefore, channel assignment schemes are necessary for nodes to decide which channels it should tune their radios to and when.

When assigning a channel to a radio, a switch delay is incurred. A radio switching between two channels may cause a delay typically ranging from a few tens of microseconds to a few hundred microseconds [26]. However, current transceiver technology enables radios to switch from one channel to the other within 1μs [44].

Existing research on channel assignment algorithms can be classified in many ways [114]: the systems can have one radio per node [16, 102, 115] or multiple radios per node [2, 106, 107]; the radios can be IEEE 802.11 radios [2] or radios using other protocols [65, 98]; the channel assignment algorithms can be classified into static [2, 106], dynamic [16, 107, 115] or hybrid [81, 127] schemes; and the channel assignment algorithms can also be classified into centralized algorithms [106], coordinated algorithms [107] or localized algorithms [98].

### 2.4.1 Channel Assignment in MANETs

Nasipuri *et al.* [98] proposed a multi-channel CSMA protocol for ad hoc networks, which detects idle channels by carrier sensing and employs a soft channel reservation. In their scheme, each node monitors all channels continuously and puts idle channels into a list. Their protocol selects the channel that was used for the last successful transmission. If that channel is not available, an idle channel will be randomly picked. They showed by simulations that their scheme gives higher throughput than a pure random channel selection scheme when the number of active nodes is large. Later, Jain *et al.* [65] proposed a similar scheme with the differences that they used a control channel for message exchanges and the metric that they used for choosing a channel is based on maximizing the signal-to-interference plus noise ratio at the receiver.

Wu *et al.* [127] proposed a multi-channel MAC protocol with a goal of reducing transmit power and increasing channel reuse. Their protocol includes an on-demand channel assignment scheme that dynamically selects data channels via negotiation on a common control channel between a sender and a receiver. Hung *et al.* [53] proposed a similar two-radio solution that negotiates a free channel via a common control channel and balances the load of all channels.

So *et al.* [115] proposed a multi-channel MAC (MMAC) protocol for wireless ad hoc networks that utilizes multiple channels via only one transceiver per node. Their idea is to divide time into small fixed intervals, with each interval starting with a small window used to negotiate a channel for that interval. Each node keeps a preferable channel list (PCL) that records the usage of channels of the nodes within the transmission range and exchanges PCL to negotiate and switch to the channel with the least scheduled traffic.

Porwal *et al.* [102] proposed an on-demand channel switching (ODC) MAC protocol for ad hoc wireless networks where each node has a single transceiver. Each node counts the traffic received and sent on its current channel during a period and estimates the traffic rate. Their ODC protocol selects channels according to channel traffic conditions and stays at the same channel until its traffic share exceeds a threshold. Their simulations showed that performance varies with the traffic flow distribution and the ODC protocol generally performs better than the MMAC protocol [115].

Kyasanur and Vaidya [81] proposed a hybrid channel assignment scheme for multi-radio wireless networks, in which some radios are statically assigned to fixed channels while others

can switch dynamically between the remaining channels. They suggested that the static radios are selected according to some hash functions or by exchanging messages. However, they didn't give any implementations or experiment results.

Bahl *et al.* [16] proposed a channel assignment scheme for ad hoc networks called Slotted Seeded Channel Hopping (SSCH) that uses only one radio to switch across multiple channels without any modifications on the IEEE 802.11 hardware. In their scheme, time is divided into slots, and each node updates its channel slot schedules and periodically exchanges them with other nodes by broadcasting. Their extensive simulations showed that the scheme significantly improves the capacity in both single hop and multi-hop wireless scenarios.

### 2.4.2 Channel Assignment in WMNs

Raniwala *et al.* [106] proposed a centralized channel assignment algorithm for WMNs, based on the assumption that network traffic can be known by measurement or other methods. Their algorithm first estimates the traffic on each link by aggregated traffic flow and calculates the expected total traffic load on each link. Then the centralized channel assignment algorithm sorts those expected traffic on links and assigns the least-traffic channel to the current highest traffic link and keeps existing connections at the same time. The algorithm estimates the amount of traffic on channels according to channel usage within the interference zone.

Based on their previous centralized algorithms [106], Raniwala *et al.* [105, 107] further proposed two distributed channel assignment schemes for a new WMN architecture called Hyacinth. The goal of their channel assignment in a multi-channel WMN is to switch radios to channels in such a way that the available data rate on the channels can satisfy the traffic loads on the radios. The two distributed algorithms differ in whether a control channel is used. The physical control network [105] uses a dedicated control channel for the control traffic, while the virtual control network [107] uses data channels for both data and control traffic in order to reduce hardware costs. Their load-aware channel assignment problem has two parts: neighbour interface binding and interface channel assignment. Their neighbour interface binding solves the channel dependency problem, i.e., whenever one node tries to change its channel, the nearby nodes may have to change their channels accordingly and cause a ripple effect. To solve this problem, they separated the node NICs into UP-NICs and DOWN-NICs, so that channel changes in DOWN-NICs will not affect UP-NICs. For interface channel assignment, the problem is how

to determine the least-traffic channels around a node. Their algorithm then allows each node to send messages and collect channel usage information in a neighbourhood within $k+1$ hops ($k$ is 2 or 3), which is assumed to include all the potential interfering nodes according to their wireless model. Based on such information, a node can determine the least-traffic-load channel and switch to it.

Adya *et al.* [2] proposed a link layer protocol for WMNs called the Multi-radio Unification Protocol, which from the network layer point of view unifies the two radios of a node as one. Their protocol aims to efficiently use the hard-coded, pre-assigned channels. It monitors the channel quality by using probing messages and measures one-hop round trip time in order to decide which radio/channel to use.

BelAir Networks [18] has a dual-radio mesh design, in which a node has one radio used for client access and the other used for network backbones. A typical channel assignment in such systems uses channels in 2.4 GHz (used by 802.11b/g) for local access and channels in 5 GHz (used by 802.11a) for network backbones.

Das *et al.* [34] proposed a fixed channel assignment scheme for WMNs that uses two integer linear programming models to maximize the number of possible simultaneous transmissions under interference constraints.

Zhu *et al.* [136] proposed a Minimum Interference Channel Selection (MIX) algorithm for cluster-based WMNs. Their WMN is divided into access point clusters, and a common channel is used for all inter-cluster communications. The MIX algorithm is designed for intra-cluster communications so that different clusters can utilize different channels. The MIX algorithm minimizes the co-channel interference in terms of energy.

Ko *et al.* [75] proposed a distributed self-stabilizing channel assignment algorithm for improving the network capacity of wireless mesh networks. They introduced a channel interference cost function that measures the spectral overlapping level between channels. They proved that their algorithm will reach a stable state in a finite number of steps because each node's greedy choice to improve its local objective results in improvement in the global objective of total interference level and eventually leads to channel assignment in which all nodes are satisfied with their channel choice.

Ramachandran *et al.* [103] proposed a centralized breadth-first-search channel assignment algorithm that is performed by a central server which periodically collects dynamically-changing

channel interference information, including the number of interfering radios and channel utilization. In their algorithms, all nodes have one radio tuned on a default channel in order to prevent topology changes.

Avallone *et al.* [13] proposed a centralized channel assignment algorithm for multi-radio wireless mesh networks, called the MCCA (Max-flow-based Centralized Channel Assignment) algorithm, in order to maintain the network connectivity and maximize throughput. Their channel assignment algorithm does not depend on the traffic profile but depends on the criticality of a link, which further depends on the capacity and locations of the links.

Marina *et al.* [92] modelled the channel assignment problem as a topology control problem, which reduces network-wide interference. They showed that the topology control optimization problem is NP-complete and proposed a greedy heuristic channel assignment algorithm, called Connected Low Interference Channel Assignment (CLICA) algorithm, to find connected and low interference topologies based on the connectivity graph and the conflict graph.

Subramanian *et al.* [117] studied the channel assignment problem with a goal of minimizing network-wide interference. They proposed centralized and distributed algorithms for the channel assignment problem that is modelled as a Max $K$-cut problem with interface constraints. The centralized algorithm is based on Tabu search, a popular heuristic search technique designed for graph coloring problems. The distributed algorithm is based on a greedy approximation algorithm for the Max $K$-cut problem in graphs.

Skalli *et al.* [113] proposed a centralized greedy channel assignment algorithm, called Mesh based Traffic and interference aware Channel (MesTiC) assignment. The MesTiC algorithm assigns channels with minimum interference to nodes with highest priority. The priority is based on three factors, including the aggregate traffic of the node, the number of radios of the node and the minimum number of hops to the gateway of the node.

Avonts *et al.* [14] proposed a channel assignment algorithm that is independent of routing and uses only locally distributed information with a goal of minimizing interference. They used weights to indicate the importance of different links, and they showed that the channel assignment problem can become a weighted conflict graph coloring problem that minimizes the number of coloring conflicts.

Shin [111] proposed a distributed heuristic channel assignment algorithm, called SAFE (Skeleton Assisted partition FrEe). The SAFE algorithm uses only local information and is

independent of routing. The idea of SAFE is that it uses distributed random channel assignment while keeping the network connected by using a spanning sub-graph technique.

## 2.5 Routing

In contrast to wired network routing that usually is independent of the lower layers of the network stack, routing in wireless networks often needs cross-layer information. For example, WMNs may achieve higher throughput if routing can take advantage of lower layer information, such as transmit power and bit rates. This section introduces some published routing protocols related to WMNs.

### 2.5.1 Routing in MANETs

Because WMNs and MANETs are both types of wireless ad hoc networks, routing protocols designed for MANETs can also be used in WMNs with minor modifications. For example, Dynamic Source Routing (DSR) [67], Ad Hoc On-Demand Distance Vector routing (AODV) [101], and Destination-Sequenced Distance-Vector routing (DSDV) [99] are the three popular MANET routing protocols, and they can be modified for WMN routing protocols, such as MIT's routing protocol for its Rooftop network [32] and Microsoft's mesh routing protocol [36].

However, routing metrics designed for MANETs usually do not provide high performance in WMNs. One reason is that MANETs need to deal with a mobile environment, where the prime goal is network connectivity, so network throughput and delay are sacrificed as a trade-off. For example, Dube *et al.* [38] found that ad hoc wireless networks suffer from frequent link failures so routing protocols should take into account current link conditions. They proposed a distributed Signal-Stability-based Adaptive routing protocol (SSA) for mobile ad hoc networks. The SSA protocol on-demand selects longer-lived routes based on signal strength and location stability. Since mobility is variable and node location is hard to predict, the SSA protocol adopts signal strength as the criterion, and takes location stability into account only where applicable.

Another reason for the poor applicability of MANET routing strategies in WMN is that MANETs usually have only one radio per node and one channel, but WMNs may have multiple radios per node and multiple channels. In multi-radio networks, some radios (such as 802.11b) have a longer range than others (such as 802.11a), so MANET routing protocols like DSR will choose the radios with longer range to obtain a shorter path (measured by the hop count). Unfortunately, longer-range links usually have worse link quality and may result in lower

throughput.

In addition, one-radio routing algorithms for MANETs do not take channel diversity into account [36]. A path consisting of the same channels (for example, with all links using channel 1) will have significantly worse throughput than a path with a variety of channels (for instance, where every link uses different channels) because of interference.

Therefore, in order to improve network performance, WMNs cannot use the routing metrics of MANETs and need find new metrics.

### 2.5.2 Routing in WMNs

This section reviews routing algorithms that have been proposed for WMNs. In general, routing algorithms may be concerned with throughput, end-to-end delay, load balancing, route robustness, security, etc. For example, wireless links have limited bit rates and some of them can easily be congested in WMNs. By performing load balancing, routing may circumvent network bottlenecks and utilize idle wireless links. Routing robustness provides fault tolerance of path failures and routing security protects routing protocols from attacks. Among these concerns, most routing studies focus on high throughput routing metrics.

Shepard [110] proposed minimum-energy routing for a wireless network which is similar to a WMN. The studied network is a scalable self-organizing multi-hop packet radio network, which is supposed to scale to millions or billions of nodes in a metropolitan area, with each node communicating with its nearby neighbours at a raw rate of hundreds of megabits per second as the system continues to scale. A minimum-energy routing protocol is proposed based on some physical layer models that take interference into account. A network consisting of 1,000 fully connected nodes under a worst-case traffic load (transmitters are busy all the time) was simulated, and all packets could be received. Although minimum-energy routing is important for system performance, Shepard did not show how to find and optimize routes in large-scale networks. Supposing that the 59-64 GHz band is available in the future and spread-code chip rates can be about 2 GHz, Shepard calculated that each node is able to transmit at about 50 Kbps. However, his work did not consider network congestion, so the traffic must be confined to some degree of locality in order to avoid congestion in a large-scale system. It may be necessary to deploy some wired tunnels to solve the congestion problem in real systems.

Raniwala *et al.* [106] proposed and evaluated their channel assignment and routing algorithms

in a multi-channel, multi-hop WMN with standard 802.11 hardware and the multiple NICs of a node operating on non-overlapping channels. They assumed that network traffic can be known by measurement or other methods, and they proposed centralized channel assignment and routing methods for WMNs. Their routing algorithms include shortest path routing that considers link bit rates and least hop-count, and randomized load-balanced multi-path routing, which uses randomization to achieve load-balanced routing. The details of the two routing algorithms are not provided.

Based on their previous centralized algorithms [106], Raniwala and Chiueh [105, 107] proposed two distributed algorithms. Assuming the raw capacity of links is fixed and the link load information can be known, they proposed a load-balancing routing algorithm, which is based on IEEE 802.1D's spanning tree formation algorithm, with changes in the routing metrics. They examined three routing metrics: hop count, gateway link capacity, and path capacity. The gateway link capacity metric supposes that the bottleneck is always the gateway link, but the path capacity metric allows the bottleneck to be any links on the path. They used a special type of packet to prevent route flaps (changing back and forth) caused by the second and third metrics above. The authors also discussed the problem of node failure and recovery and showed that their algorithms could handle these problems correctly. The authors used cross-section goodput of a network as their evaluation metric, which is defined as:

$$X = \sum_{a} \min\left( \sum_{i} C\left(a, g_i\right), B(a) \right),$$

where $C\left(a, g_i\right)$ is the available network throughput between a node $a$ and a gateway $g_i$, and $B(a)$ is the required traffic demand between a node $a$ and the wired network. The definition ensures that the user traffic demand is limited by network transmission ability. They conducted both simulations and experiments and showed that their algorithms could improve throughput about 6 to 7 times higher than a single-channel architecture, even with only 2 NICs per node.

Couto *et al.* [32] use ETX (Expected Transmission Count) as their routing metric to find high-throughput paths in a multi-hop wireless network, where each node has a single 802.11 radio. ETX measures the expected number of transmissions of a packet over a link. To do that, the system must first measure the loss probability in both directions of a link. In 802.11 environments, the 802.11 MAC will retransmit a packet if it is not transmitted successfully, and

the expected number of transmissions depends on the loss rate. For a link from node x to node y, ETX= $1/p$, where $p$ is the probability that packet transmission from node x to node y is successful (including transmission of the data packet and its ACK). The path metric is the sum of the ETX for all links in the path. The routing protocol then chooses the path that has the minimum sum of ETX, which takes into account the total number of hops and link loss rate along the path. ETX assumes packet loss on links is independent of packet size. Experiments showed that ETX can find higher throughput paths than shortest-path routing, but ETX doesn't find optimal paths in a multi-radio scenario [36] because ETX doesn't consider link bit rates and it will prefer shorter paths if loss rates on that path are not significantly higher.

Awerbuch *et al.* [15] designed a routing metric called the Medium Time Metric (MTM) for selecting high throughput paths in multi-rate ad hoc wireless networks. The MTM metric avoids long-distance links that often have the slowest rate, and it prefers shorter, high throughput, and reliable links. The MTM metric is given by:

$$\mathrm{MTM}(\pi_{ij}, p) = \sum_{\forall e \in \pi_{ij}} \tau(e, p),$$

where $\pi_{ij}$ is the path from node $i$ to $j$, and $\tau(e, p)$ is the time required to transmit packet $p$ over edge $e$. They advocated that link information could be obtained from inter-layer communication, so they did not measure or calculate the link transmission time. They observed that routing protocols that use MTM gained up to 17 times improvement in TCP throughput over those using Minimum Hop Count or ETX. The authors argued that the WCETT metric [36] is the combination of their original MTM metric, the ETX metric and its own additional channel diversity metric.

Draves *et al.* [36] proposed a new metric based on Expected Transmission Time (ETT). ETT not only considers the loss rate of a link, but also considers the bit rate of a link, so it performs better than ETX. ETT is defined as $\mathrm{ETT} = \mathrm{ETX} \cdot S / B$, where $S$ is the packet size and $B$ is the bit rate of the link. The path metric is called Weighted Cumulative ETT (WCETT), which combines both ETT and another metric that reflects link diversity in the path. The formula of the routing metric is given by:

$$\mathrm{WCETT} = (1-\beta) \cdot \sum_{i=1}^{n} \mathrm{ETT}_i + \beta \cdot \max_{1 \le j \le k} X_j,$$

where $n$ is the total number of hops, $\beta$ is a tuneable parameter ($0 \le \beta \le 1$) and $\mathrm{ETT}_i$ is the ETT on hop $i$ of the path. The $X_j$ is the sum of the transmission times of the hops on channel $j$ and is given by:

$$X_j = \sum_{\text{Hop } i \text{ is on channel } j} \mathrm{ETT}_i, 1 \le j \le k .$$

where $k$ is the number of channels. They implemented a routing protocol called MR-LQSR, which includes a DSR-like routing protocol and the above WCETT metric. To examine the performance of the MR-LQSR protocol, they set up a testbed consisting of 23 stationary nodes placed inside a 61m×32m office building floor. Their experiments using two 802.11 radios per node show that MR-LQSR takes full advantage of the additional capacity brought by the second radio, and achieves better performance (in terms of throughput) than ETX and shortest-path routing protocols. However, Draves *et al.* did no experiments with more than two radios per node because they found that two or more 802.11g or 802.11a wireless cards in the same node will interfere with one another. Also their testbed was so small that most of the links in the network interfere with others.

The WCETT routing metric captures only the intra-flow interference of a short path but does not reflect the interflow interference. Therefore, Yang *et al.* [129] proposed the Metric of Interference and Channel-switch (MIC), which considers both inter-flow interference and intra-flow interference. The MIC metric of path $p$ is given by:

$$\mathrm{MIC}(p) = \frac{1}{N \cdot \min(\mathrm{ETT})} \sum_{link\ l \in p} \mathrm{IRU}_l + \sum_{node\ h \in p} \mathrm{CSC}_h ,$$

where $N$ is the number of nodes and min(ETT) is the minimum ETT in the network. The $\mathrm{IRU}_l$ denotes the aggregated channel time that link $l$ consumes at its nearby nodes and is given by $\mathrm{IRU}_l = \mathrm{ETT}_l \cdot N_l$, where $N_l$ is the number of nodes that link $l$ interferes with. The $\mathrm{CSC}_h$ favours channel diversity for the intra-flow interference. If the channel assigned for the link of a node is different from its previous link, $\mathrm{CSC}_h = w_1$ and otherwise $\mathrm{CSC}_h = w_2$, where $0 \le w_1 < w_2$.

Jiang *et al.* [66] analyzed intra-flow interference for long paths and proposed the Weighted Cumulative Consecutive Expected Transmission Time (WCCETT) routing metric. The WCCETT metric redefines the $X_j$ in the WCETT metric by:

$$X_j = \sum_{\text{Hop } i \text{ is on segment } j} \text{ETT}_i, 1 \le j \le k,$$

where $k$ is the number of channels, and segment $j$ is defined as the set of hops on channel $j$ that are consecutive and interfere with each other.

Liu *et al.* [88] proposed a high-throughput routing metric for multi-channel, multi-radio and multi-rate WMNs, called the Bottleneck Link Capacity (BLC) routing metric, which is later renamed the Normalized Bottleneck Link Capacity (NBLC) routing metric [89]. The NBLC metric is quite complex and it takes into account link quality, interference, number of hops and traffic load on links. The NBLC metric requires each node to have its radios periodically measure the channel busy time on their current channels. These nodes then broadcast the channel busy time information to their *k*-hop neighbours through a common control channel, where *k* hops are assumed to include all the interfering nodes. Based on the collected channel busy time, each node estimates the Residual Link Capacity (RLC) of its links as the lowest residual channel time. Each node further estimates the Cumulative Expected Busy Time (CEBT) on paths. The CEBT for a link on a path is given by the accumulated ETT values for all the links on the path that are on the same channel and interfere with this link. Finally, the NBLC metric for a path $p$ of $H$ hops is calculated by:

$$\text{NBLC}_p = \min_{link\ l \in p} \left( \frac{\text{RLC}_l}{\text{CEBT}_{l,p}} \right) \cdot \mu^{-H},$$

where $\mu$ is a tuneable parameter. They further developed an on-demand routing protocol called Capacity-Aware Routing (CAR), which selects paths with the maximum NBLC values for nodes.

Bicket *et al.* [23] introduced a routing protocol called Srcr in the MIT Roofnet [95]. Srcr uses source routing to avoid routing loops. Srcr uses the estimated transmission time (ETT) metric, derived from ETX [32] as its routing metric. Each node periodically sends 1500-byte broadcasts at each bit rate and 60-byte broadcasts at 1 Mbps (representing packets and ACKs, respectively). Srcr chooses the lowest ETT value, which indicates the estimated transmission time of that path. Srcr assumes that only one hop can send at a time along the path, which is only reasonable for short routes and tends to underestimate throughput for long routes. The ETT used in Srcr is different from the ETT used in WCETT [36] in that it does not measure link bit rates directly in order to reduce measurement overhead.

Draves *et al.* [35] compared three link-quality routing metrics: ETX, Per-hop Round Trip Time (RTT), and Per-hop Packet Pair Delay (PktPair, which measures the delay between a pair of back-to-back probes) with the minimum hop-count metric in static wireless ad hoc networks via experiments in Microsoft's 23-node static wireless testbed in an office environment. They found that ETX performs best in their testbed. RTT and PktPair introduce load-sensitivity and self-interference and thus perform poorly. The minimum hop-count metric performs best only in a mobile scenario, where it responds to topology changes faster than link-quality metrics.

Biswas and Morris [24] proposed Opportunistic Multi-hop Routing (ExOR), which aims to increase throughput in multi-hop wireless networks. ExOR is special in that it can make use of long range and high loss rate radio links. The basic idea is as follows. The source broadcasts a packet, and some nodes may receive the packet. The protocol discovers which node receives the packet and is closest to the destination, and that node will broadcast the packet. This process continues until the packet reaches the destination. ExOR takes advantage of transmissions that reach unexpectedly far (long progress via lossy links) or unexpectedly short (short progress via reliable links) distances. Their experiments showed a factor of 2 to 4 improvement in throughput when senders and receivers are far apart.

Zhao *et al.* [134] proposed a new cross-layer routing metric called PARMA, which takes into account link speed and channel congestion. To avoid overhead in direct measurement, they estimated channel access delay that reflects the offered traffic at the MAC layer. They assumed the channel to be an M/M/1 queue and calculated the channel access delay as $T_q = T_s \frac{u}{1-u}$, where $u$ is the utilization of the channel, and $T_s$ is the service time. Since the utilization and service time can be observed, the channel access delay estimation is convenient. Their routing metric is packet end-to-end delay $D$, defined as:

$$D = \sum_{\forall links \in path} (T_{Transmit} + T_{access} + T_{queuing}) \approx \sum_{\forall links \in path} (\frac{L_{pkt}}{R_s} + T_{access}),$$

where $L_{pkt}$ is the packet size, $R_s$ is the link speed, so $T_{Transmit} = L_{pkt} / R_s$ is the packet transmission time and $T_{access}$ is estimated by $T_q$. The $D$ metric assumes that the number of transmission is approximately 1, and the queueing delay $T_{queuing}$ is omitted by assuming a low-saturation network. The implementation of PARMA is based on the distance vector routing protocol (DSDV) [99].

By simulations, they showed that PARMA could choose high rate links and avoid congestion.

## 2.6 Transport Layer

An important transport layer protocol for the Internet is the Transmission Control Protocol (TCP), whose main research challenges are congestion avoidance and control algorithms [40, 63]. TCP accounts for a significant amount of Internet traffic. Approximately 95% of the bytes and 90% of the packets on the Internet were found to be transferred using TCP in a 2003 study [70]. Therefore, research on TCP is important in order to improve the performance of WMNs.

An important transport layer research in WMNs is to find an effective and efficient mechanism for TCP to distinguish the reason for packet losses. Wireless links are lossy, and packets may be lost in transmissions instead of congestion. However, since TCP treats all packet losses as resulting from network congestion, it may decrease the sending rate inappropriately, and its throughput may suffer in wireless networks.

Liu *et al.* [87] proposed ad hoc TCP (ATCP), which deals with both route failures and high link loss rates. ATCP inserts an ATCP layer between the TCP and IP layers, and the ATCP layer listens to Explicit Congestion Notification (ECN) messages and "Destination Unreachable" ICMP messages from the network. ATCP enters a persisting state if it receives "Destination Unreachable" messages and will stop sending until a new path is found. ATCP executes a congestion control mechanism if it receives an ECN message.

# CHAPTER 3
# CAPACITY BOUNDS FOR CMESH CELLS

The major task of a CMESH cell is to deliver user packets between user nodes and the gateway. The capacity of a CMESH cell describes how many user packets (in bits) the cell can deliver between each user node and the gateway per second. There are many factors that affect the cell capacity, such as the number of user nodes and their locations, wireless relay node deployment, the number of radios per node, the number of orthogonal channels and their assignment, routing and transmission scheduling.

Research on theoretical cell capacity seeks to find the capacity limit of a CMESH cell, and the possible ways to approach the capacity limit. A basic research question about cell capacity is the following: given $C$ orthogonal channels and $N$ user nodes randomly and uniformly located in a cell of radius $R$, among all the possible schemes of wireless relay node deployment, routing, channel assignment and transmission scheduling, what is the maximum expected throughput that can be guaranteed to each user node?

This question can be extended to arbitrary cells as follows. Given $C$ orthogonal channels and the locations of $N$ user nodes in a cell, among all the possible schemes of wireless relay node deployment, routing, channel assignment and transmission scheduling, what is the maximum throughput that can be guaranteed to each user node?

A city-wide CMESH may consist of thousands of CMESH cells. Random CMESH cells may have independent capacity, if their gateways are spaced with enough distance so that significant mutual interference exists only in border areas. This is because the traffic pattern in a cell is only between user nodes and the gateway; spatial reuse may provide enough extra channel capacity for relatively light accumulated traffic in these border areas.

Existing research on the capacity of wireless networks uses mainly two tools: asymptotic analysis and linear programming. After Gupta and Kumar [47] published their pioneering work on the asymptotic analysis of the capacity of wireless networks, much follow-up research was conducted using this method on wireless networks [12, 73, 82], mobile ad hoc networks [46, 79,

84, 86] and wireless mesh networks [68]. Research using linear programming [7, 64, 77, 119] focuses primarily on the joint optimization of the channel assignment, routing and packet scheduling problems.

It is challenging to use asymptotic analysis and linear programming, however, to answer the above capacity questions for a CMESH cell for two main reasons. First, a typical CMESH cell has tens or hundreds of user nodes, and this scale is too small for asymptotic analysis to reveal network capacity [5]. Second, most analysis using linear programming requires deterministic topologies (or conflict graphs [64]), but the topologies of CMESH cells are partially unknown (the locations of relay nodes, as an important way to increase cell capacity, are unknown).

To answer the above research questions about the capacity of CMESH cells, this chapter introduces a new concept called Channel Transport Capacity (CTC). The CTC describes the ability of a wireless transmitter to use a channel to transmit bits over distance per second. In general, a wireless transmitter can either transmit more bits over shorter distance or fewer bits over longer distance per second. This chapter analyzes how this one-hop channel transport capacity limits multi-hop cell capacity in CMESHs. The main results of this chapter are analytic expressions for capacity bounds for multi-radio, multi-channel, multi-rate, multi-hop and carrier-sense-based cells in CMESHs. The analytic results are validated with simulations.

The remainder of this chapter is organized as follows. The research problem and assumptions are described in Section 3.1. The concept of channel transport capacity and its supply and demand are introduced in Section 3.2. The analytic expressions for upper and lower bounds on the capacity of a single-channel CMESH cell are derived in Section 3.3, and these bounds are extended to multiple channels in Section 3.4. In Section 3.5, the analytic results are validated with simulations. Section 3.6 summarizes the work presented in this chapter.

## 3.1 Problem Formulation

This section states the research problem and assumptions, focusing particularly on a multi-channel, multi-rate and carrier-sense-based wireless model.

### 3.1.1 The System Model and Assumptions

Consider a CMESH cell in a planar area, where one gateway provides Internet access for $N$ user nodes by utilizing $C$ orthogonal channels and omni-directional radios. The gateway has $C$

radios, operating on different channels. Two types of CMESH cells are considered: an arbitrary CMESH cell, where a user node $n$ ($n = 1...N$) is arbitrarily located Euclidian distance $L_n$ from the gateway, and a random CMESH cell, where user nodes are uniformly distributed at random inside a cell of radius $R$ centred at the gateway.

Let $x$ denote the throughput that is achievable by each user node with infinite traffic demand, and cell capacity is defined as the maximum $x$. The goal of this chapter is to find analytic expressions for the upper and lower bounds of cell capacity.

The basic assumption for upper bounds is a multi-channel, multi-rate and carrier-sense-based wireless model, as described in Section 3.1.2. In short, this model says that all radios operating on a channel use a common carrier sense range for all the allowed bit rates on that channel. Another interpretation of this model is that channel transport capacity (see section 3.2) at any bit rates can be recreated after a common channel spatial reuse distance.

A lower bound on cell capacity is given by finding a joint scheme of wireless relay node deployment, routing, channel assignment and transmission scheduling that delivers a certain number of bits between user nodes and the gateway per second. Note that wireless relay node deployment is indispensable in CMESH cells with sparse user nodes to keep the network connected and is an important approach to improve cell capacity. This chapter uses a simple algorithm that achieves throughput close to the upper bounds by adding a sufficient but not necessary condition: for each user node, a few wireless relay nodes are deployed along its straight-line path to the gateway. Cells with dense user nodes may achieve the lower bounds without any wireless relay nodes, because user nodes may play the role of relay nodes. Recall that both user nodes and relay nodes are modem-like wireless outdoor devices under network management (see Section 1.2.2).

Note that the definition of network capacity as the maximum $x$ (equal throughput achievable by each user node) is to provide network-wide fair throughput allocation among user nodes independent of their locations, as required by max-min fairness (see Section 1.2.4 and Section 4.1.3) that maximizes the minimum throughput of user nodes [119].

### 3.1.2 A Multi-Channel, Multi-Rate and Carrier Sense Based Wireless Model

The IEEE 802.11 standards adopt multiple bit rates and a carrier sense multiple access with collision avoidance (CSMA/CA) scheme. This chapter assumes a compatible multi-channel,

multi-rate and carrier-sense-based wireless model.

A carrier-sense-based wireless model is necessary because the carrier sense range/threshold introduces the inherent exposed terminal problem [21], which is not modeled by the existing protocol model and physical model [47]. Thus, the two existing models may overestimate the capacity of carrier-sense-based CMESH cells.

This wireless model can also be interpreted as a multi-rate extension to the wireless model in traditional cellular networks: if two transmitters on the same channel are spaced with enough distance (no less than a common spatial reuse distance $D$ for all the channels, as given below), then they can successfully send packets to their own receivers that are within the transmission range at a certain transmission rate without interfering with each other; higher transmission rates have reduced transmission ranges.

The multi-channel, multi-rate and carrier-sense-based wireless model is as follows. Let the set $\{w_{ki} \mid i = 1...m_k\}$ denote all the $m_k$ allowed bit rates on orthogonal channel $k$, $k = 1...C$ and the set $\{d_{ki} \mid i = 1...m_k\}$ denote the corresponding transmission ranges (the maximum transmission distance). The wireless model requires that all radios on channel $k$ use a common carrier sense range $D_k$, so that on channel $k$:

1) a transmitter defers its transmission if there are other active transmitters within $D_k$;

2) otherwise, it can successfully send bits to a receiver at any bit rate $w_{ki}$ if only the receiver is within $d_{ki}$.

The wireless model can be derived from a propagation model and an interference model. The rest of this section gives the derivation for an arbitrary channel $k$, so $k$ in subscripts is omitted for brevity.

Assume that all radios follow the following propagation model for the received signal power $P_{rx}$:

$$P_{rx} = M \cdot P_{tx} / r^{\gamma}, \tag{3.1}$$

where $P_{tx}$ is transmit power, $M = G_{tx} G_{rx} \lambda^2 / (4\pi)^2$ in the free space model (see Section 2.2.1) and $M = (h_{tx} h_{rx})^2 G_{tx} G_{rx}$ in the plane earth model, $r$ is the distance between the transmitter and the receiver and $\gamma$ is the path-loss coefficient, typically ranging from 2 to 4. In the above two

formulas for $M$, $\lambda$ is the wavelength, $G_{tx}$ and $h_{tx}$ are the power gain and the effective height of the transmitter's antenna, respectively; $G_{rx}$ and $h_{rx}$ are the power gain and the effective height of the receiver's antenna, respectively.

Let SINR denote signal to interference and noise ratio. It can be calculated as:

$$\text{SINR} = \frac{P_{rx}}{P_N + \sum_{f=1}^{K} P_f}, \tag{3.2}$$

where $P_f$ is the interference power contributed by an interfering radio $f$ that is concurrently transmitting on the same channel, $K$ is the total number of these interfering radios, and $P_N$ is the noise power including thermal noise and noise from other sources.

Let $d_i$ denote the transmission range for bit rate $w_i$, $i = 1...m$. By Equation (3.1), $d_i$ is calculated as:

$$d_i = \left(M \cdot P_{tx} / X_i\right)^{1/\gamma}, \tag{3.3}$$

where $X_i$ is the receiver sensitivity threshold for bit rate $w_i$.

Assume that a receiver can decode a signal at bit rate $w_i$ correctly if the following two requirements are met:

$$\begin{cases} P_{rx} \geq X_i \ \ (\text{i.e.}, r \leq d_i) \\ \text{SINR} \geq \text{SINR}_i, \end{cases} \tag{3.4}$$

where $\text{SINR}_i$ is the SINR threshold for bit rate $w_i$.

First, consider the single interfering radio model, which has only one interfering radio. In Figure 3.1, transmitter TX is located distance $r$ from receiver RX, and the interfering radio TX1 is located distance $I$ from RX. Ignoring $P_N$, the SINR at RX is given by:

$$\text{SINR} = \left(I/r\right)^{\gamma}. \tag{3.5}$$

To satisfy the SINR requirement and prevent the hidden terminal problem [121], Zhu *et al.* [135] showed that the carrier sense range $D_i$ for bit rate $w_i$ in the single interfering radio model can be set to:

$$D_i = d_i(1 + \text{SINR}_i^{1/\gamma}). \tag{3.6}$$

Zhai and Fang [133] found that $D_i$ does not change much in IEEE 802.11 networks because a larger $w_i$ requires a larger $\text{SINR}_i$ and $X_i$ (and thus a smaller $d_i$). In addition, they found that multiple carrier sense ranges may introduce additional collisions that may cause the failure of the carrier sense scheme. Therefore, a common carrier sense range $D$ is recommended for all bit rates and can be set to:

$$D = \max\{D_i \mid i = 1...m\}. \tag{3.7}$$

If there are multiple interfering radios, $D$ can be set to larger values, including those associated with the worst scenarios [74, 133].

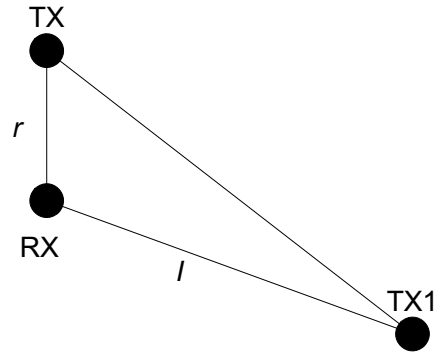


Figure 3.1: Single interfering radio model

In conclusion, on a multi-rate channel it is theoretically feasible to derive a common carrier sense range $D$, which allows a transmitter to successfully send data at any bit rate whose transmission range can reach the receiver if there are no other active transmitters within distance $D$ on the channel, as described by the assumed wireless model. Note that the common carrier sense range $D$ can also be interpreted as a channel spatial reuse distance: after the channel reuse spatial distance $D$, channel transport capacity (see section 3.2) at any bit rates can be recreated.

### 3.2 Channel Transport Capacity (CTC): Supply and Demand

This section introduces a new notion called Channel Transport Capacity (CTC), and then introduces its supply (CTCS) and demand (CTCD).

Gupta and Kumar [47] proposed Network Transport Capacity (NTC). Given $p$ source-destination pairs $(S_1, T_1),...,(S_p, T_p)$ and a vector of feasible rates for these pairs $\vec{x} = (x_1, x_2, ..., x_p)$,

$$\text{NTC} = \max\left\{\sum_i (|S_i T_i| \cdot x_i) \mid All\ \ feasible\ \vec{x}\right\}, \tag{3.8}$$

where $|S_i T_i|$ is the Euclidian distance between $S_i$ and $T_i$.

This chapter shows that the network's transport capacity (NTC) is constrained by the channels' transport capacity (CTC) in CMESH cells. Section 3.2.2 shows that NTC is related to a special case of CTCD. Note that BDiP [133], which is defined as the product of the data rate and the hop distance at a hop (note: NOT transmission range), is none of CTC, CTCS or CTCD.

### 3.2.1 Channel Transport Capacity Supply

The CTC of a channel describes the ability of the channel operated by a transmitter to transport bits over distance per second over a single link.

Recall that set $\{w_{ki} \mid i = 1...m_k\}$ includes all the bit rates allowed on channel $k$, $k = 1...C$. Let $\text{CTC}_{ki}$ be defined as the product of $w_{ki}$ and its transmission range $d_{ki}$:

$$\text{CTC}_{ki} = w_{ki} \cdot d_{ki},\ i = 1...m_k. \tag{3.9}$$

The maximum CTC of channel $k$, denoted by $c_k$, is the maximum $\text{CTC}_{ki}$ on channel $k$ and thus is given by:

$$c_k = \max\{w_{ki} \cdot d_{ki} \mid i = 1...m_k\}. \tag{3.10}$$

Let $(w_{kc}, d_{kc})$ denote the pair of $(w_{ki}, d_{ki})$ that has $w_{ki} d_{ki} = c_k$. If there are multiple such pairs whose $d_{ki}$ are $d_{kc1}, d_{kc2,}..., d_{kcn}$, then $d_{kc}$ is chosen as $\min\{d_{kc1}, d_{kc2,}..., d_{kcn}\}$ and $w_{kc} = c_k / d_{kc}$. Thus, $w_{kc}$ is the maximum bit rate among all the $w_{ki}$ in these pairs.

The channel transport capacity supply (CTCS) of multiple orthogonal channels in a CMESH cell area describes the maximum ability of these channels operated by transmitters inside the CMESH cell area to transport some bits over some distance per second. Define $\text{CTCS}_{ki}$ of channel $k$ at bit rate $i$ as:

$$\text{CTCS}_{ki} = u_k w_{ki} d_{ki},\ i = 1...m_k, \tag{3.11}$$

where $u_k$ is a spatial reuse factor (recall that a common $D_k$ is used for all bit rates on channel $k$). The maximum $\text{CTCS}_{ki}$ of channel $k$ is defined as $\text{CTCS}_k$: $\text{CTCS}_k = u_k c_k$.

Because orthogonal channels do not interfere with each other, the CTCS of $C$ orthogonal channels is defined as the sum of $\text{CTCS}_k$ :

$$\text{CTCS} = \sum_{k=1}^{C} (u_k c_k) \tag{3.12}$$

### 3.2.2 Discussion of the Maximum CTC

This section discusses the maximum CTC, i.e., $c_k$ , for an arbitrary channel $k$, so $k$ in the subscripts is omitted for brevity.

The wireless model in Section 3.1.2 assumes that CTC at any bit rate can be recreated after a fixed spatial reuse distance (or the common carrier sense range) $D$. In a single interfering radio model, $D$ limits the noise level at a receiver, and thus limits the transmission range at a bit rate. The following proposition reveals the relation of Shannon's channel capacity and $D$ to the maximum CTC, i.e., $c$ , in the single interfering radio model.

**Proposition 1**. For the propagation model and the single interfering radio model in Section 3.1.2, if $D$ is fixed, then $c$ exists and there is a unique $(w_c, d_c)$ pair that gives $c = w_c \cdot d_c$.

Proof. According to Shannon's channel capacity formula, the bit rate $w$ on a channel of bandwidth $B$ (e.g., 20 MHz in IEEE 802.11a) is given by:

$$w = B \cdot \log_2(1 + \text{SINR}). \tag{3.13}$$

Let $r$ denote the distance between the transmitter and the receiver and let $d$ denote the transmission range at bit rate $w$. Because the carrier sense range $D$ is fixed and given, the nearest possible simultaneous transmitter is $D - r$ away from the receiver, and the SINR in this case is $\text{SINR} = (D - r)^{\gamma} / r^{\gamma}$. Recall that $\gamma$ is the path-loss coefficient. Because the transmission range $d$ need take this worst case into account, CTC at bit rate $w$ is:

$$\text{CTC} \triangleq w \cdot d = B \cdot \log_2\left(1 + \left(\frac{D}{d} - 1\right)^{\gamma}\right) \cdot d. \tag{3.14}$$

Thus, $c$ is given by:

$$c \triangleq \max(\text{CTC}) = B \cdot \log_2\left(1 + \left(\frac{D}{d_c} - 1\right)^{\gamma}\right) \cdot d_c, \tag{3.15}$$

where $d_c$ is given by:

$$d_c = \arg\max_d(c) = \arg\max_d\left(\log_2\left(1+\left(\frac{D}{d}-1\right)^{\gamma}\right)\cdot d\right), \tag{3.16}$$

and $w_c$ is given by $w_c = c/d_c$. □

Let $V(\text{CTC})$ be the variable part of CTC, given by:

$$V(\text{CTC}) = \frac{\text{CTC}}{BD} = \log_2\left(1+\left(\frac{1}{(d/D)}-1\right)^{\gamma}\right)(d/D). \tag{3.17}$$

The behaviour of $V(\text{CTC})$ is shown in Figure 3.2, where $d_c$ is approximately located at $D/4$ ($d/D$ equals 0.241, 0.223 and 0.219 for $\gamma$=2, 3 and 4, respectively).

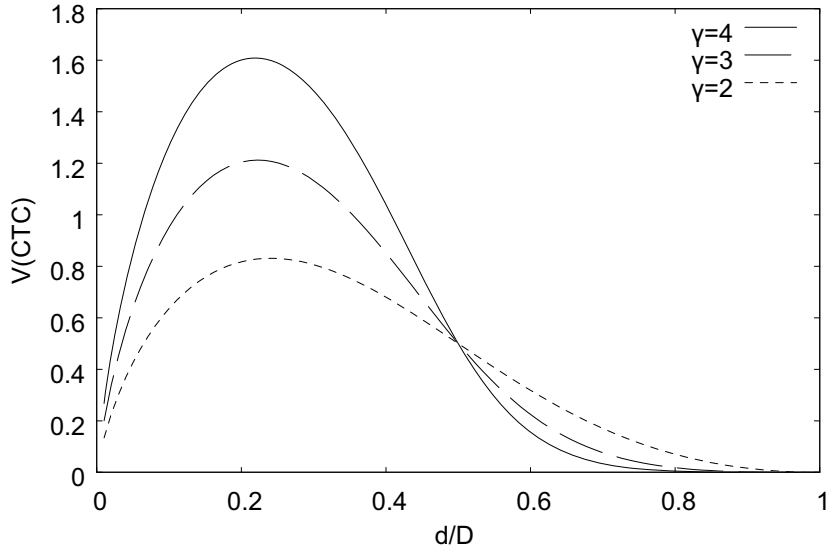


Figure 3.2: Locating $d_c$ when $D$ is fixed

For real wireless transmissions, the value of $c$ will be bounded because $P_{tx}$, $B$, $RX_{th}$ and $P_N$ (at least white Gaussian noise) are all bounded (larger than 0 and smaller than a finite value). Then, from Equation (3.3), the maximum transmission distance $d$ exists, so $0 < d \le \max(d)$; from Equation (3.2) and Equation (3.13) the maximum bit rate $w$ exists, so $0 < w \le \max(w)$, and thus $0 < c = \max(w \cdot d) \le \max(w) \cdot \max(d)$, is also bounded.

### 3.2.3 Channel Transport Capacity Demand

The Channel Transport Capacity Demand (CTCD) of a CMESH cell in its entire cell area describes the demand for the transmitters in the CMESH cell to use channels to transport bits over links/hops along paths between user nodes and the gateway per second in order to achieve throughput $x$ per user node.

For user node $n$ ( $n \in 1...N$ ) to achieve throughput $x$ via $P_n$ sub-paths, where subpath $p$, $p \in P_n$ has a path length $\tilde{L}_{np}$ and throughput $x_{np}$, CTCD is defined as:

$$\text{CTCD} = \sum_{n=1}^{N} \sum_{p=1}^{P_n} \left( x_{np} \cdot \tilde{L}_{np} \right) \tag{3.18}$$

As a special case, if user node $n$ ( $n = 1...N$ ) achieves throughput $x$ via a straight-line path whose length is $L_n$, then this CTCD, denoted by $\text{CTCD}_\text{L}$, is given by:

$$\text{CTCD}_\text{L} = x \sum_{n=1}^{N} L_n . \tag{3.19}$$

The straight-line paths are the shortest paths between user nodes and the gateway, so $\text{CTCD}_\text{L} \le \text{CTCD}$. Note that the $\text{CTCD}_\text{L}$ in the entire network area is equal to the NTC in Equation (3.8) with all rates set to $x$ and all destinations set to the gateway.

The CTCD of a CMESH cell in a network (sub)area is also defined by Equation (3.18) except that $\tilde{L}_{np}$ becomes the length of the part of user node $n$'s sub-path $p$ whose transmitters are inside the network (sub)area.

**Lemma 1**. If a CMESH cell has a network (sub)area that allows no spatial reuse for any orthogonal channels, then any achievable CTCD of the CMESH cell in the (sub)area is no more than the CTCS of these channels in the (sub)area.

Proof. Define a transmission in this proof as the process that is continuous in time and during which a certain transmitter sends bits to a certain receiver over a certain wireless link that has a constant distance and a constant bit rate. If CTCD is achievable in a network (sub)area in a CMESH cell, there exists a joint wireless relay node deployment, routing, channel assignment and transmission schedule scheme that activates a set of transmissions per time unit, denoted by $S_T$. The transmitters in $S_T$ are inside the network (sub)area and the sum of their bit-distance products is CTCD.

Consider channel $k$. Let $S_k$ denote all the transmissions using channel $k$ in $S_T$. Let $w_j$, $d_j$ and $t_j$ denote the bit rate, distance and duration time of transmission $j$, $j \in S_k$, respectively. Without spatial reuse in the network (sub)area, the transmitters of the transmissions in $S_k$ have to transmit one by one, so $\sum_{j \in S_k} t_j \le 1$. Let $\mathrm{CTCD_k}$ denote the part of CTCD produced by the transmissions in $S_k$, and:

$$\mathrm{CTCD_k} = \sum_{j \in S_k} (t_j \cdot w_j \cdot d_j) \le \sum_{j \in S_k} (t_j \cdot c_k) \le c_k \cdot \sum_{j \in S_k} t_j \le c_k .$$

Because spatial reuse is not allowed in the network (sub)area for all channels, $u_k = 1$. Furthermore, because orthogonal channels do not interfere with each other:

$$\mathrm{CTCD} = \sum_{k=1}^{C} \mathrm{CTCD_k} \le \sum_{k=1}^{C} c_k = \sum_{k=1}^{C} (u_k \cdot c_k) = \mathrm{CTCS} \,\square$$

### 3.3 Capacity Bounds for Single-Channel CMESH Cells

In this section, capacity bounds for a single-channel CMESH cell are derived, so $k$ in subscripts is omitted for brevity.

Let $w_{\max}$ denote the maximum bit rate among all $w_i$, $i = 1...m$. Then the cell capacity has an upper bound $\hat{x}_W$:

$$\hat{x}_W = w_{\max} / N . \tag{3.20}$$

In multi-hop scenarios, $\hat{x}_W$ can be very loose, but it works as a supplement to the other upper bounds derived in this section. Let $\hat{x}_{down}$ denote the downstream cell capacity (from the gateway to user nodes).

#### 3.3.1 Downstream Capacity for Arbitrary CMESH Cells

Recall that in arbitrary CMESH cells, user nodes are arbitrarily located, and the Euclidian distance between user node $n$ ($n = 1...N$) and the gateway is $L_n$.

For the downstream traffic, the following theorem holds.

**Theorem 1**. In an arbitrary CMESH cell, the $\hat{x}_{down}$ has an upper bound $x_U$:

$$\hat{x}_{down} \le x_U , \tag{3.21}$$

where $x_U = \dfrac{c}{\sum_{L_n < D/2} L_n + \sum_{L_n \ge D/2} (D/2)}$.

Note that in the above expression $L_n < D/2$ (or $L_n \ge D/2$) below the summation symbol means user node $n$ whose $L_n < D/2$ (or $L_n \ge D/2$).

Proof. Let $A_G$ denote the area enclosed by the circle (with the circle itself removed) of radius $D/2$ centred at the gateway (see Figure 3.4). Let $S_G$ and $N_G$ denote the set and the number of user nodes located inside $A_G$, respectively.

In downstream scenarios, for any wireless relay node deployment, routing and transmission scheduling schemes, the CTCD inside $A_G$ has $\text{CTCD} \ge x \sum_{n \in S_G} L_n + x\left(N - N_G\right) D/2$. Because spatial reuse is impossible inside $A_G$ ($u = 1$), the CTCS inside $A_G$ is $c$. By Lemma 1, $\text{CTCD} \le c$. Thus (3.21) is derived. □

**Theorem 2**. If every user node has $L_n < D/2$, then by deploying no more than $\lceil L_n / d_c \rceil - 1$ wireless relay nodes for each user node, there is an algorithm that guarantees:

$$\hat{x}_{down} \ge x_N , \tag{3.22}$$

where $x_N = \dfrac{c}{d_c \sum_n \lceil L_n / d_c \rceil}$.

If $L_n / d_c = \lceil L_n / d_c \rceil$, the lower bound reaches the upper bound in Theorem 1, i.e., $x_N = x_U$.

Proof. Let $\overrightarrow{ab}$ denote the directional line segment that starts at node or location $a$ and ends at $b$. Let $G$ denote the gateway. For each user node $n$, the wireless relay node deployment scheme deploys $h_n - 1$ ($h_n = \lceil L_n / d_c \rceil$) wireless relay nodes to a straight-line path on $\overline{Gn}$ consisting of $h_n$ links of bit rate $w_c$ and length $d_c$, except the last link at user node $n$ whose length is no more than $d_c$. There are a total of $h = \sum_n h_n$ links.

The transmission scheduling scheme is as follows. For each time unit, let each user node $n$ ($n = 1...N$) activate its links one by one along path $\overrightarrow{Gn}$, with each transmission lasting $1/h$ time

unit. Because $h(1/h)=1,$ the transmission scheme is schedulable.

This algorithm achieves per user node throughput:

$$x_N = \frac{w_c}{\sum_n h_n} = \frac{w_c d_c}{d_c \sum_n \lceil L_n / d_c \rceil} = \frac{c}{d_c \sum_n \lceil L_n / d_c \rceil}.$$

If $L_n/d_c = \lceil L_n/d_c \rceil,$

$$x_N = \frac{c}{d_c \sum_n \lceil L_n/d_c \rceil} = \frac{c}{\sum_n L_n} = x_U \,.\ \square$$

Next, define symmetrical user node locations as follows. In a polar coordinate system where the gateway is located at $(0,0)$, user nodes are said to be symmetrically located if whenever there is a user node located at $(r,\beta)$, there is another user node located at $(r,\beta+\pi)$. In this case, the following theorem holds.

**Theorem 3**. If user nodes are symmetrically located around the gateway, then by deploying no more than $\lceil L_n/d_c \rceil - 1$ wireless relay nodes for each user node, there is an algorithm that guarantees:

$$\hat{x}_{down} \geq x_E \,, \tag{3.23}$$

where $x_E = \dfrac{c}{d_c\left(\sum\limits_{L_n<(D+d_c)/2}\left\lceil \dfrac{L_n}{d_c}\right\rceil + \sum\limits_{L_n\geq(D+d_c)/2}\left\lceil \dfrac{D+d_c}{2d_c}\right\rceil\right)}.$

If $(D+d_c)/(2d_c) = \lceil (D+d_c)/(2d_c) \rceil$ and the user nodes with $L_n < (D+d_c)/2$ have $L_n/d_c = \lceil L_n/d_c \rceil$, then as $d_c \to 0$, the lower bound approaches the upper bound in Theorem 1, i.e., $x_E \to x_U$.

Proof. Let $A_E$ denote the area enclosed by the circle of radius $(D+d_c)/2$ centred at the gateway (with the circle itself removed). Let $S_E$ and $N_E$ denote the set and the number of user nodes located inside $A_E$, respectively.

For each user node $n$, the relay node deployment scheme deploys relay nodes on a straight-line path on $\overline{Gn}$ so that inside $A_E$ user node $n$ has $\lceil L_n/d_c \rceil$ ( $n \in S_E$ ) or $\lceil (D+d_c)/(2d_c) \rceil$

( $n \notin S_E$ ) links of rate $w_c$ and length $d_c$ except the last link. Thus, there are a total of $h = \sum_{n \in S_E} \lceil L_n / d_c \rceil + (N - N_E) \lceil (D + d_c)/(2d_c) \rceil$ links inside $A_E$. In each time unit, the transmission scheduling scheme activates the $h$ links inside $A_E$ once, one by one, with each transmission lasting $1/h$ time unit. Because $h(1/h) = 1$, the transmission scheme inside $A_E$ is schedulable.

Next, the following shows that while the links inside $A_E$ are activated once, all the links outside $A_E$ on the paths of all user nodes can be simultaneously activated once, with each transmission lasting $1/h$ time unit. The spatial reuse pattern for the user nodes on any straight line passing $G$ is shown in Figure 3.3, where the user nodes activate their links in two steps: the first step for the transmitters on the grey arrows and the second step for the transmitters on the black arrows, each arrow with a length $(D + d_c)/2$. The grey arrow marked as $\overrightarrow{Gc}$ in Figure 3.3 is also shown as $\overrightarrow{Gc}$ in Figure 3.4, which has $\lceil (D + d_c)/(2d_c) \rceil$ hops. In Figure 3.4, $\overrightarrow{Ga}$ is the first hop and $\overrightarrow{bc}$ is the last hop on the grey arrow $\overrightarrow{Gc}$ in Figure 3.3. Also in Figure 3.4, $\overrightarrow{de}$ is the first hop on the grey arrow $\overrightarrow{dz}$ in Figure 3.3. Note that $\overrightarrow{Ga}$ and $\overrightarrow{de}$ both have a length $d_c$, but $\overrightarrow{bc}$ may have a length shorter than $d_c$ since it is the last hop.

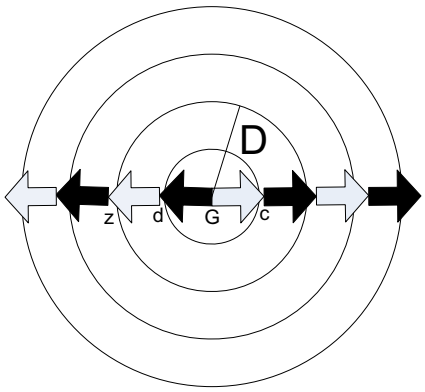


Figure 3.3: Downstream spatial reuse pattern for symmetrical topology
(see Figure 3.4 for the hops $\overrightarrow{Ga}$, $\overrightarrow{bc}$ and $\overrightarrow{de}$ on the two marked grey arrows $\overrightarrow{Gc}$ and $\overrightarrow{dz}$)

The following proves that while all links at the hop $\overrightarrow{bc}$ are activated once, all links at the hop $\overrightarrow{de}$ can be activated once simultaneously. Notice that:

1) User nodes are symmetrically located and the length of $\overrightarrow{Gb}$, denoted by $|Gb|$, is less than $|Gd|$, so the number of links (also transmissions) on $\overrightarrow{bc}$ is no less than on $\overrightarrow{de}$.

2) With a queue of size $w_c / h$ bits at each relay node, in stable states, $w_c / h$ bits can be sent by a sender and stored by a receiver.

3) $|Gb| \geq (D - d_c)/2$, so $|bd| \geq D$ and thus transmitters at $b$ and $d$ can transmit simultaneously.

Because of 1), 2) and 3), during the time period that the links on $\overrightarrow{bc}$ are activated once, the links on $\overrightarrow{de}$ can also be activated once.

Similarly, all links outside $A_E$ on the paths of all user nodes can be activated once while all links inside $A_E$ are activated once. Thus each user node achieves throughput $x = w_c / h = x_E$.

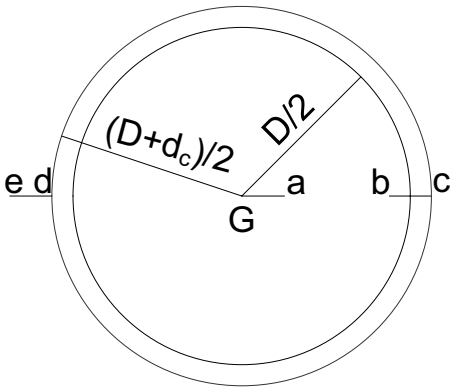


Figure 3.4: Transmission schedule for symmetrical topology
($\overrightarrow{Ga}$ is the first hop and $\overrightarrow{bc}$ is the last hop on $\overrightarrow{Gc}$, and $\overrightarrow{de}$ is the first hop on $\overrightarrow{dz}$, where $\overrightarrow{Gc}$ and $\overrightarrow{dz}$ are the two marked grey arrows in Figure 3.3)

As $d_c \to 0$, $S_E \to S_G$ and $N_E \to N_G$. Further if user nodes inside the area $A_E$ have $L_n / d_c = \lceil L_n / d_c \rceil$ and $\lceil (D + d_c)/(2d_c) \rceil = (D + d_c)/(2d_c)$, $x_E$ has:

$$x_E = \frac{c}{\sum_{n \in S_E} L_n + (N - N_E)(D + d_c)/2} \to \frac{c}{\sum_{n \in S_G} L_n + (N - N_G) D/2} = x_U . \square$$

In some areas such as corridors or highways, all nodes are deployed approximately on a line with the gateway at one end. In this case, the following theorem holds.

**Theorem 4**. If user nodes are located on a line with the gateway at one end, then by deploying no more than $\lceil L_n/d_c \rceil - 1$ wireless relay nodes for each user node, there is an algorithm that guarantees:

$$\hat{x}_{down} \geq x_D, \tag{3.24}$$

where $x_D = \dfrac{c}{d_c(\sum_{L_n<D} \lceil L_n / d_c \rceil + \sum_{L_n \geq D} \lceil D / d_c \rceil)}$.

Proof. The proof is similar to the proofs of Theorems 2 and 3. Let $A_D$ denote the area enclosed by the circle of radius $D$ centred at the gateway (with the circle itself removed). Let $S_D$ and $N_D$ denote the set and the number of user nodes located inside $A_D$, respectively.

For each user node $n$, the wireless relay node deployment scheme deploys relay nodes on a straight-line path on $\overline{Gn}$ so that inside $A_D$ user node $n$ has $\lceil L_n/d_c \rceil$ ($n \in S_D$) or $\lceil D/d_c \rceil$ ($n \notin S_D$) links of rate $w_c$ and length $d_c$ except the last link. Thus, there are a total of $h = \sum_{n \in S_D} \lceil L_n / d_c \rceil + (N - N_D)\lceil D / d_c \rceil$ links inside $A_D$.

In each time unit, the transmission scheduling scheme activates the $h$ links inside $A_E$ once, one by one, with each transmission lasting $1/h$ time unit. Because $h(1/h) = 1$, the transmission scheme inside $A_D$ is schedulable. Next, the following shows that all the links outside $A_D$ on the paths of all user nodes can be activated once simultaneously during the time period that the links inside $A_D$ are activated once, with each transmission lasting $1/h$ time unit. The spatial reuse pattern for the user nodes on the line is shown in Figure 3.5, where each arrow has a length $D$ and contains $\lceil D/d_c \rceil$ hops. The two arrows $\overrightarrow{Gc}$ and $\overrightarrow{cf}$ in Figure 3.5 are also shown as $\overrightarrow{Gc}$ and $\overrightarrow{cf}$ in Figure 3.6. In Figure 3.6, $\overrightarrow{Ga}$ is the first hop and $\overrightarrow{bc}$ is the last hop on $\overrightarrow{Gc}$. Also in Figure 3.6, $\overrightarrow{cd}$ is the first hop and $\overrightarrow{ef}$ is the last hop on $\overrightarrow{cf}$. Note that $\overrightarrow{Ga}$ and $\overrightarrow{cd}$ both have a length $d_c$, but $\overrightarrow{bc}$ and $\overrightarrow{ef}$ may have a length shorter than $d_c$ since they are the last hops.

In Figure 3.6, because $|Gc| \geq D$, transmitters $G$ and $c$ can transmit simultaneously. Further because the number of links (also transmissions) on $\overrightarrow{Ga}$ is no less than on $\overrightarrow{cd}$, while the links on $\overrightarrow{Ga}$ are activated once, the links on $\overrightarrow{cd}$ can also be activated once.

Similarly, all links outside $A_D$ on the paths of all user nodes can be simultaneously activated once while the links inside $A_D$ are activated once, and thus each user node achieves throughput $x = w_c / h = x_D$ .□

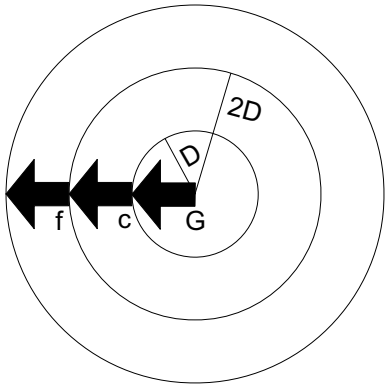


Figure 3.5: Downstream spatial reuse pattern for line topology
(see Figure 3.6 for the hops $\overrightarrow{Ga}$, $\overrightarrow{bc}$, $\overrightarrow{cd}$ and $\overrightarrow{ef}$ on the two marked arrows $\overrightarrow{Gc}$ and $\overrightarrow{cf}$ )

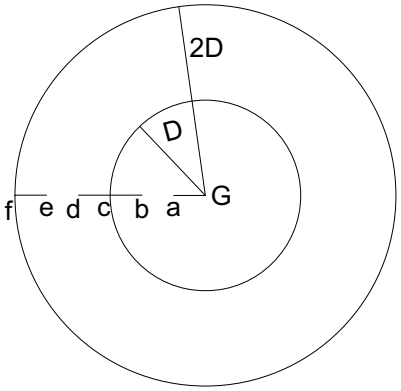


Figure 3.6: Transmission schedule for line topology
( $\overrightarrow{Ga}$ is the first hop and $\overrightarrow{bc}$ is the last hop on $\overrightarrow{Gc}$, and $\overrightarrow{cd}$ is the first hop and $\overrightarrow{ef}$ is the last hop on $\overrightarrow{cf}$, where $\overrightarrow{Gc}$ and $\overrightarrow{cf}$ are the two marked arrows in Figure 3.5)

The above analyzes two extreme cases of user node topology: the case of symmetrical topology and the case of line topology (the most highly asymmetrical topology). The following discusses the general lower bound for arbitrary CMESH cells. A general lower bound for an arbitrary CMESH cell is $x_D$ because $\hat{x}_{down} \geq x_D$ holds for arbitrary user node locations. However,

for most CMESH cells, the lower bound $x_D$ can be very loose. Theorem 3 suggests that if the wireless relay node deployment scheme constructs a symmetrical path consisting of two sub-paths for each user node and the traffic of each user node is split equally onto the two sub-paths, $x_E$ can be a much tighter lower bound:

$$\hat{x}_{down} \geq x_E , \tag{3.25}$$

where $x_E = \dfrac{c}{d_c\left(\sum_{L_n<(D+d_c)/2}\left\lceil\dfrac{L_n}{d_c}\right\rceil + \sum_{L_n\geq(D+d_c)/2}\left\lceil\dfrac{D+d_c}{2d_c}\right\rceil\right)}$.

If $L_n/d_c = \lceil L_n/d_c \rceil$, $(D+d_c)/(2d_c) = \lceil (D+d_c)/(2d_c) \rceil$, then as $d_c \to 0$, $x_E \to x_U$.

The proof of this result is omitted because the two sub-path scheme shown in Figure 3.7 is clearly impractical: it needs to deploy too many relay nodes and occupy too large areas in order to achieve the lower bound $x_E$.

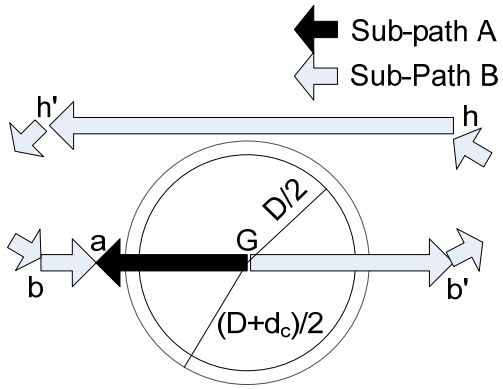


Figure 3.7: The two sub-path scheme for arbitrary topology
(For a user node outside $A_E$ located at $a$, sub-path A is the line segment from $G$ to $a$, and sub-path B is a "flat" curve from $G$ along $b'$, $h$, $h'$ and $b$ to $a$)

The following is a simple explanation of the two sub-path scheme. Each user nodes inside $A_E$ (recall: the area inside the circle of radius $(D+d_c)/2$ centred at the gateway) sets up a single straight-line path. As shown in Figure 3.7, user node $n$ outside $A_E$ located at $a$ sets up two sub-paths: sub-path A from $G$ to $a$ and sub-path B from $G$ along $b'$, $h$, $h'$ and $b$ to $a$. User node $n$ sends $x_E/2$ traffic onto each of its sub-paths. The spatial reuse pattern is similar

to Figure 3.3, where the links on the two sub-paths of user node $n$ are activated in two steps, denoted by a grey arrow $s1$ and a black arrow $s2$. Let $|s1|$ and $|s2|$ denote the lengths of $s1$ and $s2$, so $|s1| = |s2| = (D + d_c)/2$. Because $|s1| + |s2| = D + d_c > D$, if $s1$ and $s2$ on the sub-path B are designed to be similar in shape to two line segments, then $s1$ and $s2$ can alternate (i.e., $s1, s2, s1, s2, \ldots$), and the links on the paths of user node $n$ outside $A_E$ can be activated simultaneously with the links inside $A_E$, once for each link. Similar to the proof of Theorem 3, this scheme allows each user node to achieve throughput $x_E$.

This result indicates that for asymmetric user node locations including the line topology in Theorem 4, some wireless relay node deployment and routing schemes can make $x$ closer to $x_E$. Thus, for arbitrary user node locations, $x$ is achievable between $x_E$ and $x_D$.

### 3.3.2 Downstream Capacity for Random CMESH Cells

Recall that in random CMESH cells, user nodes are randomly located following a uniform distribution inside the circular area of radius $R$ ($R > 0$) centred at the gateway. This model may be natural because the user nodes active during a certain period of time usually are randomly located, even if the locations of residential houses are not random, e.g., in a grid pattern.

The following two corollaries provide expected downstream capacity bounds for a random CMESH cell, which may be used to estimate cell capacity.

**Corollary 1**. If user nodes are randomly located following a uniform distribution inside a CMESH cell of radius $R$ ($R < D/2$) centred at the gateway,

1) the $\hat{x}_{down}$ has an expected upper bound:

$$\overline{\hat{x}}_{down} \le \overline{x}_U = \frac{3c}{2NR}. \tag{3.26}$$

2) By deploying no more than $\lceil L_n / d_c \rceil - 1$ wireless relay nodes for each user node, the expected $\hat{x}_{down}$ has a lower bound:

$$\overline{\hat{x}}_{down} > \frac{3c}{2NR + 3Nd_c}. \tag{3.27}$$

Derivation. 1) Because $N$ user nodes are randomly located following a uniform distribution

inside a cell of radius $R$, the expected user node density $\rho$ is $\rho = N/(\pi R^2)$. From (3.21) and $R < D/2$,

$$\bar{\hat{x}}_{down} \le \bar{x}_U = \frac{c}{\int_0^R r\rho 2\pi r dr} = \frac{3c}{2NR}.$$

2) From (3.22),

$$\bar{\hat{x}}_{down} \ge \bar{x}_N > \frac{c}{\int_0^R r\rho 2\pi r dr + Nd_c} = \frac{3c}{2NR + 3Nd_c}.\square$$

**Corollary 2**. If user nodes are randomly located following a uniform distribution inside a CMESH cell of radius $R$ ($R \ge D/2$) centred at the gateway,

1) the $\hat{x}_{down}$ has an expected upper bound:

$$\bar{\hat{x}}_{down} \le \bar{x}_U = \frac{24R^2 c}{12R^2 ND - ND^3}. \tag{3.28}$$

2) By deploying no more than $\lceil L_n/d_c \rceil - 1$ wireless relay nodes for each user node, the expected $\hat{x}_{down}$ has an approximate lower bound:

$$\tilde{\bar{\hat{x}}}_{down} > \frac{24R^2 c}{12NR^2 D - N(D+d_c)^3 + 36NR^2 d_c}. \tag{3.29}$$

Derivation. 1) Similar to Corollary 1, the expected user node density $\rho$ is $\rho = N/(\pi R^2)$, and from (3.21),

$$\bar{\hat{x}}_{down} \le \bar{x}_U = \frac{c}{\int_0^{D/2} r\rho 2\pi r dr + \left(N - \rho\pi D^2/4\right) D/2}$$
$$= \frac{24c}{12ND - \rho\pi D^3} = \frac{24R^2 c}{12R^2 ND - ND^3}.$$

2) Because user nodes are randomly located following a uniform distribution, they are approximately symmetrically located around the gateway. Thus, from (3.23),

$$\tilde{\bar{\hat{x}}}_{down} \ge \bar{x}_E > \frac{c}{\int_0^{\frac{D+d_c}{2}} r\rho 2\pi r dr + (N - \rho\pi(D+d_c)^2/4)(D+d_c)/2 + Nd_c}$$
$$= \frac{24R^2 c}{12NR^2 D - N(D+d_c)^3 + 36NR^2 d_c}. \square$$

### 3.3.3 Upstream Capacity

The following theorem is about the upstream capacity. Further study of upstream capacity is left for future research.

**Theorem 5**. The upstream capacity is no less than the downstream capacity in a CMESH cell.

Proof. The proof is based on the following observation: if the traffic in all the above proofs for the downstream capacity changes direction, all the upper and lower capacity bounds also hold for upstream traffic. □

### 3.3.4 Bi-directional Stream Capacity

The cell capacity for bi-directional streams depends on the proportion of the downstream traffic to upstream traffic. Let $\hat{x}_{\frac{1}{2}up+\frac{1}{2}down}$ denote the cell capacity in the case that the amounts of upstream and downstream throughput are equal. The following theorem holds.

**Theorem 6**. In an arbitrary CMESH cell, if user nodes are located symmetrically around the gateway, there is an algorithm that allows downstream and upstream traffic to share the same single-path routing and guarantees:

$$\hat{x}_{\frac{1}{2}up+\frac{1}{2}down} \geq x_G , \tag{3.30}$$

where $x_G = \dfrac{c}{d_c(\sum_{L_n<D/2} \lceil L_n / d_c \rceil + \sum_{L_n \geq D/2} \lceil D/(2d_c) \rceil)}$.

Proof. The proof is similar to Theorem 3 and the details are omitted. The spatial reuse pattern is shown in Figure 3.8, where each arrow has a length $D/2$. □

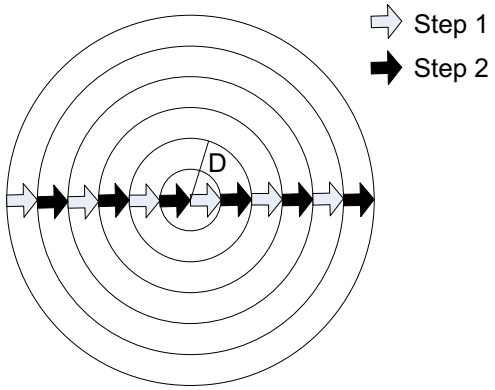


Figure 3.8: Spatial reuse pattern for symmetrical topology (bi-directional traffic)

It can be observed that bi-directional traffic may increase the capacity lower bound compared to downstream traffic.

### 3.4 Capacity Bounds for Multi-Channel CMESH Cells

This section extends the capacity bounds for single-channel CMESH cells to multi-channel CMESH cells.

First, the multi-channel expressions for the upper bound $\hat{x}_G$ in Section 3.3 can be extended as follows. Because orthogonal channels do not interfere with each other, the upper bound for the capacity of a multi-channel CMESH cell is the sum of the upper bounds for its capacity on each orthogonal channel, i.e.:

$$x_U = \sum_{k=1}^{C} \frac{c_k}{\sum_{L_n < D_k/2} L_n + \sum_{L_n \geq D_k/2} (D_k/2)}, \tag{3.31}$$

The expected upper bound for a multi-channel random CMESH cell is:

$$\overline{x}_U = \sum_{D_k > 2R} \frac{3c_k}{2NR} + \sum_{D_k \leq 2R} \frac{24R^2 c_k}{12R^2 N D_k - N D_k^3}. \tag{3.32}$$

In the above expression $D_k > 2R$ (or $D_k \leq 2R$) below the summation symbol means channel $k$ whose $D_k > 2R$ (or $D_k \leq 2R$).

Next, the multi-channel expressions for the lower bounds $x_N$, $x_E$, $x_D$ and $x_G$ in Section 3.3 can be extended as follows. Let $x_k$ denote any of these lower bounds on channel $k$. For example, if $x_k$ denotes $x_N$ on channel $k$, it is given by adding subscript $k$ to Theorem 2, i.e.:

$$x_k(\text{as } x_N \text{ on channel } k) = \frac{c_k}{d_{kc} \sum_n \lceil L_n / d_{kc} \rceil}.$$

Under the same conditions of the lower bounds in Section 3.3 (relay nodes, etc), the multi-channel expressions for these lower bounds depend on the number of radios per user node, denoted by $Y$, and have a uniform expression $x_C$:

$$x_C = \begin{cases} \sum_{k=1}^{C} x_k, & \text{if } Y \geq Y_0 = \left\lceil \sum_{k=1}^{C} \frac{x_k}{w_{kc}} \right\rceil. \\ Y \cdot \min\{w_{kc} \mid k = 1...C\}, & \text{if } Y < Y_0 \end{cases} \tag{3.33}$$

In particular, if $Y \geq Y_0$, the approximate expected lower bound on the capacity for a multi-channel random CMESH cell is:

$$\tilde{\tilde{\hat{x}}}_{down} > \sum_{D_k > 2R} \frac{3c_k}{2NR + 3Nd_{kc}} + \sum_{D_k \leq 2R} \frac{24R^2 c_k}{12NR^2 D_k - N(D_k + d_{kc})^3 + 36NR^2 d_{kc}}. \tag{3.34}$$

## 3.5 Simulation Validation

This section validates the derived expected capacity bounds for random CMESH cells by comparison with simulation results, where throughputs are calculated by Jun and Sichitiu's bottleneck collision domain (BCD) algorithm [68].

The wireless parameter values for the simulations are taken from a specification of the Cisco Aironet 1240AG series 802.11.a access points [29]. The transmission ranges and bit rates are shown in Table 3.1. There are 12 orthogonal channels ($C = 12$) each with identical parameters. The specification does not provide $SINR_i$, so the simulations assume that the common carrier sense range $D$ used by all bit rates is given by $D = 4d_c$ (see Section 3.2.2 for its reason). The $\text{CTC}_i$ is shown in Figure 3.9, where it can observed that $\text{CTC}_i$ reaches its maximum value $c$ at bit rate 36 Mbps. Thus, $w_c = 36$ Mbps, $d_c = 130\,\text{m}$ and $D = 520\,\text{m}$.

Table 3.1: Cisco 1240AG access point specification
(outdoor 802.11a)

| Bit rate (Mbps) | Transmission range (m) |
|---|---|
| 54 | 30 |
| 48 | 91 |
| 36 | 130 |
| 24 | 152 |
| 18 | 168 |
| 12 | 183 |
| 9 | 190 |
| 6 | 198 |

Two simulations were performed, one for a small random CMESH cell in order to validate Corollary 1 and the other for a large random CMESH cell in order to validate Corollary 2. Here

small cells refer to cells in which all wireless links interfere with each other (i.e., cell radius $R < D/2$). In the small-cell simulation, $R = 200$ m, $N$ is varied from 10 to 100 and each user node has two radios. In the large-cell simulation, $R = 600$ m (an area of about 1.13 $km^2$), $N$ is varied from 50 to 350 and each user node has one radio.

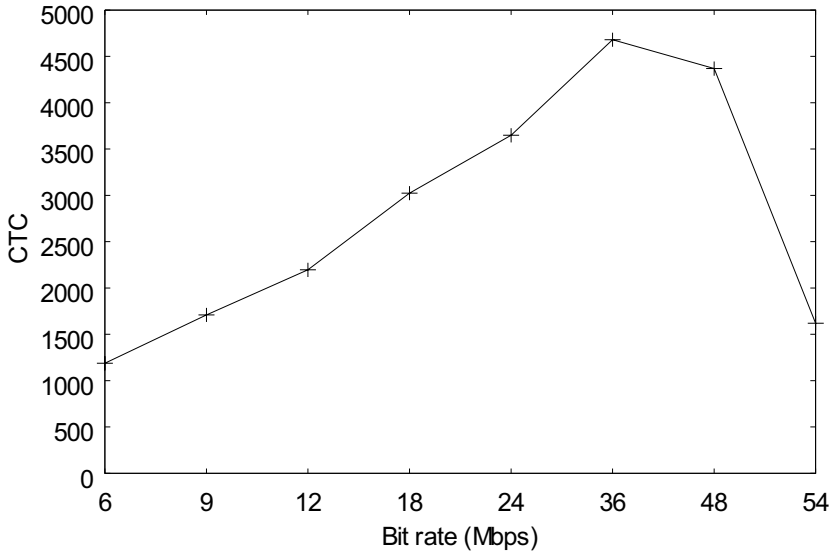


Figure 3.9: CTC at the bit rates in the Cisco 802.11a access point specification

Because the $C$ channels are orthogonal and have the same parameters, the expected upper and lower bounds for the downstream capacity are calculated by the results of Corollaries 1 and 2 times $C$. The results are shown in Figure 3.10 and Figure 3.11, where the expected upper bound is the top curve and the expected lower bound is the bottom curve.

In both simulations, in order to calculate the mean throughput for each value of $N$, 500 topologies are generated randomly, one run is made for each topology, and the mean throughput of these 500 runs is calculated.

The routing scheme is the same as the one used in the proofs. Wireless relay nodes are deployed on a straight-line path from the gateway to each user node, consisting of links of rate $w_c$ and length $d_c$, except for the last link at the user node, whose length may be less than $d_c$.

Jun and Sichitiu's bottleneck collision domain (BCD) algorithm [68] is used to calculate the throughput per user node. The collision domain of a link is formed by all of its nearby links that have to remain idle while the link is active. Note that the BCD algorithm may underestimate

achievable throughput by neglecting spatial reuse among interfering links, so it actually provides a conservative throughput per user node in the simulations.

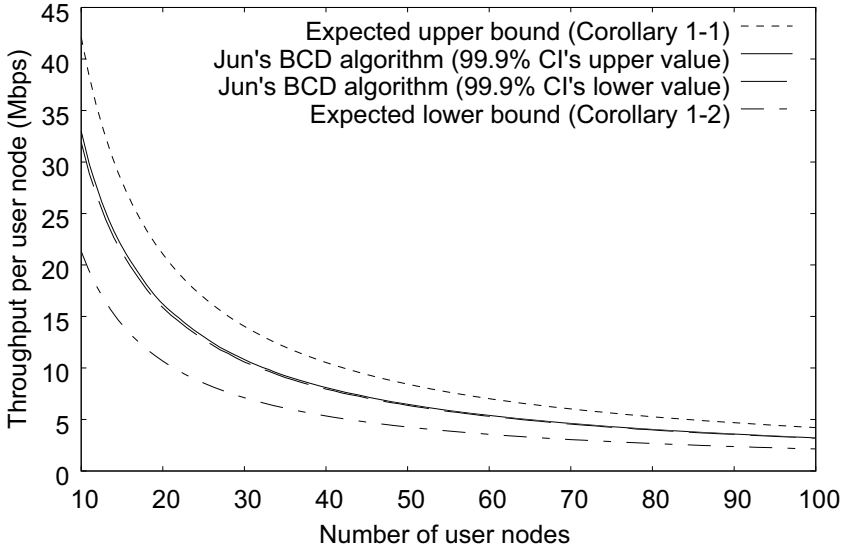


Figure 3.10: Results for small CMESH cell capacity ( $R = 200$ m; $R < D / 2$ )

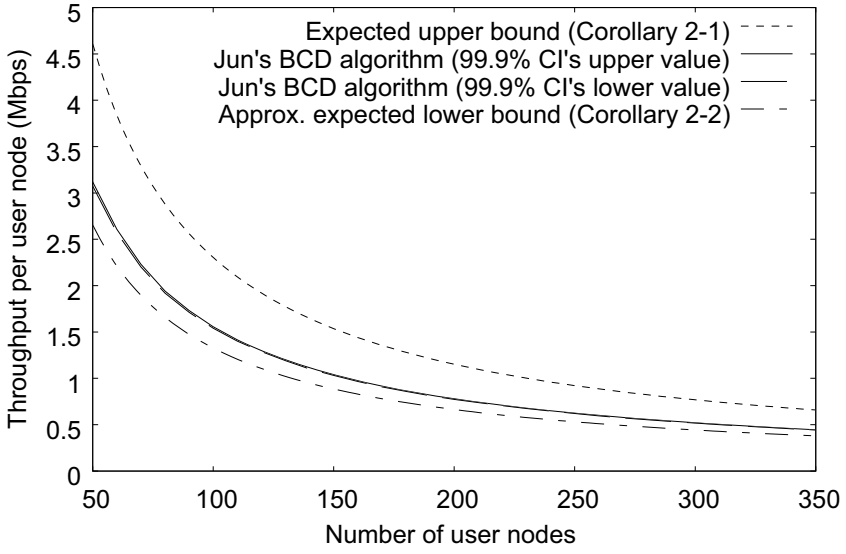


Figure 3.11: Results for large CMESH cell capacity ( $R = 600$ m; $R \geq D / 2$ )

The simulation results are shown in Figure 3.10 and Figure 3.11. Because even the 99.9% confidence interval (CI) is too small to be shown well by error bars, the 99.9% CI's upper value

and lower value are drawn instead, and they are very close to each other (the middle two curves) in both figures. It can be observed that the achieved average throughputs fall between the expected upper and lower bounds, as Corollaries 1 and 2 indicate.

## 3.6 Summary

This chapter presented analytic expressions for the upper and lower bounds on the capacity of CMESH cells. A novel method is proposed for analyzing theoretical cell capacity, which derives the capacity upper bounds by analyzing the supply and demand of a new notion called channel transport capacity and derives capacity lower bounds by finding a joint scheme of wireless relay node deployment, routing, channel assignment and transmission scheduling that achieves a certain throughput. The results are proven within the abstract models.

To validate the analytic results, simulations were conducted with wireless parameter values from the specification of a Cisco 802.11a product. In the simulations, Jun and Sichitiu's BCD algorithm [75] was used to calculate throughputs and these were compared with the expected capacity bounds calculated with the analytic expressions.

# CHAPTER 4
# NOMINAL CAPACITY OF CMESH CELLS

Chapter 3 addressed the theoretical capacity of CMESH cells where only the locations (or their distribution) of user nodes are known but the optimal schemes of wireless relay node deployment, routing, channel assignment and transmission scheduling are all unknown. In other words, Chapter 3 treated user node locations (or their distribution) as a constant and wireless relay node deployment, routing, channel assignment and transmission scheduling as variables, and it studied the cell capacity that allows all these variables to be optimized.

The rest of this thesis assumes that wireless relay nodes have been deployed in a CMESH cell so that all user nodes are connected to the gateway, and the complete topology of the cell is given and fixed. Thus, hereafter wireless relay node deployment becomes a constant, in contrast to Chapter 3. The main research interest for the rest of this thesis is to study the schemes (i.e., variables) of channel assignment, routing and transmission scheduling in order to maximize cell capacity, in terms of the max-min throughput (see Section 4.1.3). Note that cell capacity in this thesis is addressed at different levels in chapters 3, 4, 5 and 6, where the constants and variables are different, and it does not take protocol overhead into account within the abstract models.

Much existing research [7, 64, 77, 106, 124] has shown that the joint channel assignment, routing and transmission scheduling problem for maximizing throughput in WMNs is NP-hard, and the optimal solution is not computable for any practical network scale. Therefore, this thesis studies these three problems separately in order to keep the problem simpler.

This chapter assumes that the topology, bit rates, loss rates, channels and interference relationships of wireless links and the single-path routes in a CMESH cell are all given and fixed. Based on this assumption, this chapter studies interference-free transmission scheduling in order to maximize cell capacity in CMESHs. In general, however, the interference-free transmission scheduling problem is still NP-hard [7], so this chapter studies approximation algorithms only.

The roadmap of this chapter is as follows. This chapter first proposes the Maximum Channel Collision Time (MCCT) algorithm, which derives the nominal cell capacity. Then, this chapter

proves that the nominal cell capacity is achievable and is the exact cell capacity for small cells within the abstract models. The MCCT algorithm is extended further to take into account packet loss and arbitrary traffic demands of user nodes. Finally, the MCCT algorithm is adjusted to estimate the usable cell capacity that takes protocol overhead into account, and the usable cell capacity is compared with ns-2 simulation results in 802.11a-compatible random cells.

The MCCT algorithm is an extension to Jun and Sichitiu's BCD algorithm [68], Aoun *et al.*'s max-min variant [10, 11] and Akhtar and Moessner's multi-channel variant [4]. Both this research and their research focus on a single-gateway WMN. Compared with their research, this research makes following contributions.

- The MCCT algorithm works for multi-radio, multi-channel, multi-rate and multi-hop WMNs. In contrast, Jun and Sichitiu's and Aoun *et al.*'s algorithms do not work for multi-channel and multi-rate WMNs, and Akhtar and Moessner's algorithm does not work for multi-rate WMNs.
- This chapter proves that the nominal capacity derived from the MCCT algorithm is achievable and is the exact cell capacity for small cells within the abstract models. In contrast, none of the previous research proved that their capacity is achievable.
- This chapter drives an expression for the nominal capacity of a multi-radio, multi-channel, multi-rate and multi-hop CMESH cell, which has not been given by previous research.

With a similar goal, Tang *et al.* [119] presented linear programming algorithms for max-min throughput allocation. Compared with their algorithms, the MCCT algorithm has the following differences.

- Tang *et al.*'s algorithms work only for single-rate WMNs, but the MCCT algorithm also works for multi-rate WMNs.
- Their algorithms need to rely on multi-path flow routing, but the MCCT algorithm works for single-path routing.
- Their algorithms work only for infinite traffic demands of nodes, but the MCCT algorithm is extended to arbitrary traffic demands of nodes.
- Their algorithms are based on linear programming, which models the network capacity problem by a group of constraints, but the MCCT algorithm models cell capacity directly in mathematical expressions, which reveal the internal relationship between cell capacity and its major factors.

The remainder of this chapter is organized as follows. Section 4.1 presents the research problem and the assumptions, and gives the definitions of cell capacity. Section 4.2 gives the MCCT algorithm and its related proofs and algorithm extensions. Section 4.3 validates the nominal cell capacity derived from the MCCT algorithm via ns-2 simulations. Section 4.4 summarizes the work presented in this chapter.

## 4.1 Problem Formulation

This section presents the research problem and assumptions. It gives the default definition and the general definition of cell capacity and introduces the nominal cell capacity.

### 4.1.1 The System Model and Assumptions

Consider a CMESH cell, where a single gateway has the only direct Internet connection and provides Internet access for up to hundreds of mesh nodes in the its service area by utilizing multiple radios, multiple orthogonal channels, multi-rate wireless transmissions and multi-hop packet deliveries. User traffic in the cell is only between user nodes and the gateway. See Section 1.2.2 for details.

This chapter makes the following assumptions. First, relay nodes have been deployed in the cell so that all the mesh nodes are connected to the gateway and the cell topology is given. Second, single-path routing is used so that for any mesh node there is exactly one path between the mesh node and the gateway and the path is given. Note that multi-path routing is not used because it has the packet reordering problem, which may degrade cell performance. Finally, the wireless model described in Section 4.1.2 is assumed. In summary, the wireless model gives the bit rates, channels and interference relationships for all the wireless links in the cell. Note that packet loss is addressed in Section 4.2.3 as an extension to the MCCT algorithm, which makes a special assumption that packet loss on wireless links is independent of packet size.

This chapter and Chapters 5 and 6 use $\vec{v}$ to denote a vector named $v$ and use $\hat{v}$ to denote a set named $v$. In order to use set operations, a vector $\vec{v} = (v_1, ...v_n)$ is implicitly converted to its corresponding set $\hat{v} = \{v_1, ...v_n\}$ when it is defined.

Let $\hat{C} = \{1...C\}, C \geq 1$ denote the set of available orthogonal channels. A CMESH cell can be modelled by a directed graph $\vec{\Omega} = (\vec{V}, \vec{E})$. The vertex vector $\vec{V} = (\vec{N}, \vec{G})$, where $\vec{N} = (N_1, ..., N_{m'})$

represents all the $m'$ nodes in the cell and $\vec{G} = (G_1, ..., G_m)$ represents all the $m$ $(1 \le m \le C)$ radios of the gateway $G$. Each mesh node has one or multiple radios. Vector $\vec{E}$ represents the directed wireless links, called edges, among the radios in the cell. Note that radios of mesh nodes are implicitly modelled by edges.

If a vector is defined with a subscript $V$ or $E$, such as $\vec{B}_V$ or $\vec{B}_E$, the vector is based on $\vec{V}$ or $\vec{E}$, which means their elements are in the same sequence and have a one-to-one relationship. If $v \in \hat{V}$ or $e \in \hat{E}$ appears as the subscript of a vector name that is defined with a subscript $V$ or $E$, it denotes the vector's element index, which is equal to the index of $v$ or $e$ in vector $\vec{V}$ or $\vec{E}$. For example, if $\vec{V} = (a, b, c)$ and $\vec{B}_V = (1, 2, 3)$, then $B_c$ is used to refer to the third element in $\vec{B}_V$, i.e., $B_c = 3$ since $c$ is the third element in $\vec{V}$.

Let vector $\vec{R}_V = (\hat{R}_1, ...\hat{R}_{|\vec{V}|})$ denote the single-path routes between the mesh nodes and the gateway radios in a cell. For any $v \in \hat{G}$, let $\hat{R}_v = \varnothing$. For any $v \in \hat{N}$, let $\hat{R}_v = \{e_1, ..., e_g\}$ denote the set of the edges on the path of mesh node $v$ in either the upstream direction (from mesh nodes to gateway radios) or the downstream direction (from gateway radios to mesh nodes).

A user node is called an active user node if its traffic demand is greater than zero. Let $\vec{a} = (a_1, a_2, ...a_n)$, where $\hat{a} \subseteq \hat{N}$, denote the vector of all the $n$ active user nodes in the cell. In real deployments of CMESH cells, active user nodes can be determined by the following rule. When a user node's traffic (in both directions) exceeds a threshold, it is identified as an active user node; an active user node is considered inactive only if its traffic falls below the threshold for an hour. This rule can keep the vector of active user nodes in a cell stable.

The set of mesh nodes whose paths to the gateway (in either direction) pass an edge $e \in \hat{E}$ is called the sub-tree of edge $e$, and is denoted by $\hat{V}_e$, i.e., $\hat{V}_e = \{v \mid \forall v \in \hat{V}, e \in \hat{R}_v\}$.

The number of active user nodes in $\hat{V}_e$ is denoted by $A_e$:

$$A_e = |\hat{a} \cap \hat{V}_e| = \left|\hat{a} \cap \{v \mid \forall v \in \hat{V}, e \in \hat{R}_v\}\right|. \tag{4.1}$$

An edge $e$ is called an active edge if its $A_e > 0$. The set of all the active edges is denoted by $\hat{E}_A$: $\hat{E}_A = \{e \mid \forall e \in \hat{E}, A_e > 0\}$.

### 4.1.2 The Wireless Model

Recall that vector $\vec{E}$ represents the edges in a cell. The edges can be determined by a propagation model such as the one in Section 3.1.2. Recall that set $\widehat{C} = \{1...C\}, C \geq 1$ denotes the set of available orthogonal channels. Let vector $\vec{w}_E = (w_1,...,w_{|\vec{E}|})$ denote the bit rates of all the edges. Let vector $\vec{C}_E = (C_1,...,C_{|\vec{E}|})$ denote the channels on all the edges, where $C_e \in \widehat{C}, \forall e \in \widehat{E}$.

Let $\vec{I}_E = (\widehat{I}_1,...,\widehat{I}_{|\vec{E}|})$ denote the interference vector, where $\widehat{I}_e$ denotes the set of edges that interfere (the definition of interference is given in the Glossary of Terms) with edge $e \in \widehat{E}$ if they are on the same channel as edge $e$, and whether two edges interfere with each other is not affected by other edges. Set $\widehat{I}_e$ can be determined by an interference model, such as the one in Section 3.1.2, or by a conflict graph [64] that specifies interference between any two wireless links. In a conflict graph, a vertex corresponds to a wireless link in a connectivity graph, and an edge is drawn if the two wireless links interfere with each other and cannot be activated simultaneously. Note that in this type of interference model, whether two edges interfere with each other is not affected by other edges.

Let $\widehat{I}_e(k)$ denote the set of edges on channel $k \in \widehat{C}$ in $\widehat{I}_e$, i.e., $\widehat{I}_e(k) = \{e' \mid \forall e' \in \widehat{I}_e, C_{e'} = k\}$. Let $\widehat{I}_e^+(C_e)$ denote the set $\{e\} \bigcup \widehat{I}_e(C_e)$, i.e.:

$$\widehat{I}_e^+(C_e) = \{e\} \bigcup \{e' \mid \forall e' \in \widehat{I}_e, C_{e'} = C_e\}. \tag{4.2}$$

### 4.1.3 The Nominal Cell Capacity

As discussed in Section 1.2.4, a CMESH cell needs to use max-min fairness for throughput allocations among user nodes,. In the original definition of max-min fairness [19] (also called lexicographical max-min by Tang *et al.* [119]), a feasible allocation of throughput $\vec{x}$ is max-min fair if and only if an increase of any throughput by any feasible allocation must come at the cost of a decrease of some already smaller throughput, i.e., for any other feasible throughput allocation $\vec{y}$, if $y_i > x_i$ then there must exist some $j$, such that $y_j < x_j < x_i$.

Max-min fairness is described by a throughput vector, but network capacity is typically described by a single throughput. Therefore, this thesis chooses a single throughput to define cell capacity, and this throughput is termed the "max-min throughput". In the default definition

of cell capacity that is used throughout this thesis, the max-min throughput refers to the maximized minimum throughput of active user nodes each with infinite traffic demand. The max-min throughput in the general definition of cell capacity (see below) refers to the maximized minimum throughput of unsatisfied user nodes. The following first gives the default definition of cell capacity, which is consistent with Gupta and Kumar's network throughput capacity [47] and Jun and Sichitiu's network nominal capacity [68].

Let $\vec{x} = (x_1, x_2, ..., x_n)$ denote a vector of feasible throughput allocations for the vector of active user nodes $\vec{a} = (a_1, a_2, ...a_n)$ each with infinite traffic demand. Let $x$ denote the minimum throughput in $\vec{x}$: $x = \min(\vec{x}) = \min\{x_1, x_2, ..., x_n\}$. Cell capacity is defined as the maximum $x$ among all the feasible $\vec{x}$.

Note that the definition of cell capacity in Chapter 3 also follows this default definition because all user nodes in Chapter 3 are active user nodes. Chapter 3 does not explicitly introduce the term active user nodes because research on theoretical cell capacity studies only the case that all user nodes have infinite traffic demands.

Note that cell capacity can be in either the downstream or the upstream direction, which is implied in the routing vector $\vec{R}_V$. Cell capacity can be extended to bi-stream user traffic if the composition of downstream and upstream traffic of each user node is given.

The goal of this chapter is to find an algorithm and an expression for a conservative cell capacity $\hat{x}$, which is named the nominal cell capacity [68]. The nominal cell capacity does not take protocol overhead into account and allows a transmission on an edge to be arbitrarily short in time. The nominal cell capacity is the exact cell capacity for small cells (see Section 4.2.2) but can be less than the exact cell capacity for large cells (see Section 4.2.2).

The definition of cell capacity or the max-min throughput is based on the simple definition of max-min fairness given by Tang *et al.* [119]: $\vec{x}$ is a max-min throughput allocation vector if and only if for any other feasible throughput allocation $\vec{y}$, $\min(\vec{x}) \geq \min(\vec{y})$. Their definition of max-min throughput also assumes that all nodes have infinite traffic demands.

For arbitrary traffic demands of user nodes, cell capacity or the max-min throughput is no longer given by the minimum throughput of active user nodes even if a max-min mechanism is enforced and a bottleneck is reached in the cell. For example, if the minimum throughput is achieved by a user node only because the user node has little traffic demand (e.g., nearly zero), it

cannot represent a throughput allocation under the constraint of max-min fairness.

Therefore, this thesis further proposes a general definition of cell capacity, referring to the maximized minimum throughput of unsatisfied user nodes. Consider an arbitrary profile of the traffic demands of active user nodes $\vec{a}$, given by vector $\vec{m} = (m_1, m_2, ..., m_n)$. Then any feasible throughput has $x_i \le m_i$, $1 \le i \le n$. If $x_i = m_i$, the user node of $x_i$ is said to have been satisfied; otherwise $x_i < m_i$ and the user node of $x_i$ is said to be unsatisfied. The general definition of cell capacity, in terms of the max-min throughput is as follows. The $\min\{x_i \mid 1 \le i \le n, x_i < m_i\}$ is the max-min throughput if and only if for any other feasible throughput allocation $\vec{y}$:

$$\min\{x_i \mid 1 \le i \le n, x_i < m_i\} \ge \min\{y_i \mid 1 \le i \le n, y_i < m_i\}.$$

Note that the concept of cell capacity or the max-min throughput is meaningful only if the cell has reached a bottleneck, so the general definition of cell capacity assumes that there is at least one unsatisfied user node to ensure this condition.

Algorithms based on the default definition of cell capacity can be extended to the general definition of cell capacity (see Section 4.2.4) and can be extended to the original definition of max-min fairness [10, 119].

## 4.2 The Maximum Channel Collision Time (MCCT) Algorithm

The MCCT algorithm is a multi-channel and multi-rate extension to Jun and Sichitiu's Bottleneck Collision Domain (BCD) algorithm [68]. The BCD algorithm defines the collision domain of a wireless link $e$ as a set of links formed by wireless link $e$ and all other wireless links that have to be inactive for transmissions on wireless link $e$ to be successful. This chapter models link directions by edges, so it defines the collision domain of an edge $e$ as $\widehat{I}_e \bigcup \{e\}$.

The MCCT Algorithm introduces the Channel Collision Domain (CCD) of an edge $e$, which is defined as $\widehat{I}_e^+(C_e)$. This means that the collision domain of edge $e$ is split into several groups according to the channels of its edges. The CCD of an edge $e$ depends on which channel is assigned to edge $e$ by channel assignment algorithms.

Let $T_e$ denote the channel time spent on edge $e$ per second, for each active user node to achieve 1bps throughput. There are $A_e$ active user nodes whose single-path routes pass edge $e$, so $A_e$ bits will pass edge $e$ in each second. Recall that $w_e$ is the bit rate of edge $e$, so $T_e$ is:

$$T_e = A_e / w_e . \tag{4.3}$$

Define the Channel Collision Time (CCT) of edge $e$ as the sum of the channel time in the CCD of edge $e$ per second for each active user node to achieve 1 bps throughput, given by:

$$\mathrm{CCT}_e = \sum_{e' \in \widehat{I}_e^+(C_e)} T_{e'} = \sum_{e' \in \widehat{I}_e^+(C_e)} (A_{e'} / w_{e'}) . \tag{4.4}$$

### 4.2.1 Specification of the MCCT Algorithm

The MCCT algorithm is given as Algorithm 1. Note that the $\vec{D}_E$ in step 3 can be an input directly, when $\vec{I}_E$ is not independent of channels.

Algorithm 1: The MCCT algorithm

Input: $\vec{V}$, $\vec{E}$, $\vec{a}$, $\vec{R}_V$, $\vec{C}_E$, $\vec{I}_E$, $\vec{w}_E$.

Output: the nominal cell capacity $\hat{x}$.

1. Get $\vec{A}_E = (A_1, ..., A_{|\vec{E}|})$ via $\vec{V}$, $\vec{E}$, $\vec{a}$ and $\vec{R}_V$ (Equation (4.1)).
2. Get $\widehat{E}_A = \{e \mid \forall e \in \widehat{E}, A_e > 0\}$ via $\vec{A}_E$ and $\vec{E}$.
3. Get $\vec{D}_E = \left( \widehat{I}_1^+(C_1), ..., \widehat{I}_{|\vec{E}|}^+(C_{|\vec{E}|}) \right)$ via $\vec{I}_E$ and $\vec{C}_E$ (Equation (4.2)).
4. Get $\widehat{\mathrm{CCT}} = \{\mathrm{CCT}_e \mid \forall e \in \widehat{E}_A\}$ via $\vec{A}_E$, $\vec{D}_E$ and $\vec{w}_E$ (Equation (4.4) ).
5. Get $\mathrm{MCCT} = \max(\widehat{\mathrm{CCT}})$.
6. Get $\hat{x} = 1 / \mathrm{MCCT}$.

The implication of $\hat{x} = 1/\mathrm{MCCT}$ in Algorithm 1 is clear: maximizing the nominal cell capacity $\hat{x}$ is equivalent to minimizing the maximum $\mathrm{CCT}_e$, $\forall e \in \widehat{E}_A$. This is the theoretical basis that guides the research on channel assignment in Chapter 5 and on routing in Chapter 6 to find greedy algorithms that improve cell capacity.

### 4.2.2 Properties of the Nominal Cell Capacity

The nominal cell capacity $\hat{x}$ derived from the MCCT algorithm is achievable within the abstract models. The following gives its proof.

**Theorem 7**. The nominal cell capacity given by the MCCT algorithm (Algorithm 1) is achievable within the abstract models, i.e., per active user node throughput $\hat{x}$ is achievable.

Proof. From step 6 in the MCCT algorithm, MCCT=$1/\hat{x}$. From step 5, the above formula is equivalent to $\hat{x} = 1/\max\left\{\mathrm{CCT}_e \mid \forall e \in \widehat{E}_A\right\}$.

Proving that per active user node throughput $\hat{x}$ is achievable amounts to proving that if $\hat{x} = 1/\max\left\{\mathrm{CCT}_e \mid \forall e \in \widehat{E}_A\right\}$ holds, there exists an interference-free transmission scheme that delivers $\hat{x}$ bits from/to each active user node to/from the gateway in each time unit.

If $\hat{x} = 1/\max\left\{\mathrm{CCT}_e \mid \forall e \in \widehat{E}_A\right\}$ holds, $\hat{x} \cdot \mathrm{CCT}_e \le 1,\ \forall e \in \widehat{E}_A$. From step 4, it is equivalent to $\hat{x} \cdot \sum_{e' \in \widehat{I}_e^+(C_e)} (A_{e'} / w_{e'}) \le 1,\ \forall e \in \widehat{E}_A$. Recall $\widehat{I}_e^+(C_e) = \widehat{I}_e(C_e) \bigcup \{e\}$, so the inequality is equivalent to:

$$\hat{x} \cdot A_e / w_e \le 1 - \sum_{e' \in \widehat{I}_e(C_e)} (\hat{x} \cdot A_{e'} / w_{e'}),\ \forall e \in \widehat{E}_A. \tag{4.5}$$

Thus, proving that per active user node throughput $\hat{x}$ is achievable amounts to proving that if inequality (4.5) holds, there exists an interference-free transmission scheme that delivers $\hat{x}$ bits from/to each active user node to/from the gateway in each time unit. The rest of the proof is similar to Lemma 3 in Alicherry *et al.* [7]. Note that different from Alicherry *et al.*'s [7] and some other researchers' [64] work that seeks to use linear programming to solve network capacity, this chapter seeks to find algorithms and expressions for cell capacity.

Recall that $\widehat{E}_A$ is the set of all active edges that have transmissions, and inactive edges have no transmissions and need no transmission scheduling. Thus, if each edge $e \in \widehat{E}_A$ can transmit $\hat{x} \cdot A_e / w_e$ time units in each time unit, in each time unit, each active user node has its $\hat{x}$ bits delivered on each edge $e$ on its path to the gateway in $\hat{x} / w_e$ time units, and thus throughput $\hat{x}$ is achieved for each active user node in a stable state. So the following needs only to prove that if inequality (4.5) holds, there is an interference-free transmission scheme that allocates each edge $e \in \widehat{E}_A$ transmissions of $\hat{x} \cdot A_e / w_e$ time units in each time unit.

Transmission scheme $\mathbb{Z}$ that allocates each edge $e \in \widehat{E}_A$ transmissions of $\hat{x} \cdot A_e / w_e$ time units in each time unit is as follows. Define a time slot as a continuous period of time variable in length. In the first step, the scheme arbitrarily orders all the edges in $\widehat{E}_A$ and gets a sequence $\mathbb{S}$,

so as to allocate time slots for them one by one in this sequence. Note that the selection of $\mathbb{S}$ has no impact on the feasibility of scheme $\mathbb{Z}$ (see below). In the second step, for any edge $e$ in $\mathbb{S}$, it searches, starting from the beginning of the time unit on channel $C_e$, and allocates the first encountered unused time slot, denoted by $\Delta_1$, to edge $e$ (the time slot represents a transmission of $e$). If $\Delta_1 < x \cdot A_e / w_e$, it continues searching and allocates the second unused time slot on channel $C_e$, denoted by $\Delta_2$, to edge $e$, and so on until exactly $x \cdot A_e / w_e$ time units are allocated to edge $e$. Finally, the second step is repeated until all the edges in $\mathbb{S}$ are treated.

The following uses mathematical induction to prove that if inequality (4.5) holds, the transmission scheme $\mathbb{Z}$ is able to allocate time slots (also transmissions) of $x \cdot A_e / w_e$ time units to each active edge $e$ in $\mathbb{S}$ and is free of interference.

1) Basis: allocating time slots of $\hat{x} \cdot A_e / w_e$ for the first active edge $e$ in $\mathbb{S}$ is clearly feasible, because inequality (4.5) gives $\hat{x} \cdot A_e / w_e \le 1$ and the allocated transmissions do not interfere with each other (they all belong to $e$ and their time slots do not overlap).

2) Inductive step: assume that allocating the time slots for the $i$th $(1 \le i \le \left|\hat{E}_A\right| - 1)$ active edge in $\mathbb{S}$ is feasible. Let $e$ denote the $i+1$th active edge in $\mathbb{S}$. Let $\hat{J}_e$ denote all the active edges that have been allocated time slots and interfere with $e$. Then, if inequality (4.5) holds, because $\hat{J}_e \subseteq \hat{I}_e(C_e)$, $\hat{x} \cdot A_e / w_e + \sum_{e' \in \hat{J}_e} (\hat{x} \cdot A_{e'} / w_{e'}) \le 1$, and thus transmission scheme $\mathbb{Z}$ is able to allocate edge $e$ time slots of $\hat{x} \cdot A_e / w_e$ which do not overlap with the time slots allocated to each edge in $\hat{J}_e$. Thus, the transmissions of edge $e$ does not interfere with those of each edge in $\hat{J}_e$. By the definition of $\hat{J}_e$, the transmissions of edge $e$ does not interfere with those of the active edges that have been allocated time slots but are not in $\hat{J}_e$. Notice further that the beginning of the inductive step assumes that before edge $e$ is allocated time slots, the transmissions of the active edges that have been allocated time slots do not interfere with each other and their interference relationships are not affected by the transmissions of edge $e$ (see Section 4.1.2). Thus, after edge $e$ is allocated time slots, the transmissions of the active edges that have been allocated time slots (including edge $e$) do not interfere with each other.

Since both the basis and the inductive step have been proved, it has now been proved by mathematical induction that if inequality (4.5) holds, scheme $\mathbb{Z}$ is able to allocate transmissions of $x \cdot A_e / w_e$ time units to each active edge $e$ in $\mathbb{S}$ and is free of interference.

It is thus concluded that per active user node throughput $\hat{x}$ is achievable. □

The nominal cell capacity derived from the MCCT algorithm is a conservative capacity for large cells because it may neglect the possibility of channel spatial reuse inside the CCD of any active edge $e$: two edges that interfere with edge $e$ may not necessarily interfere with each other due to channel spatial reuse.

However, Theorem 8 proves that, for small cells, the nominal cell capacity $\hat{x}$ derived from the MCCT algorithm (Algorithm 1) is the exact cell capacity within the abstract models. In other words, any achievable throughput per active user node cannot be higher than the nominal capacity $\hat{x}$. Here, small cells refer to CMESH cells in which all wireless links interfere with each other if they are on the same channel. In other words, $\{e\} \bigcup \widehat{I}_e = \widehat{E}$, $\forall e \in \widehat{E}$.

**Theorem 8**. For small cells, the nominal cell capacity $\hat{x}$ given by the MCCT algorithm (Algorithm 1) is the exact cell capacity within the abstract models, i.e., any achievable per active user node throughput $x$ cannot be higher than $\hat{x}$.

Proof. If each active user node can achieve throughput $x$ bits per time unit, then $x \cdot \mathrm{CCT}_e = x \cdot \sum_{e' \in \widehat{I}_e^+(C_e)} (A_{e'} / w_{e'})$, $\forall e \in \widehat{E}_A$.

By definition, in small cells, $\{e\} \bigcup \widehat{I}_e = \widehat{E}$, $\forall e \in \widehat{E}_A$, so edges in $\widehat{I}_e^+(C_e) = \{e' \mid e' \in \widehat{E}, C_{e'} = C_e\}$ interfere with each other, and their transmissions have to be activated one by one, so the sum of their transmission time in a time unit cannot be larger than 1, i.e., $x \cdot \mathrm{CCT}_e \le 1$, $\forall e \in \widehat{E}_A$. This gives $x \cdot \max(\widehat{\mathrm{CCT}}) = x \cdot \max\{\mathrm{CCT}_e \mid \forall e \in \widehat{E}_A\} \le 1$. Thus, $x \le 1 / \max(\widehat{\mathrm{CCT}}) = \hat{x}$. □

### 4.2.3 Accounting for Packet Loss

The MCCT algorithm (Algorithm 1) can be easily extended to take packet loss on edges into account. In this case, it calculates the expected nominal cell capacity.

This extension of the MCCT algorithm makes an additional assumption. It assumes that packet loss on edges is independent of packet size. Let $p_e$ denote the packet loss rate on edge $e \in \widehat{E}$. Thus, the expected number of transmissions for a packet to be successfully delivered

over edge $e$ is $1/(1\text{-}p_e)$. The expected transmission time [36] for a packet of size $S$ to be delivered over edge $e$, denoted by $\mathrm{ETT}_e$, is $\mathrm{ETT}_e = S / w_e / (1 - p_e)$. For the MCCT algorithm to take packet loss into account and calculate the expected nominal cell capacity, the following $\mathrm{CCT}_e$ should replace Equation (4.4):

$$\mathrm{CCT}_e = \sum_{e' \in \widehat{I}_e^+(C_e)} (A_{e'} \cdot \mathrm{ETT}_{e'} / S) = \sum_{e' \in \widehat{I}_e^+(C_e)} (A_{e'} / w_{e'} / (1 - p_{e'})). \tag{4.6}$$

The above ETT can further incorporate the backoff time before accessing a channel, as required by IEEE 802.11 protocols. Draves *et al.* [36] give an alternative version of ETT that includes the backoff time caused by packet losses. They do not, however, consider the backoff time caused by collision avoidance among competing nodes. If all active user nodes have infinite traffic demands, it is likely that the backoff time caused by packet collisions depends on the number of active edges in channel collision domains. There has been research [39] on this topic, but this thesis leaves further investigation for future research.

### 4.2.4 Accounting for Arbitrary Traffic Demands of User Nodes

The MCCT algorithm can be further extended to take into account arbitrary traffic demands of user nodes. In this case, it calculates the nominal cell capacity based on the general definition of cell capacity.

For the vector of active user nodes $\vec{a} = (a_1, a_2, ...a_n)$, consider its corresponding vector of arbitrary traffic demand $\vec{m} = (m_1, m_2, ..., m_n)$. The extended MCCT algorithm for $\vec{m}$ is given as Algorithm 2. Note that in the loop of Algorithm 2, the values of $\vec{R}_V$, $\vec{C}_E$, $\vec{I}_E$, $\vec{w}_E$, $\widehat{E}_A$ and $\widehat{I}_e^+(C_e)$ are fixed, but the values of $\vec{a}$, $\vec{m}$, $A_e$, $T_e$ and $x$ are updated in each round of the loop.

The variable $x$ in Algorithm 2 records the maximum throughput among the currently allocated throughputs of unsatisfied user nodes. When Algorithm 2 ends, for any active user node, its throughput is either $x$ if its traffic demand is unsatisfied or its initial traffic demand if its traffic demand is satisfied.

**Theorem 9**. The throughputs allocated to the active user nodes in a cell by Algorithm 2 are achievable within the abstract models.

Proof. Notice that inequality (4.5) still holds in Algorithm 2. According to the proof of Algorithm 1, inequality (4.5) guarantees that the throughputs allocated to the active user nodes in

a cell by Algorithm 2 are achievable within the abstract models. □

Algorithm 2: The extended MCCT algorithm

Input: $\vec{V}$, $\vec{E}$, $\vec{a}$, $\vec{m}$, $\vec{R}_V$, $\vec{C}_E$, $\vec{I}_E$, $\vec{w}_E$.

Output: the nominal cell capacity $\hat{x}$ (by the general definition).

1. Initialize $A_e$ for each $e \in \hat{E}$ via $\vec{V}$, $\vec{E}$, $\vec{a}$ and $\vec{R}_V$ (Equation (4.1)).
2. Get $\hat{E}_A = \{e \mid \forall e \in \hat{E}, A_e > 0\}$ via $A_e$ and $\vec{E}$.
3. Get $\hat{I}_e^+(C_e)$, for each $e \in \hat{E}_A$ via $\vec{C}_E$ and $\vec{I}_E$ (Equation (4.2)).
4. Initialize $x = 0$, and for each $e \in \hat{E}_A$, initiate $L_e = 1$.

Loop {

5. Get $\mathrm{CCT}_e$, for each $e \in \hat{E}_A$ via $A_e$, $\hat{I}_e^+(C_e)$ and $\vec{w}_E$ (Equation (4.4)).
6. Get $\Delta x_e = L_e / \mathrm{CCT}_e$, for each $e \in \hat{E}_A$.
7. Get $\Delta x = \min\{\min\{\Delta x_e \mid e \in \hat{E}_A\}, \min(\hat{m})\}$.
8. Update $x \leftarrow x + \Delta x$.
9. Update $L_e \leftarrow L_e - \Delta x \cdot \mathrm{CCT}_e$, for each $e \in \hat{E}_A$.
10. Get $S_{satisfied} = \{i \mid m_i \in \hat{m}, m_i - \Delta x = 0\}$ and update $\vec{m} \leftarrow \vec{m} - \Delta x$.
11. If $|S_{satisfied}| = 0$ or $|S_{satisfied}| = |\hat{m}|$, Then $\hat{x} = x$ is found and this algorithm exits.

  Else {

    11.1) Update $\vec{a}$ and $\vec{m}$ by removing elements whose indexes are in $S_{satisfied}$.

    11.2) Update $A_e$ via $\vec{V}$, $\vec{E}$, $\vec{a}$ and $\vec{R}_V$ (Equation (4.1)).

  } End Else

} End Loop

### 4.3 Simulation Validation

In this section, the nominal cell capacity derived from the MCCT algorithm (Algorithm 1) is first adjusted to estimate the usable cell capacity and then is compared with ns-2 simulation results in 802.11a-compatible random CMESH cells. In order to simulate 802.11a-compatible

CMESH cells, the ns-2 simulator [120] needed to be modified to support the necessary features of CMESH cells, including multiple radios per node, multiple channels, multiple bit rates, IEEE 802.11a and a max-min fairness mechanism. These modifications are discussed in Section 4.3.1 and Section 4.3.2.

### 4.3.1 The Max-Min Fairness Mechanism

Because cell capacity is defined with max-min fairness, it was necessary to add a max-min fairness mechanism to the ns-2 simulator to enforce the max-min throughput. Otherwise, user nodes will encounter severe unfairness in throughput (see an example in Section 1.2.4), which cannot be solved by channel assignment or routing algorithms.

The max-min fairness mechanism added to the ns-2 simulator includes two schemes. The first is a source rate control scheme, which enforces max-min user node throughputs at the cell-level (macro-level). The second is a scheme of round robin queues and group packet transmissions, which provides max-min packet transmissions at the node-level (micro-level). The DCF mechanism (see Section 2.3.3) in the IEEE 802.11 standards provides max-min packet transmissions among all nodes in a WLAN, where any transmission involves the access point and the RTS/CTS scheme is used to coordinate all transmissions. However, in CMESH cells, there is no such common node that coordinates all transmissions, so the DCF mechanism can no longer provide max-min packet transmissions among interfering nodes. In addition, the DCF mechanism has no impact on max-min packet transmissions inside a node that has packets from its sub-tree nodes. Therefore, the proposed two schemes are necessary to overcome the two weaknesses of the DCF mechanism in CMESH cells. The research details of the two schemes are beyond the scope of this thesis, so the following only briefly introduces them.

#### The Source Rate Control Scheme

The source rate control scheme has two components: the computation of the source rate threshold and the operations of source rate control. The source rate threshold computation is performed by the gateway, and the operations of the source rate control is performed by both the gateway and all the user nodes.

From the gateway's perspective, there is a bi-directional packet "pipe" between each user node and itself. The gateway calculates the current source rate threshold $X$ (similar to a valve in a

pipe that controls the amount of the inside flow) and works with user nodes to ensure that the throughputs in these pipes conform to max-min fairness.

A simplified scheme for the calculation of the source rate threshold was added to the ns-2 simulator. It works as follows. The gateway sets a global source rate threshold $X$ representing the max-min bi-directional throughput of user nodes. The source rate threshold $X$ is adjusted as follows. The gateway initializes $X$ to a conservative value that allows traffic to start but will not result in congestion. The gateway monitors the real throughputs of user nodes $\hat{x} = \{x_1, ...x_n\}$ and whether their traffic demands have been satisfied. The gateway increases $X$ to $X' = X + \Delta$, $\Delta > 0$, and updates $\hat{x}$ to $\hat{x}' = \{x_1', ...x_n'\}$. In the simulations, all active user nodes have infinite traffic demands, so it is expected that $\forall x' \in \hat{x}'$, $X \le x' \le X'$. If there exists $x'$, $x' < X$, the gateway knows that the cell capacity has been exceeded, so it sets $X'$ back to $X$. Note that in real applications, it would be more practical to check the violation of max-min fairness by $\exists x_i' \in \hat{x}'$, $x_i' < x_i \in \hat{x}$, for the unsatisfied user nodes.

The source rate threshold $X$ considers bi-directional traffic. The gateway may use two methods to determine the upstream and downstream throughputs of a user node, denoted by $X_{\text{up}}$ and $X_{\text{down}}$, respectively. The gateway allows only the maximum amount of $X_{\text{down}}$ traffic for the user node to enter the cell from the Internet; and the user node allows only no more than $X_{\text{up}}$ of its local traffic to enter the cell. One method is that the gateway monitors the upstream throughput of the user node $X_{\text{up}}$, and calculates the downstream throughput by $X_{\text{down}} = X - X_{\text{up}}$. The other method is to set $X_{\text{up}}$ to a fixed rate and let $X_{\text{down}} = X$. In the simulation design in this section, only downstream user traffic is examined, i.e., $X_{\text{up}} = 0$, so the two methods give the same result: $X_{\text{down}} = X$.

The gateway and mesh nodes use the leaky bucket technology [123] for the operations of source rate control. Each user node has two packet leaky buckets: one at the user node itself for its upstream traffic and the other at the gateway for its downstream traffic. All incoming packets first flow into a leaky bucket, and then "leak" out at a steady rate, either $X_{\text{up}}$ or $X_{\text{down}}$, which is controlled by the gateway. In the event the incoming packet rate exceeds the controlled rate for a certain time, overflow packets will be dropped. The leaky bucket scheme for a user node in a CMESH cell is illustrated in Figure 4.1.

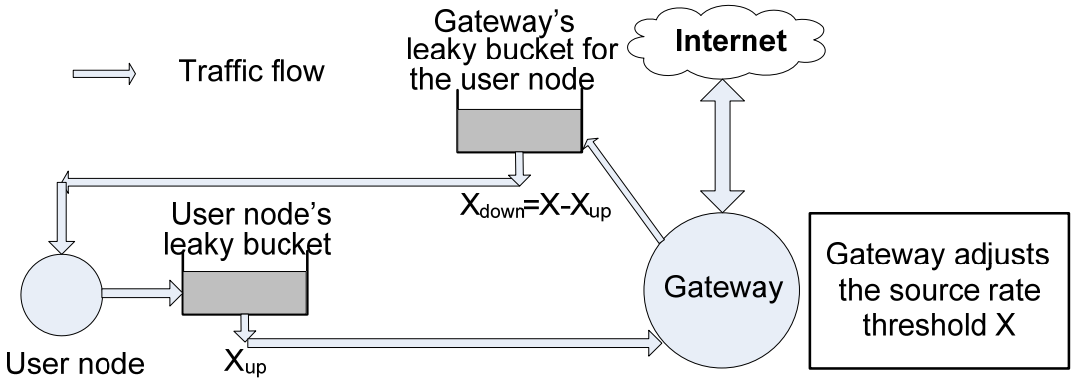


Figure 4.1: The scheme of source rate control

**The Scheme of Round Robin Queues and Group Packet Transmissions**

The scheme of round robin queues and group packet transmissions is designed to enforce max-min packet transmissions at the node level (among interfering nodes and inside nodes among their sub-tree nodes).

A mesh node transmits not only its own packets but also the packets of its sub-tree nodes (i.e., nodes whose routes to the gateway pass through the mesh node). The mesh node uses round robin queues [112] for all the incoming packets, in order to provide max-min packet transmissions at the node level. Otherwise, severe unfairness in user node throughputs may occur (see Section 1.2.4). Figure 4.2 shows the comparison of a group of small round robin queues with a big First-in-First-out (FIFO) queue for upstream traffic. A number in the figure represents a packet coming from the user node represented by the number. For example, a number 2 represents a packet originated from user node 2. If round robin queues are used, when packets from user nodes 1, 2 and 3 enter node 1, they will enter their private small queues instead of a single big queue. For example, packets from user node 2 will enter queue 2. When node 1 prepares for the next round of transmissions, it selects one packet from each queue, if the queue is not empty.

If a standard IEEE 802.11 MAC is used by nodes, after node 1 has collected the group of packets from the round robin queues for the next round of packet transmissions, it can transmit only one of these packets each time it acquires the channel. Then, each packet in the group will experience its own random contention delay and may experience collision avoidance delay and RTS/CTS frame delay.

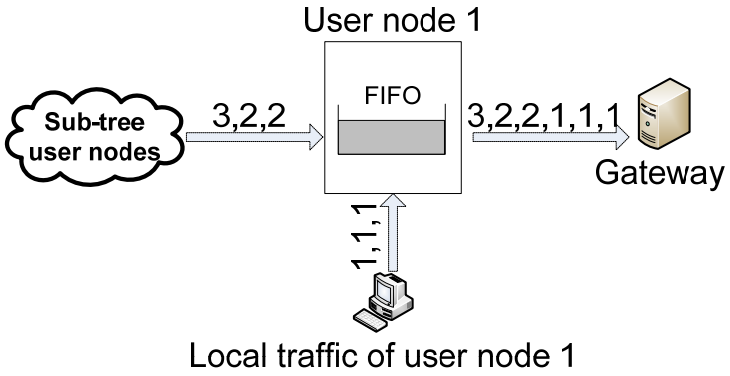


(a) A single FIFO queue

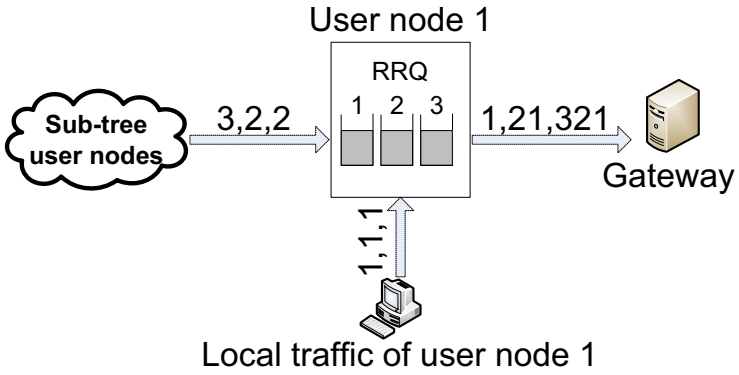


(b) Round robin queues

Figure 4.2: The scheme of round robin queues and group packet transmissions

If node 1 has a large sub-tree of active user nodes, the overall delay costs for transmitting the whole group of packets with the standard IEEE 802.11 MAC will be very high. In addition, because the DCF mechanism seeks to give interfering nodes equal opportunity to acquire their shared channel, node 1 and its sub-tree active user will suffer significant throughput unfairness compared with its interfering nodes with small sub-trees in its interference range. Therefore, group packet transmissions are necessary in CMESH cells, so that even if node 1 has a large group of packets (consisting of at most one packet for each user node in its sub-tree) to send, these packets wait for node 1 to acquire the channel only once and then are sent back-to-back.

A similar batch transmission scheme was introduced by Yuan *et al.* [132], and their experiments showed that their batch transmission scheme can increase the throughput by 112% and reduce average delay by 54% compared with the standard IEEE 802.11 MAC.

### 4.3.2 Modifications to ns-2

For the experiments, all simulations use the ns-2 network simulator version 2.30 [120]. The ns-2 simulator is a popular discrete event simulator designed for network research. As a packet-level simulator, the ns-2 simulator implements various network protocols, such as the IEEE 802.11 DCF mechanism, so its simulation results include the costs of these protocols. Much research [52, 62] has validated the ns-2 simulator as a reliable tool for the evaluation of multi-hop wireless networks.

However, the ns-2 version 2.30 cannot directly simulate CMESH cells because it does not support multi-radio, multi-channel, multi-rate and IEEE 802.11a networks, such as CMESH cells. In addition, as discussed in Section 4.3.1, the max-min fairness mechanism including the source rate control, round robin queues and group packet transmissions needed to be added to the ns-2 simulator. As a result, the following modifications were made to the ns-2 simulator.

1. The ns-2 simulator was modified to support multiple radios per node and multiple orthogonal channels. Each mesh node supports three radios (a down radio, an up radio and a helper radio) and the gateway supports $C$ down radios, where $C$ is the number of orthogonal channels in a cell.
2. The ns-2 simulator was modified to support multiple bit rates. The transmission ranges for the bit rates in IEEE 802.11.a are taken from a specification of the Cisco Aironet 1240AG series 802.11.a access points (see Section 3.5), as shown in Table 3.1. The specification does not provide the SINR thresholds required by these bit rates, so they were calculated based on a common carrier sense range $D = 4d_c$ (see Section 3.2.2 for the reason) using the formulas in Section 3.1.2. In brief, the bit rate of a packet transmission is determined by its transmission distance; and the packet transmission at the bit rate will succeed if the SINR at its receiver is above the required threshold, otherwise it will fail due to errors.
3. The ns-2 simulator does not provide IEEE 802.11a parameters, so the parameters listed in Table 4.1 were set according to the IEEE 802.11a standard [56].
4. A new mesh layer was inserted into the ns-2 simulator between the link layer and the MAC layer, and interface queues were replaced by round robin queues. The mesh layer is responsible for switching channels, management of the round robin queues and group packet transmissions and interactions with the MAC layer.

5. The MAC layer in the ns-2 simulator was modified to support the functions of group packet transmissions and the detection of the channel busy state (required by the DPLB algorithm). These functions cooperate with the mesh layer.
6. The packet capture function in the ns-2 simulator was modified to reflect current technologies. In ns-2, if a new packet arrives while the receiver is receiving an earlier packet, the new packet is always dropped. However, Kochut *et al.* [76] and Chen *et al.* [27] reported that real wireless cards accept packets with stronger signals even if they arrive after reception has started. Therefore, the following packet capture function was used in simulations: if the new packet has sufficiently higher power than the earlier packet, it can be successfully received and the earlier packet is dropped.
7. The max-min fairness mechanism introduced in Section 4.3.1, including the source rate control scheme and the scheme of round robin queues and group packet transmissions, was added to the ns-2 simulator.

Table 4.1: The 802.11a parameters in the ns-2 simulations

| **Parameter in ns-2** | **Description** | **Value** |
|---|---|---|
| freq_ | Radio frequency | 5.15 GHz |
| CWMin_ | Minimum contention window | 16 |
| CWMax_ | Maximum contention window | 1024 |
| SlotTime_ | Time used for defining periods | 9 μs |
| SIFS_ | Short inter-frame space | 16 μs |
| PreambleLength_ | Length of preamble | 96 bits |
| PLCPHeaderLength_ | Length of the header of the physical layer convergence protocol | 24 bits |
| ShortRetryLimit_ | Maximum number of retries for short frames | 7 |
| LongRetryLimit_ | Maximum number of retries for long frames | 4 |
| basicRate_ | Bit rate used by control frames | 6 Mbps |
| PLCPDataRate_ | Bit rate used by PLCP header and preamble | 6 Mbps |

### 4.3.3 Experiment Design

Four simulation experiments—experiment 1 to experiment 4—were performed, with each varying one of the following four factors: the number of channels, the number of user nodes, the number of traffic flows and the cell area size. In each experiment, the other three factors are fixed to their default levels, which are given in Table 4.2.

These four factors are chosen from four major system parameters: channels, radios (the transmit units), user traffic and cell areas.

A cell provides three factors: the number of channels, the number of user nodes and the cell area size. A cell consists of three basic components: its coverage area, its channels and its radios. The first two components provide two factors directly. The third component, radios, includes the gateway radios and node radios. The gateway radios are located at the centre of a cell and their number is set to the number of channels, so they are fixed parameters. In random cells, user nodes are randomly uniformly located, and relay nodes are deployed using fixed algorithms (see below). The cells in the simulations use a two-data-radio node design, where each node has two data radios, consisting of a down radio and an up radio (see Section 1.2.2). Therefore, in all simulations, the radio component can be determined by the number of user nodes.

The user traffic in a cell gives the last factor: the number of traffic flows. Recall that the simulation experiments in this section are designed to find cell capacity, whose definition requires that user nodes either have no traffic or have infinite traffic (active user nodes). These active user nodes are selected randomly from all user nodes based on an assumption that only a random group of user nodes are active at the same time in a CMESH cell. Then, the user traffic in a cell can be represented by the number of traffic flows in the cell.

The levels of the four factors are selected to reflect the network goal of a CMESH cell: a CMESH cell is designed to serve a large number of user nodes in a large area by utilizing multiple channels. For this reason, single-channel cells, single-hop cells and cells with less than 20 user nodes (a typical scale for WLANs) are not examined in the simulation experiments.

Table 4.2: Experimental factors

| **Factor** | **Corresponding experiment #** | **Levels** | **Default level** |
|---|---|---|---|
| Number of channels | 1 | 2-20 | 12 |
| Number of user nodes | 2 | 20, 30, …, 100 | 100 |
| Number of traffic flows | 3 | 20, 30, …, 100 | 100 |
| Side length of the coverage area | 4 | 600m, 800m, …, 2000m | 1000m |

The default levels of the four factors were chosen to represent the following application goal of a CMESH cell: the cell is designed to use IEEE 802.11a channels (12 orthogonal channels) to serve a large number of user nodes (100 user nodes) in the worst case that all the user nodes have

infinite traffic demands (100 traffic flows) as a solution for the "last-kilometre" problem (cell side length of 1 km).

The four simulation experiments share a common set of 50 cell topologies. In each topology, the gateway is always located at the centre of a square cell area. User node locations are generated randomly inside the cell area following a discrete uniform distribution (on 1m×1m grids). For each factor value in each simulation experiment, one simulation was run for each topology, and the mean throughput of these 50 runs was calculated.

Wireless relay nodes are deployed to solve two problems: network disconnection and long hops. Because user nodes are located randomly, a cell can be disconnected if some nodes are out of the maximum transmission ranges of all other nodes. Therefore, it is necessary to deploy relay nodes in the cell to keep all user nodes connected to the gateway. The long-hop problem exists only in experiment 4, in which the side length of the cell coverage area increases. In experiment 4, the maximum transmission range keeps fixed as the distance between the furthest node and the gateway increases, so the maximum hop count will increase. If the number of hops is too large, packets may suffer high delay and losses, so long hops should be avoided.

In each topology, wireless relay nodes are deployed using the Least-RN (Least number of Relay Nodes) algorithm. The Least-RN algorithm first selects the closest two nodes, one from the nodes that are connected to the gateway (or the gateway itself) and one from the user nodes that are disconnected from the gateway. Then it deploys relay nodes, spaced with a distance of the maximum transmission range, on the straight line between the two nodes. Finally, it repeats the above process until all user nodes are connected to the gateway. The Least-RN algorithm guarantees that the least number of wireless relay nodes are deployed.

In experiment 4, which varies the cell area size, the Cut-Hop algorithm is applied after the Least-RN algorithm to reduce long hops. Cut-Hop first calculates a routing tree rooted at the gateway using the MinHops routing algorithm (see below), and then cuts off the sub-trees that have more than 10 hops (note that the cell has no real routes yet; hops are only calculations by Cut-Hop). Finally, it deploys the least number of relay nodes to connect all these sub-trees to the gateway group, which is defined as the group including the gateway and the existing relay nodes.

The up radio of a mesh node uses the MinHops routing algorithm to select the path that minimizes the total number of hops from the mesh node to the gateway. The down radio of a mesh node use the Random channel assignment algorithm to select a channel randomly from all

the available channels. The up radio of a mesh node connects to its next-hop down radio by switching to the same channel.

Active user nodes were selected randomly from all user nodes, and their traffic was generated by Constant Bit Rate (CBR) sources that always have UDP packets to send. The data payloads in each UDP packet are 1000 bytes. TCP could not be used in the simulation experiments because its congestion control mechanism punishes flows with more hops and thus conflicts with the max-min fairness used by cell capacity.

The RTS/CTS scheme in 802.11 MAC was disabled in simulations. The RTS/CTS scheme is designed to solve the hidden-terminal problem in single-hop WLANs, where any two transmissions involve the base station. However, in multi-hop networks, such as CMESH cells, two transmissions no longer share a common mesh node, so the RTS/CTS scheme does not work well. Therefore, the RTS/CTS scheme in 802.11 MAC is disabled in CMESH cells.

In each simulation, throughput and packet delay for an active user node are measured for 10 seconds after the source rate control scheme enters a steady state. The steady state is determined as follows. The gateway increases the source rate threshold by 10 kbps if it finds that all the throughputs of active user nodes exceed the last threshold. The gateway sets the current threshold back to the last lower threshold if some throughputs of active user nodes are below the last threshold. After the gateway has decreased the source rate threshold three times, it will no longer increase the threshold and enters the steady state, in which throughputs and packet delay of user nodes are measured.

Other system parameters are all fixed. As mentioned earlier, the number of gateway radios is set to the number of channels, and each gateway radio operates on a different channel. Table 4.3 summarizes the major system parameters and their values.

The nominal cell capacity $\hat{x}$ derived from the MCCT algorithm (Algorithm 1) does not take protocol overhead into account. To compare with the throughput (data payload) achieved by a ns-2 simulation, the $\hat{x}$ was adjusted to estimate the usable cell capacity in the following two steps. In the first step, the $T_e$ in the MCCT algorithm was replaced by:

$$T_e = \frac{A_e}{l}\left(\frac{l}{w_e} + T_o\right), \tag{4.7}$$

where $l$ is the packet payload size and $T_o$ is the time spent on the protocol overhead for

transmitting the packet over edge $e$.

Table 4.3: Major parameters in the nominal cell capacity experiments

| **Parameter** | **Value** |
|---|---|
| Number of gateway radios | Number of channels |
| User node location distribution | Discrete uniform distribution |
| Number of cell topologies | 50 |
| Relay node deployment scheme | Least-RN (and Cut-Hop in experiment 4) |
| Channel assignment algorithm | Random |
| Routing algorithm | MinHops |
| Traffic direction | Downstream |
| Traffic type | UDP/CBR |
| Packet payload size | 1000 Bytes |
| Source rate adjustment step | 10 kbps |
| RTS/CTS scheme | Disabled |

The calculation of $T_e$ in this section takes the packet overhead of UDP and the deterministic protocol overhead in IEEE 802.11a into account, but it does not take collision-related overhead into account, and so may overestimate cell capacity. Thus, a capacity loss factor $\alpha$, $0 < \alpha \leq 1$, was introduced to model such unexplored cell capacity loss in the second step. The estimated usable cell capacity, denoted by $\hat{x}'$ is given by the nominal cell capacity $\hat{x}$ (using the adjusted $T_e$) multiplied by $\alpha$:

$$\hat{x}' = \hat{x} \cdot \alpha . \tag{4.8}$$

In Equation (4.8), $\alpha = 0.9$ is used (by curve-fitting) in the simulations, and the nominal cell capacity $\hat{x}$ is derived from the MCCT algorithm (Algorithm 1), with $T_e$ calculated by Equation (4.7) instead of Equation (4.3). Research on the improvement of the calculation accuracy of $T_e$ is left for future work.

### 4.3.4 Simulation Results

The results of estimated usable cell capacity calculated by Equation (4.8) and the ns-2 simulation results for random CMESH cells are shown in Figure 4.3. The mean throughput per active user node is drawn with its 95% confidence interval. It can be observed that the two sets of results match well for each experiment.

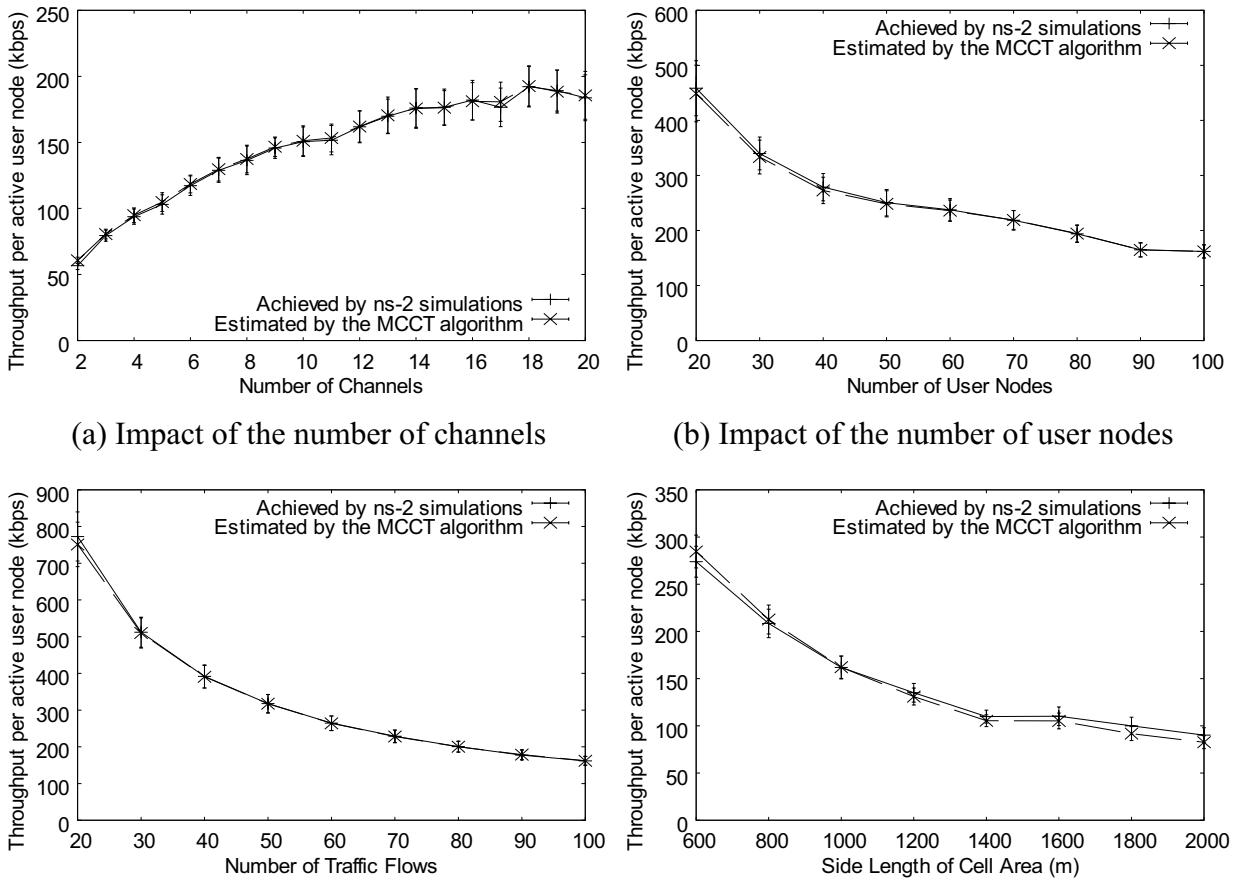


(a) Impact of the number of channels

(b) Impact of the number of user nodes

(c) Impact of the number of traffic flows

(d) Impact of the cell coverage area

Figure 4.3: Matching the estimated usable cell capacity to ns-2 simulation results

The estimation error of Equation (4.8) was calculated for the individual cell scenario (determined by the factor levels and the specific cell topology). For a specific cell, if Equation (4.8) estimates the throughput per active user node at $\hat{x}'$, but an ns-2 simulation achieved $\hat{x}_{ns}$, the estimation error $\delta$ is defined as $\delta = \frac{|\hat{x}' - \hat{x}_{ns}|}{\hat{x}_{ns}} \times 100\%$.

Table 4.4 summarizes the estimation errors in the four simulation experiments. Note that a major reason for the estimation errors of Equation (4.8) is the use of $\alpha$ to estimate the collision-related protocol overhead. Also notice that Figure 4.3 and Table 4.4 present different results because of their different interest: Figure 4.3 focuses on the capacity of random CMESH cells, while Table 4.4 focuses on the accuracy of the MCCT algorithm, so the former shows mean throughput and the latter shows statistics for individual estimation errors.

Table 4.4: Summary of the estimation errors

| Experiment # | Number of simulations | Estimation error ($\delta$) | |
|---|---|---|---|
| | | Mean | Standard deviation |
| 1 | 950 | 4.73% | 6.33 % |
| 2 | 450 | 4.34% | 3.98% |
| 3 | 450 | 3.99% | 3.54% |
| 4 | 400 | 5.83% | 5.47% |

## 4.4 Summary

This chapter assumed that the topology, the bit rates, loss rates, channels and interference relationships of wireless links and the single-path routes in a CMESH cell are all given and fixed. Based on this assumption, the Maximum Channel Collision Time (MCCT) algorithm was proposed, which is a multi-channel and multi-rate extension to Jun and Sichitiu's Bottleneck Collision Domain (BCD) algorithm. The MCCT algorithm gives an expression for the nominal capacity of a multi-radio, multi-channel, multi-rate and multi-hop cell in CMESHs. It is proved that the nominal cell capacity is achievable and is the exact cell capacity for small cells within the abstract models. The MCCT algorithm was further extended to take into account packet loss on edges and arbitrary traffic demands of user nodes.

To validate the nominal cell capacity derived from the MCCT algorithm, ns-2 simulations were performed in random CMESH cells. The simulations took wireless parameter values from the IEEE 802.11a standard and the specification of a Cisco 802.11a product, and used a max-min fairness mechanism to enforce the max-min throughput. The nominal cell capacity was first adjusted to estimate the usable cell capacity and was then compared with the ns-2 simulation results, and the two results were found to match well.

The nominal cell capacity is the theoretical basis for the channel assignment algorithms in Chapter 5 and the routing algorithms in Chapter 6 to improve cell capacity.

# CHAPTER 5
# CHANNEL ASSIGNMENT IN CMESH CELLS

As was discussed in Section 1.2.1, an important advantage of a CMESH is that it can utilize abundant high radio frequencies. In a CMESH, its all available radio frequencies are divided into multiple orthogonal channels that do not interfere with each other. For example, IEEE 802.11a has 12 orthogonal channels in the 5 GHz spectrum [56]. Fully and efficiently utilizing these available channels increases the aggregate bandwidth in a CMESH cell and can improve cell capacity. Therefore, channel assignment is an important research topic for a CMESH.

The channel assignment problem for a CMESH cell is as follows. The CMESH cell in the problem has a two-data-radio node design, where each node has an up radio and a down radio. The up radio of a node finds a path to the gateway, and the down radio of the node serves as a next-hop candidate for the up radios of other nodes to use its path to access the gateway. Once the up radio of a node has selected the down radio of another node as its next hop, it has to switch to the same channel used by the down radio, because two radios can communicate with each other only if they are on the same channel. Therefore, the channel assignment problem for a CMESH cell is to select channels for the down radios in the cell, with a goal of maximizing cell capacity, in terms of the max-min throughput.

The channel assignment problem can be studied either alone or jointly with the routing problem in CMESH cells. However, studying channel assignment and routing jointly in wireless networks increases the computational complexity of the problem [7, 81], so this thesis chooses to study them separately. This chapter studies the channel assignment problem only and assumes that the routes of nodes in a cell are given and fixed.

Channel assignment in multi-radio wireless networks is known to be an NP-hard problem [34, 106, 111, 117]. For example, Raniwala *et al.* [106] proved that with complete knowledge of network topology and traffic on links, the channel assignment problem with a goal of satisfying the expected load on links is NP-hard. This chapter shows that even the problem of channel assignment in small cells (offering no spatial reuse) is NP-hard (see Section 5.2.1). Because of

the large scale of a CMESH cell, it is not typically feasible to find the optimal channel assignment scheme. Thus, this chapter seeks to present only heuristic algorithms.

The roadmap of this chapter is as follows. This chapter first proves that the problem of channel assignment in small cells is equivalent to the multiprocessor scheduling problem [33]. Since the LPT (Longest Processing Time) algorithm works well for the multiprocessor scheduling problem, its counterpart, the CPLB-Cell algorithm, is used for channel assignment in small cells. In large cells, CPLB-Cell has a weakness that it does not take channel spatial reuse into account. Thus, this chapter proposed two modified algorithms for large cells: a centralized algorithm called CPLB and a distributed algorithm called DPLB. Then the weakness of CPLB in large cells is identified. To overcome the weakness of CPLB, this chapter further proposes two greedy algorithms based on the MCCT algorithm, called GMCCT-LB and CPLB-GMCCT. Finally, the performance of the proposed channel assignment algorithms are compared with some existing channel assignment algorithms through ns-2 simulations.]

Among the previous channel assignment algorithms (see Section 2.4), Raniwala and Chiueh's distributed channel assignment algorithm [107], named the Distributed Priority Least Traffic (DPLT) algorithm in this thesis, is of particular interest because it is closest to the DPLB algorithm proposed in this chapter and is used for performance comparison in the simulation experiments. Although the details of the DPLT algorithm are not fully disclosed in its original publication [107], the following differences between DPLT and DPLB can be observed.

- The DPLT algorithm assumes single-rate WMNs, but the DPLB algorithm also works for multi-rate WMNs.
- The DPLT algorithm relies on message exchanges among interfering nodes, but the DPLB algorithm can use carrier sense technology, which needs no message exchanges and thus saves network capacity. In addition, DPLB may perform better than DPLT in open systems where license-exempt radio bands such as that for IEEE 802.11a is used. This is because interference from other systems is inevitable in license-exempt radio bands. DPLT relies on message exchanges to share the traffic information within the system, but the information no longer reflects the real traffic due to interference from other systems. In contrast, DPLB may still work by carrier sensing other systems.
- The DPLT algorithm forbids lower priority (i.e., longer hops) radios from using the channels already used by higher priority radios within interference ranges, but the DPLB

algorithm allows this, if these channels are not fully utilized by higher priority radios.

The remainder of this chapter is organized as follows. The channel assignment problem and its assumptions are described in Section 5.1. Section 5.2 studies channel assignment in small cells and proves that this problem is equivalent to the multiprocessor scheduling problem, and thus introduces the CPLB-Cell algorithm. Section 5.3 studies channel assignment in large cells, and proposes the CPLB and DPLB algorithms and two greedy algorithms based on the MCCT algorithm. Section 5.4 evaluates the performance of the proposed algorithms by comparison with the DPLT algorithm and a Random algorithm through ns-2 simulations. Section 5.5 summarizes the work presented in this chapter.

## 5.1 Problem Formulation

Consider a CMESH cell, where a single gateway provides Internet access for up to hundreds of mesh nodes in the cell coverage area by utilizing multiple orthogonal channels, multi-rate wireless transmissions and multi-hop packet deliveries. The gateway has the only direct Internet connection in the cell. User traffic in the cell is only between user nodes and the gateway. See Section 1.2.2 for details.

Each mesh node has two data radios: an up radio and a down radio. The details for this two-data-radio node design has been discussed in Section 1.2.2. The gateway has multiple (up to the number of available orthogonal channels in the cell) down radios.

### 5.1.1 Assumptions

The following assumptions for channel assignment in CMESH cells are made in this chapter.

First, this chapter assumes that the cell topology and the single-path routes between mesh nodes and the gateway in a cell are all given and are stable. Relay nodes have been deployed in a cell so that all user nodes are connected to the gateway. The stability of cell topology is an advantage of CMESHs (see Section 1.2), and routing stability is a basic requirement in a CMESH (see Section 6.1.2). The stability of the cell topology and routing is important: channel assignment optimization is meaningful only if the cell topology and the routing in a cell do not change quickly so that channel assignment algorithms have time to adapt to their changes.

Second, this chapter assumes that the bit rates, loss rates and interference relationships of the wireless links in a cell are given and stable and are independent of channels. The stability of wireless links is an advantage of CMESHs (see Section 1.2). Field measurements [118] show

that 802.11a links for stationary nodes are stable but a few channels may perform poorly on some links because their received signal strength (RSS) happen to cross below a threshold. However, CMESHs may solve this problem by choosing a conservative RSS threshold for all channels. If this method fails and some links still have different quality on different channels, routing algorithms can avoid choosing these links. If both of the methods fail, channel assignment algorithms may choose channels from only a subset of candidate channels on which link quality is similar.

Finally, for simplicity purposes, this chapter assumes that a cell has only downstream user traffic (from the gateway to user nodes). In many cases, the problem of channel assignment for upstream traffic is different from the one for downstream traffic only in the description of traffic direction, which can be rather trivial and tedious. The algorithms proposed in this chapter can be easily extended to upstream user traffic because they are based on the MCCT algorithm which allows user traffic in both directions. This chapter chooses to present downstream traffic instead of upstream traffic because local access network users may have more interest in downstream traffic. For example, the network speed cited for local access networks using DSL and cable technologies typically refers only to downstream user traffic. Also, Section 3.3.3 showed that the upstream cell capacity is theoretically no less than the downstream cell capacity. For these reasons, this chapter assumes downstream user traffic only.

### 5.1.2 The System Model

For a vector $\vec{v} = (v_1, ...v_n)$, let $\hat{v}$ denote its set form, i.e., $\hat{v} = \{v_1, ...v_n\}$. Let $\hat{C} = \{1...C\}$, $C \geq 1$, denote the set of available orthogonal channels.

A CMESH cell can be modelled by a directed graph $\vec{\Omega} = (\vec{V}, \vec{E})$. A vector of vertexes $\vec{V} = (\vec{N}, \vec{G})$, where $\vec{N} = (N_1, ..., N_{m'})$ represents all the $m'$ nodes in the cell or their down radios (because each node has exactly one down radio) and $\vec{G} = (G_1, ..., G_m)$ represents all the $m$ ($1 \leq m \leq C$) down radios of the gateway $G$. Thus, the total number of down radios is $\left|\hat{V}\right| = m' + m$. Let edge vector $\vec{E}$ represent all the directed wireless links in the cell. Recall that this chapter assumes downstream traffic only, and let edge $e_{u,v} \in \hat{E}$ denote the directed wireless link from down radio $u \in \hat{V}$ to the up radio of node $v \in \hat{N}$.

If a vector is defined with a subscript $V$ or $E$, such as $\vec{B}_V$ or $\vec{B}_E$, the vector is based on $\vec{V}$ or $\vec{E}$, which means its elements have a one-to-one relationship to $\vec{V}$ or $\vec{E}$ in the same sequence. If $v \in \hat{V}$ or $e \in \hat{E}$ appears as the subscript of a vector name that is defined with a subscript $V$ or $E$, it denotes the vector's element index, which is equal to the index of $v$ or $e$ in vector $\vec{V}$ or $\vec{E}$. For example, if $\vec{V} = (a,b,c)$ and $\vec{B}_V = (1,2,3)$, then $B_c$ is used to refer to the third element in $\vec{B}_V$, i.e., $B_c = 3$, since $c$ is the third element in $\vec{V}$.

The single-path route of node $v \in \hat{N}$ is given by a set of edges $\hat{R}_v = \{e_{g,\cdot}, ..., e_{\cdot,v}\}$, where $e_{g,\cdot}$ denotes the edge starting from $g \in \hat{G}$, and $e_{\cdot,v}$ denotes the edge ending at $v$ on the path of $v$. Let $\vec{R}_V = (\hat{R}_1, ... \hat{R}_{|\hat{V}|})$ denote the vector of the single-path routes in a cell, where $\forall v \in \hat{G}$, $\hat{R}_v = \varnothing$. The set of mesh nodes whose routes to $G$ include edge $e \in \hat{E}$ is called the sub-tree of edge $e$, denoted by $\hat{V}_e$, given by $\hat{V}_e = \{v \mid \forall v \in \hat{V}, e \in \hat{R}_v\}$.

A user node is called an active user node if its traffic demand is greater than zero. Let $\vec{a} = (a_1, a_2, ... a_n)$, where $\vec{a} \subseteq \hat{N}$, denotes the vector of all the $n$ active user nodes in the cell.

The number of active user nodes in $\hat{V}_e$ is denoted by $A_e$, i.e.:

$$A_e = |\vec{a} \cap \hat{V}_e| = \left|\vec{a} \cap \{v \mid \forall v \in \hat{V}, e \in \hat{R}_v\}\right| \tag{5.1}$$

Edge $e$ is called an active edge if its $A_e > 0$. The set of all the active edges is denoted by $\hat{E}_A$: $\hat{E}_A = \{e \mid \forall e \in \hat{E}, A_e > 0\}$.

Define a child edge of $\forall v \in \hat{V}$ as edge $e_{v,u}$, where $u \in \hat{N}$ and $e_{v,u} \in \hat{R}_u$. The set of all the child edges of $\forall v \in \hat{V}$ is denoted by $\hat{E}_v$:

$$\hat{E}_v = \{e_{v,u} \mid \forall u \in \hat{N}, e_{v,u} \in \hat{R}_u\}. \tag{5.2}$$

Note that the above expression for $\hat{E}_v$ is simplified because this chapter assumes downstream user traffic only. Otherwise, in the case of upstream traffic, $\hat{E}_v = \{e_{u,v} \mid \forall u \in \hat{V}, e_{u,v} \in \hat{R}_u\}$.

### 5.1.3 The Wireless Model

This chapter uses the same wireless model as Section 4.1.2. It is summarized as follows.

Let vector $\vec{w}_E = (w_1, ..., w_{|\vec{E}|})$ denote the bit rates of all the edges in $\vec{E}$. Let vector $\vec{C}_E = (C_1, ..., C_{|\vec{E}|})$, where $\forall e \in \hat{E}$, $C_e \in \hat{C}$, denote the current channels on all the edges in $\vec{E}$. Let $\vec{I}_E = (\hat{I}_1, ..., \hat{I}_{|\vec{E}|})$ denote the interference vector, where $\forall e \in \hat{E}$, $\hat{I}_e$ denotes the set of edges that interfere with edge $e$ if they are on the same channel as edge $e$.

Let $\hat{I}_e(k)$ denote the set of edges on channel $k \in \hat{C}$ in $\hat{I}_e$:

$$\hat{I}_e(k) = \{e' \mid \forall e' \in \hat{I}_e, C_{e'} = k\}. \tag{5.3}$$

Let $\hat{I}_e^+(C_e)$ denote the set $\{e\} \bigcup \hat{I}_e(C_e)$, i.e.:

$$\hat{I}_e^+(C_e) = \{e\} \bigcup \{e' \mid \forall e' \in \hat{I}_e, C_{e'} = C_e\}. \tag{5.4}$$

Let $\tau_e$ denote the channel time spent on edge $e$, $e \in \hat{E}$ for transmitting one bit, which is calculated by:

$$\tau_e = 1 / w_e. \tag{5.5}$$

Note that the above expression for $\tau_e$ is simplified, and it can be extended to take into account the loss rate on edge $e$ (see Section 4.2.3).

Let $T_e$ denote the channel time spent on edge $e$ per second, for each active user node to achieve throughput of 1 bps. Because of single-path routing, $T_e$ is given by:

$$T_e = A_e \cdot \tau_e. \tag{5.6}$$

Note that $T_e$ in Equation (5.6) does not take into account protocol overhead. Thus, in the simulation experiments in Section 5.4, where IEEE 802.11a-compatible CMESH cells were studied, $T_e$ was adjusted by Equation (4.7), which takes into account the packet overhead of UDP and the deterministic protocol overhead in IEEE 802.11a, but it does not take into account collision-related overhead, which is left for future research.

Let $\vec{T}_V = (T_1, ..., T_{|\vec{V}|})$, where $T_v$ denotes the sum of channel time spent on all the edges in $\hat{E}_v$, $\forall v \in \hat{V}$ per second, for each active user node to achieve throughput of 1 bps:

$$T_v = \sum_{e \in \hat{E}_v} T_e. \tag{5.7}$$

### 5.1.4 The Channel Assignment Problem

For any $v \in \widehat{V}$, let $C_v \in \widehat{C}$ denote the channel assigned to the down radio $v$. Then the output of a channel assignment algorithm is a vector $\vec{C}_V = (C_1, ..., C_{|\widehat{V}|})$, which denotes the channels assigned on all the down radios in $\vec{V}$.

Because the up radio of a node has to follow the channel of its next-hop down radio as discussed earlier, channel assignment on edges is subject to the following constraint: if a down radio $v \in \widehat{V}$ switches to a channel $k \in \widehat{C}$, all its child edges $\widehat{E}_v$ must switch to the same channel $k$. In other words, $\forall v \in \widehat{V}$ and $\forall e \in \widehat{E}_v$, $C_e = C_v$.

Let $\vec{x} = (x_1, x_2, ..., x_n)$ denote a vector of feasible throughput allocations for the vector of active user nodes $\vec{a} = (a_1, a_2, ...a_n)$, each with infinite traffic demand. Let $x$ denote the minimum throughput in $\hat{x}$: $x = \min(\hat{x}) = \min\{x_1, x_2, ..., x_n\}$. The goal of the channel assignment problem is to find the vector $\vec{C}_V = (C_1, ..., C_{|\widehat{V}|})$ that maximizes $x$.

This chapter proposes greedy channel assignment algorithms based on the MCCT algorithm (see Chapter 4). For small cells, the MCCT algorithm gives the exact cell capacity within the abstract models. For large cells, although the MCCT algorithm gives only a conservative cell capacity, the simulation results in Chapter 4 suggest that it predicts cell capacity fairly accurately. Therefore, the MCCT algorithm can be used to guide the channel assignment algorithms in this chapter to improve cell capacity.

Note that the channel assignment problem is described with the default definition of cell capacity, where each active user node has infinite traffic demand. Thus, the proposed channel assignment algorithms in this chapter are based on the MCCT algorithm (Algorithm 1). The channel assignment problem and the proposed channel assignment algorithms can be extended to an arbitrary profile of traffic demands of user nodes by using the general definition of cell capacity (see Section 4.1.3) and the extended MCCT algorithm (Algorithm 2).

## 5.2 Channel Assignment in Small Cells

Recall that small cells refer to CMESH cells in which all the wireless links interfere with each other if they are on the same channel, i.e., $\forall e \in \widehat{E}$, $\{e\} \bigcup \widehat{I}_e = \widehat{E}$. The channel assignment

problem is simpler in small cells than in large cells because of this interference model.

This section proves that the problem of channel assignment in small cells is equivalent to the multiprocessor scheduling problem [33], and thus introduces the CPLB-Cell channel assignment algorithm for small cells.

### 5.2.1 An Equivalent Problem

The problem of channel assignment in small cells is equivalent to a well-known NP-hard optimization problem called the multiprocessor scheduling problem [33], as given by the following theorem. Note that it follows that the problem of channel assignment in small cells is also NP-hard.

**Theorem 10**. In small cells, the problem of channel assignment that maximizes cell capacity is equivalent to the multiprocessor scheduling problem that schedules all the tasks in set $\widehat{V}$, where $\forall v \in \widehat{V}$ has time length $T_v$, on $C$ processors and seeks to minimize the maximum accumulated time on these processors.

Proof. Theorem 8 proved that within the abstract models the exact cell capacity for small cells is the nominal cell capacity $\hat{x}$, given by $\hat{x} = 1/\max(\widehat{\text{CCT}})$, where $\widehat{\text{CCT}}=\{\text{CCT}_e \mid \forall e \in \widehat{E}_A\}$, $\text{CCT}_e = \sum_{e' \in \widehat{I}_e^+(C_e)} (A_{e'} / w_{e'})$ and $\widehat{I}_e^+(C_e) = \{e\} \bigcup \{e' \mid e' \in \widehat{I}_e, C_{e'} = C_e\}$.

Define $\widehat{E}_k = \{e \mid \forall e \in \widehat{E}, C_e = k\}$ and $\text{CCT}_k = \sum_{e \in \widehat{E}_k} (A_e / w_e)$, $\forall k \in \widehat{C}$. By the definition of small cells, $\forall e \in \widehat{E}$, $\{e\} \bigcup \widehat{I}_e = \widehat{E}$. Thus, $\forall e \in \widehat{E}_A$ and $\forall e' \in \widehat{E}_A$, if $C_e = C_{e'} = k$, $\widehat{I}_e^+(C_e) = \widehat{I}_{e'}^+(C_{e'}) = \widehat{E}_k$ and $\text{CCT}_e = \text{CCT}_{e'} = \text{CCT}_k$. $\forall k \in \widehat{C}$, if $\widehat{E}_k = \varnothing$, $\text{CCT}_k = 0$. Thus the following holds:

$$\max(\widehat{\text{CCT}}) = \max\{\text{CCT}_e \mid \forall e \in \widehat{E}_A\} = \max\{\text{CCT}_k \mid k = 1...C\}. \tag{5.8}$$

In Equation (5.8), $\text{CCT}_k$ is defined by the edges on channel $k \in \widehat{C}$ in a cell. Reorganizing these edges by down radios on channel $k$, $\text{CCT}_k$ can be written as:

$$\text{CCT}_k = \sum_{\forall v \in \widehat{V}, C_v = k} T_v . \tag{5.9}$$

From $\hat{x} = 1/\max(\widehat{\text{CCT}})$, to maximize cell capacity $\hat{x}$ is to minimize the $\max(\widehat{\text{CCT}})$, which,

in other words, is to minimize $\max\{\text{CCT}_k \mid k=1...C\} = \max\{\sum_{\forall v \in \widehat{V}, C_v = k} T_v \mid k=1...C\}$. That is, the problem is equivalent to the multiprocessor scheduling problem that schedules all the tasks in set $\widehat{V}$, where $\forall v \in \widehat{V}$ has time length $T_v$, on $C$ processors and seeks to minimize the maximum accumulated time on these processors. □

Note that the original multiprocessor scheduling problem can be stated as follows. Given a set $T$ of tasks and number $M$ of processors, where task $T_i \in T$ has time length $L_i$, the problem seeks to find the minimum finish time required to schedule all the tasks on the processors.

### 5.2.2 The CPLB-Cell Algorithm

The multiprocessor scheduling problem has a simple and often used algorithm called the LPT (Longest Processing Time) algorithm, which sorts the tasks by their time lengths and then assigns them to the processor that has the minimum time of the existing assigned tasks. The LPT algorithm achieves within a factor of $4/3 - 1/(3M)$ of the optimal solution [45], where $M$ is the number of processors.

Since the problem of channel assignment in small cells is equivalent to the multiprocessor scheduling problem, the LPT algorithm can be used for channel assignment in small cells. The corresponding algorithm is named CPLB-Cell, which is given as Algorithm 3.

The notation "CPLB" in "CPLB-Cell" stands for Centralized Priority Least Busy. CPLB-Cell is called a centralized algorithm because it runs at only the gateway, which calculates the results and then notifies mesh nodes to switch channels. In the problem of channel assignment in small cells, the procedure of LPT is described by PLB (Priority Least Busy), which sorts all the down radios by their $T_v$ in descending order and then assigns them to the least busy channel (i.e., the channel with the minimum accumulated $T_v$).

The notation "Cell" in "CPLB-Cell" indicates that the algorithm assumes that any two wireless links in the cell interfere with each other if they are on the same channel. This assumption is true in small cells by definition.

## 5.3 Channel Assignment in Large Cells

In large cells, channel spatial reuse (i.e., two simultaneous transmissions on the same channel can succeed if they are out of each other's interference range) makes the channel assignment

problem more difficult than that for small cells. This section studies the problem of channel assignment in large cells.

Algorithm 3: The CPLB-Cell channel assignment algorithm

Input: $\vec{V}$, $\vec{E}$, $\vec{a}$, $\vec{R}_V$, $\vec{w}_E$, $\widehat{C}$.

Output: $\vec{C}_V = (C_1, ..., C_{|\vec{V}|})$.

1. Get $\vec{A}_E = (A_1, ..., A_{|\vec{E}|})$ via $\vec{V}$, $\vec{E}$, $\vec{a}$ and $\vec{R}_V$ (Equation (5.1)).
2. Get $\vec{E}_V = (E_1, ..., E_{|\vec{V}|})$ via $\vec{V}$ and $\vec{R}_V$ (Equation (5.2)).
3. Get $\vec{T}_V = (T_1, ..., T_{|\vec{V}|})$ via $\vec{A}_E$, $\vec{E}_V$ and $\vec{w}_E$ (Equation (5.7) ).
4. Get $\vec{V}'$ as sorted $\vec{V}$ so that $\forall v \in \widehat{V}'$, $T_v \in \widehat{T}_V$ is in descending order.
5. Initialize vector $\vec{B} = (B_1, ..., B_C) = 0$.
6. For each sorted element $v$ in $\vec{V}'$:
   - 6.1) Get $k$ as the first element in $\widehat{K} = \{k \mid k \in \widehat{C}, B_k = \min(\widehat{B})\}$.
   - 6.2) Update $C_v \leftarrow k$.
   - 6.3) Update $B_k \leftarrow B_k + T_v$.

### 5.3.1 The Centralized PLB Algorithm

Although the CPLB-Cell channel assignment algorithm is designed for small cells, the core idea behind PLB can also be used in large cells. However, the following modification needs to be made.

The idea of PLB is that each down radio $v \in \widehat{V}$ selects the least busy channel within its interference range for all its child edges in $\widehat{E}_v$. Unlike in small cells, each child edge $e \in \widehat{E}_v$ in large cells may have a different set of interfering edges on channels: $\{\widehat{I}_e(k) \mid k = 1...C\}$. Recall $\widehat{I}_e(k) = \{e' \mid e' \in \widehat{I}_e, C_{e'} = k\}$. Therefore, in large cells, it is necessary to determine the set of interfering edges "seen" by a down radio $v \in \widehat{V}$ on channels, denoted by $\{\widehat{I}_v(k) \mid k = 1...C\}$. The choice made by this chapter is to set:

$$\hat{I}_v(k) = \bigcup_{e \in \hat{E}_v} \hat{I}_e(k) - \hat{E}_v . \tag{5.10}$$

Then the busy channel time "seen" by $v \in \hat{V}$ on channel $k$, denoted by $B_v(k)$, is:

$$B_v(k) = \sum_{e \in \hat{I}_v(k)} T_e . \tag{5.11}$$

The centralized PLB channel assignment algorithm for large cells, named CPLB, assigns any down radio $v \in \hat{V}$ the least busy channel calculated from $\vec{B}_v = (B_v(1), ..., B_v(C))$. The CPLB algorithm is given by Algorithm 4. Before the CPLB algorithm starts, all the down radios in a cell are not assigned to any channels, and $\vec{C}_V = (C_1 = -1, ..., C_{|\hat{V}|} = -1)$ denotes this initial state.

The CPLB algorithm runs only at the gateway. Before running the CPLB algorithm, the gateway needs to collect necessary information from the cell, including the cell topology, the routes of all mesh nodes and the bit rates (or the ETT in Section 4.2.3 for packet loss) and the interference vector of wireless links. The gateway uses the information collected as input, runs the CPLB algorithm to calculate the channel assignment result, and notifies the related mesh nodes to switch their down radios to the new channels.

The CPLB channel assignment algorithm uses infinite traffic demands of active user nodes as input to predict the channel time $T_v$ of the down radios in a cell. If channel assignment need not adapt to the real-time dynamic traffic demands, CPLB can be a low-cost and stable algorithm. This is because it is costly to collect real-time traffic information, and sometimes the real-time traffic may be too dynamic for channel assignment algorithms to follow.

### 5.3.2 The Distributed PLB Algorithm

If channel assignment is required to adapt to the real-time traffic in a CMESH cell, a distributed PLB algorithm (such as DPLB in this section) may be preferable to a centralized PLB algorithm because it has lower cost in this case. A distributed PLB algorithm runs at both mesh nodes and the gateway, which select channels for their down radios based on only information collected in their local areas.

A distributed PLB algorithm can have even lower cost if the MAC layer uses carrier sense technology as described in Section 3.1.2, because a down radio using carrier sense technology can directly sense the busy state of channels and find the least busy channel without sending

packets for exchanging channel usage information among neighbours.

If some types of 802.11 devices do not allow channel assignment algorithms to access channel busy states, it is still practical to estimate the channel busy time by sending probe packets to measure the round-trip time on wireless links [2]. Another way to obtain channel busy state information is to allow all the mesh nodes within the interference range of a mesh node (estimated by the number of hops to the mesh node [107]) to exchange the information of the traffic and the ETT (see Section 4.2.3) values of their wireless links. Then the mesh node can estimate the expected busy time that would have been sensed by its down radios.

Algorithm 4: The CPLB channel assignment algorithm

Input: $\vec{V}$, $\vec{E}$, $\vec{a}$, $\vec{R}_V$, $\vec{I}_E$, $\vec{w}_E$, $\widehat{C}$.

Output: $\vec{C}_V = (C_1,...,C_{|\vec{V}|})$.

1. Get $\vec{A}_E = (A_1,...,A_{|\vec{E}|})$ via $\vec{V}$, $\vec{E}$, $\vec{a}$ and $\vec{R}_V$ (Equation (5.1)).
2. Get $\vec{E}_V = (E_1,...,E_{|\vec{V}|})$ via $\vec{V}$ and $\vec{R}_V$ (Equation (5.2)).
3. Get $\vec{T}_E = (T_1,...,T_{|\vec{E}|})$ via $\vec{E}$, $\vec{A}_E$ and $\vec{w}_E$ (Equation (5.6)).
4. Get $\vec{T}_V = (T_1,...,T_{|\vec{V}|})$ via $\vec{T}_E$ and $\vec{E}_V$ (Equation (5.7)).
5. Get $\vec{V}'$ as sorted $\vec{V}$ so that $\forall v \in \widehat{V}', T_v \in \widehat{T}_V$ is in descending order.
6. Update $C_v \leftarrow C \in \widehat{C}$, $\forall v \in \widehat{V}$, $T_v \in \widehat{T}_V$ and $T_v = 0$.

Loop {

7. For each sorted element $v$ in $\vec{V}'$, $T_v > 0$:
   - 7.1) Get $\vec{B}_v = \left(B_v(1),...,B_v(C)\right)$ via $\vec{T}_E$ and $\vec{I}_E$ (Equation (5.11)).
   - 7.2) Get $\widehat{K} = \{k \mid k \in \widehat{C}, B_v(k) = \min(\widehat{B}_v)\}$.
   - 7.3) Get $k = C_v$ if $C_v \in \widehat{K}$; otherwise, get $k$ as the first element in $\widehat{K}$.
   - 7.4) Update $C_v \leftarrow k$ if $C_v \neq k$.
8. If no $C_v$ is updated in this iteration of the loop, then this algorithm exit.

} End Loop

To simplify the algorithm descriptions, the proposed distributed PLB algorithm, called DPLB, assumes that carrier sense technology is available and each mesh node also has a helper radio (see Section 1.2.2). For DPLB to work, a down radio needs to know its priority among all the down radios in a cell in order to determine the timing of its channel switches. In other words, if two down radios are both on channel $k \in \widehat{C}$ and both find another channel to be less busy, a priority policy is necessary for them to decide which should switch its channel first. Otherwise, they may both leave channel $k$ and their sudden simultaneous leaving may cause channel $k$ to again become the least busy channel for them.

The DPLB algorithm determines the priority of any down radio $v \in \widehat{V}$ in a cell based on its number of hops to the gateway, denoted by $h_v$. Because the traffic pattern of a cell is between user nodes and the gateway, traffic from different user nodes will accumulate as it approaches the gateway. Therefore, down radios close to the gateway generally have heavier traffic and larger $T_v$, so they should be granted higher priority in channel selection. Down radios with higher priority are designed to experience fewer collisions and take up more transmission time by driving away down radios with lower priority from a channel if necessary.

The DPLB algorithm allows a mesh node $v$ to switch channels for its down radio only at the specific timings, which are calculated based on $h_v$. The down radio and the helper radio sense and record the accumulated busy time of a channel during a sensing period of $P_{\mathrm{s}}$ seconds. The down radio senses only its current channel, and the helper radio senses the other channels. Thus, each node can use $P_{\mathrm{u}} = (C-1)P_{\mathrm{s}}$ seconds to finish sensing $C$ channels. Note that if nodes do not have helper radios, they may let down radios sense the busy time of all channels by sampling and $P_{\mathrm{u}}$ could be calculated in a different way.

Let $H$ denote the maximum number of hops in a cell. The period for all the down radios in the cell to finish sensing and switching channels based on their priority (the number of hops to the gateway) is $HP_{\mathrm{u}}$ seconds. The down radio of mesh node $v$ whose number of hops to the gateway is $h_v$ switches channels only at the end of a time interval $P_v = (H - h_v + 1)P_{\mathrm{u}}$. A variance of time $\alpha P_{\mathrm{u}}$, where $\alpha$ is a random number uniformly distributed between 1 and $(H - h_v + 1)$, is added to $P_v$ when the algorithm is started in order to avoid synchronization among mesh nodes with the same number of hops.

By this design, the down radios of nodes closer to the gateway will switch their channels less frequently and keep their channel stable. This is important because down radios closer to the gateway are likely to have heavy traffic. When down radios with heavy traffic switch channels, they significantly change the channel busy status of both the old channel and the new channel, and thus are more likely to cause the performance of a cell to be unstable.

The DPLB algorithm is given as Algorithm 5. Before the algorithm starts, the gateway and the mesh nodes need to prepare the necessary information, including $\widehat{C}$, $H$, $P_s$ and $h_v$, for any down radio $v \in \widehat{V}$. Note that DPLB simply seeks to adapt to the real-time traffic in a cell, so it needs to work with the max-min fairness mechanism (see Section 4.3.1) in order to provide max-min throughput for user nodes.

In the second step in the DPLB channel assignment algorithm, the mesh node or the gateway measures channel busy time as follows. A channel is considered to be busy if a radio detects the accumulated received signal strength on the sensed channel is above a carrier sensing threshold. A down radio senses its current channel only when it is not sending or receiving packets so that the measured busy channel time does not include the time for its own traffic. The helper radio senses the other channels continuously. The down radio of a mesh node or its helper radio measures the accumulated busy time of channel $k \in \widehat{C}$ during $P_s$ seconds.

Algorithm 5: The DPLB channel assignment algorithm

Input for $v \in \widehat{V}$: $H$, $P_s$, $\widehat{C}$ and $h_v$.

Output for $v$: $C_v$.

1. The mesh node or the gateway starts a $P_v$ timer for its down radio $v$, where $P_v = (H - h_v + 1)(C-1)P_s$, after a random delay $\alpha(C-1)P_s$, where $\alpha$ is a random number between 1 and $(H - h_v + 1)$ and $C = \left|\widehat{C}\right|$.
2. The mesh node or the gateway senses the busy time of each channel in $\widehat{C}$ during the last $(C-1)P_s$ seconds right before the $P_v$ timer expires.
3. When the $P_v$ timer expires, the mesh node or the gateways switches its down radio $v$ to the least busy channel if it is not the radio's current channel.

### 5.3.3 The GMCCT-LB Algorithm

In a large cell, the CPLB channel assignment algorithms may not be able to maximize the nominal cell capacity given by the MCCT algorithm, i.e., to minimize the maximum CCT of the active edges in the cell (see Section 4.2). This is because CPLB seeks to minimize the CCT "seen" by each down radio in a cell greedily, but is unaware of the maximum CCT of the active edges in the entire cell.

To overcome the weakness of CPLB, greedy channel assignment algorithms based on the MCCT algorithm are proposed, which greedily minimize the maximum $\text{CCT}_e$, $\forall e \in \widehat{E}_A$ under the channel assignment constraint: $\forall v \in \widehat{V}$ and $\forall e \in \widehat{E}_v$, $C_e = C_v$. Such an algorithm can start either from scratch or from the result of the CPLB channel assignment algorithms.

The MCCT algorithm requires $\vec{C}_E = (C_1, ..., C_{|\bar{E}|})$ as input, but channel assignment algorithms deal with $\vec{C}_V = (C_1, ..., C_{|\bar{V}|})$. Therefore, it is necessary to convert $\vec{C}_V$ to $\vec{C}_E$. Let $\vec{C}_E(\vec{C}_V)$ denote the result of the process that converts $\vec{C}_V$ to $\vec{C}_E$, which is given by $C_e = C_v$, where $e \in \widehat{E}_v$. Let $\vec{C}_V(C_v = k)$ denote the new channel assignment scheme $\vec{C}_V$ if down radio $v$ in the current $\vec{C}_V$ is assigned to channel $k \in \widehat{C}$ and the other down radios remain on their current channels.

The following proposes a greedy MCCT-based channel assignment algorithm for large cells, called GMCCT-LB. Here, the term "greedy" indicates that each decision of assigning a channel to a down radio is to minimize the maximum CCT of the active edges in a cell, although this does not guarantee the final channel assignment scheme is optimal. If there are multiple candidate channels, the GMCCT-LB algorithm selects the least busy (LB) channel among them.

The GMCCT-LB channel assignment algorithm is given as Algorithm 6. Before the algorithm starts, the down radios in a cell are not assigned to any channels, and let $\vec{C}_V = (C_1 = -1, ..., C_{|\bar{V}|} = -1)$ denote this initial state.

### 5.3.4 The CPLB-GMCCT Algorithm

The GMCCT-LB algorithm is based on the MCCT algorithm and selects the least busy channel only when MCCT gives multiple candidate channels. The MCCT algorithm can also be used to help the CPLB channel assignment algorithm to overcome its weakness that the down

radios are unaware of the global channel usage in the cell.

Algorithm 6: The GMCCT-LB channel assignment algorithm

Input: $\vec{V}$, $\vec{E}$, $\vec{a}$, $\vec{R}_V$, $\vec{I}_E$, $\vec{w}_E$, $\widehat{C}$.

Output: $\vec{C}_V = (C_1, ..., C_{|\vec{V}|})$.

1. Get $\vec{A}_E = (A_1, ..., A_{|\vec{E}|})$ via $\vec{V}$, $\vec{E}$, $\vec{a}$ and $\vec{R}_V$ (Equation (5.1)).
2. Get $\vec{E}_V = (E_1, ..., E_{|\vec{V}|})$ via $\vec{V}$ and $\vec{R}_V$ (Equation (5.2)).
3. Get $\vec{T}_E = (T_1, ..., T_{|\vec{E}|})$ via $\vec{E}$, $\vec{A}_E$ and $\vec{w}_E$ (Equation (5.6)).
4. Get $\vec{T}_V = (T_1, ..., T_{|\vec{V}|})$ via $\vec{T}_E$ and $\vec{E}_V$ (Equation (5.7)).
5. Get $\vec{V}'$ as sorted $\vec{V}$ so that $\forall v \in \widehat{V}', T_v \in \widehat{T}_V$ is in descending order.
6. Update $C_v \leftarrow C \in \widehat{C}$, $\forall v \in \widehat{V}$ and $T_v = 0$.

Loop {

7. For each sorted element $v$ in $\vec{V}', T_v > 0$:
   - 7.1) Get $\vec{M} = (M_1, ..., M_C)$, where $M_k, k \in \widehat{C}$ is the $\max(\widehat{\text{CCT}})$ in Algorithm 1 with $\vec{V}$, $\vec{E}$, $\vec{a}$, $\vec{R}_V$, $\vec{C}_E\left(\vec{C}_V(C_v = k)\right)$, $\vec{I}_E$, $\vec{w}_E$ as input.
   - 7.2) Get $\widehat{K} = \{k \mid k \in \widehat{C}, M_k = \min(\widehat{M})\}$.
   - 7.3) Get $\widehat{B}_v = \{B_v(k) \mid \forall k \in \widehat{K}\}$ via $\vec{T}_E$ and $\vec{I}_E$ (Equation (5.11)).
   - 7.4) $\widehat{K}' = \{k \mid \forall k \in \widehat{K}, B_v(k) = \min(\widehat{B}_v)\}$.
   - 7.5) Get $k = C_v$ if $C_v \in \widehat{K}'$; otherwise get $k$ as the first element in $\widehat{K}'$.
   - 7.6) Update $C_v \leftarrow k$ if $C_v \neq k$.
8. If no $C_v$ is updated in this iteration of the loop, then this algorithm exits.

} End Loop

The CPLB-GMCCT algorithm is based on CPLB (it starts and ends with the CPLB algorithm) but uses the MCCT algorithm to minimize $\max(\widehat{\text{CCT}})$ (i.e., the maximum $\text{CCT}_e$, $\forall e \in \widehat{E}_A$) in a

cell. CPLB-GMCCT greedily switches the down radios whose edges are used in the calculation of $\max(\widehat{\text{CCT}})$ to other less busy channels if such a channel switch can minimize $\max(\widehat{\text{CCT}})$.

The CPLB-GMCCT algorithm is given as algorithm 7. Before the algorithm starts, the down radios in a cell are not assigned to any channels. $\vec{C}_V = (C_1 = -1, ..., C_{|\vec{V}|} = -1)$ denotes this initial state. Note that in step 8.3a the CPLB algorithm assigns channels to the down radios of a cell, except down radio $v$, which is fixed to channel $k$.

### 5.4 Performance Comparisons

In this section, the performance of the proposed channel assignment algorithms is evaluated by comparison with the DPLT algorithm [107] and a random channel assignment algorithm in 802.11a-compatible random CMESH cells through ns-2 simulations.

To simulate 802.11a-compatible CMESH cells, the ns-2 simulator was modified to support multiple radios per node, multiple channels, multiple bit rates, IEEE 802.11a and a max-min fairness mechanism, as introduced in Section 4.3.1 and Section 4.3.2.

Because the goal of the channel assignment algorithms is to maximize cell capacity, the major performance metric is the max-min throughput. The average throughput and the average packet delay of active user nodes are also shown, but they are treated as secondary performance metrics. The average packet delay is shown to examine three concerns: what is the range of average packet delay, whether the improvement in cell capacity comes at the cost of increased average packet delay, and how system factors impact the average packet delay.

For the same reasons as Section 4.3.3, four experiments—experiment 1 to experiment 4—were performed, with each varying one of the following four factors respectively: the number of channels, the number of user nodes, the number of traffic flows and the cell area size. In each experiment, the other three factors are fixed to their default levels. The levels and default levels of the four factors are listed in Table 4.2. The reason for selecting these values is the same as in Section 4.3.3.

In each experiment, seven channel assignment algorithms—Random, DPLT [107], DPLB, CPLB-Cell, CPLB, GMCCT-LB and CPLB-GMCCT—are compared. The Random algorithm selects a channel from all the available channels in a cell randomly for each down radio.

Algorithm 7: The CPLB-GMCCT channel assignment algorithm

Input: $\vec{V}$, $\vec{E}$, $\vec{a}$, $\vec{R}_V$, $\vec{I}_E$, $\vec{w}_E$, $\widehat{C}$.

Output: $\vec{C}_V = (C_1, ..., C_{|\vec{V}|})$.

1. Get $\vec{A}_E = (A_1, ..., A_{|\vec{E}|})$ via $\vec{V}$, $\vec{E}$, $\vec{a}$ and $\vec{R}_V$ (Equation (5.1)).

2. Get $\vec{E}_V = (E_1, ..., E_{|\vec{V}|})$ via $\vec{V}$ and $\vec{R}_V$ (Equation (5.2)).

3. Get $\vec{T}_E = (T_1, ..., T_{|\vec{E}|})$ via $\vec{E}$, $\vec{A}_E$ and $\vec{w}_E$ (Equation (5.6))

4. Get $\vec{T}_V = (T_1, ..., T_{|\vec{V}|})$ via $\vec{T}_E$ and $\vec{E}_V$ (Equation (5.7)).

Loop {

5. Get $\vec{C}_V = (C_1, ..., C_{|\vec{V}|})$ via the CPLB algorithm (Algorithm 4) with $\vec{V}$, $\vec{E}$, $\vec{a}$, $\vec{R}_V$, $\vec{I}_E$, $\vec{w}_E$, $\widehat{C}$ as input.

6. Get $M = \max(\widehat{\text{CCT}})$ in the MCCT algorithm (Algorithm 1) with $\vec{V}$, $\vec{E}$, $\vec{a}$, $\vec{R}_V$, $\vec{C}_E(\vec{C}_V)$, $\vec{I}_E$, $\vec{w}_E$ as input and find the corresponding $\widehat{I}_e^+(C_e)$ that gives $M$.

7. Get $\vec{V}'$ that includes all elements in $\{v \mid \forall e' \in \widehat{I}_e^+(C_e), \forall v \in \widehat{V}, e' \in \widehat{E}_v\}$ and that $\forall v \in \widehat{V}', T_v \in \widehat{T}_V$ is in descending order.

8. For each sorted element $v$ in $\vec{V}'$, $T_v > 0$:

   8.1) Get $\vec{B}_v = \left(B_v(1), ..., B_v(C)\right)$ via $\vec{T}_E$ and $\vec{I}_E$ (Equation (5.11)).

   8.2) Get $\vec{C}'$ as sorted $\vec{C}$ so that $\forall k \in \widehat{C}', B_v(k)$ is in ascending order.

   8.3) For each sorted element $k$ in $\vec{C}'$, $k \neq C_v$.

      8.3a) Get $\vec{C}'_V = (C'_1, ..., C'_{|\vec{V}|})$ via the CPLB algorithm, fixing $C_v = k$.

      8.3b) Get $M' = \max(\widehat{\text{CCT}})$ via Algorithm 1, with $\vec{C}_E(\vec{C}'_V)$ as channel input.

      8.3c) Update $C_v \leftarrow k$ and go back to Loop if $M' < M$.

9. If no $C_v$ is updated in this iteration of the loop, then this algorithm exits.

} End Loop

The four simulation experiments share a common set of 50 cell topologies. In each topology, the gateway is always located at the centre of a square cell area. User node locations are randomly generated following a discrete uniform distribution (on 1m×1m grids) inside the cell area. For each factor value in each experiment, one simulation is run for each topology, and the mean throughput and delay of these 50 runs are calculated. In the figures showing the max-min throughput, bars show the 95% confidence intervals.

Relay nodes are deployed to handle two problems: network disconnection and long hops. The Least-RN algorithm in Section 4.3.3 is used to keep the network connected. It deploys the least number of relay nodes into the cell in order to keep all user nodes connected to the gateway. The long-hop problem exists only in experiment 4, when the cell area sizes increases to a large value. Thus, in experiment 4, the following Cut-Hop algorithm (note: not the one in Section 4.3.3) is used to replace the Least-RN algorithm. The Cut-Hop algorithm introduces a concept called the gateway group, consisting of the gateway and all relay nodes. Cut-Hop starts with a relay node deployment process that deploys the least number of relay nodes that connect all the disconnected sub-networks to the gateway group. Then Cut-Hop uses the MTM routing algorithm [15] to calculate a routing tree rooted at the gateway, and cuts off sub-trees whose nodes have more than 10 hops on the routing tree. Finally, Cut-Hop repeats the above relay node deployment process by treating these sub-trees as disconnected sub-networks.

The routing algorithm used in all the four experiments is based on the MTM algorithm. The MTM algorithm is selected by the following two criteria. First, the selected routing algorithm should not use the channel information in a cell as input, because channel assignment algorithms have not run yet (recall that this chapter assumes that routing algorithms have run before channel assignment). Second, the selected routing algorithm should provide good performance for multi-hop wireless networks; otherwise, it is likely to become the bottleneck issue and cause all channel assignment algorithms to perform poorly. For example, the MinHops routing algorithm should not be used because it performs poorly in multi-hop wireless networks [15, 31]. Filtered by the two criteria, the MTM algorithm is one of the most suitable existing routing algorithms because it is designed for multi-rate and multi-hop wireless networks and is independent of channel assignment (see Section 2.5.2).

However, the MTM routing algorithm has a weakness: it cannot distinguish candidate paths that have the same MTM metric value. This case can be common in CMESH cells, so two

modifications are made to the MTM routing algorithm. First, the MTM routing algorithm is modified to select the path with the minimum hop count among candidate paths with the same MTM value. Second, the MTM routing algorithm is modified to perform traffic load balancing among the gateway radios. This is because the up radios of nodes whose next-hop candidates are gateway radios will find that all these radios have the same MTM value and hop count. The modified MTM routing algorithm is named the MTM-LB (LB stands for Load Balancing) routing algorithm.

In order to be fair to DPLT, MTM-LB performs traffic load balancing among the gateway radios by selecting the gateway radio with the least traffic (instead of least busy time, which favours the proposed PLB algorithms) for the up radios of nodes whose next-hop candidates are gateway radios. If two gateway radios have equal traffic, the one with a smaller number of sub-tree nodes is selected.

Other parameters are set in the same way as in Section 4.3.3. Table 5.1 summarizes the major parameters and their values.

Table 5.1: Major parameters in the channel assignment experiments

| **Parameter** | **Value** |
|---|---|
| Number of gateway radios | Number of channels |
| User node location distribution | Discrete uniform distribution |
| Number of cell topologies | 50 |
| Relay node deployment scheme | Least-RN/Cut-Hop |
| Routing algorithm | MTM-LB |
| Traffic direction | Downstream |
| Traffic | UDP/CBR |
| Packet payload size | 1000 Bytes |
| Source rate adjustment step | 10 kbps |
| RTS/CTS scheme | Disabled |

### 5.4.1 Impact of the Number of Channels

Experiment 1 examines the performance of the channel assignment algorithms in random CMESH cells as the number of channels increases. The results are shown in Figure 5.1.

It is not surprising that Random gives the lowest cell capacity in Figure 5.1(a), because it is unaware of routes, traffic and link quality and thus cannot allocate channels to where they are

needed for traffic delivery. Figure 5.1(c) shows that the average throughput is above but close to the max-min throughput. This is because the max-min fairness mechanism in the simulations stops increasing the source rate threshold after the max-min throughput is reached.

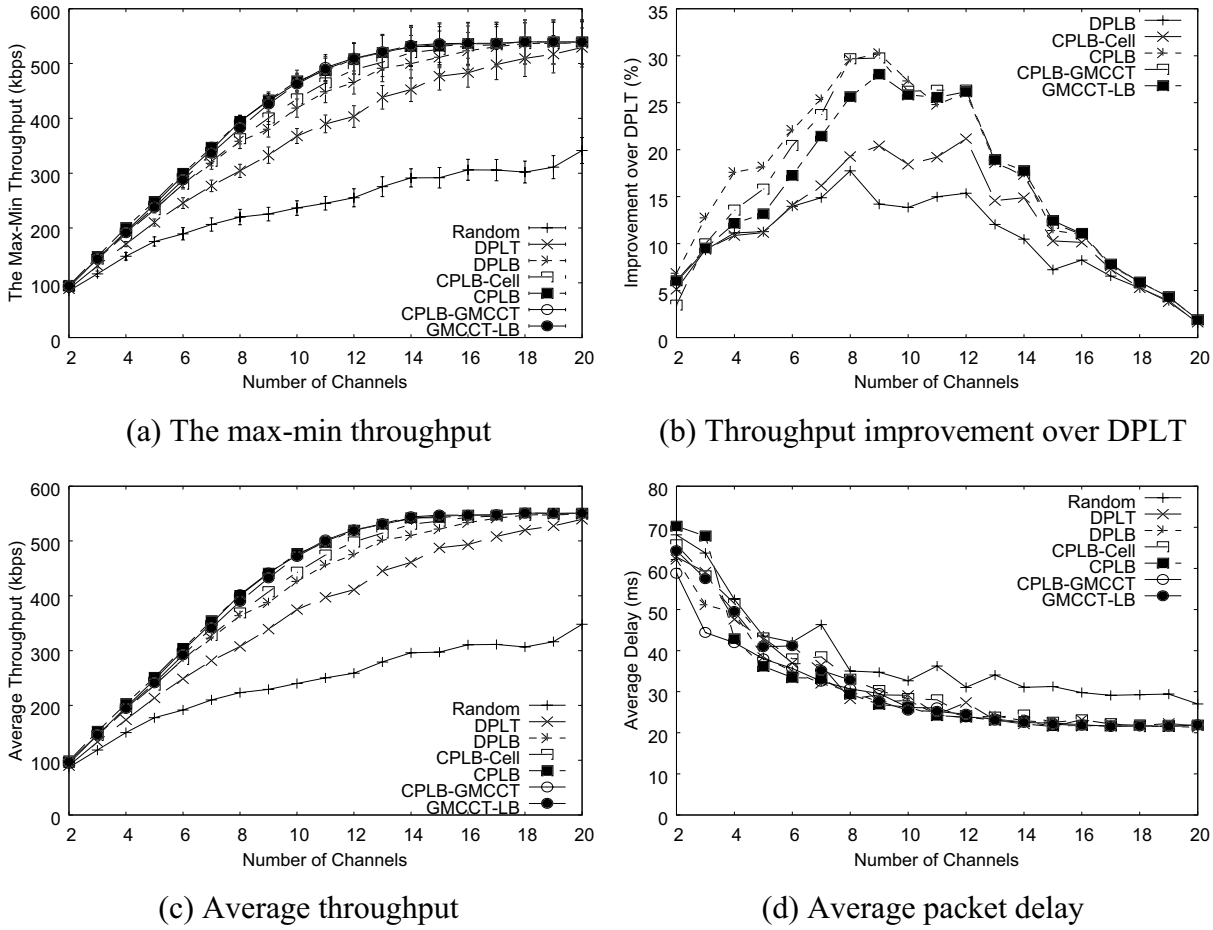


(a) The max-min throughput

(b) Throughput improvement over DPLT

(c) Average throughput

(d) Average packet delay

Figure 5.1: Impact of the number of channels on channel assignment algorithms (Run after the MTM-LB routing algorithm)

Recall that CPLB-GMCCT is proposed to overcome the weakness of CPLB, which is unaware of the channel usage in the entire cell. However, in most ns-2 simulation results, CPLB-GMCCT does not show significant cell capacity improvement over CPLB. This is because CPLB-GMCCT does not take into account collision-related overhead, which leads to estimation errors for the usable cell capacity (see Section 4.3.3). These estimation errors mislead CPLB-GMCCT and prevent it from outperforming CPLB. Thus, once collision-related overhead is accurately modelled, CPLB-GMCCT will outperform CPLB in ns-2 simulations.

Because the above three observations hold in all experiments, they will not be discussed again in the rest of this chapter.

Figure 5.1(a) shows the max-min throughput with its 95% confidence interval. It can be observed that the proposed channel assignment algorithms achieve significantly higher cell capacity than the DPLT algorithm when the number of channels is below 14. Figure 5.1(b) shows that the proposed algorithms increase the max-min throughput by up to 30% above DPLT.

As the number of channels increases above 14, the MTM-LB routing algorithm starts to become the major factor that limits cell capacity, so DPLT and the proposed algorithms achieve similar the max-min throughput. For example, as the number of channels exceeds 18, it is found that all the proposed channel assignment algorithms encounter a bottleneck wireless link that exclusively uses a channel within its interference range. This means that cell capacity is maximized by means of channel assignment and cannot be increased further unless routing algorithms help to remove some traffic from the bottleneck wireless link. The above analysis is validated in Section 6.3.3, which redoes the channel assignment simulations by using a proposed routing algorithm called GMCCT-CPLB. The simulation results for this experiment in Section 6.3.3 show that the bottleneck is removed and the proposed channel assignment algorithms achieve up to 55% max-min throughput improvement over DPLT.

Among the proposed channel assignment algorithms, Figure 5.1(a) and Figure 5.1(b) show that the proposed CPLB, GMCCT-LB and CPLB-GMCCT algorithms generally perform better than the DPLB and CPLB-Cell algorithms. In Figure 5.1(b), when the number of channels is small, CPLB performs slightly better than GMCCT-LB and CPLB-GMCCT because MCCT predicts cell capacity less accurately due to packet collisions and misleads GMCCT-LB and CPLB-GMCCT.

Figure 5.1(d) shows that the proposed channel assignment algorithms have average packet delay similar to DPLT as the number of channels increases. This means that the improvement in cell capacity over other algorithms does not come at the cost of higher average packet delay. In addition, it can be observed that for all algorithms, the average packet delay generally decreases as the number of channels increases. This is because packets need less waiting time for idle channels and encounter fewer collisions and retransmissions as the number of channels increases. Finally, the average packet delay in the simulations is on the order of tens of milliseconds, which may be decreased further by future research.

In summary, the simulation results for this experiment show that the proposed channel assignment algorithms significantly increase the max-min throughput and have average packet delay similar to DPLT. In addition, the capacity of random CMESH cells improves as the number of channels increases until a threshold is reached. Above this threshold, a bottleneck caused by the MTM-LB routing algorithm is encountered, and channel assignment algorithms cannot further increase cell capacity by themselves without the help from routing or relay node deployment algorithms.

### 5.4.2 Impact of the Number of User Nodes

Experiment 2 examines the performance of the channel assignment algorithms in random CMESH cells as the number of user nodes increases. The results are shown in Figure 5.2.

Figure 5.2(a) shows that the proposed channel assignment algorithms increase the max-min throughput significantly compared to DPLT when a cell has more than 70 user nodes. Up to a roughly 27% increase is observed in Figure 5.2(b). In addition, Figure 5.2(b) shows that the throughput gain generally increases as the number of user nodes increases. The reason is as follows. As the number of user nodes is small, the major factor that limits cell capacity is the poor quality of wireless links, caused by long transmission distances, instead of channel assignment algorithms. As the number of user nodes increases, there are more high-quality links in the cell. The proposed channel assignment algorithms can then utilize these high-quality links to improve cell capacity, but DPLT cannot even identify them.

Figure 5.2(d) shows that the proposed channel assignment algorithms have similar average packet delay to DPLT as the number of channels increases. This suggests that the improvement in cell capacity over other algorithms does not come at the cost of higher packet delay. In addition, it can be observed that for all the algorithms presented here, the average packet delay generally decreases as the number of user nodes increases because the bit rates of wireless links in general increase as the number of user nodes increases and the average packet transmission delay is significantly reduced accordingly. Finally, the average packet delay in the simulations is on the order of tens of milliseconds, which may be decreased further by future research.

Figure 5.2(a) and Figure 5.2(c) show that the throughput per user node tends to decrease as the number of user nodes increases, but the rate of decrease is slow and the per-user-node throughput even increases at some points. This phenomenon does not contradict the theoretical

results in Chapter 3, which say that the per-user-node throughput is inversely proportional to the number of user nodes. The first reason is that the theoretical results in Chapter 3 assume that relay nodes are deployed along the straight-line paths between user nodes and the gateway. However, in this experiment only the minimum relay nodes are deployed for the purpose of network connectivity. As shown in Figure 5.3, the average number of relay nodes per topology is very small. The second reason is that when the number of user nodes is small, these user nodes are likely to suffer poor-quality wireless links on paths because of poor network connectivity. As the number of user nodes increases, there will be more high-quality wireless links on paths because of increased connectivity. Therefore, the per-user-node throughput increase caused by new high-quality links will partially compensate for the per-user-node throughput loss caused by new user nodes as the number of user nodes increases.

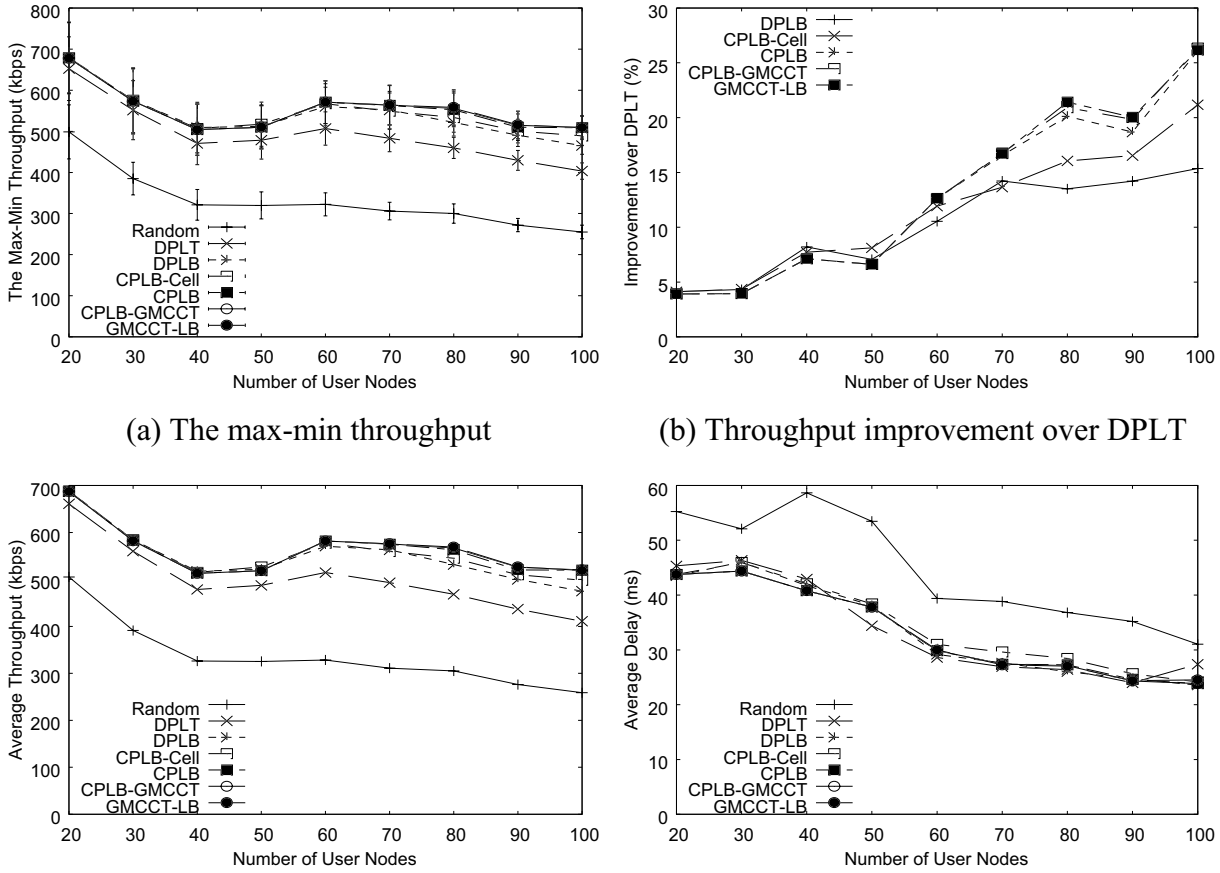


(a) The max-min throughput

(b) Throughput improvement over DPLT

(c) Average throughput

(d) Average packet delay

Figure 5.2: Impact of the number of user nodes on channel assignment algorithms (Run after the MTM-LB routing algorithm)

This experiment shows an important advantage of CMESHs: adding user nodes to a cell may not necessarily decrease per-user-node throughput or increase the average packet delay, because adding user nodes can increase network connectivity and improve the quality of wireless links.

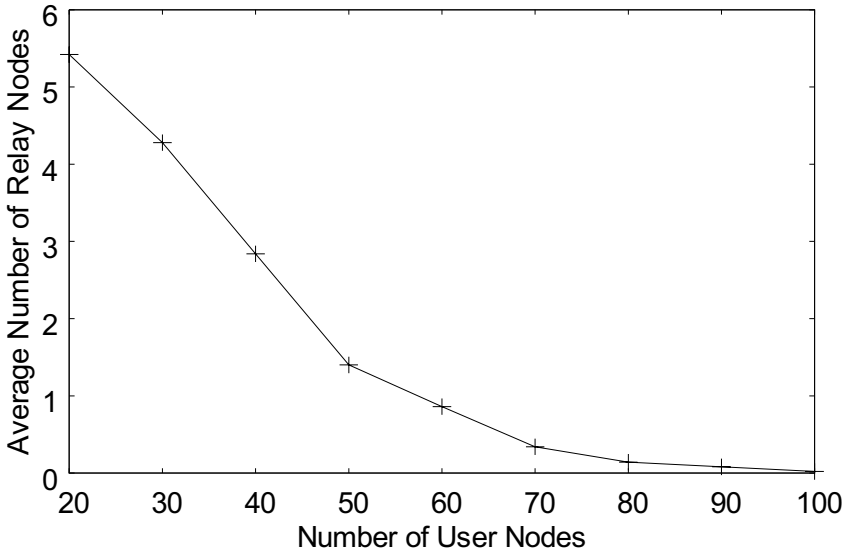


Figure 5.3: The average number of relay nodes per topology in experiment 2
(In experiment 1 and 3, the number of user nodes is fixed to 100)

### 5.4.3 Impact of the Number of Traffic Flows

Experiment 3 examines the performance of the channel assignment algorithms in random CMESH cells as the number of traffic flows increases. As discussed in Section 4.3.3, the number of traffic flows is equivalent to the number of active user nodes, which are randomly selected because a real CMESH cell is likely to have only a group of random active user nodes at the same time. Because this experiment has 100 user nodes in a cell and one active user node has exactly one traffic flow, the number of traffic flows is also equal to the percentage of active user nodes among all user nodes. The results are shown in Figure 5.4.

Figure 5.4(a) shows that the proposed channel assignment algorithms significantly increase the max-min throughput compared to DPLT in this experiment. Up to a roughly 27% increase can be observed in Figure 5.4(b), and the proposed channel assignment algorithms achieve relatively stable throughput gain compared to DPLT as the number of traffic flows increases, mainly because the quality of wireless links on paths is stable.

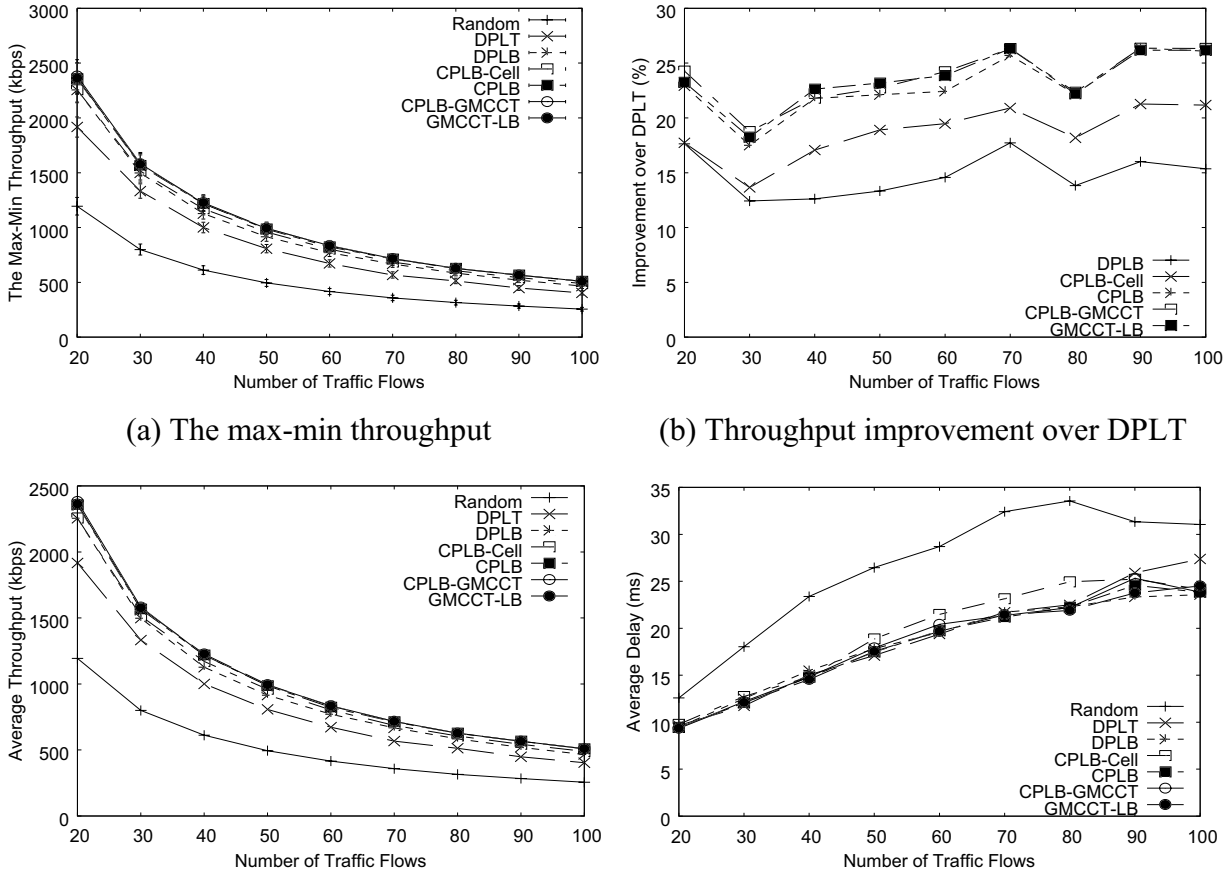


(a) The max-min throughput

(b) Throughput improvement over DPLT

(c) Average throughput

(d) Average packet delay

Figure 5.4: Impact of the number of traffic flows on channel assignment algorithms (Run after the MTM-LB routing algorithm)

Figure 5.4(a) also shows that cell capacity decreases as the number of traffic flows increases. This is consistent with the theoretical results in Chapter 3, which say that per-user-node throughput is inversely proportional to the number of user nodes. Recall that traffic flows in this experiment represent active user nodes, which correspond to user nodes in Chapter 3, while inactive user nodes in this experiment correspond to a part of relay nodes in Chapter 3. In this experiment, the topology, the routes of user nodes and link quality in a cell do not change as the number of active user nodes increases. Therefore, it is expected that per flow throughput will be approximately inversely proportional to the number of traffic flows.

Figure 5.4(d) shows that the proposed channel assignment algorithms have average packet delay similar to DPLT. In addition, it can be observed that the average packet delay generally increases as the number of traffic flows increases. This is because packets from an active user

node need to compete with packets from more active user nodes as the number of traffic flows increases. Finally, the average packet delay in the simulations is on the order of tens of milliseconds, which may be decreased further by future research.

### 5.4.4 Impact of the Cell Coverage Area

Experiment 4 examines the performance of the channel assignment algorithms in random CMESH cells as the cell coverage area increases. The results are shown in Figure 5.5.

Recall that this experiment uses a special relay node deployment algorithm, called Cut-Hop, to handle the problem of long hops. Therefore, the results shown in Figure 5.5 are different from those in the other three experiments.

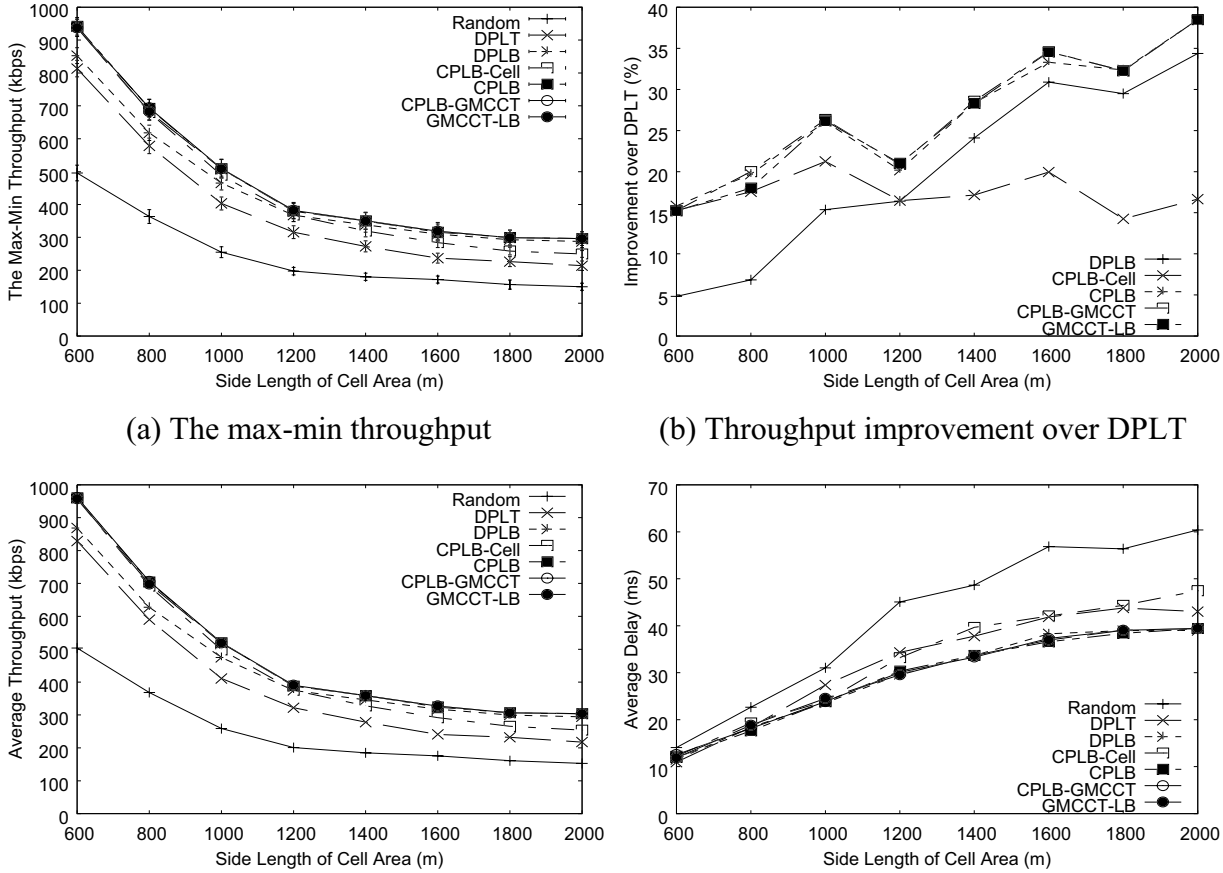


(a) The max-min throughput

(b) Throughput improvement over DPLT

(c) Average throughput

(d) Average packet delay

Figure 5.5: Impact of the cell coverage area on channel assignment algorithms (Run after the MTM-LB routing algorithm)

Figure 5.5(a) shows that the proposed channel assignment algorithms increase the max-min throughput significantly compared to the DPLT algorithm in this experiment. Up to a roughly 40% increase is observed in Figure 5.5(b). In addition, Figure 5.5(b) shows that the throughput gain (except for CPLB-Cell) generally increases as the cell coverage area increases, mainly because the Cut-Hop algorithm for relay node deployment provides high-quality wireless links (see below), which can be utilized by the proposed channel assignment algorithms but cannot be utilized by DPLT.

Figure 5.5(a) and Figure 5.5(c) show that per-user-node throughput generally decreases but becomes less significant as the cell coverage area increases. Per-user-node throughput stops decreasing as the side length of the cell reaches 1800m. This is consistent with the theoretical results in Chapter 3, which implies that per-user-node throughput has a lower bound as the cell radius increases. As a necessary factor that supports this phenomenon, enough wireless relay nodes need to be deployed in a cell. Figure 5.6 shows that the number of wireless relay nodes deployed by Cut-Hop significantly increases as the size of the cell coverage area increases.

This experiment shows another important advantage of CMESHs: if enough relay nodes can be deployed, increasing the coverage area of a cell above a certain threshold may not further decrease per-user-node throughput.

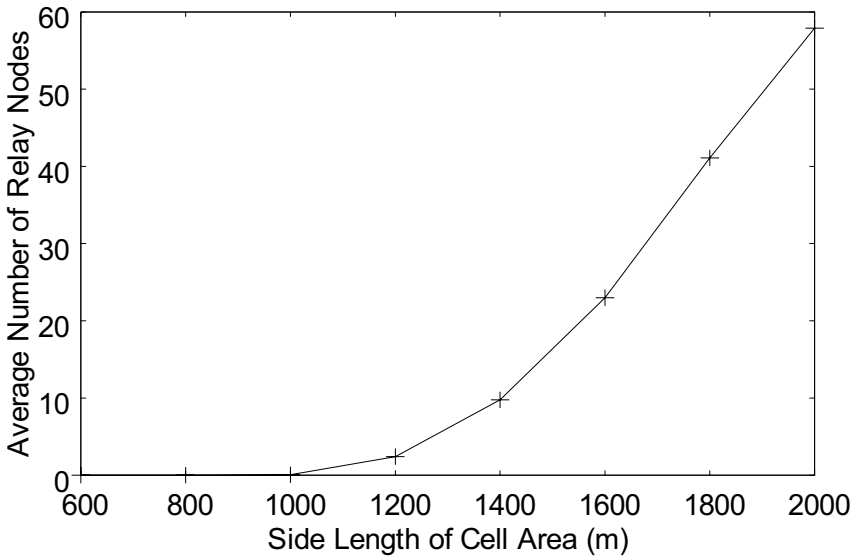


Figure 5.6: The average number of relay nodes per topology in experiment 4

Among the proposed algorithms, Figure 5.5(a) and Figure 5.5(b) show that CPLB-Cell performs worse than other proposed algorithms as the cell coverage area increases. This is because CPLB-Cell neglects channel spatial reuse and cannot utilize the recreated channel time, which is plentiful in large cell coverage areas.

Figure 5.5(d) shows that the proposed channel assignment algorithms (except CPLB-Cell) generally have lower average packet delay compared with DPLT. In addition, it can be observed that average packet delay generally increases as cell coverage area increases because a packet needs to travel more hops. Finally, the average packet delay in the simulations is on the order of milliseconds, which may be decreased further by future research.

## 5.5 Summary

This chapter studied the channel assignment problem in CMESH cells, with the goal of maximizing cell capacity, in terms of the max-min throughput.

This chapter first proved that the problem of channel assignment in small cells is equivalent to the multiprocessor scheduling problem, and thus introduced the CPLB-Cell algorithm. CPLB-Cell was further modified into two channel assignment algorithms for large cells: a centralized algorithm called CPLB and a distributed algorithm called DPLB. Then it was shown that CPLB may not be able to reach the nominal cell capacity given by the MCCT algorithm in large cells. Therefore, two MCCT-based greedy channel assignment algorithms—GMCCT-LB and CPLB-GMCCT—were proposed for large cells.

Simulation results showed that in random CMESH cells the proposed channel assignment algorithms can significantly improve cell capacity compared to the DPLT algorithm [107] and to a random channel assignment algorithm, and up to a roughly 40% capacity improvement over DPLT can be observed in the ns-2 simulation results.

The MTM routing algorithm with necessary modifications that favour DPLT was used in the channel assignment simulations in this chapter. Analysis of the simulation results found that channel assignment algorithms may encounter link bottlenecks caused by MTM. Chapter 6 revisited the channel assignment simulations in this chapter using a routing algorithm proposed by this thesis. The ns-2 simulation results in Section 6.3.3 showed that the proposed channel assignment algorithms increase cell capacity by up to nearly 70% compared to DPLT.

# CHAPTER 6
# ROUTING IN CMESH CELLS

As suggested by the word "mesh" in the name "wireless mesh network", WMNs, including CMESHs, will generally have a large number of wireless links that operate at different bit rates and loss rates on different channels. Therefore, it is important that routing algorithms utilize these abundant and diverse wireless links and channels to improve network performance.

Previous research on WMNs has proposed and evaluated many routing algorithms designed for high network throughput (see Section 2.5). This is different from MANET routing, which usually is not designed to provide high network throughput. One reason is that mobile nodes in MANETs may encounter frequent network disconnections, and these nodes typically have only one radio operating on a common channel; these disadvantages significantly limit the network throughput of MANETs. In contrast, a WMN can be a multi-channel and multi-radio wireless network, whose nodes are stationary and wireless links are more stable and have higher quality. These advantages make it possible for WMN routing algorithms to find high throughput paths.

Following the same direction, routing research in CMESHs also finds routing algorithms that provide high throughput for user nodes. Moreover, as a local access network, a CMESH cell needs to allocate user node throughput based on max-min fairness (see Section 1.2.4). Thus, the goal of routing algorithms in CMESHs is to find the routes of nodes that maximize cell capacity, in terms of the max-min throughput.

The routing problem in a CMESH cell is as follows. The routing problem prescribes three constraints. First, because user traffic in a cell is only between user nodes and the gateway (see Section 1.2.2), routing in a cell finds only paths between mesh nodes and the gateway. Second, routing in a cell studies single-path routes only. Multi-path routing is not of interest because it has the packet reordering problem which may degrade cell performance. Third, a cell has a two-data-radio node design, where each node has an up radio and a down radio. The up radio of a node finds a path to the gateway, and the down radio of the node serves as a next-hop candidate for the up radios of other nodes to use its path to access the gateway. Once the up radio of a

node selects the down radio of another node as its next hop, it has to switch to the channel used by the down radio because two radios can communicate with each other only if they are on the same channel. Because of the three constraints, the problem of routing in a cell is to select the next-hop down radios for the up radios in the cell with a goal of maximizing cell capacity.

The routing problem can be studied either alone or jointly with the channel assignment problem. However, studying channel assignment and routing jointly increases the computational complexity [7, 81]. The channel assignment problem alone is known to be an NP-hard problem [34, 106, 111, 117]. Therefore, this thesis studies them separately. This chapter studies routing algorithms only, assuming that channel assignment algorithms either have run before them or will run after them. Thus, two types of routing algorithms are investigated in this chapter: post-CA algorithms that run after channel assignment algorithms, and pre-CA algorithms that run before channel assignment algorithms.

As a benefit of the traffic pattern in a CMESH cell (i.e., user traffic is only between user nodes and the gateway), routing for a CMESH can avoid complex routing protocols such as DSR [67] and use a centralized simple routing process in which the gateway collects necessary information from the nodes in the cell, calculates their paths and notifies them. The routing process has two parts: an upstream process (from mesh nodes to the gateway) and a downstream process (from the gateway to mesh nodes), described as follows.

The upstream routing process allows mesh nodes to find their upstream paths to the gateway. First, mesh nodes collect information such as wireless links to their neighbours and the quality of these links, and report to the gateway at the scheduled time. Using the collected information, the gateway calculates the upstream paths for all mesh nodes. Finally, the gateway notifies mesh nodes of the new next-hop down radios for their up radios.

The downstream routing process allows mesh nodes to find the downstream paths to their sub-tree nodes. There are two possible ways to do this. One way is to let the gateway tell each node its downstream routing table directly. The shortcoming of this method is that for any route change of a node, the gateway has to notify not only the node but also all the nodes between the node and the gateway. The other way is to let nodes learn their downstream routing table from their own upstream traffic. When the down radio of a node receives an upstream packet from a previous-hop up radio, the node records the source IP address of the packet and the MAC address of the up radio in its downstream routing table. Later, when the down radio of the node

receives a downstream packet whose destination IP address is in the downstream routing table, the node looks up the recorded MAC address and forwards the packet to the recorded up radio. In this way, for any route change of a node, the gateway notifies only the node. Then the node uses the new path to reply with an acknowledgement packet, and this will update the downstream routing tables of all the nodes along the new path.

By using this simple routing process, a CMESH can gain the following advantages. First, nodes need not run any complex routing protocols and thus may reduce their cost. Second, the overheads introduced by distributed routing protocols are eliminated. For any route change of a node, the gateway sends only a single packet to the node, and the node replies with a single acknowledgement packet. In contrast, a typical distributed routing protocol needs to flood routing update information to the entire network. Finally, the simple routing process eliminates the calculation of routes between any two mesh nodes, which are not used (see Section 1.2.2).

The roadmap of this chapter is as follows. The problem of post-CA routing in small cells is addressed first. This problem is translated into an equivalent problem, which presents the strength and weaknesses of the MTM routing algorithm [15]. To overcome the weaknesses of MTM, two greedy algorithms based the MCCT algorithm are proposed, called GMCCT and GMCCT-Cell, and their performance is compared with existing routing algorithms through ns-2 simulations. Then pre-CA routing algorithms that run before channel assignment are studied. Because the CPLB channel assignment algorithm in Chapter 5 is simple and performs well, the two proposed post-CA routing algorithms are converted into two pre-CA routing algorithms, called GMCCT-CPLB and GMCCT-CPLB-Cell, by preparing routes for CPLB. Finally, the performance of the proposed pre-CA routing algorithms is evaluated and the impact of GMCCT-CPLB on the performance of the channel assignment algorithms in Chapter 5 is examined.

The remainder of the chapter is organized as follows. The routing problem and assumptions are described in Section 6.1. Section 6.2 proposes post-CA routing algorithms that run after channel assignment algorithms. Section 6.3 proposes pre-CA routing algorithms that run before channel assignment algorithms. The performance of the proposed post-CA and pre-CA routing algorithms are compared with some existing routing algorithms through ns-2 simulations in Section 6.2 and Section 6.3. The performance of the channel assignment algorithms in Chapter 5 is revisited by using a proposed pre-CA routing algorithm in Section 6.3. Section 6.4 summarizes the work presented in this chapter.

## 6.1 Problem Formulation

Consider a CMESH cell, where a single gateway provides Internet access for up to hundreds of mesh nodes in the cell coverage area by utilizing multiple orthogonal channels, multi-rate wireless transmissions and multi-hop packet deliveries. The gateway has the only direct Internet connection in the cell. User traffic in the cell is only between user nodes and the gateway. See Section 1.2.2 for details.

Each mesh node has two data radios: an up radio and a down radio. The details for this two-data-radio node design has been discussed in Section 1.2.2. The gateway has multiple (up to the number of available orthogonal channels in the cell) down radios.

### 6.1.1 Assumptions

The following assumptions related to routing in CMESH cells are made in this chapter.

First, this chapter assumes that the topology, bit rates, loss rates and interference relationships of the wireless links in a cell are all given and are stable. Wireless relay nodes have been deployed in the cell so that all user nodes are connected to the gateway. The stability of cell topology and wireless links are advantages of CMESHs (see Section 1.2). Field measurements [118] have also validated that 802.11a links are stable.

Second, for simplicity purposes, this chapter assumes downstream user traffic only. In many cases, the upstream routing problem is different from the downstream routing problem only in the description of traffic direction, which can be rather trivial and tedious. The algorithms proposed in this chapter can be easily extended to upstream user traffic because all these algorithms are based on the MCCT algorithm (Algorithm 1), which allows user traffic in both directions. This chapter chooses to present downstream user traffic instead of upstream user traffic because local access network users may have more interest in downstream user traffic. For example, the transmission speed cited for local Internet access networks using DSL and cable technologies typically refers only to downstream user traffic. Also, Section 3.3.3 showed that the upstream cell capacity is theoretically no less than the downstream cell capacity. For these reasons, this chapter assumes downstream user traffic only.

Finally, post-CA routing algorithms assume that channel assignment algorithms have assigned channels to the down radios in a cell, and the assignment is given and fixed. In contrast, pre-CA routing algorithms assume that channel assignment algorithms have not assigned

channels to the down radios in a cell but will run after them and use their routes as input.

### 6.1.2 Routing Stability

In general, a routing algorithm may adapt to changes in network topology, link quality and user traffic in order to improve network throughput. In a CMESH cell, cell topology and link quality are assumed to be stable (see Section 6.1.1), but the real-time traffic demands of user nodes can be quite dynamic. If routing algorithms adapt to the real-time user traffic demands, routes may change frequently. However, routing instability is very harmful to the performance of WMNs [104, 129] and should be avoided. The following gives some reasons.

First, route changes may cause packet loss, which may severely decrease network throughput. When a node changes routes from its old path to a new path, many packets that are still in the queues on the old path may encounter routing failures and have to be dropped. In addition, because upper network layers, such as TCP, treat packet loss as a signal of network congestion, they will decrease sending rates, and thus throughput may drop significantly.

Second, route changes may cause packet reordering, which also may severely degrade network throughput. As a node changes its old path to a new path, packets sent along the new path may arrive at their destination earlier. The receiver at their destination may infer that the delayed packets have been lost and require the sender to retransmit them. For example, three out-of-order packets will trigger TCP's congestion control mechanism. When this happens, the TCP sender will decrease its sending rate and throughput will drop significantly.

Third, if channel assignment algorithms use the routes of nodes in a cell as input, route changes may cause channel assignment instability. If routes in a cell change too frequently, channel assignment algorithms may not have enough time to converge, and the performance of a cell may become unpredictable.

Finally, route changes may lead to a negative user experience because the old paths and the new paths may have different lengths and bit rates, and thus bring different throughput and delay. For this reason, frequent route changes can be detrimental to some real-time applications, and users may feel the network instability and refuse to use it.

In conclusion, unstable routes may significantly degrade the performance of CMESH cells, so routing algorithms in a CMESH cell should avoid adapting to the real-time traffic demands of user nodes (see Section 6.1.5).

### 6.1.3 The System Model

For a vector $\vec{v} = (v_1, ...v_n)$, let $\hat{v}$ denote its set form, i.e., $\hat{v} = \{v_1, ...v_n\}$. Let $\hat{C} = \{1...C\}$, $C \geq 1$, denote the set of available orthogonal channels in a cell. A CMESH cell can be modelled by a directed graph $\vec{\Omega} = (\vec{V}, \vec{E})$. A vector of vertexes $\vec{V} = (\vec{N}, \vec{G})$, where $\vec{N} = (N_1, ..., N_{m'})$ represents all the $m'$ mesh nodes in the cell or either of their up radios or down radios (because each node has exactly one up radio and one down radio) and $\vec{G} = (G_1, ..., G_m)$ represents all the $m$ ( $1 \leq m \leq C$ ) down radios of the gateway $G$. Thus, the total number of down radios is $\left|\hat{V}\right| = m' + m$. Let edge vector $\vec{E}$ represent all the directed wireless links in the cell. Since this chapter assumes downstream traffic only, let edge $e_{u,v} \in \hat{E}$ denote the directed wireless link from down radio $u \in \hat{V}$ to up radio $v \in \hat{N}$.

As described in Chapter 5, if a vector is defined with a subscript $V$ or $E$, such as $\vec{B}_V$ or $\vec{B}_E$, the vector is based on $\vec{V}$ or $\vec{E}$. If $v \in \hat{V}$ or $e \in \hat{E}$ appears as the subscript of a vector name that is defined with a subscript $V$ or $E$, it denotes the vector's element index, which is equal to the index of $v$ or $e$ in vector $\vec{V}$ or $\vec{E}$. See Section 5.1.2 for details.

Let $\vec{H}_V = (H_1, ..., H_{|\hat{N}|})$ denote the vector of the next-hop down radios for the up radios of mesh nodes in a cell, so $\forall v \in \hat{N}$, $H_v \in \hat{V}$. Because of the constraints discussed at the beginning of this chapter, each up radio $v$ has a unique $H_v$. Then, $\forall v \in \hat{N}$, let $e_v$ denote the unique edge $e_{H_v,v} \in \hat{E}$, and let $\vec{e}_V = (e_1, ..., e_{|\hat{N}|})$ denote the vector of such edges for all the mesh nodes in a cell. The single-path route of node $v \in \hat{N}$ is given by a set of edges: $\hat{R}_v = \{e_{g,\cdot}, ..., e_v\}$, where $e_{g,\cdot}$ denotes the edge starting from $g \in \hat{G}$ on the path of $v$. Let $\vec{R}_V = (\hat{R}_1, ..., \hat{R}_{|V|})$ denote the vector of all the single-path routes in a cell, where $\forall v \in \hat{G}$, $\hat{R}_v = \varnothing$.

Let $\vec{R}_V(\vec{H}_V)$ denote the result of the process that converts $\vec{H}_V$ to $\vec{R}_V$, whose algorithm is straight-forward and is omitted. Let $\vec{H}_V(H_v = u)$ denote the new vector $\vec{H}_V$ in case that $H_v$ in the current $\hat{H}_V$ is set to down radio $u \in \hat{V}$ and other elements remain unchanged.

The set of mesh nodes whose routes to $G$ include edge $e \in \hat{E}$ is called the sub-tree of edge $e$,

denoted by $\hat{V}_e$, which is given by:

$$\hat{V}_e = \{v \mid \forall v \in \hat{V}, e \in \hat{R}_v\} \tag{6.1}$$

A user node is called an active user node if its traffic demand is greater than zero. Let $\vec{a} = (a_1, a_2, ...a_n)$, where $\hat{a} \subseteq \hat{N}$, denote the vector of all the active user nodes in a cell.

The number of active user nodes in $\hat{V}_e$ is denoted by $A_e$, i.e.:

$$A_e = |\hat{a} \bigcap \hat{V}_e| = \left|\hat{a} \bigcap \{v \mid \forall v \in \hat{V}, e \in \hat{R}_v\}\right| \tag{6.2}$$

An edge is called an active edge if its $A_e > 0$. The set of all the active edges is denoted by $\hat{E}_A$: $\hat{E}_A = \{e \mid \forall e \in \hat{E}, A_e > 0\}$.

### 6.1.4 The Wireless Model

This chapter uses the same wireless model as in Chapter 4, which is summarized as follows. Details of the model can be found in Section 4.1.2.

Let vector $\vec{C}_E = (C_1, ..., C_{|\vec{E}|})$, where $\forall e \in \hat{E}$, $C_e \in \hat{C}$, denote the current channels on all the edges in $\vec{E}$. Let vector $\vec{C}_V = (C_1, ..., C_{|\vec{V}|})$ denote the channels assigned on all the down radios in a cell. Because of the assumption of the two-data-radio node design (see Section 6.1.1), $\vec{C}_E$ and $\vec{C}_V$ have the channel assignment constraint (see Section 5.1.4): $\forall v \in \hat{V}$ and $\forall e \in \hat{E}_v$, $C_e = C_v$. Let $\vec{C}_E(\vec{C}_V)$ denote the result of the process that converts $\vec{C}_V$ to $\vec{C}_E$, i.e., $C_e = C_v$, where $e \in \hat{E}_v$.

Let vector $\vec{w}_E = (w_1, ..., w_{|\vec{E}|})$ denote the bit rates of all the edges in $\vec{E}$. Let $\vec{I}_E = (\hat{I}_1, ..., \hat{I}_{|\vec{E}|})$ denote the interference vector, where $\forall e \in \hat{E}$, $\hat{I}_e$ denotes the set of edges that interfere with edge $e$ if they are on the same channel as edge $e$.

Let $\hat{I}_e(k)$, $k \in \hat{C}$ denote the set of edges on channel $k$ in $\hat{I}_e$:

$$\hat{I}_e(k) = \{e' \mid \forall e' \in \hat{I}_e, C_{e'} = k\}. \tag{6.3}$$

Let $\hat{I}_e^+(C_e)$ denote the set $\{e\} \bigcup \hat{I}_e(C_e)$, i.e.:

$$\hat{I}_e^+(C_e) = \{e\} \bigcup \{e' \mid \forall e' \in \hat{I}_e, C_{e'} = C_e\}. \tag{6.4}$$

Let $\tau_e$ denote the channel time spent on edge $e$, $\forall e \in \hat{E}$, for transmitting one bit, which is given by:

$$\tau_e = 1 / w_e . \tag{6.5}$$

Note that the above expression for $\tau_e$ is simplified and can be extended to take into account packet loss rate on edge $e$ (see Section 4.2.3).

Let $T_e$ denote the channel time spent on edge $e$, $\forall e \in \hat{E}$ per second, for each active user node to achieve throughput of 1 bps. Because of single-path routing, $T_e$ is given by:

$$T_e = A_e \cdot \tau_e . \tag{6.6}$$

Note that $T_e$ in Equation (6.6) does not take protocol overhead into account. In the simulation experiments in this chapter, where IEEE 802.11a-compatible CMESH cells were studied, $T_e$ was adjusted by Equation (4.7) which takes into account the packet overhead of UDP and the deterministic protocol overhead in IEEE 802.11a, but it does not take into account collision-related overhead, which is left for future research.

### 6.1.5 The Routing Problem

Let $\vec{x} = (x_1, x_2, ..., x_n)$ denote a vector of feasible throughput allocations for the vector of active user nodes $\vec{a} = (a_1, a_2, ...a_n)$, each with infinite traffic demand. Let $x$ denote the minimum throughput in $\hat{x}$: $x = \min(\hat{x}) = \min\{x_1, x_2, ..., x_n\}$. The goal of the routing problem is to find the vector $\vec{H}_V = (H_1, ...H_{|\hat{N}|})$ that maximizes $x$.

Recall that this chapter studies two types of routing algorithms: post-CA algorithms that run after channel assignment algorithms, and pre-CA routing algorithms that run before channel assignment algorithms. For each of the two types of algorithms, this chapter proposes greedy routing algorithms based on the MCCT algorithm (see Section 4.2.1), which gives the nominal cell capacity. For small cells, the MCCT algorithm gives the exact cell capacity within the abstract models (see Section 4.2.2). For large cells, although the MCCT algorithm gives a conservative cell capacity, the ns-2 simulation results in Chapter 4 suggest that it predicts cell capacity fairly accurately in CMESH cells. Therefore, the MCCT algorithm can be used to guide routing algorithms to improve the capacity of CMESH cells.

Note that the routing problem is described with the default definition of cell capacity, where each active user node has infinite traffic demand. Thus, the proposed routing algorithms in this chapter are based on the MCCT algorithm (Algorithm 1). The routing problem and the proposed routing algorithms can be extended to an arbitrary profile of traffic demands of user nodes by using the general definition of cell capacity (see Section 4.1.3) and the extended MCCT algorithm (Algorithm 2).

When the general definition of cell capacity is addressed, because of the importance of routing stability (see Section 6.1.2), routing algorithms should adapt to a stable profile of the traffic demands of user nodes instead of the dynamic real-time traffic demands of user nodes. This can be done by setting the traffic demands of user nodes to their maximum allowable throughputs, based on factors such as users' payment or the traffic history of user nodes.

## 6.2 Post-CA (Channel Assignment) Routing Algorithms

Routing algorithms that run after channel assignment are called post-CA routing algorithms. Post-CA routing algorithms assume that $\vec{C}_V$ is given and fixed. They use $\vec{C}_V$ as an input and seek to find the routes that maximize cell capacity, in terms of the max-min throughput.

This section first translates the post-CA routing problem for small cells into an equivalent problem. By analyzing this equivalent problem, the strength and weaknesses of the MTM routing algorithm [15] in CMESH cells are considered and two greedy MCCT algorithms are proposed to overcome its weaknesses.

### 6.2.1 Analysis of the Post-CA Routing Problem in Small Cells

Recall that small cells refer to CMESH cells in which all the wireless links interfere with each other if they are on the same channel. In other words, $\forall e \in \widehat{E}$, $\{e\} \bigcup \widehat{I}_e = \widehat{E}$. When analyzing small cells, a channel is also referred to as a channel bucket that contains channel time.

**Theorem 11**. For a small cell, finding the post-CA routes that maximize cell capacity is equivalent to finding the vector of edges $\vec{e}_V = (e_1, ..., e_{|\widehat{N}|})$ that satisfies the following: after each $e \in \vec{e}_V$ (whose associated channel time $T_e$ is given by Equation (6.6) and associated channel is $C_e \in \widehat{C}$) is put into channel bucket $C_e$, the maximum accumulated channel time across the $C$ channel buckets is minimized.

Proof. Theorem 8 proved that within the abstract models the exact cell capacity for small cells is the nominal cell capacity $\hat{x}$, given by $\hat{x} = 1/\max(\widehat{\text{CCT}})$, where $\widehat{\text{CCT}}=\{\text{CCT}_e \mid \forall e \in \hat{E}_A\}$, $\text{CCT}_e = \sum_{e' \in \hat{I}_e^+(C_e)} T_{e'}$ and $\hat{I}_e^+(C_e) = \{e\} \bigcup \{e' \mid e' \in \hat{I}_e, C_{e'} = C_e\}$.

For any $k \in \hat{C}$, define $\hat{E}_k = \{e \mid \forall e \in \hat{E}, C_e = k\}$ and $\text{CCT}_k = \sum_{e \in \hat{E}_k} T_e$. By the definition of a small cell, $\forall e \in \hat{E}$, $\{e\} \bigcup \hat{I}_e = \hat{E}$. Therefore, $\forall e \in \hat{E}_A$ and $\forall e' \in \hat{E}_A$, if $C_e = C_{e'} = k$, then $\hat{I}_e^+(C_e) = \hat{I}_{e'}^+(C_{e'}) = \hat{E}_k$ and $\text{CCT}_e = \text{CCT}_{e'} = \text{CCT}_k$. For any $k \in \hat{C}$, if $\hat{E}_k = \varnothing$, then $\text{CCT}_k = 0$. Thus, $\max(\widehat{\text{CCT}}) = \max\{\text{CCT}_e \mid \forall e \in \hat{E}_A\} = \max\{\text{CCT}_k \mid k = 1...C\}$.

For any $k \in \hat{C}$, define $\hat{E}_k' = \{e \mid \forall e \in \hat{e}_V, C_e = k\}$ and notice $\forall e \notin \hat{e}_V$, $T_e = 0$, so $\text{CCT}_k = \sum_{e \in \hat{E}_k'} T_e$.

Thus, $\max(\widehat{\text{CCT}}) = \max\{\text{CCT}_k \mid k = 1...C\} = \max\{\sum_{e \in \hat{E}_k'} T_e \mid k = 1...C\}$.

From $\hat{x} = 1/\max(\widehat{\text{CCT}})$, to maximize cell capacity $\hat{x}$ is to minimize the $\max(\widehat{\text{CCT}})$, which is equivalent to minimizing $\max\{\sum_{e \in \{e' \mid \forall e' \in \vec{e}_V, C_{e'} = k\}} T_e \mid k = 1...C\}$. That is, for a small cell, finding the post-CA routes that maximize cell capacity is equivalent to finding the $\vec{e}_V$ that leads to minimized the maximum accumulated channel time across all channel buckets. □

**Corollary 3**. For a small cell that has only one channel ($C = 1$), finding the post-CA routes that maximize cell capacity is equivalent to finding the vector of edges $\vec{e}_V = (e_1, ..., e_{|\hat{N}|})$ that minimizes $\sum_{e \in \vec{e}_V} T_e$.

Proof. The proof of Theorem 11 showed that to maximize cell capacity of a small cell is to minimize $\max\{\sum_{e \in \{e' \mid \forall e' \in \vec{e}_V, C_{e'} = k\}} T_e \mid k = 1...C\}$. If $C = 1$, $\max\{\sum_{e \in \{e' \mid \forall e' \in \vec{e}_V, C_{e'} = k\}} T_e \mid k = 1...C\} = \sum_{e \in \vec{e}_V} T_e$. That is, for a small cell, finding the routes that maximize cell capacity is equivalent to finding $\vec{e}_V$ so that $\sum_{e \in \vec{e}_V} T_e$ is minimized. □

Awerbuch *et al.*'s MTM routing algorithm [15] defines the MTM metric of node $v \in \hat{N}$ as $\text{MTM}_v = \sum_{\forall e \in R_v} \tau_e$, where $\tau_e$ is given by Equation (6.5). They proved a theorem that is equivalent

to saying that the MTM metric maximizes the capacity of small networks where wireless links interfere with each other. Their theorem is consistent with Corollary 3. Notice that:

$$\sum_{e\in\tilde{e}_V} T_e = \sum_{e\in\tilde{e}_V} (A_e / w_e) = \sum_{v\in\bar{N}} \sum_{e\in R_v} (1/w_e) = \sum_{v\in\bar{N}} \sum_{e\in R_v} \tau_e = \sum_{v\in\bar{N}} \mathrm{MTM}_v,$$

and $\tau_e$ (see above) is independent of each other, so the MTM metric is equivalent to $\sum_{e\in\tilde{e}_V} T_e$ (the proof is omitted here). Therefore, the strength of the MTM metric is that it is the optimal routing metric in single-channel small cells.

In multi-channel small cells, however, the MTM routing metric is no longer optimal because Theorem 11 says that the optimal routing in multi-channel small cells is the one that minimizes $\max\{\sum_{e\in\{e'|\forall e'\in\tilde{e}_V, C_{e'}=k\}} T_e \mid k=1...C\}$. In a multi-channel small cell, the GMCCT algorithm (see Section 6.2.2) can be used to improve the cell capacity.

Figure 6.1 shows a simple example that is used to analyze the weakness of the MTM routing algorithm in multi-channel small cells. In Figure 6.1, the routing decision of MTM is compared with the routing decision of the GMCCT algorithm. In the example, a small cell has two channels and the gateway G has two down radios, each operating on a different channel. The small cell has three nodes, named A, B and C, each with infinite traffic demand. Node A and node B have their up radios connect to the two down radios of the gateway as illustrated in Figure 6.1. The up radio of node C has two candidates for its next hop: the down radio of node A on channel 2 with $\tau = 5$ and the down radio of node B on channel 1 with $\tau = 2$, where $\tau$ is the channel time required to transmit one bit over the edge from A or B to C.

Figure 6.1(a) shows the routing decision of the MTM algorithm based on metric $\sum_{e\in\tilde{e}_V} T_e$ which is equivalent to the MTM metric as discussed above. The MTM algorithm selects node B as the next hop of node C because the sum of channel time of the two buckets is 18, which is smaller than the 19 in case (b). This route decision can be verified by the MTM metric, which seeks to minimize the sum of $\tau$ on a path, and thus will also select node B, whose sum of $\tau$ on this path is 6+2=8 which is smaller than 4+5=9 on the path through node A.

The GMCCT algorithm will select node A as the next hop of node C because the maximum sum of the channel time across the two buckets is 11, which is smaller than the 12 if node B is selected. According to Theorem 11, the GMCCT algorithm achieves higher cell capacity than

the MTM algorithm in this example.

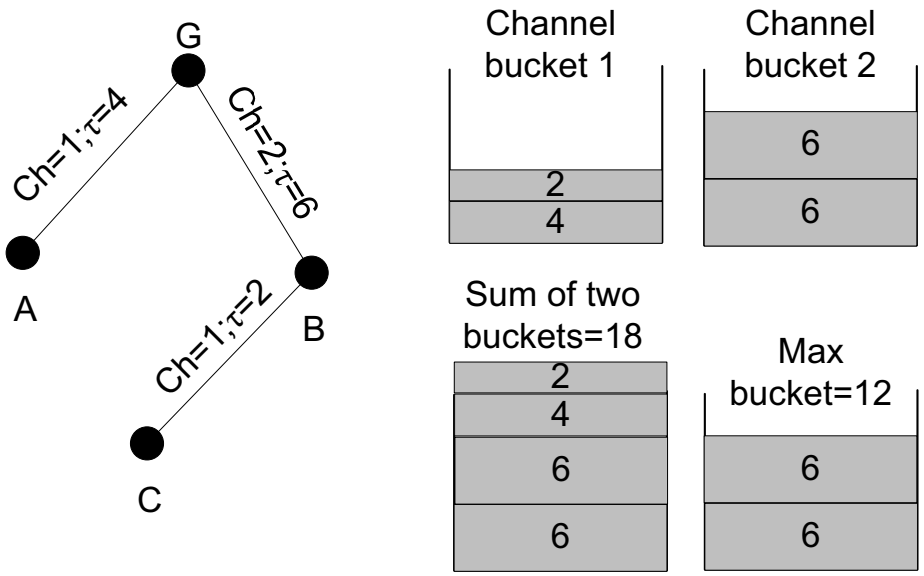


(a) The MTM algorithm selects node B as node C's next hop because the sum of the channel time in the two buckets is 18, which is smaller than the 19 in case (b) (below).

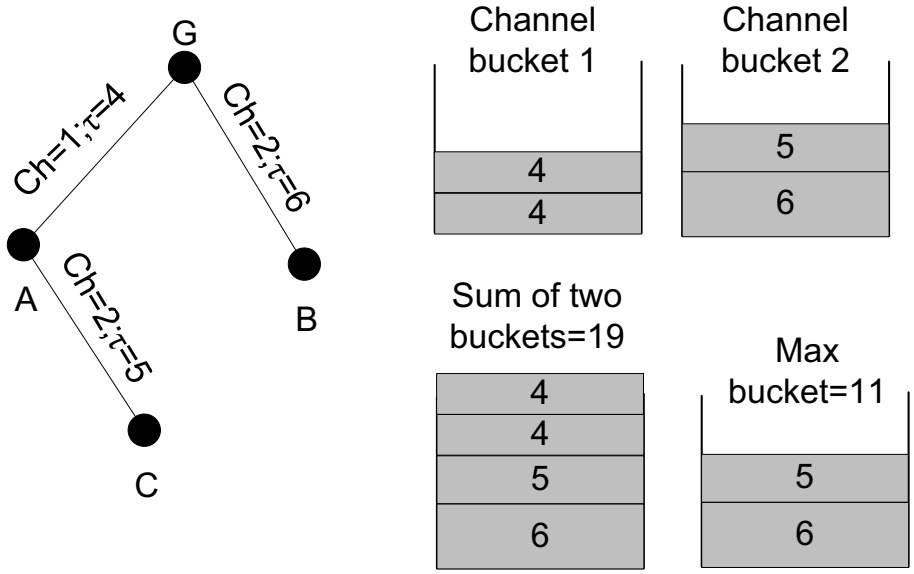


(b) The GMCCT algorithm selects node A as node C's next hop because the maximum sum of the channel time across the two buckets is 11, which is smaller than the 12 in case (a) (above).

Figure 6.1: Comparison of the MTM and GMCCT routing algorithms

In this example, the idea used by the GMCCT algorithm to improve cell capacity is clear: in multi-channel small cells, although decreasing the channel time in the bottleneck channel bucket

may increase the overall channel time in all channel buckets (i.e., sacrifice some bit-transmission efficiency of the overall channel time), it may achieve better channel time load balancing among all channel buckets (i.e., achieve better fairness for the active user nodes to use the overall channel time), and thus may increase cell capacity.

### 6.2.2 The GMCCT and GMCCT-Cell Routing algorithms

The analysis in Section 6.2.1 shows that MTM is a channel-time efficient routing algorithm. However, MTM has the following three weaknesses in CMESH cells. First, MTM cannot distinguish between two candidate paths that have the same MTM metric value. In CMESH cells this case can be common and needs to be handled. Second, based on the analysis in Section 6.2.1, MTM cannot fairly utilize all available channels for user node traffic and thus may lose cell capacity in multi-channel cells. Finally, in large cells, even including single-channel large cells, MTM is no longer optimal, because it neglects channel spatial reuse.

To overcome these three weaknesses of MTM, two greedy MCCT routing algorithms are proposed: the GMCCT and GMCCT-Cell routing algorithms. They are designed for both small cells and large cells, and both start with another proposed routing algorithm called CETT-HL (Cumulative Expected Transmission Time plus Hop count and Load balancing among gateway radios), which deals with the first weakness of MTM.

To overcome the second weakness of MTM, the two proposed greedy algorithms perform load balancing of channel time among channels. To deal with the third weakness of MTM, GMCCT takes into account channel spatial reuse by adjusting routes to greedily minimize the maximum $\mathrm{CCT}_e$, $\forall e \in \widehat{E}_A$. Here, the term "greedy" is used to indicate that the maximum $\mathrm{CCT}_e$ decreases monotonously in each adjustment in order to allow the algorithms to finish quickly.

The proposed CETT-HL algorithm makes the following two modifications to MTM. When two candidate paths have the same MTM metric value, CETT-HL selects the path with fewer hops. When the next-hop candidates of the up radio of a node are gateway radios, these candidate paths may have the same MTM metric value and hop count. Because gateway radios are operating on different orthogonal channels, CETT-HL performs further load balancing among gateway radios by selecting the least busy gateway radio. If two gateway radios are equally busy, the gateway radio that has fewer associated nodes may be selected. The CETT-HL routing algorithm is given as Algorithm 8.

Algorithm 8: The CETT-HL routing algorithm

Input: $\vec{V}$, $\vec{E}$, $\vec{a}$, $\vec{w}_E$.

Output: $\vec{H}_V = (H_1, ...H_{|\vec{N}|})$.

1. Initialize vectors: $\vec{M}_V = \vec{h}_V = \left( \overbrace{\infty, ..., \infty}^{|\vec{N}|}, \overbrace{0, ..., 0}^{|\vec{G}|} \right)$

2. Get $\vec{\tau}_E = (\tau_1, ..., \tau_{|\vec{E}|})$ via $\vec{w}_E$ (Equation (6.5)).

3. Initialize sets: $\hat{Y} = \hat{G}$ and $\hat{O} = \hat{N}$.

Loop until $\hat{O} = \varnothing$ {

4. Get $\hat{L} = \{e_{g,o} \mid \forall g \in \hat{Y}, \forall o \in \hat{O}, e_{g,o} \in \hat{E}\}$ and its $\hat{J} = \{J_{e_{g,o}} = M_g + \tau_{e_{g,o}} \mid \forall e_{g,o} \in \hat{L}\}$.

5. Get $\hat{Q} = \{e_{g,o} \mid e_{g,o} \in \hat{L}, J_{e_{g,o}} = \min(\hat{J})\}$ and its $\hat{P} = \{P_{e_{g,o}} = h_g + 1 \mid \forall e_{g,o} \in \hat{Q}\}$.

6. Get $e_{g,o}$ as the first element in set $\{e_{g,o} \mid e_{g,o} \in \hat{Q}, P_{e_{g,o}} = \min(\hat{P})\}$.

7. Update $H_o \leftarrow g$, $h_o \leftarrow h_g + 1$, $M_o \leftarrow M_g + \tau_{e_{g,o}}$, $\hat{O} \leftarrow \hat{O} - \{o\}$ and $\hat{Y} \leftarrow \hat{Y} \bigcup \{o\}$.

} End Loop

7. Get $\vec{A}_E = (A_1, ..., A_{|\vec{E}|})$ via $\vec{V}$, $\vec{E}$, $\vec{a}$ and $\vec{R}_V(\vec{H}_V)$ (Equation(6.2)).

8. Get $\vec{T}_E = (T_1, ..., T_{|\vec{E}|})$ via $\vec{A}_E$ and $\vec{\tau}_E$ (Equation (6.6)).

9. Initialize vector $\vec{B}_V = \left( \overbrace{\infty, ..., \infty}^{|\vec{N}|}, \overbrace{0, ..., 0}^{|\vec{G}|} \right)$.

9. Get $\vec{Z}$ that includes all elements in $\{v \mid \forall v \in \hat{N}, H_v \in \hat{G}\}$ and that $\forall v \in \hat{Z}$, $T_{e_v} \in \hat{T}_E$ is in descending order.

10. For each sorted element $v$ in $\vec{Z}$:

    10.1) Get $u$ as the first element in $\{u \mid u \in \hat{G}, B_u = \min(\hat{B})\}$.

    10.2) Update $H_v \leftarrow u$.

    10.3) Update $B_u \leftarrow B_u + T_{e_v}$.

The proposed GMCCT algorithm requires the gateway to collect the following information from mesh nodes: the channels on their down radios, their wireless links and bit rates (see Section 6.1.4 for loss rates) and the set of interfering wireless links if they are on the same channel. The GMCCT algorithm is given as Algorithm 9.

Algorithm 9: The GMCCT routing algorithm

Input: $\vec{V}$, $\vec{E}$, $\vec{a}$, $\vec{C}_V$, $\vec{I}_E$, $\vec{w}_E$.

Output: $\vec{H}_V = (H_1, ...H_{|\vec{N}|})$.

1. Get $\vec{H}_V$ via the CETT-HL algorithm (Algorithm 8) with $\vec{V}$, $\vec{E}$, $\vec{a}$, $\vec{w}_E$ as input.

Loop {

2. Get $M = \max(\widehat{\text{CCT}})$ and the corresponding $\hat{I}_e^+(C_e)$ via the MCCT algorithm (Algorithm 1) with $\vec{V}$, $\vec{E}$, $\vec{a}$, $\vec{R}_V(\vec{H}_V)$, $\vec{C}_E(\vec{C}_V)$, $\vec{I}_E$, $\vec{w}_E$ as input.
3. Get $\vec{V}_E = (\hat{V}_1, ..., \hat{V}_{|\vec{E}|})$ via $\vec{V}$, $\vec{E}$ and $\vec{R}_V(\vec{H}_V)$ (Equation(6.1)).
4. Get $\vec{T}_E = (T_1, ..., T_{|\vec{E}|})$ via $\vec{V}_E$, $\vec{a}$ and $\vec{w}_E$ (Equation (6.2) and Equation (6.6)).
5. Get $\vec{Q}$ that includes all elements in $\hat{I}_e^+(C_e)$ and that $\forall e \in \hat{Q}$, $T_e \in \hat{T}_E$ is in descending order.
6. For each sorted element $e$ in $\vec{Q}$, $T_e > 0$:
   6.1) Get $\vec{Z}$ that includes all elements in $\hat{V}_e$ and that $\forall v \in \hat{Z}$, $T_{e_v} \in \hat{T}_E$ is in descending order.
   6.2) For each sorted element $v$ in $\vec{Z}$, $T_{e_v} > 0$:
      6.2.1) For each element $u$ in set $\{u \mid u \in \hat{V}, e_{u,v} \in \hat{E}\}$, $e \notin \hat{R}_u$:
         6.2.1a) Get $M' = \max(\widehat{\text{CCT}})$ via the MCCT algorithm (Algorithm 1) with $\vec{V}$, $\vec{E}$, $\vec{a}$, $\vec{R}_V(\vec{H}_V(H_v = u))$, $\vec{C}_E(\vec{C}_V)$, $\vec{I}_E$, $\vec{w}_E$ as input.
         6.2.1b) If $M' < M$ then update $H_v \leftarrow u$ and go back to loop
7. If no $H_v$ is updated in this iteration of the loop, then this algorithm exits.

} End Loop

For $e_{u,v} \in \widehat{E}$, let $f_{e_{u,v}} = \{e'_{u,v'} \mid \forall v' \in \widehat{N}, e'_{u,v'} \in \widehat{E}\}$. A simple version of the GMCCT algorithm is given by replacing the condition $e \notin \widehat{R}_u$ at step 6.2.1 in Algorithm 9 with the following condition: for each $e' \in f_e$, $e' \notin \widehat{R}_u$. This simple version reduces the number of candidate routes for search and thus is used in the simulation experiments in this chapter.

It could be difficult for a large cell to collect the interference vector $\vec{I}_E$. Thus, the GMCCT-Cell algorithm is proposed to handle this difficulty. It assumes that all the wireless links in a cell interfere with each other if they are on the same channel. The GMCCT-Cell algorithm is given as Algorithm 10.

Algorithm 10: The GMCCT-Cell routing algorithm

Input: $\vec{V}$, $\vec{E}$, $\vec{a}$, $\vec{C}_V$, $\vec{w}_E$.

Output: $\vec{H}_V = (H_1, ...H_{|\vec{N}|})$.

1. Get $\vec{I}_E = (\widehat{E} - \{e_1\}, ..., \widehat{E} - \{e_{|\vec{E}|}\})$.
2. Get $\vec{H}_V$ via the GMCCT algorithm (Algorithm 9) with $\vec{V}$, $\vec{E}$, $\vec{a}$, $\vec{C}_V$, $\vec{I}_E$, $\vec{w}_E$ as input.

### 6.2.3 Performance Comparisons

This section evaluates the performance of the proposed post-CA routing algorithms (GMCCT and GMCCT-Cell) through ns-2 simulations by comparison with four existing post-CA routing algorithms: MinHops, MTM, WCETT and NBLC (see Section 2.5.2).

The four existing routing algorithms are selected to represent four common types of routing algorithms in WMNs. The MinHops algorithm is independent of link quality, channel diversity and traffic load; the MTM algorithm is a link-aware routing algorithm that is independent of channel diversity and traffic load; the WCETT algorithm is a link-aware and channel-aware routing algorithm that is independent of traffic load; and the NBLC algorithm is a link-aware, channel-aware and load-aware routing algorithm.

For MinHops, MTM and WCETT, the up radio of a node whose next-hop candidates are gateway radios will find that these candidate paths have the same metric value in the simulations.

It is natural for the up radio to select a gateway radio randomly in order to reduce the chances that the up radios of other nodes also select the gateway radio. Otherwise, the gateway radio may become the bottleneck factor that severely degrades cell capacity. In contrast, NBLC is a traffic-load-aware algorithm, so it can perform load balancing among the gateway radios by itself.

In the simulations for MinHops, each node selects the path that minimizes the total number of hops to the gateway. In the simulations for MTM, the MTM metric for any node $v$ is calculated by $\text{MTM} = \sum_{\forall e \in R_v} (1/w_e)$, where $R_v$ is a candidate path of node $v$, $e$ is a wireless link on the path and $w_e$ is the bit rate of wireless link $e$. In the simulations for WCETT, the WCETT metric for any node $v$ is calculated by $\text{WCETT} = (1-\beta)\cdot\text{MTM}+\beta\cdot\max_{1\le k\le C} X_k$, where $X_k$ is the sum of $1/w_e$ for each wireless link $e \in R_v$ that is operating on channel $k$. The parameter $\beta$ is set to 0.5, which is the default value used by the original paper [36].

In the simulations for NBLC (see Section 2.5.2), the parameter $\mu$ is set to 1.2, as in the original paper [88]. In order to calculate the NBLC metric, each node needs to measure the traffic load in terms of channel busy time within the interference range. The routing protocol for NBLC is an on-demand routing protocol, so the activation sequence of traffic flows impacts the NBLC metric and path selections. The simulations in this section assume that the traffic flow of a user node is activated immediately after the user node finds its path by a greedy NBLC algorithm. In the greedy NBLC algorithm, each of its steps finds the path of one node that has no path yet, until the paths of all nodes are found. In each step, the greedy NBLC algorithm finds the NBLC metric values among all the possible routes of the nodes that have no routes yet, and then selects the path of a node that has the maximum NBLC metric value. If the node is an active user node, its traffic flow is activated, and all nodes in the cell update their current measured traffic load information. Finally, greedy NBLC repeats the above step until the paths of all nodes are found. Note that when a node is about to select a path, it cannot know the decision of nodes at latter hops, and neither it can know the channels at latter hops. Because of these two shortcomings [88], the paths selected by NBLC may not be optimal.

To simulate 802.11a-compatible CMESH cells, the ns-2 simulator was modified to support multiple radios per node, multiple channels, multiple bit rates, 802.11a features and a max-min fairness mechanism. These modifications were introduced in Section 4.3.1 and Section 4.3.2.

For the same reasons as in Section 4.3.3, four simulation experiments—experiment 1 to experiment 4—were performed, with each varying one of the following four factors while holding the others constant at their default levels: the number of channels, the number of user nodes, the number of traffic flows and the cell area size. The default levels are listed in Table 4.2. The reason for selecting these values is the same as in Section 4.3.3.

In each experiment, the six routing algorithms—MinHops, MTM, WCETT, NBLC, GMCCT-Cell and GMCCT—are compared. Because the goal of routing in CMESHs is to maximize cell capacity, the major performance metric is the max-min throughput. The average throughput and the average packet delay of active user nodes are also shown, but they are treated as secondary performance metrics. See Section 5.4 for details.

Other major parameters are set in the same way as in Section 4.3.3. Table 6.1 summarizes the major parameters and their values.

Table 6.1: Major parameters in the post-CA routing experiments

| **Parameter** | **Value** |
|---|---|
| Number of gateway radios | Number of channels |
| User node location distribution | Discrete uniform distribution |
| Number of cell topologies | 50 |
| Relay node deployment scheme | Least-RN/Cut-Hop |
| Channel assignment algorithm | Random |
| Traffic direction | Downstream |
| Traffic type | UDP/CBR |
| Packet payload size | 1000 Bytes |
| Source rate adjustment step | 10 kbps |
| RTS/CTS scheme | Disabled |

As shown in Table 6.1, the four simulation experiments share a common set of 50 cell topologies. In each topology, the gateway is always located at the centre of a square cell area. The locations of user nodes are randomly generated following a discrete uniform distribution (on 1m×1m grids) inside the cell area. Wireless relay nodes are deployed by either the Least-RN algorithms or the Cut-Hop algorithms, as introduced in Section 5.4. For each factor value in each experiment, one simulation is run for each topology, and the mean throughput and delay of the 50 runs are calculated. In the figures showing the max-min throughput, bars show the 95% confidence intervals.

The post-CA routing algorithms need to work with a channel assignment algorithm, which had to be selected. Because the selected channel assignment algorithm must run before routing algorithms, it cannot acquire routing or traffic information (because traffic cannot be delivered without routes). Thus, the Random channel assignment algorithm was selected, which assigns channels to all the down radios in a cell randomly. Its channel assignment output was then fixed for all post-CA routing algorithms. Note that in the experiments for WCETT [36], each node had two radios: one fixed to 802.11a channel 36 and the other fixed to 802.11g channel 10. The experiments for NBLC [88] also used a random channel assignment algorithm.

**Impact of the Number of Channels**

The first experiment examines the performance of the post-CA routing algorithms in random CMESH cells as the number of channels increases. The results are shown in Figure 6.2.

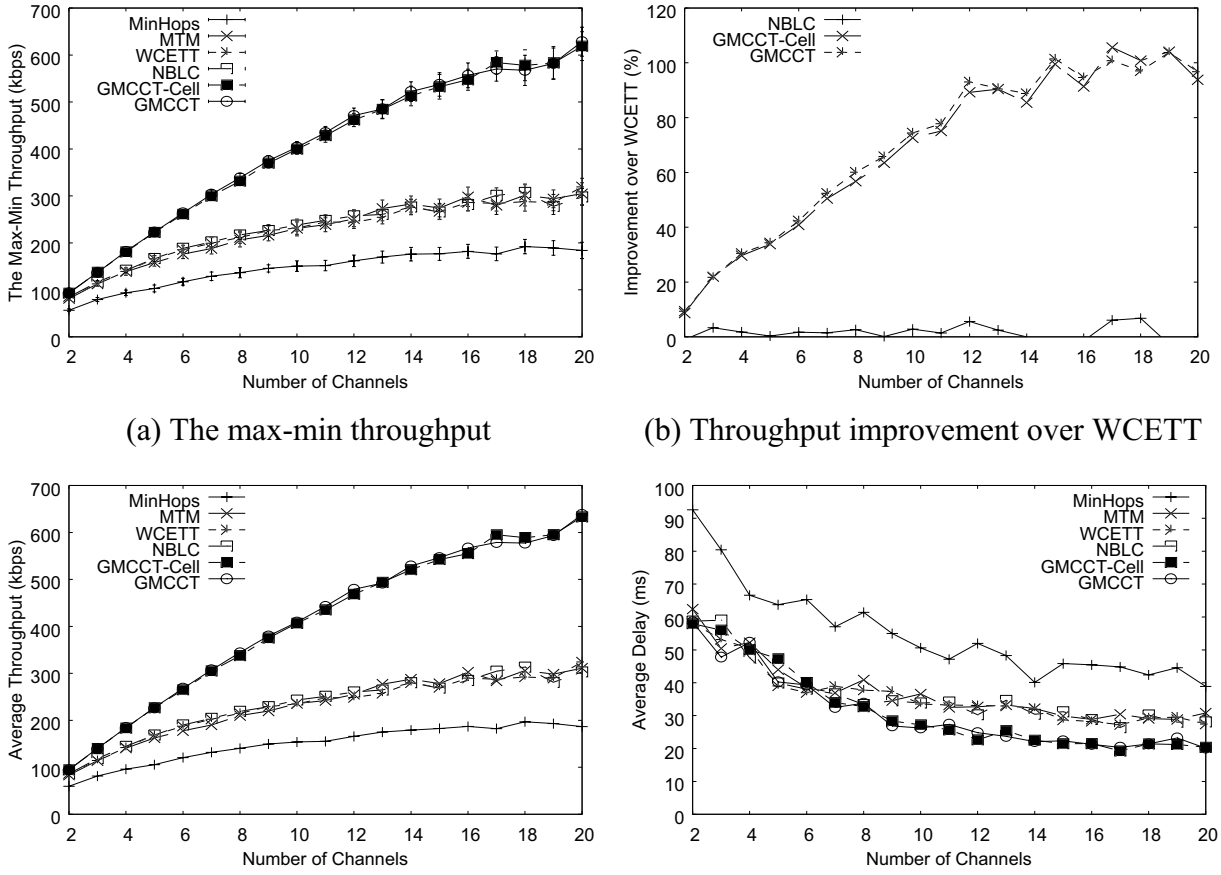


(a) The max-min throughput

(b) Throughput improvement over WCETT

(c) Average throughput

(d) Average packet delay

Figure 6.2: Impact of the number of channels on post-CA routing algorithms

It is not surprising that MinHops gives the poorest performance because it is unaware of the link quality, channel diversity and traffic load; thus it cannot find routes that utilize the diversity of wireless links and channels fully and efficiently. A comparison of Figure 6.2(a) and Figure 6.2(c) shows that the average throughput is above but close to the max-min throughput. This is because the max-min fairness mechanism in the simulations stops increasing the source rate threshold after the max-min throughput is reached. The above two observations hold in all experiments, so they will not be discussed again in the rest of this section.

Figure 6.2(a) shows the max-min throughput with 95% confidence intervals. It can be observed that the max-min throughput generally increases as the number of channels increases, and the six routing algorithms divide into three groups: the first group (containing MinHops) performs the worst; the second group (containing MTM, WCETT and NBLC) performs better; and the third group (containing GMCCT and GMCCT-Cell) performs the best. Figure 6.2(b) shows that the throughput gain generally increases as the number of channels increases, and up to 100% throughput improvement over WCETT is observed.

Figure 6.2(a) and Figure 6.2(b) show that the proposed GMCCT and GMCCT-Cell algorithms have similar max-min throughput in this experiment. This indicates that the load balancing of the accumulated channel time among channels is the primary reason for the improvement of cell capacity. In this experiment, the cell area size is not large enough for GMCCT to outperform GMCCT-Cell by utilizing channel spatial reuse.

Figure 6.2(d) shows that the proposed routing algorithms generally have lower average packet delay than the four existing routing algorithms as the number of channels increases. This means that the throughput improvement over other algorithms does not come at the cost of higher packet delay. It can also be observed that for all algorithms, the average packet delay generally decreases as the number of channels increases. This is because packets wait less time for idle channels and encounter fewer collisions and retransmissions as the number of channels increases. Finally, the average packet delay in the simulations is on the order of tens of milliseconds, which may be decreased further by future research.

**Impact of the Number of User Nodes**

The second simulation experiment examines the performance of the post-CA routing algorithms in random CMESH cells as the number of user nodes increases. The results are

shown in Figure 6.3.

Like the first experiment, in Figure 6.3(a), the six routing algorithms divide into three groups according to the max-min throughputs, with the two proposed routing algorithms significantly (with 95% confidence) outperforming the others when the number of user nodes exceeds 40. Figure 6.3(b) shows that the throughput gain achieved by the proposed algorithms generally increases as the number of user nodes increases, and up to 90% improvement over WCETT is observed. Note that the maximum improvement in this experiment is smaller than in experiment 1 because this experiment has fewer channels.

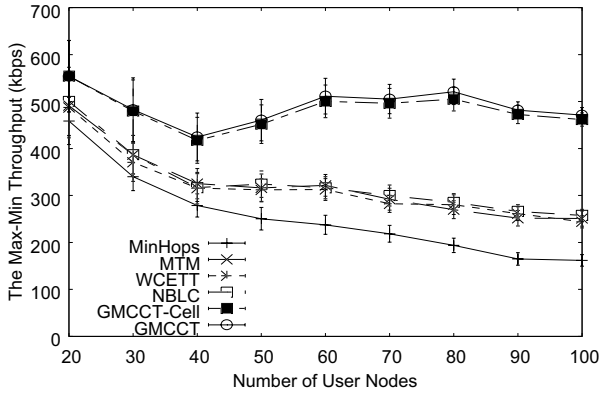


(a) The max-min throughput

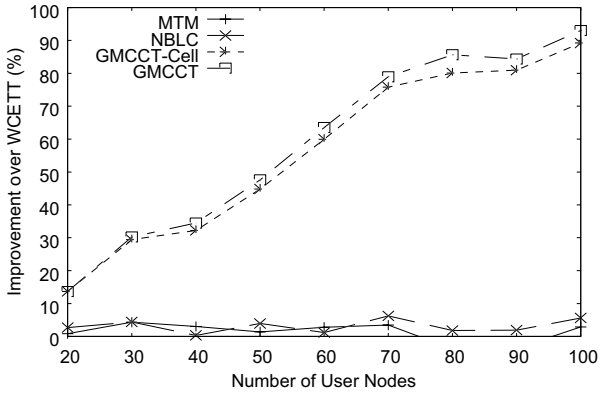


(b) Throughput improvement over WCETT

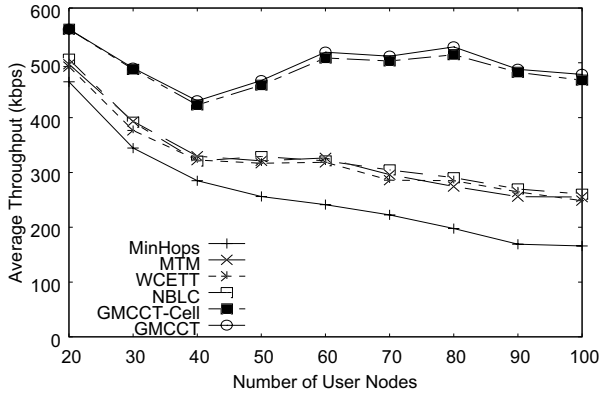


(c) Average throughput

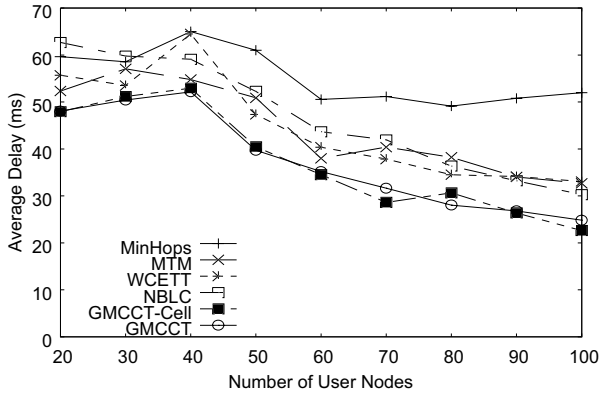


(d) Average packet delay

Figure 6.3: Impact of the number of user nodes on post-CA routing algorithms

Like experiment 2 in Section 5.4.2, Figure 6.3(a) shows an appealing phenomenon of CMESH cells, namely that per-user-node throughput may not decrease significantly as the number of user nodes increases, because adding user nodes can increase network connectivity

and improve link quality in a random cell.

Figure 6.3(d) shows that the proposed routing algorithms have similar average packet delay compared to the four existing routing algorithms as the number of user nodes increases. This suggests that the improvement in cell capacity over other algorithms does not come at the cost of higher packet delay. In addition, it can be observed that for most algorithms, the average packet delay generally decreases as the number of user nodes increases for the same reason articulated in Section 5.4.2. Finally, the average packet delay in the simulations is on the order of tens of milliseconds, which may be decreased further by future research.

**Impact of the Number of Traffic Flows**

The third experiment examines the performance of the post-CA routing algorithms in random CMESH cells as the number of traffic flows increases. The results are shown in Figure 6.4.

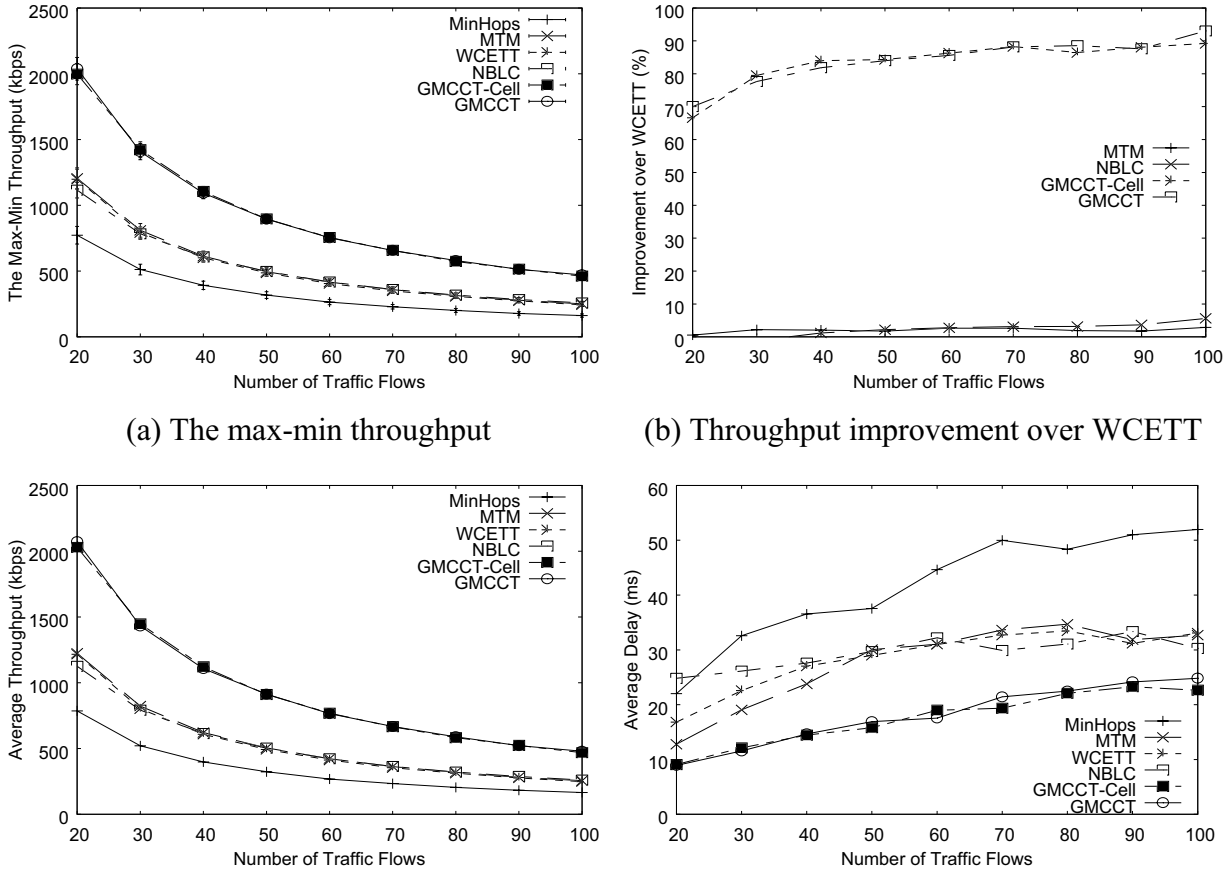


(a) The max-min throughput

(b) Throughput improvement over WCETT

(c) Average throughput

(d) Average packet delay

Figure 6.4: Impact of the number of traffic flows on post-CA routing algorithms

Like the previous two experiments, Figure 6.4(a) shows that the six routing algorithms divide into three groups according to their max-min throughputs, and the proposed routing algorithms outperform the others. Figure 6.4(b) shows that the throughput gain achieved by the proposed algorithms generally increases as the number of traffic flows increases, and up to 90% improvement over WCETT is observed.

Figure 6.4(a) shows that the max-min throughput decreases as the number of flows increases, which is consistent with the theoretical results in Chapter 3, which say that per-user-node throughput is inversely proportional to the number of user nodes. The reason is the same as in Section 5.4.3.

Figure 6.4(d) shows that the proposed routing algorithms generally have lower average packet delay than the four existing routing algorithms as the number of traffic flows increases. In addition, it can be observed that the average packet delay generally increases as the number of traffic flows increases. Finally, the average packet delay in the simulations is on the order of tens of milliseconds, which may be decreased further by future research.

**Impact of the Cell Coverage Area**

The fourth experiment examines the performance of the post-CA routing algorithms in random CMESH cells as the cell area size increases. The results are shown in Figure 6.5.

Recall that this experiment uses a special relay node deployment algorithm, called Cut-Hop, to handle the problem of long hops. For this reason, the results in Figure 6.5 are different from those in the other three experiments.

Like the previous experiments, Figure 6.5(a) shows that the six routing algorithms divide into three groups according to the max-min throughput, and the proposed algorithms outperform the others. Figure 6.5(b) shows that the proposed algorithms increase cell capacity by up to 90% compared to WCETT. It can be observed that the throughput gain generally decreases as the cell coverage area increases, and GMCCT performs better than GMCCT-Cell. However, the improvement is not very significant because the Random channel assignment algorithm does not optimize channel assignment and prevents GMCCT from fully utilizing channel spatial reuse.

Like in Section 5.4.4, Figure 6.5(a) shows another appealing phenomenon of CMESH cells: if enough relay nodes can be deployed, increasing the coverage area of a cell above a certain threshold may not further decrease per-user-node throughput.

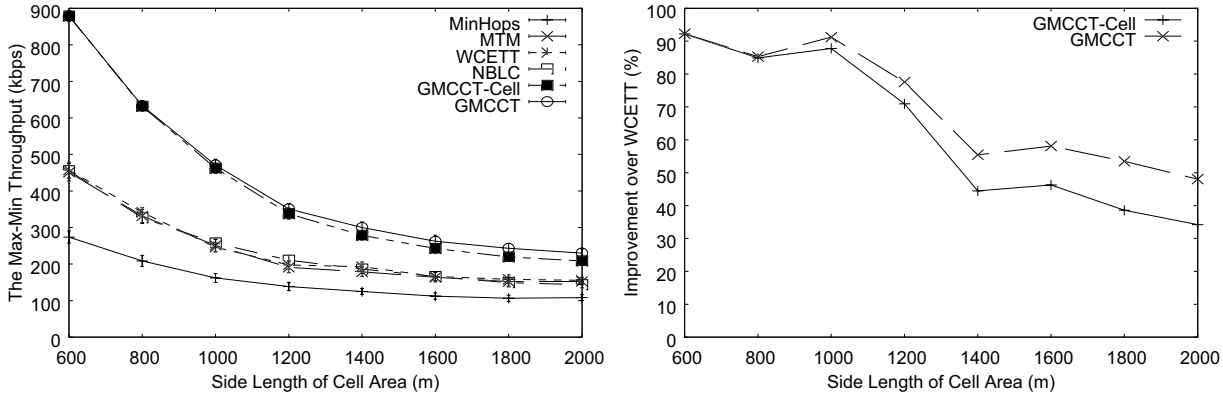


(a) The max-min throughput




(b) Throughput improvement over WCETT

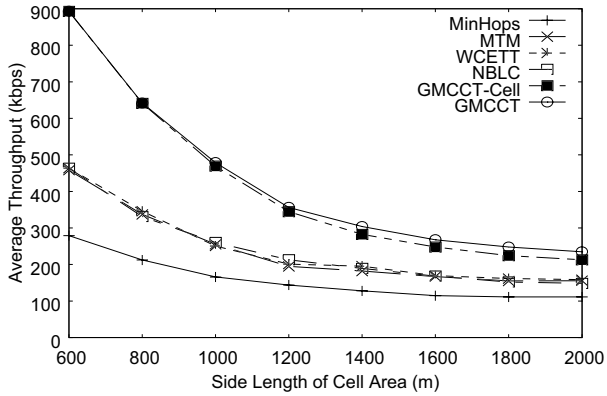


(c) Average throughput

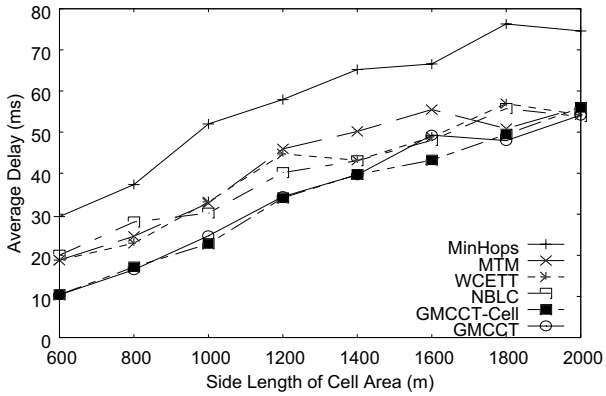


(d) Average packet delay

Figure 6.5: Impact of the cell coverage area on post-CA routing algorithms

Figure 6.5(d) shows that the proposed routing algorithms generally have similar average packet delay compared to the existing routing algorithms as the cell coverage area increases. In addition, it can be observed that the average packet delay generally increases as the cell coverage area increases. This is because user packets need to travel more hops and thus need more transmission time. Finally, the average packet delay is on the order of tens of milliseconds.

## 6.3 Pre-CA (Channel Assignment) Routing Algorithms

This section studies pre-CA routing algorithms that run before channel assignment. Pre-CA routing algorithms run without the knowledge of $\vec{C}_V$, but they know that channel assignment algorithms will run after them and will use their routes as input.

Simulation experiments in Chapter 5 showed that channel assignment algorithms need pre-CA routing algorithms to help them circumvent bottleneck wireless links. Therefore, pre-CA

routing algorithms should anticipate and prepare the routes required by channel assignment algorithms, designed for maximizing cell capacity.

### 6.3.1 The GMCCT-CPLB and GMCCT-CPLB-Cell Routing algorithms

Because the CPLB channel assignment algorithm is relatively simple and shows satisfying performance (see Chapter 5), the post-CA GMCCT algorithm in Section 6.2.2, can be modified to a pre-CA routing algorithm by preparing routes for the CPLB channel assignment algorithm. This new pre-CA routing algorithm, named GMCCT-CPLB, is given as Algorithm 11.

GMCCT-CPLB needs the interference vector $\vec{I}_E$ as input, which may not always be easily collected in a large cells. Therefore, GMCCT-CPLB-Cell is proposed. It does not require $\vec{I}_E$ as input by assuming that all wireless links in a cell interfere with each other if they are on the same channel. The term "Cell" in the name is used to indicate this assumption. GMCCT-CPLB-Cell is given as Algorithm 12.

### 6.3.2 Performance Comparisons

This section evaluates the performance of the proposed pre-CA routing algorithms (GMCCT-CPLB and GMCCT-CPLB-Cell) by comparison with two existing pre-CA routing algorithms: MinHops and MTM (see Section 6.2.3). Experiments were conducted in 802.11a-compatible random CMESH cells through ns-2 simulations.

MinHops and MTM were selected for comparison because they belong to the family of pre-CA routing algorithms, i.e., they do not require any channel information in a cell to find paths of nodes. In contrast, WCETT and NBLC cannot be selected because they do not belong to pre-CA routing algorithms, i.e., they require the channel information in a cell as input.

The experiment design is similar to that in Section 6.2.3, except for the channel assignment algorithm. In the simulation experiments designed for pre-CA routing algorithms, no channel assignment algorithm has run before the routing algorithms, and the CPLB channel assignment algorithm runs after them. CPLB is selected because it is simple and performs well in the channel assignment simulation experiments in Section 5.4.

The results are shown in Figure 6.6, Figure 6.7 and Figure 6.8. The average throughput is not presented because it is always above but close to the max-min throughput due to the max-min fairness mechanism used in the simulations (see Section 6.2.3).

Algorithm 11: The GMCCT-CPLB routing algorithm

Input: $\vec{V}$, $\vec{E}$, $\vec{a}$, $\vec{I}_E$, $\vec{w}_E$, $\widehat{C}$.

Output: $\vec{H}_V = (H_1, ...H_{|\vec{N}|})$.

1. Get $\vec{H}_V$ via the CETT-HL algorithm (Algorithm 8) with $\vec{V}$, $\vec{E}$, $\vec{a}$, $\vec{w}_E$ as input.
2. Get $\vec{C}_V = (C_1, ..., C_{|\vec{V}|})$ via the CPLB algorithm (Algorithm 4) with $\vec{V}$, $\vec{E}$, $\vec{a}$, $\vec{R}_V(\vec{H}_V)$, $\vec{I}_E$, $\vec{w}_E$, $\widehat{C}$ as input.

Loop {

3. Get $M = \max(\widehat{\text{CCT}})$ and the corresponding $\widehat{I}_e^+(C_e)$ via the MCCT algorithm (Algorithm 1) with $\vec{V}$, $\vec{E}$, $\vec{a}$, $\vec{R}_V(\vec{H}_V)$, $\vec{C}_E(\vec{C}_V)$, $\vec{I}_E$, $\vec{w}_E$ as input.
4. Get $\vec{V}_E = (\widehat{V}_1, ..., \widehat{V}_{|\vec{E}|})$ via $\vec{V}$, $\vec{E}$ and $\vec{R}_V(\vec{H}_V)$ (Equation(6.1)).
5. Get $\vec{T}_E = (T_1, ..., T_{|\vec{E}|})$ via $\vec{V}_E$, $\vec{a}$ and $\vec{w}_E$ (Equation (6.2) and Equation (6.6)).
6. Get $\vec{Q}$ that includes $\widehat{I}_e^+(C_e)$ and that $\forall e \in \widehat{Q}, T_e \in \widehat{T}_E$ is in descending order.
7. For each sorted element $e$ in $\vec{Q}$, $T_e > 0$:
   7.1) Get $\vec{Z}$ that includes $\widehat{V}_e$ and that $\forall v \in \widehat{Z}_e, T_{e_v} \in \widehat{T}_E$ is in descending order.
   7.2) For each sorted element $v$ in $\vec{Z}$, $T_{e_v} > 0$:
      7.2.1) For each node $u$ in set $\{u \mid e_{u,v} \in \widehat{E}\}$, $e \notin \widehat{R}_u$:
         7.2.1a) Get $\vec{C}'_V = (C_1, ..., C_{|\vec{V}|})$ via the CPLB algorithm (Algorithm 4) with $\vec{V}$, $\vec{E}$, $\vec{a}$, $\vec{R}_V(\vec{H}_V(H_v = u))$, $\vec{I}_E$, $\vec{w}_E$, $\widehat{C}$ as input.
         7.2.1b) Get $M' = \max(\widehat{\text{CCT}})$ via the MCCT algorithm (Algorithm 1) with $\vec{V}$, $\vec{E}$, $\vec{a}$, $\vec{R}_V(\vec{H}_V(H_v = u))$, $\vec{C}_E(\vec{C}'_V)$, $\vec{I}_E$, $\vec{w}_E$ as input.
         7.2.1c) If $M' < M$ then update $H_v \leftarrow u$ and go back to loop
8. If no $H_v$ is updated in this iteration of the loop, then this algorithm exits.

} End Loop

Algorithm 12: The GMCCT-CPLB-Cell routing algorithm

Input: $\vec{V}$, $\vec{E}$, $\vec{a}$, $\vec{C}_V$, $\vec{w}_E$.

Output: $\vec{H}_V = (H_1, ...H_{|\vec{N}|})$.

1. Get $\vec{I}_E = (\hat{E} - \{e_1\}, ..., \hat{E} - \{e_{|\vec{E}|}\})$.
2. Get $\vec{H}_V$ via the GMCCT-CPLB algorithm (Algorithm 11) with $\vec{V}$, $\vec{E}$, $\vec{a}$, $\vec{C}_V$, $\vec{I}_E$, $\vec{w}_E$ as input.

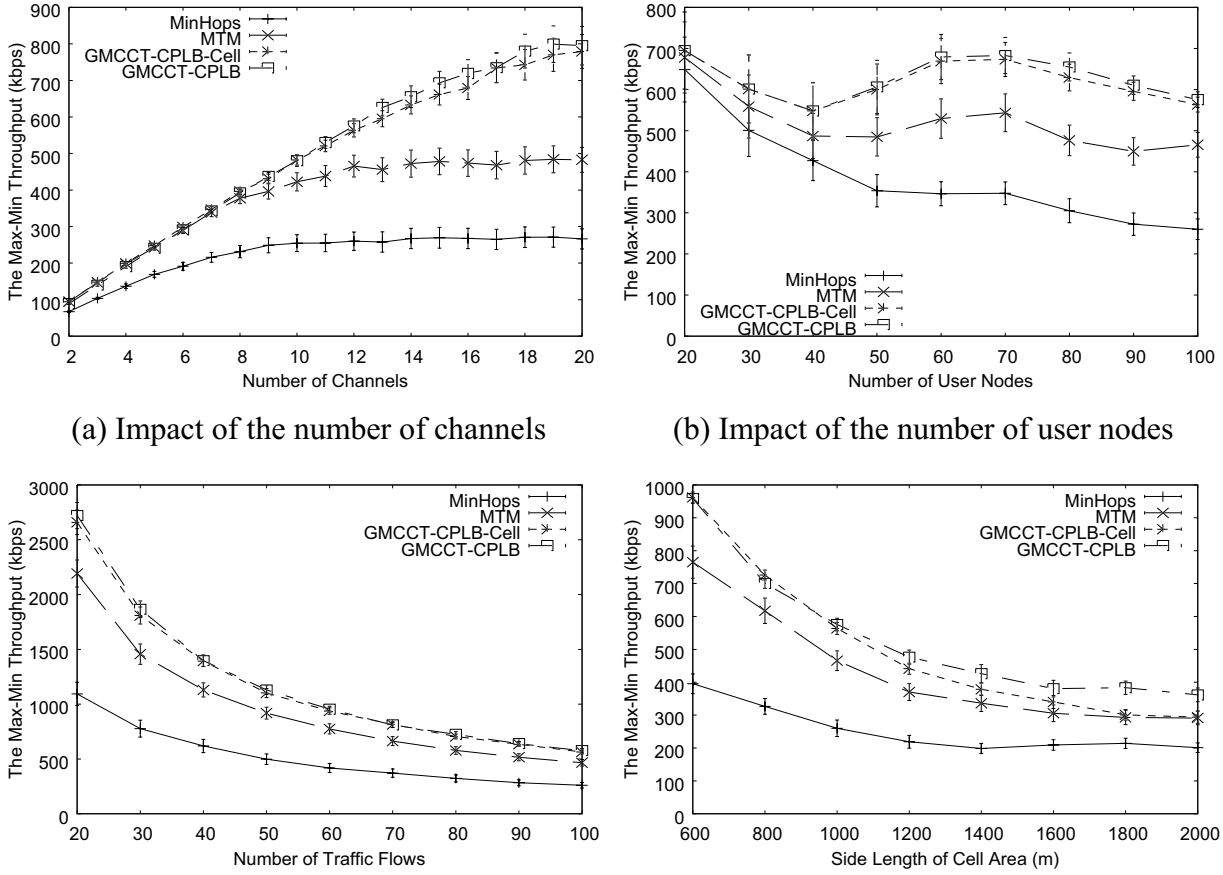


(a) Impact of the number of channels

(b) Impact of the number of user nodes

(c) Impact of the number of traffic flows

(d) Impact of the cell coverage area

Figure 6.6: The max-min throughput in the pre-CA routing simulation results (Routing is followed by the CPLB channel assignment algorithm)

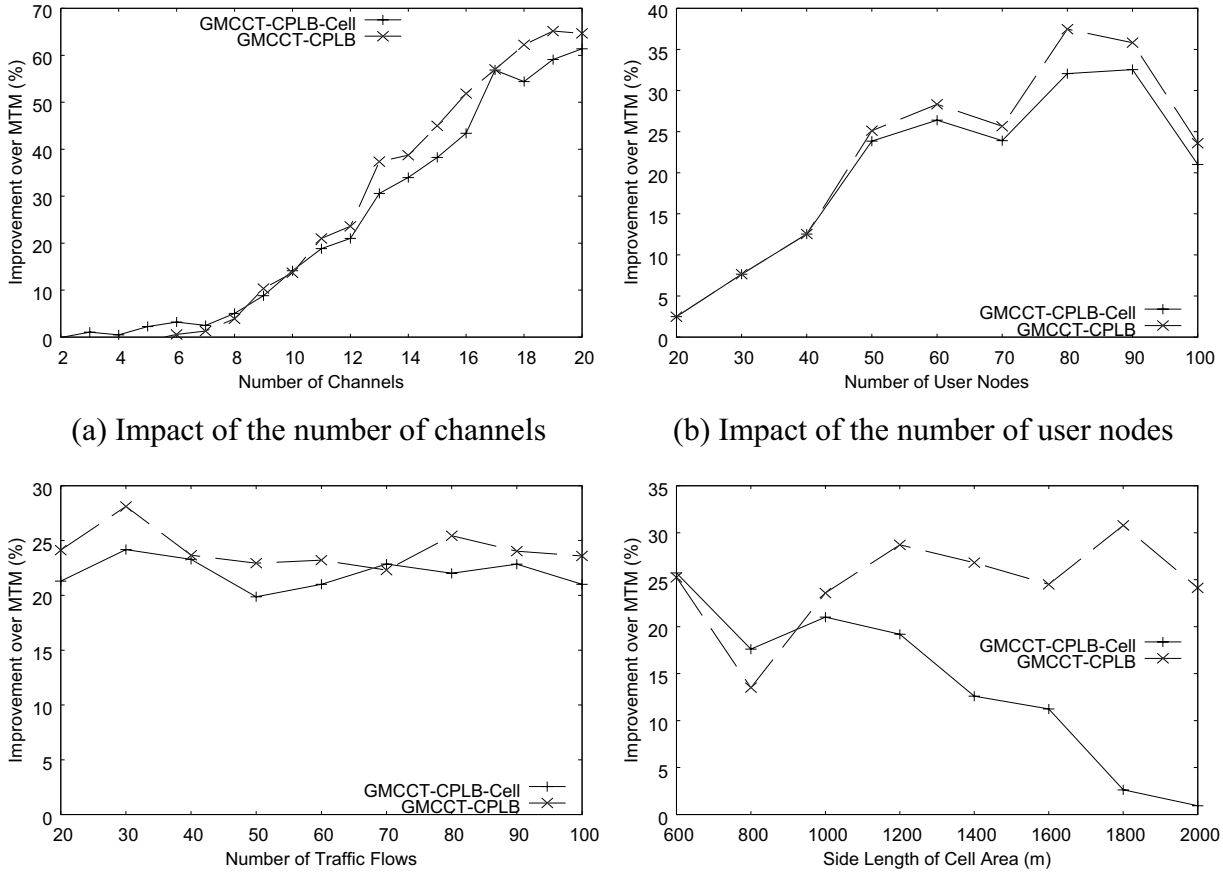


(a) Impact of the number of channels

(b) Impact of the number of user nodes

(c) Impact of the number of traffic flows

(d) Impact of the cell coverage area

Figure 6.7: The improvement over MTM in the pre-CA routing simulation results (Routing is followed by the CPLB channel assignment algorithm)

Figure 6.6 shows the max-min throughput with 95% confidence intervals. Except for Figure 6.6(d), the four routing algorithms divide into three groups according to their max-min throughputs: MinHops performs the worst; MTM performs better; the third group (containing the proposed GMCCT-CPLB and GMCCT-CPLB-Cell) performs the best.

Figure 6.6(d) shows that GMCCT-CPLB-Cell degrades to MTM as the cell coverage area increases. This is because the CPLB channel assignment algorithm makes up for the second weakness of MTM (see Section 6.2.2) by performing load balancing among channels after MTM. GMCCT-CPLB performs significantly better than MTM because it can makes up for the third weakness of MTM by utilizing channel spatial reuse.

In Figure 6.7, it can be observed that the throughput gain by the proposed pre-CA algorithms is lower than by the proposed post-CA algorithms in Section 6.2.3 (note that in the post-CA

experiments, although WCETT is used for comparison, it performs similarly to MTM). For example, in experiment 1 (Figure 6.7a), the maximum throughput gain achieved by the proposed pre-CA algorithms is roughly 65%, which is significantly lower than the 100% achieved by the proposed post-CA algorithms. This is because the Random channel assignment algorithm was used in the post-CA routing experiments, but the pre-CA routing experiments used the CPLB channel assignment algorithm which performs load balancing among channels, and thus makes up for the second weakness of MTM (see Section 6.2.2).

Figure 6.8 shows that the proposed routing algorithms generally have similar packet delay compared to MTM. The average packet delay in the simulations is on the order of tens of milliseconds, which may be decreased further by future research.

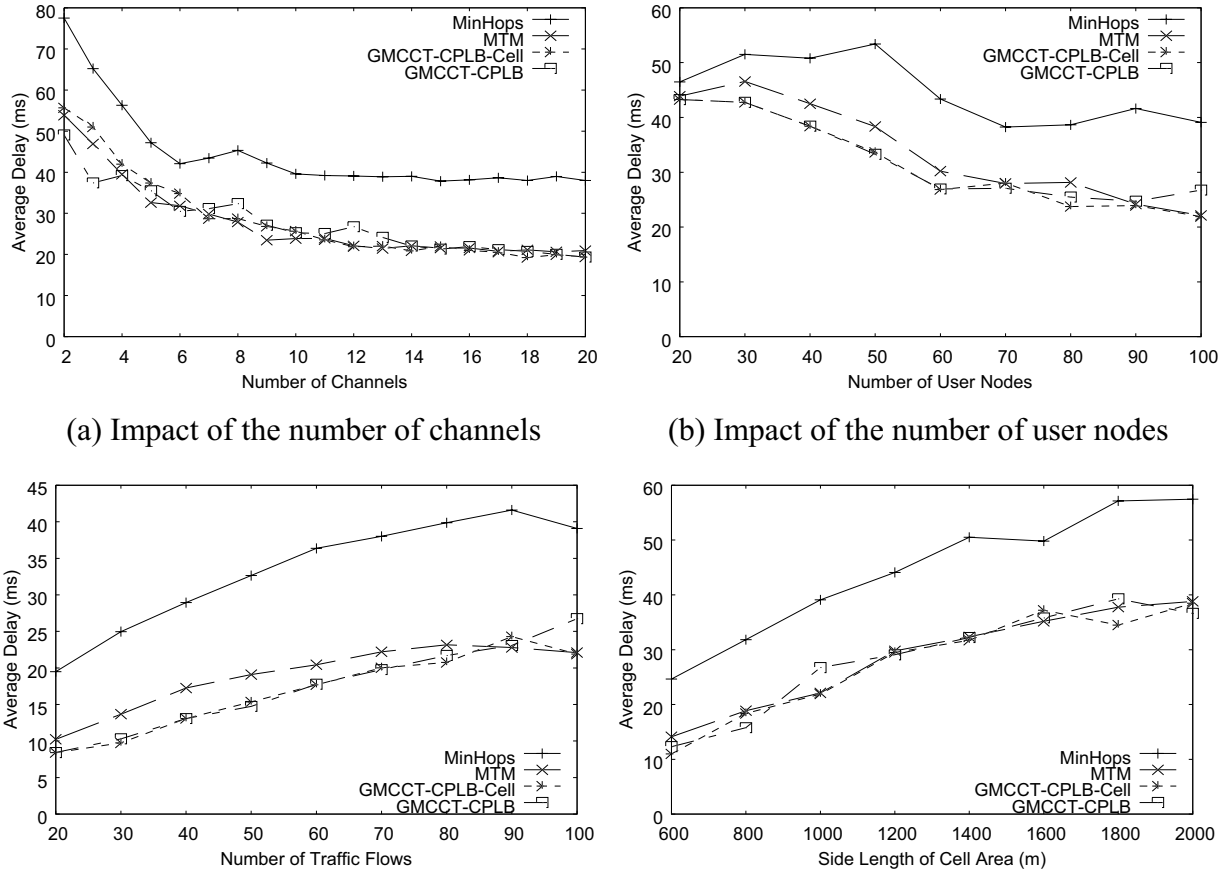


(a) Impact of the number of channels

(b) Impact of the number of user nodes

(c) Impact of the number of traffic flows

(d) Impact of the cell coverage area

Figure 6.8: The average packet delay in the pre-CA routing simulation results (Routing is followed by the CPLB channel assignment algorithm)

### 6.3.3 Revisiting the Performance of Channel Assignment Algorithms

In the channel assignment experiments in Chapter 5, the MTM-LB routing algorithm is found to have negative impacts on the performance of channel assignment algorithms. Therefore, it is necessary to use the pre-CA routing algorithms proposed in this Chapter to re-evaluate the performance of the channel assignment algorithms. GMCCT-CPLB is selected to replace MTM-LB. GMCCT-CPLB-Cell is not selected because it neglects channel spatial reuse and does not perform well in a large cell area (see Section 6.3.2).

Figure 6.9 and Figure 6.10 show the simulation results of four channel assignment algorithms: DPLT, DPLB, CPLB and CPLB-GMCCT (see Section 5.4). Figure 6.9 shows the max-min throughput with 95% confidence intervals. Figure 6.10 shows the percentage improvement of the three proposed algorithms compared to DPLT.

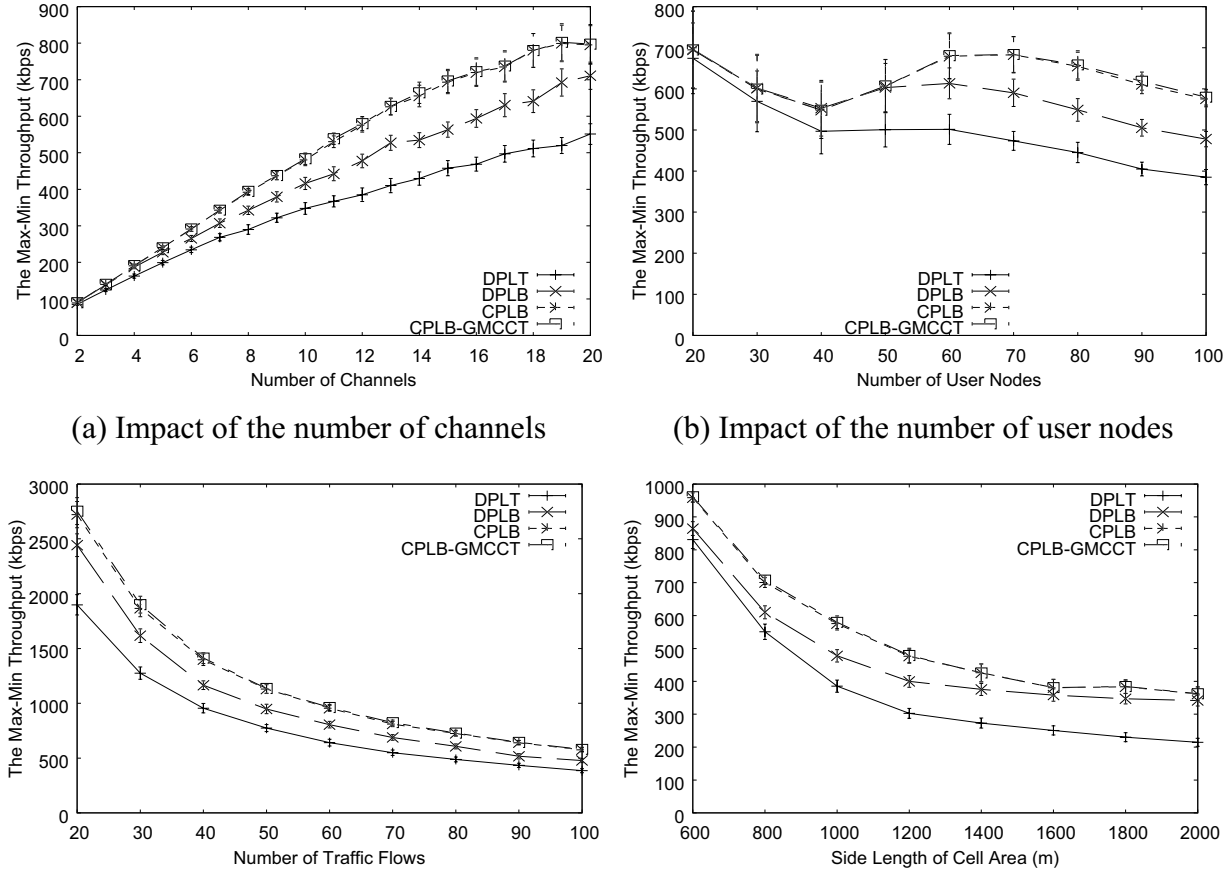


(a) Impact of the number of channels

(b) Impact of the number of user nodes

(c) Impact of the number of traffic flows

(d) Impact of the cell coverage area

Figure 6.9: Revisiting channel assignment simulations (the max-min throughput)
(Channel assignment runs after the GMCCT-CPLB routing algorithm)

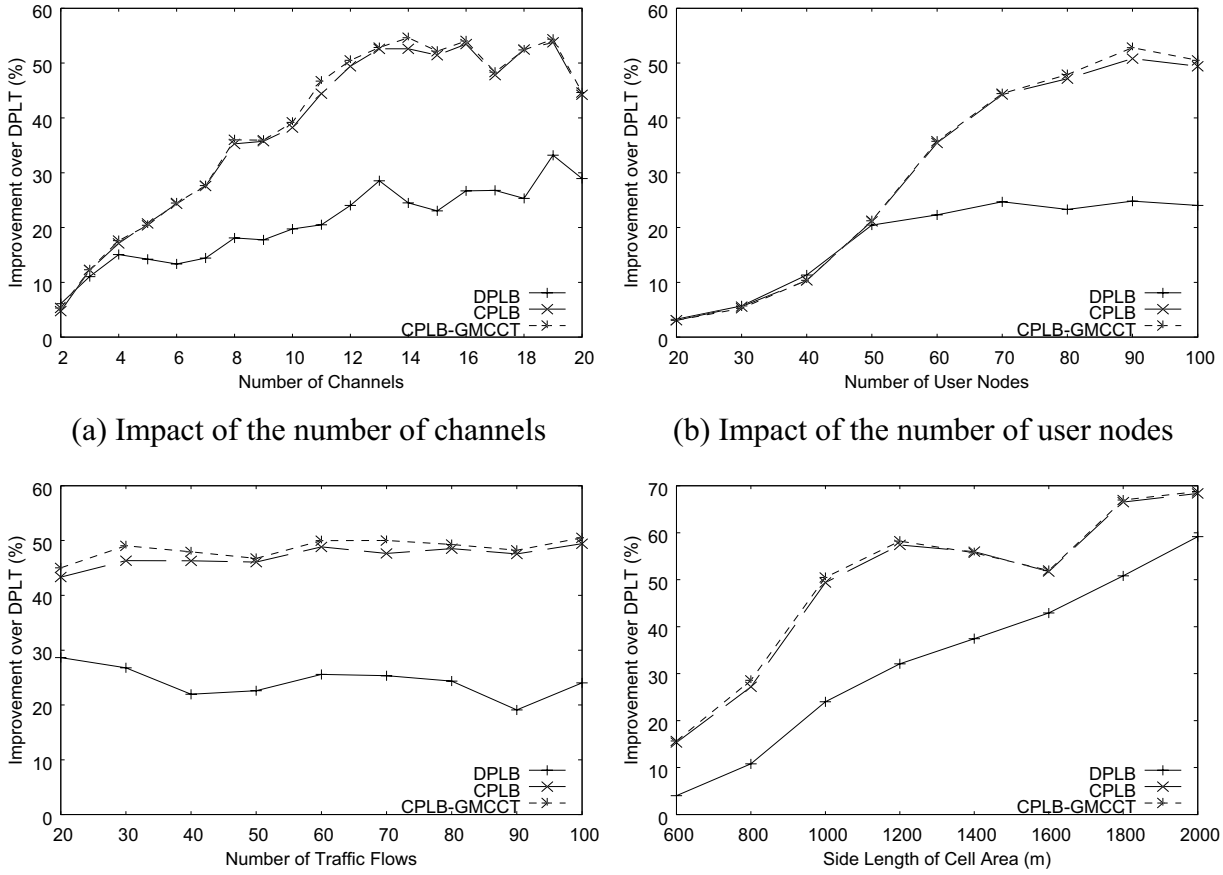


(a) Impact of the number of channels

(b) Impact of the number of user nodes

(c) Impact of the number of traffic flows

(d) Impact of the cell coverage area

Figure 6.10: Revisiting channel assignment simulations (improvement over DPLT)
(Channel assignment runs after the GMCCT-CPLB routing algorithm)

Figure 6.9(a) shows that the proposed channel assignment algorithms significantly outperform DPLT as the number of channels increases. Figure 6.10(a) shows that the throughput gain generally increases as the number of channels increases, and up to a roughly 55% increase in the max-min throughput is observed.

Figure 6.9(b) shows that the proposed channel assignment algorithms achieve significantly higher throughput than DPLT as the number of user nodes exceeds 50. Figure 6.10(b) shows that the throughput gain generally increases as the number of user nodes increases, and up to a roughly 55% improvement over DPLT is observed.

Figure 6.9(c) shows that the proposed channel assignment algorithms significantly outperform DPLT as the number of traffic flows increases. Figure 6.10(c) shows that the percentage improvement in the max-min throughput over DPLT is quite stable and up to a roughly 50%

increase in the max-min throughput is observed.

Figure 6.9(d) shows that the proposed channel assignment algorithms achieve significantly higher throughput than DPLT as the cell area size increases. Figure 6.10(d) shows that the throughput gain generally increases as the cell area size increases, and up to a nearly 70% improvement in max-min throughput over DPLT is observed.

Figure 6.10 shows that compared with the simulation results in Section 5.4 where the MTM-LB routing algorithm is used, the percentage improvement is approximately doubled by using the proposed GMCCT-CPLB routing algorithm.

## 6.4 Summary

A CMESH cell generally has a large number of wireless links that operate at different bit rates and loss rates on different channels. Therefore, it is important for routing algorithms to fully utilize these abundant and diverse wireless links and channels to maximize cell capacity, in terms of the max-min throughput. This chapter studied two types of routing algorithms that run either before or after channel assignment algorithms.

This chapter first addressed post-CA routing algorithms that run after channel assignment. By analyzing the post-CA routing problem in small cells, the strengths and weaknesses of the MTM routing algorithm were revealed. In order to overcome the weaknesses of MTM, two greedy MCCT-based algorithms were proposed, called GMCCT and GMCCT-Cell, which work for both small cells and large cells.

This chapter also studied pre-CA routing algorithms that run before channel assignment. The proposed post-CA routing algorithms were converted to pre-CA routing algorithms by preparing routes for the CPLB channel assignment algorithm.

The ns-2 simulation results showed that the proposed post-CA routing algorithms can improve the capacity of random CMESH cells by up to 100% compared to the WCETT routing algorithm, and the proposed pre-CA routing algorithms can increase the capacity of random CMESH cells by up to 65% compared to the MTM routing algorithm.

# CHAPTER 7
# SUMMARY AND CONCLUSIONS

A cellular wireless mesh network (CMESH) is envisioned as a potential solution for future ubiquitous broadband wireless access networks. It has the potential to be globally deployed to provide broadband (at least comparable to the DSL/Cable technology) wireless Internet access for the public. A CMESH can utilize abundant high radio frequencies, such as 5-50 GHz, and just as city lights can light up every corner of a city, its mesh nodes, if widely deployed, may provide high-speed Internet to every corner of a city.

Previous research on wireless mesh networks (WMNs) has investigated network capacity, channel assignment, routing and other issues. Based on this research, the thesis focuses on a CMESH, organized in multi-radio, multi-channel, multi-rate and multi-hop radio cells, where each cell has a single Internet-connected gateway and can serve a large number of user nodes in a large coverage area.

The thesis addresses performance issues in a CMESH, focusing specifically on cell capacity, expressed in terms of the max-min throughput. The research has four parts, which are addressed in four chapters: cell capacity bounds in Chapter 3, nominal cell capacity in Chapter 4, channel assignment in Chapter 5 and routing in Chapter 6.

The relationships of the four parts are shown in Figure 7.1, where cell capacity, defined as the max-min throughput, represents the main performance metric. Inside the big square box in Figure 7.1 are labels for the six main network issues in a CMESH cell. Arrows show cell capacity's reliance on these main network issues and assumptions. For example, wireless links and their interference relationships cannot be determined without the locations of user nodes and relay nodes and the assumption of a wireless model.

The remainder of this chapter is organized as follows. Section 7.1 summarizes each part of the thesis research. Section 7.2 states the main contributions. Finally, Section 7.3 briefly considers some possible areas for future research.

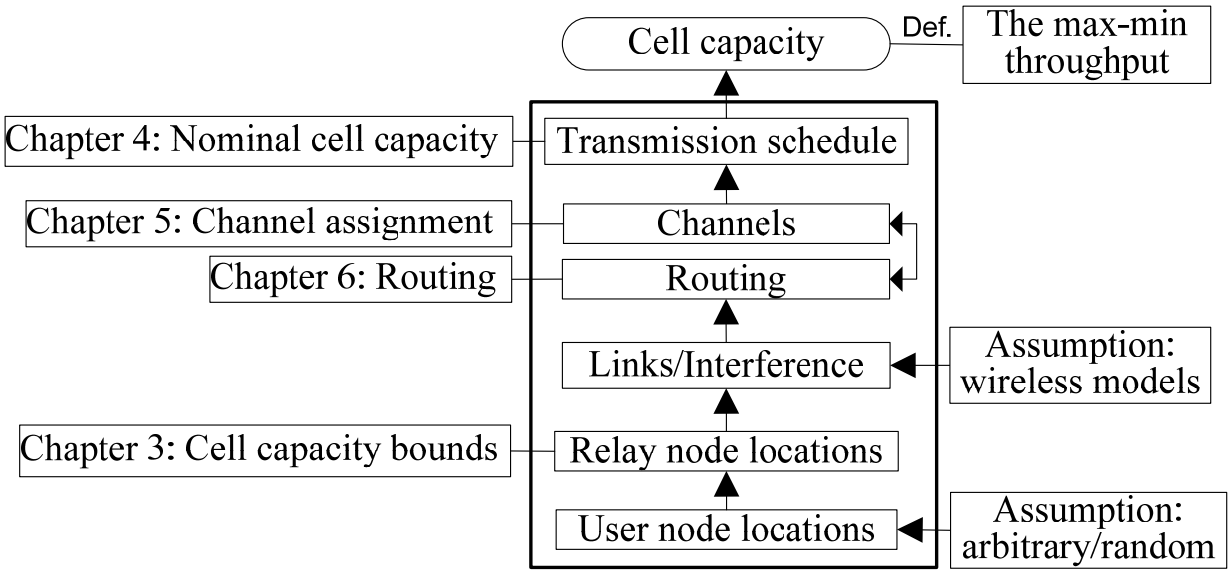


Figure 7.1: Thesis research organization

## 7.1 Thesis Summary

The thesis focuses on the capacity of multi-radio, multi-channel, multi-rate and multi-hop cells in a CMESH, in terms of the max-min throughput. The capacity of a CMESH cell is affected by many factors, such as wireless relay node deployment, channel assignment, routing and transmission scheduling. This research addresses the major factors.

### Capacity Bounds for CMESH Cells

A key research question for a CMESH is the capacity of its cells. Given $C$ orthogonal channels and $N$ user nodes randomly located in a CMESH cell of radius $R$, how much expected throughput can be guaranteed for each user node?

It is difficult to answer this question using two common research tools: linear programming and asymptotic analysis. Linear programming requires complete knowledge of cell topology and interference among wireless links to calculate cell capacity, but the locations of relay nodes in a CMESH cell are not given. Asymptotic analysis cannot reveal the capacity of a typical CMESH cell with tens or hundreds of user nodes, because the scale of the cell is too small for asymptotic analysis to derive network capacity.

Therefore, the thesis employed a new method based on a new notion called Channel Transport Capacity (CTC) and derived analytic expressions for the capacity bounds of carrier-sense-based

CMESH cells within the abstract models. Upper bounds for cell capacity were derived by analyzing the supply and demand of CTC, and lower bounds were derived by finding a joint scheme of relay node deployment, routing, channel assignment and transmission scheduling that achieves a certain throughput.

Simulation experiments showed that the derived capacity bounds are consistent with simulation results given by Jun and Sichitiu's bottleneck collision domain (BCD) algorithm [68].

**Nominal Capacity of CMESH Cells**

Jun and Sichitiu's BCD algorithm [68] and its multi-channel variant [4] and max-min fairness variants [10, 11] can calculate the nominal network capacity for a single-gateway and single-rate WMN. CMESH cells are multi-rate WMNs, however, so this thesis extended the BCD algorithm and proposed the Maximum Channel Collision Time (MCCT) algorithm, which calculates the nominal network capacity for multi-radio, multi-channel, multi-rate and multi-hop CMESH cells. It was shown that the nominal cell capacity is achievable and is the exact cell capacity for small cells within the abstract models. The MCCT algorithm was further extended to take into account packet loss on wireless links and arbitrary traffic demands of user nodes.

Simulation experiments were carried out to validate the nominal cell capacity in random CMESH cells. The simulations were conducted with a modified ns-2 simulator [120] using wireless parameter values from the IEEE 802.11a standard and the specification of a Cisco 802.11a product, and using a max-min fairness mechanism to ensure the max-min throughput. The nominal cell capacity was first adjusted to estimate the usable cell capacity and was then compared with ns-2 simulation results. The two results were found to match well.

**Channel Assignment Algorithms**

A CMESH cell is expected to have multiple orthogonal channels, and fully and efficiently utilizing these available channels can improve cell capacity. Therefore, channel assignment is an important research topic in CMESHs.

Channel assignment in CMESH cells is to assign channels to the down radios of mesh nodes in order to maximize cell capacity. Channel assignment in multi-radio wireless networks has been shown by previous research [34, 106, 111, 117] to be an NP-hard problem. Therefore, this research studies only greedy channel assignment algorithms.

This thesis first studied the problem of channel assignment in small cells. The thesis proved that this problem is equivalent to the multiprocessor scheduling problem [33], and introduces the CPLB-Cell channel assignment algorithm for small cells. CPLB-Cell was extended further to large cells, and a centralized algorithm (called CPLB) and a distributed algorithm (called DPLB) were proposed. Then the weakness of CPLB in large cells is identified. To overcome the weakness of CPLB, two greedy algorithms based on the MCCT algorithm (called GMCCT-LB and CPLB-GMCCT) were proposed.

Simulation results showed that the proposed channel assignment algorithms can significantly improve the capacity of random CMESH cells compared to the DPLT algorithm, with up to a nearly 70% increase in cell capacity.

**Routing Algorithms**

A CMESH cell generally has a large number of wireless links that operate at different bit rates and loss rates on different channels. Therefore, it is important for routing algorithms to fully utilize these abundant and diverse wireless links and channels to maximize cell capacity, in terms of the max-min throughput.

The thesis first considered routing algorithms that run after channel assignment, called post-CA algorithms. By analysis of an equivalent problem to the problem of post-CA routing in small cells, the strengths and weaknesses of the MTM routing algorithm are addressed. To overcome the weaknesses of MTM, the thesis proposed two greedy routing algorithms based on the MCCT algorithm (called GMCCT and GMCCT-Cell) for both small cells and large cells.

The thesis then considered routing algorithms that run before channel assignment, called pre-CA algorithms. A pre-CA routing algorithm has no knowledge of the channels assigned to the down radios in a cell, but it knows that a channel assignment algorithm will run after it and adapt to its routes. GMCCT and GMCCT-Cell were converted to two pre-CA routing algorithms by preparing routes for the CPLB channel assignment algorithm.

Simulation results showed that the post-CA routing algorithms proposed can improve the capacity of random CMESH cells by up to 100% compared to the WCETT routing algorithm, and the pre-CA routing algorithms proposed can increase cell capacity up to 65% compared to the MTM routing algorithm.

## 7.2 Thesis Contributions

In summary, the following are the main contributions of this thesis.

- A cellular wireless mesh network (CMESH) is proposed as a potential solution for future ubiquitous broadband wireless access networks. A CMESH can utilize high radio frequencies such as 5-50 GHz, and thus may satisfy the bandwidth requirements of future ubiquitous wireless applications.
- A new method is proposed for analyzing theoretical cell capacity based on a new concept called Channel Transport Capacity (CTC), and new analytic expressions are derived within the abstract models for capacity bounds for carrier-sense-based cells in CMESHs.
- A new algorithm is proposed, called Maximum Channel Collision Time (MCCT), which derives an expression for the nominal cell capacity. The nominal cell capacity is then proven to be achievable and to be the exact cell capacity for small cells within the abstract models. The MCCT algorithm is further extended to take into account packet loss and arbitrary traffic demands of user nodes.
- New greedy channel assignment and routing algorithms based on the MCCT algorithm are proposed. Simulation results show that these greedy algorithms can significantly improve the capacity of CMESH cells, compared with algorithms proposed by other researchers.

In addition to the main contributions, this thesis makes the following minor contributions. First, a max-min fairness mechanism is proposed for CMESH cells, which includes a source rate control scheme and a scheme of round robin queues and group packet transmissions. Second, this thesis extends the ns-2 simulator to support multi-radio, multi-channel, multi-rate and IEEE 802.11a networks. Also, this thesis designs two algorithms for wireless relay node deployment in CMESH cells, called Least-RN and Cut-Hop.

## 7.3 Future Work

There are some unexplored research issues relating to the performance of CMESHs.

1. Upstream cell capacity bounds need to be derived, and simulation experiments need to be performed for upstream traffic. This thesis focused on downstream cell capacity and Chapter 3 showed that the upstream cell capacity is theoretically no less than the downstream cell capacity.

2. The impact of inter-cell interference on cell capacity needs to be investigated. For small cells, neighbouring cells have to use a different set of channels to avoid inter-cell interference. For large random cells, it may be possible for each cell to use a common set of channels without losing each cell's capacity. However, this requires that these cells are sufficiently large, and research is needed to investigate this problem.
3. Additional schemes for wireless relay node deployment need to be explored. Deploying wireless relay nodes is an important way to improve cell capacity in CMESHs. This thesis studied straight-line deployment and proposed the Least-RN and the Cut-Hop algorithms. More schemes need to be studied in order to reduce the number of relay nodes and at the same time satisfy the cell capacity requirements.
4. In IEEE 802.11-compatible CMESH cells, collision-related protocol overhead such as backoff time needs to be modelled, so that the MCCT algorithm can predict the usable cell capacity more accurately. This can help improve the performance of the channel assignment and the routing algorithms in 802.11-compatible cells, because they use the MCCT algorithm to improve the usable cell capacity.
5. Packet delay requires further research. How to provide guaranteed low packet delay and how to provide fairness for packet delay among user nodes are important research questions. This thesis focused on throughput, and so it addressed packet delay only briefly and its simulation results showed only average packet delay.
6. TCP performance needs to be investigated. This thesis did not use TCP in the simulations because the congestion control mechanism in TCP conflicts with the max-min fairness (TCP approximately provides proportional fair rate sharing) and thus prevents the identification of cell capacity. However, significant Internet traffic uses TCP, so improving TCP performance in CMESH cells is an important research issue that needs to be investigated.

## References


[1] N. Abramson. The ALOHA system - another alternative for computer communications. In *AFIPS Conference Proceedings*, pp. 281-285, 1970.

[2] A. Adya, P. Bahl, J. Padhye, A. Wolman and L. Zhou. A multi-radio unification protocol for IEEE 802.11 wireless networks. In *IEEE BROADNETS'04*, San Jose, California, USA, pp. 344-354, 2004.

[3] D. Aguayo, J. Bicket, S. Biswas, G. Judd and R. Morris. Link-level measurements from an 802.11b mesh network. In *ACM SIGCOMM'04*, Portland, Oregon, USA, pp. 121–132, 2004.

[4] N. Akhtar and K. Moessner. On the nominal capacity of multi-radio multi-channel wireless mesh networks. *Computer Communications*, *31* (8), pp. 1475-1483, 2008.

[5] I.F. Akyildiz and X. Wang. A survey on wireless mesh networks. *IEEE Radio Communications*, *43* (9), pp. s23- s30, 2005.

[6] I.F. Akyildiz, X. Wang and W. Wang. Wireless mesh networks: A survey. *Computer Networks and ISDN Systems*, *47* (4), pp. 445-487, 2005.

[7] M. Alicherry, R. Bhatia and L.E. Li. Joint channel assignment and routing for throughput optimization in multi-radio wireless mesh networks. In *MOBICOM'05*, Cologne, Germany, pp. 58-72, 2005.

[8] H.A. Amara and V. Bahl. Residential broadband revisited: Research challenges in residential networks, broadband access, and applications. Technical Report, NSF, 2003.

[9] G. Anastasi, E. Borgia, M. Conti and E. Gregori. Wi-Fi in ad hoc mode: A measurement study. In *IEEE PERCOM'04*, Orlando, USA, pp. 145-154, 2004.

[10] B. Aoun and R. Boutaba. Max-min fair capacity of wireless mesh networks. In *IEEE MASS'06*, pp. 1-10, 2006.

[11] B. Aoun, Y. Iraqi and R. Boutaba. A closer look at the capacity of wireless mesh networks. In *Med-Hoc-Net'06*, Sicily, Italy, pp. 90-97, 2006.

[12] O. Arpacioglu and Z.J. Haas. On the scalability and capacity of wireless networks with omnidirectional antennas. In *IPSN'04*, Berkeley, CA, USA, pp. 169-177, 2004.

[13] S. Avallone and I.F. Akyildiz. A channel assignment algorithm for multi-radio wireless mesh networks. In *ICCCN'07*, Honolulu, Hawaii, USA, pp. 1034-1039, 2007.

[14] J. Avonts, N.V.D. Wijngaert and C. Blondia. Distributed channel allocation in multi-radio wireless mesh networks. In *WiMAN'07*, Honolulu, Hawaii, USA, pp. 1-6, 2007.

[15] B. Awerbuch, D. Holmer and H. Rubens. The medium time metric: High throughput route selection in multi-rate ad hoc wireless networks. Technical Report, Johns Hopkins University, 2003.

[16] P. Bahl, R. Chandra and J. Dunagan. SSCH: Slotted seeded channel hopping for capacity improvement in IEEE 802.11 ad-hoc wireless networks. In *Mobicom'04*, Philadelphia, PA, USA, pp. 216-230, 2004.

[17] Belair Networks. http://www.belairnetworks.com. Accessed on 08/09/2010.

[18] Belair Networks. Capacity of wireless infrastructure mesh networks. White paper, 2004.

[19] D. Bertsekas and R. Gallager. *Data networks.* Prentice-Hall, Englewood Cliffs, New Jersey, USA, 1992.

[20] P. Bhagwat, B. Raman and D. Sanghi. Turning 802.11 inside-out. *ACM SIGCOMM Computer Communication Review*, *34* (1), pp. 33-38, 2004.

[21] V. Bharghavan, A. Demers, S. Shenker and L. Zhang. MACAW: A media access protocol for wireless LANs. In *ACM SIGCOMM'94*, London, UK, pp. 212-225, 1994.
[22] J. Bicket. Bit-rate selection in wireless networks. M.S. dissertation, Massachusetts Institute of Technology, 2005.
[23] J. Bicket, D. Aguayo, S. Biswas and R. Morris. Architecture and evaluation of an unplanned 802.11b mesh network. In *MOBICOM'05*, Cologne, Germany, pp. 31-42, 2005.
[24] S. Biswas and R. Morris. Exor: Opportunistic multihop routing for wireless networks. In *ACM SIGCOMM'05*, Philadelphia, PA, USA, pp. 133-144, 2005.
[25] R. Bruno, M. Conti and E. Gregori. Mesh networks: Commodity multihop ad hoc networks. *IEEE Communications Magazine*, *43* (3), pp. 123-131, 2005.
[26] R. Chandra, V. Bahl and P. Bahl. Multinet: Connecting to multiple IEEE 802.11 networks using a single wireless card. In *IEEE INFOCOM'04*, Hong Kong, China, pp. 882-893, 2004.
[27] Q. Chen, F. Schmidt-Eisenlohr, D. Jiang, M. Torrent-Moreno, L. Delgrossi and H. Hartenstein. Overhaul of IEEE 802.11 modeling and simulation in ns-2. In *MSWiM'07*, Chania, Greece, pp. 159-168, 2007.
[28] D. Cheung and C. Prettie. A path loss comparison between the 5 GHz UNII (802.11a) and the 2.4 GHz ISM band (802.11b). Technical Report, Intel Labs, 2002.
[29] Cisco Systems. Cisco Aironet 1240AG series 802.11a/b/g access point. http://www.cisco.com/en/US/products/ps6521/products_data_sheet0900aecd8031c844.html. Accessed on 08/09/2010.
[30] Cisco Wireless Mesh Networking Solution. http://www.cisco.com/en/US/netsol/ns621/networking_solutions_package.html. Accessed on 08/09/2010.
[31] D. Couto, D. Aguayo, B.A. Chambers and R. Morris. Performance of multihop wireless networks: Shortest path is not enough. In *HotNets-I*, Princeton, New Jersey, USA, 2002.
[32] D. Couto, D. Aguayo, J. Bicket and R. Morris. High-throughput path metric for multi-hop wireless routing. In *MOBICOM'03*, San Diego, CA, USA, pp. 134-146, 2003.
[33] P. Crescenzi and V. Kann. A compendium of NP optimization problems. http://www.nada.kth.se/~viggo/wwwcompendium. Accessed on 08/09/2010.
[34] A. Das, H. Alazemi, R. Vijayakumar and S. Roy. Optimization models for fixed channel assignment in wireless mesh networks with multiple radios. In *IEEE SECON'05*, Santa Clara, California, USA, pp. 1-12, 2005.
[35] R. Draves, J. Padhye and B. Zill. Comparison of routing metrics for static multi-hop wireless networks. In *ACM SIGCOMM'04*, Portland, Oregon, USA, pp. 133-144, 2004.
[36] R. Draves, J. Padhye and B. Zill. Routing in multi-radio, multi-hop wireless mesh networks. In *MOBICOM'04*, Philadelphia, PA, USA, pp. 114-128, 2004.
[37] R.V. Drunen, J. Koolhaas, H. Schuurmans and M. Vijn. Building a wireless community network in the Netherlands. In *USENIX'03*, San Antonio, TX, USA, pp. 219-230, 2003.
[38] R. Dube, C. Rais, K. Wang and S. Tripathi. Signal stability based adaptive routing (SSA) for ad-hoc mobile networks. Technical Report CS-TR-3646, University of Maryland, 1996.
[39] M. Ergen and P. Varaiya. Throughput analysis and admission control for IEEE 802.11a. *Mobile Networks and Applications*, *10*, pp. 705–716, 2005.
[40] K. Fall and S. Floyd. Simulation-based comparison of Tahoe, Reno, and SACK TCP.

*Computer Communication Review*, *26* (3), pp. 5-21, 1996.
[41] Z. Fang, B. Bensaou and Y. Wang. Performance evaluation of a fair backoff algorithm for IEEE 802.11 DFWMAC. In *MobiHoc'02*, Lausanne, Switzerland, pp. 1-10, 2002.
[42] Firetide. http://www.firetide.com. Accessed on 08/09/2010.
[43] C.L. Fullmer and J.J. Garcia-Luna-Aceves. Floor acquisition multiple access (FAMA) for packet-radio networks. In *ACM SIGCOMM'95*, Cambridge, MA, USA, pp. 262-273, 1995.
[44] R. Garces and J.J. Garcia-Luna-Aceves. Collision avoidance and resolution multiple access for multichannel wireless networks. In *IEEE INFOCOM'00*, Tel Aviv, Israel, pp. 595-602, 2000.
[45] R.L. Graham. Bounds on multiprocessing timing anomalies. *SIAM Journal of Applied Mathematics*, *17* (2), pp. 416-429, 1969.
[46] M. Grossglauser and D. Tse. Mobility increases the capacity of ad hoc wireless networks. *IEEE/ACM Transactions on Networking*, *10* (4), pp. 477-486, 2002.
[47] P. Gupta and P.R. Kumar. The capacity of wireless networks. *IEEE Transactions on Information Theory*, *46* (2000), pp. 388-404, 2000.
[48] P. Gupta and P.R. Kumar. Towards an information theory of large networks: An achievable rate region. *IEEE Transactions on Information Theory*, *49* (8), pp. 1877-1894, 2003.
[49] J.M. Hernando and F. Perez-Fontan. *Introduction to mobile communications engineering.* Artech House, Boston, USA, 1999.
[50] M. Heusse, F. Rousseau, G. Berger-Sabbatel and A. Duda. Performance anomaly of 802.11b. In *IEEE INFOCOM'03*, San Francisco, CA, USA, pp. 836-843, 2003.
[51] G. Holland, N. Vaidya and P. Bahl. A rate-adaptive MAC protocol for multi-hop wireless networks. In *MOBICOM'01*, Rome, Italy, pp. 236-251, 2001.
[52] J. Hortelano, M. Nacher, J.-C. Cano, C. Calafate and P. Manzoni. Evaluating the goodness of MANETs performance results obtained with the ns-2 simulator. In *NSTools'07*, Nantes, France, pp. 1-7, 2007.
[53] W.-C. Hung, K.L.E. Law and A. Leon-Garcia. A dynamic multi-channel MAC for ad hoc LAN. In *21st Biennial Symposium on Communications*, Kingston, Canada, pp. 31-35, 2002.
[54] IEEE 802.11s Project. http://grouper.ieee.org/groups/802/11/Reports/tgs_update.htm. Accessed on 08/09/2010.
[55] IEEE Std 802.11-1999 (R2003). http://standards.ieee.org. Accessed on 08/09/2010.
[56] IEEE Std 802.11a-1999 (R2003). http://standards.ieee.org. Accessed on 08/09/2010.
[57] IEEE Std 802.11b-1999 (R2003). http://standards.ieee.org. Accessed on 08/09/2010.
[58] IEEE Std 802.11g-2003. http://standards.ieee.org. Accessed on 08/09/2010.
[59] IEEE Std 802.11n-2009. http://standards.ieee.org. Accessed on 08/09/2010.
[60] IEEE Std 802.16-2009. http://standards.ieee.org. Accessed on 08/09/2010.
[61] ITU-R IMT-Advanced. http://www.itu.int/ITU-R/go/rsg5-imt-advanced. Accessed on 08/09/2010.
[62] S. Ivanov, A. Herms and G. Lukas. Experimental validation of the ns-2 wireless model using simulation, emulation, and real network. In *WMAN'07*, Bern, Switzerland, pp. 433-444, 2007.
[63] V. Jacobson. Congestion avoidance and control. In *ACM SIGCOMM'88*, Stanford, CA, USA, pp. 314-329, 1988.

[64] K. Jain, J. Padhye, V.N. Padmanabhan and L. Qiu. Impact of interference on multi-hop wireless network performance. In *MOBICOM'03*, San Diego, CA, USA, pp. 66-80, 2003.
[65] N. Jain, S.R. Das and A. Nasipuri. A multichannel CSMA MAC protocol with receiver-based channel selection for multihop wireless networks. In *ICCCN'01*, Scottsdale, AZ, USA, pp. 432-439, 2001.
[66] W. Jiang, Z. Zhang and X. Zhong. High throughput routing in large-scale multi-radio wireless mesh networks. In *WCNC'07*, Hong Kong, China, pp. 3598-3602, 2007.
[67] D.B. Johnson, D.A. Maltz and J. Broch. DSR: The dynamic source routing protocol for multi-hop wireless ad hoc networks. *Ad Hoc Networking, Addison Wesley*, pp. 139-172, 2001.
[68] J. Jun and M. Sichitiu. The nominal capacity of wireless mesh networks. *IEEE Wireless Communications*, *10* (5), pp. 1536-1284, 2003.
[69] A. Kamerman and L. Monteban. Wavelan-II: A high-performance wireless LAN for the unlicensed band. *AT&T Bell Laboratories Technical Journal*, pp. 118-133, 1997.
[70] T. Karagiannis, M. Molle, M. Faloutsos and A. Broido. A nonstationary Poisson view of Internet traffic. In *IEEE INFOCOM'04*, Hong Kong, China, pp. 1-12, 2004.
[71] P. Karn. MACA - a new channel access method for packet radio. In *ARRL/CRRL Amateur radio 9th Computer Networking Conference*, London, Ontario, Canada, pp. 134-140, 1990.
[72] R. Karrer, A. Sabharwal and E. Knightly. Enabling large-scale wireless broadband: The case for TAPs. In *HotNets-II*, Cambridge, MA, USA, pp. 1-6, 2003.
[73] A. Keshavarz-Haddad and R. Riedi. Bounds for the capacity of wireless multihop networks imposed by topology and demand. In *MOBIHOC'07*, Montréal, Québec, Canada, pp. 256-265, 2007.
[74] T.S. Kim, J.C. Hou and H. Lim. Improving spatial reuse through tuning transmit power, carrier sense threshold, and data rate in multihop wireless networks. In *MOBICOM'06*, Los Angeles, CA, USA, pp. 366-377, 2006.
[75] B. Ko, V. Misra, J. Padhye and D. Rubenstein. Distributed channel assignment in multi-radio 802.11 mesh networks. In *WCNC'07*, Hong Kong, China, pp. 3978-3983, 2007.
[76] A. Kochut, A. Vasan, A.U. Shankar and A. Agrawala. Sniffing out the correct physical layer capture model in 802.11b. In *INCP'04*, Washington D.C, USA, pp. 252-261, 2004.
[77] M. Kodialam and T. Nandagopal. Characterizing the capacity region in multi-radio multi-channel wireless mesh networks. In *MOBICOM'05*, Cologne, Germany, pp. 73-87, 2005.
[78] D. Kotz, C. Newport and C. Elliott. The mistaken axioms of wireless-network research. Technical Report TR2003-467, Dartmouth College, 2003.
[79] U. Kozat and L. Tassiulas. Throughput capacity of random ad hoc networks with infrastructure support. In *MOBICOM'03*, San Diego, CA, USA, pp. 55-65, 2003.
[80] V.S.A. Kumar, M.V. Marathe and S. Parthasarathy. Algorithmic aspects of capacity in wireless networks. *ACM SIGMETRICS Performance Evaluation Review*, *33* (1), pp. 133-144, 2005.
[81] P. Kyasanur and N.H. Vaidya. Routing and interface assignment in multi-channel multi-interface wireless networks. In *IEEE WCNC'05*, pp. 2051-2056, 2005.
[82] P. Kyasanur and N.H. Vaidya. Capacity of multi-channel wireless networks: Impact of number of channels and interfaces. In *MOBICOM'05*, Cologne, Germany, pp. 43-57, 2005.
[83] M. Lacage, H. Manshaei and T. Turletti. IEEE 802.11 rate adaptation: A practical

approach. In *ACM MSWiM'04*, Venice, Italy, pp. 126-134, 2004.
[84] J. Li, C. Blake, D. Couto, H.I. Lee and R. Morris. Capacity of ad hoc wireless networks. In *MOBICOM'01*, Rome, Italy, pp. 61-69, 2001.
[85] Z. Li, S. Nandi and A.K. Gupta. Improving fairness in IEEE 802.11 using enhanced carrier sensing. *IEE Proceedings Communications*, *151* (5), pp. 467- 472, 2004.
[86] B. Liu, Z. Liu and D. Towsley. On the capacity of hybrid wireless networks. In *IEEE INFOCOM'03*, San Francisco, CA, USA, pp. 1-10, 2003.
[87] J. Liu and S. Singh. ATCP: TCP for mobile ad hoc networks. *IEEE Journal on Selected Areas in Communications*, *19* (7), pp. 1300-1315, 2001.
[88] T. Liu and W. Liao. Capacity-aware routing in multi-channel multi-rate wireless mesh networks. In *ICC'06*, Istanbul, Turkey, pp. 1971-1976, 2006.
[89] T. Liu and W. Liao. On routing in multichannel wireless mesh networks: Challenges and solutions. *IEEE Network*, *22* (1), pp. 13-18, 2008.
[90] H. Lundgren, E. Nordstrom and C. Tschudin. Coping with communication grey zones in IEEE 802.11b based ad hoc networks. In *IEEE WoWMoM'02*, Atlanta, Georgia, USA, pp. 49-55, 2002.
[91] MANET. http://www.ietf.org/html.charters/manet-charter.html. Accessed on 08/09/2010.
[92] M.K. Marina and S.R. Das. A topology control approach for utilizing multiple channels in multi-radio wireless mesh networks. In *Broadnets'05*, Boston, USA, pp. 381-390, 2005.
[93] R. Mazumdar, L.G. Mason and C. Douligeris. Fairness in network optimal flow control: Optimality of product form. *IEEE Transactions on Communication*, *39*, pp. 775-782, 1991.
[94] Microsoft Wireless Mesh Research. http://www.research.microsoft.com/mesh. Accessed on 08/09/2010.
[95] MIT Roofnet. http://www.pdos.lcs.mit.edu/roofnet. Accessed on 08/09/2010.
[96] Motorola Mesh Networks. http://www.motorola.com/business/v/index.jsp?vgnextoid=91c623805ae46110VgnVCM1000008406b00aRCRD. Accessed on 08/09/2010.
[97] J. Moy. OSPF version 2. *RFC 2328*, 1998.
[98] A. Nasipuri, J. Zhuang and S.R. Das. A multichannel CSMA MAC protocol for multihop wireless networks. In *IEEE WCNC'99*, New Orleans, LA, USA, pp. 1-5, 1999.
[99] C. Perkins and P. Bhagwat. Highly dynamic destination-sequenced distance vector routing (DSDV) for mobile computers. In *ACM SIGCOMM'94*, London, UK, pp. 234-244, 1994.
[100] C. Perkins. IP mobility support for IPv4. *IETF RFC 3344*, 2002.
[101] C. Perkins, E.M. Royer and I. Chakeres. Ad hoc on demand distance vector (AODV) routing. *RFC 3561*, 2003.
[102] P. Porwal and M. Papadopouli. On-demand channel switching for multi-channel wireless MAC protocols. Technical Report TR04-024, Department of Computer Science, University of North Carolina, 2005.
[103] K. Ramachandran, E.M. Belding, K.C. Almeroth and M.M. Buddhikot. Interference-aware channel assignment in multi-radio wireless mesh networks. In *IEEE INFOCOM'06*, Barcelona, Spain, pp. 1-12, 2006.
[104] K. Ramachandran, I. Sheriff, E. Belding and K. Almeroth. Routing stability in static wireless mesh networks. In *PAM'07*, Louvain la neuve, Belgium, pp. 73-82, 2007.
[105] A. Raniwala and T. Chiueh. Evaluation of a wireless enterprise backbone network

architecture. In *IEEE Hot Interconnects 12*, Stanford University, pp. 1-7, 2004.
[106] A. Raniwala, K. Gopalan and T.-C. Chiueh. Centralized channel assignment and routing algorithms for multi-channel wireless mesh networks. *Mobile Computing and Communications Review*, *8* (2), pp. 50-65, 2004.
[107] A. Raniwala and T. Chiueh. Architecture and algorithms for an IEEE 802.11-based multi-channel wireless mesh network. In *IEEE INFOCOM'05*, Miami, FL, USA, pp. 1-12, 2005.
[108] B. Sadeghi, V. Kanodia, A. Sabharwal and E. Knightly. Opportunistic media access for multirate ad hoc networks. In *MOBICOM'02*, Atlanta, Georgia, USA, pp. 24-35, 2002.
[109] A.U.H. Sheikh. *Wireless communications: Theory and techniques.* Kluwer Academics Publishers, Boston, 2004.
[110] T.J. Shepard. A channel access scheme for large dense packet radio networks. In *ACM SIGCOMM'96*, Palo Alto, California, USA, pp. 219-230, 1996.
[111] M. Shin, S. Lee and Y.-A. Kim. Distributed channel assignment for multi-radio wireless networks. In *IEEE MASS'06* Vancouver, Canada, pp. 417-426, 2006.
[112] M. Shreedhar and G. Varghese. Efficient fair queueing using deficit round robin. In *ACM SIGCOMM '95*, Cambridge, MA, USA, pp. 231-242, 1995.
[113] H. Skalli, S.K. Das, L. Lenzini and M. Conti. Traffic and interference aware channel assignment for multi-radio wireless mesh networks. Technical Report, IMT Lucca, 2006.
[114] H. Skalli, S. Ghosh, S.K. Das, L. Lenzini and M. Conti. Channel assignment strategies for multiradio wireless mesh networks: Issues and solutions. *IEEE Communications Magazine*, *45* (11), pp. 86-95, 2007.
[115] J. So and N.H. Vaidya. Multi-channel MAC for ad hoc networks: Handling multi-channel hidden terminals using a single transceiver. In *ACM MOBIHOC'04*, Tokyo, Japan, pp. 222-233, 2004.
[116] Strix System. http://www.strixsystems.com/. Accessed on 08/09/2010.
[117] A.P. Subramanian, H. Gupta and S.R. Das. Minimum interference channel assignment in multi-radio wireless mesh networks. In *SECON'07*, San Diego, USA, pp. 481-490, 2007.
[118] A.P. Subramanian, J. Cao, C. Sung and S.R. Das. Understanding channel and interface heterogeneity in multi-channel multi-radio wireless mesh networks. In *PAM'09*, Seoul, South Korea, pp. 89-98, 2009.
[119] J. Tang, G. Xue and W. Zhang. Maximum throughput and fair bandwidth allocation in multi-channel wireless mesh networks. In *IEEE INFOCOM'06*, Barcelona, Spain, pp. 1-10, 2006.
[120] The Network Simulator - ns-2. http://www.isi.edu/nsnam/ns/. Accessed on 08/09/2010.
[121] F.A. Tobagi and L. Kleinrock. Packet switching in radio channels: Part II - the hidden terminal problem in carrier sense multiple-access and the busy tone solution. *IEEE Transactions on Communications*, *23* (12), pp. 1417-1433, 1975.
[122] Tropos Networks. http://www.tropos.com/. Accessed on 08/09/2010.
[123] J.S. Turner. New directions in communications (or which way to the information age?). *IEEE Communications*, *24* (10), pp. 8-15, 1986.
[124] M. Virendra, Q. Duan, S. Upadhyaya and V. Anand. A new paradigm for load balancing in wireless mesh networks. Technical Report 2006-11, the State University of New York at Buffalo, 2006.
[125] Wi-Fi. http://www.wi-fi.org. Accessed on 08/09/2010.
[126] Wireless Ad Hoc Networks. http://w3.antd.nist.gov/wahn_home.shtml. Accessed on 08/09/2010.

[127] S. Wu, Y. Tseng, C. Lin and J. Sheu. A multi-channel MAC protocol with power control for multi-hop mobile ad hoc networks. *The Computer Journal*, *45* (1), pp. 101-110, 2002.
[128] S. Xu and T. Saadawi. Does the IEEE 802.11 MAC protocol work well in multihop wireless ad hoc networks? *IEEE Communications Magazine*, *39* (6), pp. 130-137, 2001.
[129] Y. Yang, J. Wang and R. Kravets. Interference-aware load balancing for multihop wireless networks. Technical Report UIUCDCS-R-2005-2526, Department of Computer Science, University of Illinois at Urbana-Champaign, 2005.
[130] M. Yarvis, K. Papagiannaki and W.S. Conner. Characterization of 802.11 wireless networks in the home. In *the 1st Workshop on Wireless Network Measurements (WiNMee'05)*, Garda, Italy, pp. 1-19, 2005.
[131] S. Yi, Y. Pei and S. Kalyanaraman. On the capacity improvement of ad hoc wireless networks using directional antennas. In *ACM MOBIHOC'03*, Annapolis, Maryland, USA, pp. 108-116, 2003.
[132] Y. Yuan, D. Gu, W. Arbaugh and J. Zhang. High-performance MAC for high-capacity wireless LANs. In *ICCCN'04*, Rosemont, USA, pp. 167-172, 2004.
[133] H. Zhai and Y. Fang. Physical carrier sensing and spatial reuse in multirate and multihop wireless ad hoc networks. In *IEEE INFOCOM'06*, Barcelona, Spain, pp. 1-12, 2006.
[134] S. Zhao, Z. Wu, A. Acharya and D. Raychaudhuri. PARMA: A PHY/MAC aware routing metric for ad-hoc wireless networks with multi-rate radios. In *IEEE WoWMoM'05*, Giardini Naxos, Italy, pp. 286-292, 2005.
[135] J. Zhu, X. Guo, L.L. Yang, W.S. Conner, S. Roy and M.M. Hazra. Adapting physical carrier sensing to maximize spatial reuse in 802.11 mesh networks. *Wireless Communications and Mobile Computing*, *4* (8), pp. 933-946, 2004.
[136] J. Zhu and S. Roy. 802.11 mesh networks with two-radio access points. In *ICC'05*, Seoul, Korea, pp. 3609-3615, 2005.